Rhizo-sweet : glycomolecules of the rhizosphere and plant defense

Thi Ngoc Hanh Nguyen

Normandie Université

THÈSE

Pour obtenir le diplôme de doctorat

Spécialité SCIENCES AGRONOMIQUES, BIOTECHNOLOGIES AGRO-ALIMENTAIRES

Préparée au sein de l'Université de Caen Normandie

Rhizo-sweet: glycomolecules of the rhizosphere and plant defense

Présentée et soutenue par
THI NGOC HANH NGUYEN

Thèse soutenue le 26/04/2022 devant le jury composé de		
MME BARBARA DE CONINCK	Professeur, LEUVEN - KATHOLIEKE UNIVERSITEIT	Rapporteur du jury
MME FABIENNE GUILLON	Directrice de recherche, INRAE BIA NANTES	Rapporteur du jury
MME WAFA ACHOUAK	Directrice de recherche, CEA	Membre du jury
M. AZEDDINE DRIOUICH	Professeur des universités, Université Rouen Normandie	Président du jury
MME ANNETTE BERTRAND	Maître de conférences HDR, Université Caen Normandie	Directeur de thèse
MME MAITE VICRE	Maître de conférences HDR, Université Rouen Normandie	Co-directeur de thèse

Thèse dirigée par ANNETTE BERTRAND (Écophysiologie végétale, agronomie et nutritions N.C.S. (Caen)) et MAITE VICRE

UNIVERSITÉ CAEN NORMANDIE

ED 497 NBISE
Normande de Biologie Intégrative, Santé, Environnement

Ecophysiologie Végétale, Agronomie & nutritions N,C,S

Normandie Université

THÈSE

Pour obtenir le diplôme de doctorat

Spécialité SCIENCES AGRONOMIQUES, BIOTECHNOLOGIES AGRO-ALIMENTAIRES

de l'Université de Caen Normandie

Rhizo-sweet : glycomolécules de la rhizosphère et défense des plantes

Présentée et soutenue par

THI NGOC HANH NGUYEN

Thèse soutenue le 26/04/2022 devant le jury composé de		
MME BARBARA DE CONINCK	Professeure, Katholieke Universiteit Leuven, Belgique	Rapportrice du jury
MME FABIENNE GUILLON	Directrice de recherche, INRAE, Nantes	Rapportrice du jury
MME WAFA ACHOUAK	Directrice de Recherche, CEA, Cadarache	Membre du jury
M. AZEDDINE DROUICH	Professeur des universités, Université de Rouen Normandie	Membre du jury
MME ANNETTE MORVAN-BERTRAND	Maîtresse de conférences, HDR, Université de Caen Normandie	Directrice de thèse
MME MAÏTÉ VICRÉ	Maîtresse de conférences, HDR, Université de Rouen Normandie	Co-directrice de thèse

MME MARIE-PASCALE PRUD'HOMME	*Professeure des universités, Université de Caen Normandie*	*Invitée*
MME MARIE-LAURE FOLLET-GUEYE	*Maîtresse de conférences, HDR, Université de Rouen Normandie*	*Invitée*

Thèse dirigée par ANNETTE MORVAN-BERTRAND (Ecophysiologie Végétale, Agronomie et nutritions N.C.S., Caen) et MAÏTÉ VICRÉ (Glycobiologie et Matrice Extracellulaire Végétale, Rouen)

UNIVERSITÉ CAEN NORMANDIE

UNIVERSITÉ DE ROUEN NORMANDIE

ED 497 NBISE
Normande de Biologie Intégrative, Santé, Environnement

Ecophysiologie Végétale, Agronomie & nutritions N,C,S

GLYCO-MEV EA 4358

Acknowledgements

I would like to thank the members of my thesis jury for accepting to examine this thesis. I am very honored that Barbara De Coninck and Fabienne Guillon have accepted to be the reviewers of my thesis. I would like to express my gratitude to Wafa Achouak and Azeddine Driouich for accepting to be the examiners of this thesis.

Remerciements

Tout d'abord, je tiens à remercier Philippe Laîné et Philippe Etienne, directeur et directeur adjoint de l'UMR 950 INRAE-UCN EVA, pour m'avoir accueillie en son sein au cours de mes 2 premières années de thèse à Caen. Je remercie également Jean-Claude Mollet et Muriel Bardor, directeur et directrice adjointe du laboratoire Glyco-MEV EA-4358, de m'avoir ouvert les portes du laboratoire pour mes dernières années de thèse à Rouen. Merci pour votre chaleureux accueil et votre disponibilité tout le long de cette thèse.

Je remercie la région Normandie, la Structure Fédérative de Recherche « Normandie Végétal » (FED4277), ainsi que l'Université de Caen et l'Université de Rouen, pour leur soutien financier durant ma thèse. Je remercie également l'Ecole Doctorale Normande de Biologie Intégrative, Santé et Environnement (EdNBISE497) pour l'aide financière accordée lors de mon séjour au laboratoire d'Écologie Microbienne de la Rhizosphère et de l'Environnement Extrême en 2019 à Cadarache.

Je continue mes remerciements envers l'Institut de Génétique Environnement et Protection des Plantes (INRAE, IGEPP) et plus particulièrement à Maria J. Manzanares-Dauleux et Antoine Gravot pour vos nombreux échanges scientifiques et votre collaboration, m'ayant permis de récupérer différents lots de graines de colza et de mener des études sur le rôle des FEH du colza. Je remercie également Agnès Attard de l'Institut Sophia Agrobiotech (INRAE 1355-CNRS 7254) de Sophia Antipolis pour votre conseil scientifique et votre collaboration sur le test des mutants FEHs d'Arabidopsis en relation avec *Phytophtora parasitica.* Je remercie aussi Magalie Uyttewall de l'Institut Jean-Pierre Bourgin (IJPB, Versailles) pour la formation de croisement des mutants FEHs d'Arabidopsis.

Mes remerciements s'adressent également à Laurence Padel et son équipe à BIOTEM pour les efforts conjoints dans la génération d'anticorps monoclonaux contre les fructanes, m'ayant permis de réaliser l'aspect primordial de mon travail de thèse.

J’adresse mes profonds remerciements aux membres du Laboratoire d'écologie microbienne de la rhizosphère et de l'environnement extrême (LEMiRE, CEA, Cadarache) et spécialement à Wafa Achouak et Sylvain Fochesato pour leur chaleureux accueil, leurs conseils et leur gentillesse, qui m’ont permis de faire connaissance avec *Pseudomonas brassicacearum* et d’avoir un grand plaisir à travailler avec.

Toute ma gratitude va à Juliette Delisle, Christophe Trehin, Michaël Aubert et Marc Rollin pour avoir pris part à mon Comité de Suivi Individuel (CSI) pendant trois années et d’avoir apporté vos conseils et votre perspective.

À présent, j’aimerais adresser mes plus sincères remerciements à mes quatre formidables encadrants de thèse : Annette Morvan-Bertrand, Maïté Vicré, Marie-Pascale Prud'homme, et Marie-Laure Follet-Gueye. Mesdames, merci infiniment pour la chance et la confiance que vous m’avez accordées pour réaliser cette thèse à vos côtés. Aucun mot n’est assez fort pour remercier votre précieux accompagnement tout le long de ma thèse, votre disponibilité malgré des nombreuses heures de cours et des projets de recherche, votre rigueur et passion scientifique qui m’ont permis de faire le premier pas vers les fructanes, les FEHs, les cellules bordantes et le mucilage. Merci à toutes les quatre d’avoir donné à une voyageuse comme moi l'opportunité de voyager et d'approfondir mes connaissances sur les différentes techniques et sur les divers thèmes de recherche. Merci également pour votre gentillesse, votre écoute, votre énergie et votre optimisme qui m’ont encouragé et aidé à surmonter les problèmes pour continuer cette aventure. Un immense merci pour vos nombreuses corrections, vos conseils, votre aide précieuse non seulement pour ce manuscrit mais aussi pour les présentations, la rédaction d’articles scientifiques, les papiers administratifs ou tout simplement les emails qui commencent parfois très tôt le matin et finissent très tard le soir. Merci aussi pour mon initiation au monde de l’enseignement à travers mon contrat d’ATER signé avec l’Université de Rouen. En cette fin de thèse, un grand MERCI du fond du cœur pour votre soutien sans faille tout au long de la thèse et surtout MERCI pour le titre qui me tient à cœur : « votre doctorante ».

A Caen, mes sincères remerciements vont à tous les membres de l’équipe FEAST de m’avoir fait une place et accueillie dans l’équipe « fructanes » et pour vos précieux conseils qui ont participé au développement de ce travail de thèse. Je souhaiterais aussi remercier les membres du laboratoire EVA ainsi que ceux qui ont collaboré à la réalisation de ma thèse et qui ont pris sur leur temps pour m’aider dès que j’en avais besoin. Merci aussi pour la bonne ambiance de travail et la bonne humeur générale. Un merci tout particulier à Anne-Françoise Ameline pour la mise en place de ma culture en serre, tes conseils techniques précieux, tes nombreuses aides

au quotidien non seulement pour mes plantes mais aussi pour moi. Merci à Julie Frémont, la reine de la biologie moléculaire à EVA pour tes conseils techniques ainsi que pour les nombreuses qPCR et PCR sans fin. Merci également à Aurélia Lornac pour ta participation enthousiaste et précieuse dans la préparation des extraits des glucides solubles, la purification des fructanes de ray-grass et l'analyse HPAEC-PAD. Merci aussi à Josiane Pichon pour tous les matériels que tu nous prépares toujours dans la bonne humeur et ton aide précieuse pour la culture de nos mutants d'Arabidopsis. Merci à l'équipe de PLATIN' de m'avoir hébergé pendant des jours pour faire les extractions enzymatiques.

Je tiens à exprimer toute ma gratitude à l'équipe de la plateforme CMAbio[3] et plus particulièrement à Jean-Christophe Avice, Nicolas Elie et Didier Goux pour leur aide précieuse et les conseils microscopiques dans l'observation initiale de mes racines de raygrass.

Mes pensées se tournent vers tous les anciens doctorants, Cylia, Charlotte, Emilie, Maxence, Victor et Han. Ce fut un plaisir de vous avoir connu et de partager le début de thèse avec vous. Un merci tout particulier aux doctorants, ceux qui ont partagé mon quotidien durant mes premières années de cette thèse et pour tous les bons moments passés ensemble. A Galatéa, Lethícia, Moha, Aurélien, Jérémy et Antoine, merci à tous pour votre amitié et votre soutien tout au long de cette thèse. Toutes les discussions, les sorties, les repas et les partages sur la culture française ont énormément aidé la petite Hanh perdue en Normandie se sentant comme à la maison. Tous ces moments ont été précieux et vont énormément me manquer. Merci également aux stagiaires d'EVA pour leurs sourires et leurs soutiens pendant tout le temps passé à Caen. Une immense pensée à la team « choupette », Laëtitia, Lucile et Jérémy, pour leur soutien sans faille, les encouragements quotidiens et surtout pour votre merveilleuse amitié que j'ai beaucoup de chance d'avoir.

A Rouen, j'adresse mes profonds remerciements aux membres du laboratoire GlycoMEV qui est devenu ma seconde maison de thèse. Merci infiniment pour votre accueil, votre gentillesse et vos conseils qui m'ont permis de finaliser cette thèse dans les meilleures conditions. Je tiens à exprimer toute ma reconnaissance à Azeddine Driouich pour ses conseils scientifiques et sa participation primordiale au développement de ce travail de thèse. Un grand merci à Sophie Bernard et Gaëlle Durambur pour leur aide précieuse à la préparation des échantillons microscopiques ainsi que pour leurs conseils techniques. Merci également à Carole Burel et Quentin Arnaudin pour vos conseils avisés et vos nombreuses aides techniques. Je remercie infiniment Bruno Gugi de m'avoir fourni les fameux sucres dans sa « sucrothèque » qui m'ont permis de réaliser mes immunodot-blots ainsi que pour son soutien sans faille. Merci aussi à

Isabelle Boulogne et Carole Plasson de m'avoir fourni les graines de blé et formé pour la culture in vitro. Je souhaiterais aussi remercier Sophie Pagny-Salehabadi, Arnaud Lehner, Jean-Claude Mollet, Marie-Laure Follet-Gueye et Maïté Vicré de m'avoir fait confiance et initié au rôle d'enseignant lors mon contrat ATER à Rouen.

Je tiens à exprimer toute ma reconnaissance à l'équipe de la plateforme PRIMACEN (Plate-Forme de Recherche en Imagerie Cellulaire de Normandie) et plus particulièrement à Magalie Bénard pour son importante aide et ses conseils techniques dans l'utilisation du microscope confocal.

Mes sincères remerciements vont à tous les anciens doctorants de GlycoMEV, Barbara, Marc, Coralie, Jérémy, Pierre-Louis, Maxime, Yohana, Rodolphe, Mathilde, Aline et Marie que j'ai eu le plaisir de connaître et avec qui j'ai pu travailler. Merci pour votre chaleureux accueil lors mon arrivée en retard à Rouen. Egalement un immense merci aux doctorants (Charlotte, Marie-Laure, Mélanie, Alexia, Savignien, Olwen, Eulalie, Quentin) et aux collègues rouennais (Quentin, Juliette, Cathleen, Nesrine, Melissa, Manon, Kylhan, Édouard) de m'avoir réservé une petite place à vos côtés même avant mon arrivée à Rouen. Merci infiniment pour votre soutien, les discussions mémorables, les inoubliables souvenirs enrichis de rires et votre bonne humeur qui m'ont bien changé les idées. C'était un réel plaisir de travailler avec vous.

Enfin, je remercie sincèrement ma famille, toujours là pour me soutenir malgré la grande distance géographique. Tout d'abord merci à mes parents de m'avoir donné cette précieuse vie, de m'avoir accompagné dès les premiers pas et de m'avoir encouragé sans relâche depuis toujours. Merci à mes frères et sœurs, tout particulièrement à ma sœur Vy et mon frère Laurent. Mille mercis « anh Lô và chị Vy » pour votre soutien indéfectible depuis ma première leçon de français jusqu'à présent. Merci d'être toujours à mes côtés malgré les nombreux voyages et les déménagements sans fin. Merci de m'avoir nourri, supporté et offert un abri plein d'amour dans les moments les plus difficiles.

Dành tặng cho ba má kính mến của con những thành quả mà con đạt được tới ngày hôm nay. Con cám ơn ba má rất nhiều !
«Mai con lớn lên rồi ra đi tung cánh trong đời, dù xa vô bờ vẫn nhờ đến tình mẹ cha » (Cầu cho Cha Mẹ 2-Phanxicô Nguyễn Đình Diễn).

Table of contents

List of abbreviations

Table of figures

General introduction

I. Literature review 19

A. Plant cell wall - A constitutive defense barrier in plant immunity 19

1. Primary cell walls 19

2. Secondary cell walls 21

3. Plant cell wall distinction between eudicots and grasses 21

4. Cell wall composition and biosynthesis 24

5. Role of the cell wall in root defense 33

B. Concepts of plant immunity 35

C. Plant roots: A specialized underground defense system 39

1. Specificity of root defense: Organ-specific and tissue-specific responses 39

2. Root Associated, Cap-Derived Cells (AC-DCs) – The population of root border cells (BCs) and border-like cells (BLCs) 40

3. Root mucilage 48

4. Action of border cells and root mucilage in root defense 49

5. The Root Extracellular Trap (RET) model 53

D. Fructans and the concept of "Sweet Immunity" 55

1. Fructans in microorganisms and plants 55

2. Fructan metabolism in plant and microorganisms 61

E. FEHs in non fructan-plants 66

F. Objectives 71

II. Materials and methods 75

A. Seed sterilization and plant growth conditions 75

1. Seed sterilization 75

2. Plant growth 75
B. Study of the RET in perennial ryegrass 80
1. Selection and collection of root tips 80
2. Water deficit treatment 81
3. Visualization of mucilage by counterstaining with India ink 82
4. MAMPs 82
5. Surface immunolabeling of root border cells, mucilage and root tips 82
6. High-Pressure Freezing/Freeze Substitution (HPF) sample preparation 84
7. Immunolabeling of HPF sections of root border cells, mucilage and root tips 85
8. Ultrastructural and immunogold analyses using transmission electron microscopy 86
9. Primary antibodies table 86
10. Statistical and image analysis 86
C. Characterization of two new monoclonal antibodies against β-(2,1) and β-(2,6)-plant fructans 88
1. Antibody generation 88
2. Carbohydrate samples 89
3. Immuno-dot blot assay 89
4. Immuno-dot blot analysis 90
5. Localization by immunofluorescence of fructan epitopes 91
6. Statistical analysis 91
D. Salicylic acid upregulates fructan exohydrolases (FEH) together with defense-marker genes in non-fructan plants. 91
1. Plant treatment with phytohormones 91
2. RNA extraction 92
3. RT-qPCR analysis 93
4. Statistical analysis 95

E. Involvement of bacterial levans and plant fructan exohydrolases (FEHs) in *Arabidopsis thaliana* root colonization by *Pseudomonas brassicacearum* 96

1. Bacterial strains 96

2. Arabidopsis T-DNA mutant 96

3. Bacterial inoculation 99

4. Monitoring root colonization by *P. brassicacearum* using bacterial colonies counting 99

5. Monitoring root colonization by *P. brassicacearum* using fluorescent microscopy 101

6. Observations of *P. brassicacearum* exopolysaccharide (EPS) production 101

7. Analysis of root system morphology 101

8. Statistical analysis 103

III. Results 105

1. Generation and characterization of two monoclonal antibodies that recognized β-(2,1) and β-(2,6)-fructan epitopes: new tools to unravel the functions and subcellular localizations of fructans in plants 105

2. Microscopical characterization of the root extracellular trap (RET) of perennial ryegrass (*Lolium perenne*), a fructan producing plant 129

3. Salicylic acid upregulates fructan exohydrolases (FEH) together with defense-marker genes in non-fructan plants 165

4. Involvement of bacterial levans and plant fructan exohydrolases (FEHs) in *Arabidopsis thaliana* root colonization by *Pseudomonas brassicacearum* 191

IV. General discussion and Perspectives 209

V. Appendix 215

VI. References 219

List of abbreviations

1-FEH: 1-fructan exohydrolase
1-FFT: fructan:fructan 6-fructosyl transferase
1-KEH: 1-kestotriose exohydrolase
1-SST: sucrose:sucrose 1-fructosyl transferase
6&1-FEH: 6&1-fructan exohydrolase
6-FEH: 6-fructan exohydrolase
6G-FFT: fructan: fructan 6G-fructosyl transferase
6-KEH: 6-kestotriose exohydrolase
6-SFT: sucrose:fructan 6-fructosyl transferase
ACC: 1-Aminocyclopropane-1-carboxylic acid
AC-DC: associated cap-derived cell
ACR4: Arabidopsis CRINKLY4
AFS: freeze-substitution automate
AGP: arabinogalactan protein
AOS: allene oxide synthase
Ara*f*: arabinose (furanose)
Ara-T: arabinosyltransferase
ATP: adenosyl-triphosphate
BC: root border cell
BFO: burdock fructo-oligosaccharide
BLC: root border-like cell
bp: base pair
BRN1: bearskin 1
BRN2: bearskin 2
BSA: bovine serum albumin
CAZy: carbohydrate-active enzymes database
CDF: cycling DNA-binding one zinc finger factor
cDNA: complementary DNA
CDPK: calcium-dependent protein kinase
CEA: Commisariat à l'énergie atomique et aux énergies alternatives
CESA: cellulose synthase
CLE40: clavata3/embryo surrounding region 40
CLV1: CLAVATA
COL: columella
Col-0: Columbia 0
ConA: concanavalin A
CSC: cellulose synthase complexe
CSL: cellulose synthase like
CslA to CslH: cellulose synthase like (family A to H)
CSLM: confocal scanning light microscopy
CW: cell wall
Cw-INV: cell-wall invertases
DAMP: damage-associated molecular pattern
DNA: deoxyribonucleic acid
DOF: DNA-binding one zinc finger
DP: degree of polymerization
DZ: differentiation zone
eBC: elongated border cells

EDTA: ethylenediaminetetraacetic acid
EF: elongating factor
ELISA: enzyme-linked-immunosorbent-assay
EPS: exopolysaccharide
ER: endoplasmic reticulum
ERDF: European regional development fund
ERF: ethylene responsive factor
ESF: European social fund
ET: ethylene
ETI: effector-triggered immunity
ETS: effector-triggered susceptibility
EVA: écophysiologie végétale, agronomie et nutritions N.C.S.
exDNA: external DNA
EXT: extension
EZ: elongation zone
fBLC: filamentous border-like cell
FEH: fructan exohydrolase
FLA: fasciclin-like AGP
flg: flagellin
FOS: fructo-oligoaccharides
FT: fructosyltransferase
Fucosyltransferase: Fuc-T
G: Golgi stack
GalA: galactuonic acid
GalT: galactosyltransferase
GAPDH: glyceraldehyde 3-phosphate dehydrogenase
GAX: glucuronoarabinoxylan
GFP: green fluorescent protein
GH: glycoside hydrolase
GlcA*p*: glucuronic acid (pyranose)
GlcAT: Glucuronosyltransferase
GlycoMEV: glycobiology and plant extracellular matrix
GPI: glycosylphosphatidylinositol
GRP: glycine-rich proteins
HEL: hevein like
HG: homogalacturonan
HPAEC-PAD : high performance anion exchange chromatography – pulsed amperometric detection
HPF/FS: high pressure freezing / freezed substitution
HPF: high-pressure freezing
HPGT: Hyp-*O*-galactosyltransferase
HPLC: high performance liquid chromatography
HR: hypersensitive response
HRGP: hydroxyproline-rich glycoprotein
HRP: horseradish peroxidase
iBC: intermediate border cells
IgG: immunoglobulin G
IJPB: Jean-Pierre Bourgin Institute
INRAE: Institut national de recherche pour l'agriculture, l'alimentation et l'environnement
INV: invertase

INSEE: National Institute of Statistics and Economic Studies
JA: jasmonic acid
JIM: John Innes monoclonal
KEH: kestoriose hydrolase
LEMiRE: laboratoire d'écologie microbienne de la rhizosphère et de l'environnement Extrême
LM: Leeds monoclonal
LPS: lipopolysaccharide
LRC: lateral root cap cell
LRR: leucine-rich-repeat
LRW: London Resin White
M: mitochondria
mAb: monoclonal antibody
MAMP: microbial-associated molecular pattern
MAPK: mitogen-activated protein kinase
MeGlcA*p*: methylglucuronic acid (pyranose)
MeJA: methyljasmonate
MF: cellulose microfibril units
MLG: mixed-linkage glucans
MS: Murashige and Skoog
mvb: multi-vesicular bodies
NAD: nicotinamide adenine dinucleotide
NASC: Nottingham Arabidopsis stock centre
NB: nucleotide-binding
NDS: normal donkey serum
NET Neutrophil Extracellular Trap
NGS: normal goat serum
NLR: nucleotide-binding leucine-rich repeat receptor
NPL7: NIN-like protein 7
OG: oligogalacturonides
PAMP: pathogen-associated molecular pattern
PAR: Photosynthetically Active Radiations
PBS: phosphate-buffered saline
PBST: phosphate-buffered saline with tween
PCR: polymerase chain reaction
PEG: polyethylene glycol
PFA: paraformaldehyde
PGN: peptidoglycan
PIPES: piperazine- N,N’-bis [2-ethanesulfonic acid]
PM: plasma membrane
PME: pectin methylesterase
PR: pathogenesis-related
PRP: proline-rich proteins
PRR: pattern recognition receptors
PTI: PAMP-triggered immunity
QC: quiescent center
qPCR: quantitative PCR
R: resistance proteins
RAM: root apical meristem
RBOHD: respiratory burst oxidase homologue D
RC: root cap

RCPG: root cap polygalacturonase
RET Root Extracellular Trap
RFP: red fluorescent protein
RGI: rhamnogalacturonan I
RGII: rhamnogalacturonan II
RLK: receptor-like kinase
RLP: receptor-like protein
RNA: ribonucleic acid
ROS: reactive oxygen species
RT: reverse transcription
RT: room temperature
SA: salicylic acid.
SAR: systemic acquired resistance
sBC: spherical border cells
SCR: scarecrow
SDS: sodium dodecyl sulfate
SFR: structure federative de recherche
SMB: sombrero
SV: secretory vesiclesV: vacuole
TBS: Tris-buffered saline
TBST: Tris-buffered saline with tween
TGN: trans golgi network
TZ: transition zone
UMR: unité mixte de recherche
UPRES-EA: unité propre de recherche de l'enseignement supérieur– équipe d'accueil
V-INV: vacuolar invertase
WOX: Wuschel-related homeobox
WSC: water-soluble carbohydrate
XGA: xylogalacturonan
XyG: xyloglucan
YFP: yellow fluorescent protein

Table of figures

Figure I-1. Structure and composition of the primary wall of plants. 20
Figure I-2. The model of type I and type II primary walls. 22
Figure I-3. Composition of secondary cell wall of eudicots and grasses. 23
Figure I-4. Association of cellulose molecules in the plant cell wall. 25
Figure I-5. Xyloglucan [β-D-Glcp-(1 4)]n backbone substituted with side chains as seen in pea and Arabidopsis. 26
Figure I-6. Glucuronoarabinoxylan (GAX) typical of commelinid monocots. 27
Figure I-7. Mixed linkage β-glucan 28
Figure I-8. Schematic structure of pectin showing the four pectic polysaccharides. 29
Figure I-9. Structure of arabinogalactan proteins (AGPs) 32
Figure I-10. Classical structure of extensins complemented by the enzymes responsible of their formation. 33
Figure I-11. Schematic view of plant defense signaling. 37
Figure I-12. Model of crosstalk and cooperation between ETI and PTI 38
Figure I-13. Microscopical characterization of pea (*P. sativum*) border cells. 41
Figure I-14. Root border cell morphotypes from pea (*P. sativum*) root tip. 42
Figure I-15. Microscopical characterization of Arabidopsis root border-like cells. 43
Figure I-16. Microscopical characterization of root border-like cells (BLCs) from flax (*L. usitatissimum*) 43
Figure I-17. Root cap structure and development. 44
Figure I-18. Evidence of border cells in several plant species. 45
Figure I-19. Organization of the root apex of eudicotyledonous angiosperm plants. 46
Figure I-20. Involvement of different transcription factors and signaling peptides in Arabidopsis root cap development and BLC release. 47
Figure I-21. Visualization of secreted mucilage using India ink staining. 48
Figure I-22. Role of root AC-DCs in the various stresses. 51
Figure I-23. Schematic model of RET. 54
Figure I-24. Schematic representation of the different types of fructans. 57
Figure I-25. Role of fructans in plant immunity. 60
Figure I-26. Model of fructan biosynthesis in plants. 62
Figure I-27. Schematic representation of carbohydrate metabolism in a plant cell. 64

Figure I-28. Phylogenetic tree of FEH, cell wall invertases (Cw-INV), fructosytransferases (FT) and vacuolar invertases (V-INV) of plants based on predicted amino acid sequences (ClustalW/Drawtree). 67
Figure I-29. Schematic representation of FEHs potential roles during biotic stress. 69
Figure II-1. In vitro plant growth in dishes. 77
Figure II-2. Experimental design for seedling production. 79
Figure II-3. Schematic representation of root preparation for microscopic observation. 81
Figure II-4. Schematic representation of root preparation for immunolabeling experiment. .. 83
Figure II-5. Schematic representation of high-pressure freezing/freeze substitution (HPF) sample preparation. 85
Figure II-6. Illustration of immuno-dot blot assay of the binding of anti-fructan antibodies to a series of fructans and other water soluble carbohydrate (WSC) extracts..... 90
Figure II-7. Experimental design for exogenous supply of phytohormones at the root level.. 92
Figure II-8. Separation by 1.2% agarose gel electrophoresis of total RNAs. 93
Figure II-9. Arabidopsis T-DNA mutant genotyping..... 98
Figure II-10. Schematic representation of the experiments to study the interaction between A. thaliana FEH knock-out mutants and P. brassicacearum. 100
Figure II-11. Schematic representation of image analysis of root system morphology..... 102
Figure III-1. Immuno-dot blot quantification using BTM9H2 mAb with goat anti-mouse secondary antibody. 114
Figure III-2. Immuno-dot blot quantification using BTM15A6 mAb with goat anti-mouse secondary antibody. 116
Figure III-3. Immuno-dot blot quantification using BTM9H2 mAb with chicken anti-mouse secondary antibody. 118
Figure III-4. Immuno-dot blot quantification using BTM15A6 mAb with chicken anti-mouse secondary antibody. 118
Figure III-5. Immunofluorescence detection of fructans on root tips of A. thaliana, timothy, wheat and perennial ryegrass using the monoclonal antibodies BTM9H2 and BTM15A6... 120
Figure III-7. Visualization of secreted mucilage (m) using India ink staining. 147
Figure III-6. Root border cell morphotypes. Images showing different cell morphotypes using a bright-field microscope: (A) localization of different cell types along the root tip using a bright-field microscope. 147
Figure III-8. Immunolocalisation of hemicellulose epitopes on the surface of root tips. 149
Figure III-9. Immunolocalisation of hemicellulose epitopes on the HPF sections. 150

Figure III-10. Immunolocalisation of pectin epitopes on the surface of root tips. 151
Figure III-11.Immunolocalisation of extensin epitopes on the surface of root tips. 152
Figure III-12. Immunolocalisation of arabinogalactan proteins (AGPs) epitopes at the surface of root tips. 153
Figure III-13. Immunolocalisation of arabinogalactan proteins (AGPs) epitopes on the HPF sections. 154
Figure III-14. Immunogold labeling of AGPs using mAb JIM13 on 12-d-old perennial ryegrass root border cells prepared by HPF and FS. 155
Figure III-15. Immunostaining of AGPs epitopes at the surface of Arabidopsis 156
Figure III-16. Immunostaining of AGPs epitopes at the surface of ryegrass 157
Figure III-17. Immunostaining of AGPs epitopes at the surface of ryegrass 158
Figure III-18. Histograms represent quantitative data indicating the proportion of RET surface area surrounding the root cap. 159
Figure III-19. Phytohormone treatments increased the expression of some defense-marker and FEH genes in B. napus roots. 172
Figure III-20. Phytohormone treatments increased the expression of some defense-marker and FEH genes in *B. napus* roots and shoots. 174
Figure III-21. Phytohormone treatments increased the expression of some defense-marker and FEH genes in *A. thaliana* roots and shoots. 176
Figure III-22. The expression of defense-marker and FEH genes in *B. napus* roots after SA treatment differed among genotypes. 178
Figure III-23. Level of Arabidopsis Col-0 root colonization by *P. brassicacearum*. 198
Figure III-24. Exopolysaccharide (EPS) of *P. brassicacearum* NFM421-I::gfp strain visualization using red fluorescent ConA probe. 198
Figure III-25. Visualization of Arabidopsis Col-0 root colonization of by red fluorescent protein-tagged *P. brassicacearum* NFM421 (wild-type) and Δlev (levansucrase deletion mutant) 200
Figure III-26. Arabidopsis Col-0 and FEH knock-out mutants inoculated with *P. brassicacearum* 202
Figure III-27. The effect of *P. brassicacearum* inoculation on root morphology of Arabidopsis 203
Figure III-28. Visualization by light microscopy of the mucilage forming a halo at the root tip (m) using India ink staining. 204

Table I-1. Approximate composition (% dry weight) of typical eudicot and grass primary and secondary cell walls. 24
Table I-2. Examples of occurrence found in literature of different types of fructans in plants and microorganisms. 58
Table I-3. The occurrence of GH32 enzymes in plants. 61
Table I-4. Summary of selected cDNAs from FEHs of plants. 70
Table II-1. Composition of the Hoagland ¼ nutrient solution used for the culture in hydroponics of Arabidopsis and rapeseed (*Brassica napus*). 80
Table II-2. Composition of the 'EVA' nutrient solution used for the culture in hydroponics of perennial ryegrass (*Lolium perenne*). 80
Table II-3. Primary antibodies and associated epitopes of different cell wall polysaccharides used in this project. 87
Table II-4. Primers used for qRT-PCR in this study. 95
Table II-5. T-DNA specific primers for SALK insertion mutant collection and primers used for plant genotyping. 97
Table II-6. Characteristics of FEH knockout mutants. 98
Table III-1. Immunolabeling of major glyco-polymer motifs in the RET of perennial ryegrass, timothy, wheat and Arabidopsis using immunofuorescence microscopy. 148

General introduction

With a production of 75.5 billion euros, France was the leading agricultural producer in the European Union in 2020 according to the statistical analysis of INSEE (National Institute of Statistics and Economic Studies). Agricultural activities produce not only an important source of food for humans but also feed for livestock and provide raw materials for many industrial sectors (biofuels, bioplastics, biomaterials, cosmetics, health, etc.). The major challenge for agriculture today and in the future is to improve the yield of plant productions and maintain the quality of the harvested products while being more environmentally friendly. To develop sustainable agriculture, French government projects such as "Ecophyto II+" aim to reduce the use of crop protection chemicals by 50% by 2025. Elimination of glyphosate was planned by the end of 2020 for its main uses and by 2022 for all kinds of uses (https://agriculture.gouv.fr/ecophyto). In addition, the cooperation of the French Institute INRAE and its German counterpart enabled the development of the "European Green Deal" project in 2020. One of the pillars of this project is the "2030 Biodiversity Strategy", one of the main challenges is to build agriculture free of chemical pesticides (https://ec.europa.eu/environment/strategy/biodiversity-strategy-2030_en). In an agricultural region like Normandy where agriculture and agri-food industry are sectors with great potential, the demand for natural crop protection products is increasing day by day. In the context of reducing the use and risk of chemical pesticides, the characterization of the mechanisms involved in the natural defense systems of plants is necessary for the development of sustainable alternatives to the use of synthetic products in agricultural areas (https://world.businessfrance.fr/nordic/2020/06/09/the-future-of-agriculture-is-organic-and-in-normandy/).

While the defense mechanisms against pathogens have been well studied, this question has been largely investigated regarding the aerial parts of the plants, knowledge regarding the root system is still scarce (Chuberre et al., 2018). Differences were reported between immune responses in leaves and roots which makes it difficult to extrapolate data from the aerial part to the below-ground system. It is thus necessary to get a better understanding of the root system defense (Millet et al., 2010; Mauch-Mani et al., 2017).

The rhizosphere is a privileged area of interactions between microbial flora and roots. More especially atypical living cells called "Root Border Cells" or root "associated, cap-derived cells (AC-DCs) embedded in their surrounding mucilage play a key role in root-soil borne microorganisms (Driouich et al., 2019). Root border cells are specialized in the production of

anti-microbial molecules including proteins and secondary metabolites. Interestingly, the mucilage released from the root cap of many plant species has been shown to act in conjunction with AC-DCs to form a structure defined as Root Extracellular Trap (RET) by analogy with the Neutrophil Extracellular Trap (NET) involved in mammalian immunity (Driouich et al., 2013). The RET has been shown to play a key role in root-microbe interactions (Hawes et al., 2000; Cannesan et al., 2012; Driouich et al., 2013; Hawes et al., 2016; Tran et al., 2016). Molecular characterization of the RET showed that polysaccharides such as pectins, mannans, glycoproteins (extensins), and proteoglycans (arabinogalactan proteins) are major components (Willats et al., 2001 ; Knee et al., 2001; Cannesan et al., 2012; Driouich et al., 2013; Plancot et al. 2013 ; Castilleux et al. 2018).

The number of border cells produced and the composition of the mucilage were shown to be impacted in response to elicitors (flagellin 22, chitosan, peptidoglycan…) suggesting that a modulation of the RET is probably part of root immunity (Chuberre et al., 2018; Driouich et al., 2019).

The evaluation of the role of plant- or microbial-derived carbohydrates in plant immunity has recently led to the concept of "Sweet-Immunity" (Bolouri Moghaddam and Van den Ende, 2013; Trouvelot et al., 2014; Tarkowski et al., 2019; Svara et al., 2020). Among carbohydrates capable of eliciting a defense response, fructans, which are water-soluble polymers of fructosyl residues linked by β-(2,1) and/or β-(2,6) linkages with one external or internal glucosyl residue, are considered as multi-functional molecules involved in the tolerance and resistance of plants against abiotic and biotic stresses (Vijn and Smeekens 1999; Ritsema and Smeekens 2003). Indeed, fructans, either of plant or microbial (Versluys et al. 2017) origin were shown to activate plant immune responses. In plants, the synthesis of fructans is carried out from sucrose thanks to different fructosyltransferases (FTs) and their degradation by fructan exohydrolases (FEHs). Due to the phylogenetic proximity between FEHs and Cell Wall Invertase (CW-INV) which both belong to the glycoside hydrolase 32 (GH32) family, functional characterization of purified proteins shown that some of these genes initially identified as encoding CW-INVs actually encode proteins with FEH activity. Interestingly, some studies shown the presence of genes encoding enzymes with FEH activity in the genome of several non-fructan plants such as *Beta vulgaris* (Van den Ende et al. 2003b), *Arabidopsis thaliana* (*At6&1FEH* and *At6-FEH*; De Coninck et al. 2005), and *Zea mays* (Zhao et al. 2019). The role of these FEHs is unclear and one hypothesis is that these FEHs are defense-related proteins that play a role in plant-microorganism interactions by contributing to the production

of the Pathogenesis/Microbial-associated molecular pattern (P/MAMPs) from extracellular microorganism levans and/or by weakening the bacterial biofilm (Van den Ende et al., 2005). This hypothesis was recently supported by the fact that the FEH identified in maize (Zm-6&1-FEH1) is localized in the apoplast, which would allow a direct action on microbial extracellular fructans (Zhao et al., 2019). It is also possible that following injury or pathogen attack causing disruption of the plasma membrane and/or tonoplast, vacuolar FEHs are discharged into the apoplast compartment. The FEHs thus present in the cell wall would be able to degrade the microbial fructans, leading to (*i*) a modification of the properties of the biofilm which could reduce virulence, and (*ii*) the release of fructose and fructooligosaccharides (FOSs) which could play the role of P/MAMPs. These P/MAMPs would be recognized by Pattern Recognition Receptors (PRR) thus triggering plant primary innate immunity (Pathogenesis Triggered Immunity, PTI). As a result, signaling cascades involving salicylic acid (SA), jasmonic acid (JA), and/or ethylene (ET) pathways would lead to the initiation of defense responses such as the synthesis of compounds with antimicrobial activity (Thakur and Sohal 2013; Rejeb et al., 2014).

In this context, one objective of my thesis work is to characterize the RET of perennial ryegrass and to determine whether fructans are part of the RET of the fructan-producing plants. For this, perennial ryegrass (*Lolium perenne*) was used as a fructan-producing plant model to characterize the biochemical composition of the RET using cytochemical approaches. In order to study the localization of fructans within the root system, it was first necessary to obtain antibodies specifically dedicated to fructan epitopes. Indeed, only two studies have reported the use of anti-fructan antibodies to localize fructans in plant tissues (Röber et al., 1996; Pilon-Smits et al., 1996). In these two cases, antibodies were used for the immunolocalization of levans produced in transgenic potatoes through the expression of a bacterial levansucrase gene. Pilon-Smits et al. (1996) used mAbs produced in mouse (2-l-3mAb; Hall et al., 1990) while in the case of Röber et al. (1996), the provenance of the anti-levan antibody was not given. In both cases, the cellular localization of the fructans was investigated *via* immunofluorescence and shown the presence of fructans in the intercellular space instead of the expected vacuolar localization. To our knowledge, apart from these two studies which focused on transgenic plant producing fructans, the immunolocalization of fructans has not been reported, either in transgenic or in native fructan plant species. Moreover, no anti-fructan antibodies are currently available. Due to the absence of commercially available anti-fructan antibodies, we initiated

collaboration with the company BIOTEM to generate and characterize two new monoclonal antibodies (mAbs) directed against fructan epitopes.

The specificities of these were analysed by dot blot on a wide range of oligo- and polysaccharides at the different steps of production.

Besides, to clarify the roles of FEHs in non-fructan producing plants, we tested the hypothesis according to which FEHs are defense-related proteins whose synthesis is induced during the immune response in two non-fructan species, rapeseed (*Brassica napus*) and *Arabidopsis thaliana*. To do this, defense responses were stimulated by treatments of the roots with phytohormones or their precursors, namely SA, methyl jasmonate (MeJA), and the precursor of ethylene, the 1-aminocyclopropane-1-carboxylate (ACC) and gene expression of FEHs was measured. In addition, to assess the roles of plant FEHs and bacterial fructans (levans) in plant-microorganism interactions, we performed preliminary experiments with knock-out mutants of *A. thaliana* lacking FEH genes inoculated with two strains of the non-pathogen root-colonizing bacterium *Pseudomonas brassicacearum* (strains with or without the levansucrase gene encoding the enzyme synthesizing levans).

The experimentations were financially supported by Normandy County council and the European Union (in the framework of the ERDF-ESF operational program 2014-2020) through three regional research projects (EPURE, Enhancing Plant nutRition and Health, 2017-2019; NPT, Normandy Plant Tech, 2018-2021; and BEER, Bactéries, Exsudats Et Rhizodépôts, 2019-2022). These projects were elaborated in collaboration by the three academic partners of the Normand federative research structure “NORVEGE” (SFR Normandie Végétal FED 4277FD) which are University of Caen Normandy (UMR INRAE 950 EVA), University of Rouen Normandy (UPRES-EA4358 Glyco-MEV and EA4312 LMSM) and UniLaSalle Polytechnic Institute (UP2018.C101 AGHYLE). These projects aim to improve crop production in terms of yield and quality through sustainable agroecological solutions that would eliminate (or at least limit) chemical inputs in agricultural practices. More precisely, these projects aim to contribute to a better knowledge of the mechanisms involved in plant nutrition and in root defense. The studies are carried out at different scales (whole plant, cell and molecular levels) and focus on plants of regional interest (notably rapeseed, pea, potato, and ryegrass) and a model plant (*Arabidopsis thaliana*).

As a contribution to these research objectives, my thesis focused on three plants, rapeseed (*Brassica napus*), perennial ryegrass *(Lolium perenne),* and *Arabidopsis thaliana.* The

experimental work was carried out in two laboratories, one at the University of Caen Normandy (UMR INRAE 950 EVA “Ecophysiologie Végétale, Agronomie et nutrition N.C.S”) and one at the University of Rouen Normandy (UPRES-EA 4358 Glyco-MEV “Glycobiology and Plant Extracellular Matrix”) on the basis of the expertise of each research team. During the two first years of my thesis, my research was done at the University of Caen Normandy in EVA laboratory, within the FEAST (Fructans, Environment And Sugar Transport) team. It has focused on the studies of the role of FEHs in plant defense. In parallel, collaboration with BIOTEM was initiated to produce anti-fructan antibodies and I tested the specificity of sera and cell culture supernatants during the different stages of antibody production. During the third year of my thesis, my research has been achieved at the University of Rouen Normandy in GlycoMEV laboratory. The main topic of my work there was the characterization of the RET of perennial ryegrass as well as the analysis of specificity of the two anti-fructan mAbs produced by BIOTEM.

During my thesis, I also had the opportunity to collaborate with the « Laboratoire d'Écologie Microbienne de la Rhizosphère et de l'Environnement Extrême » (LEMiRE, CEA, Cadarache). I spent two months (Oct-2019 to Dec-2019) under the supervision of Dr. Wafa Achouak who has the expertise to study the adaptive responses of bacteria to environmental fluctuations, as well as the regulation and expression of phytobeneficial traits of bacteria associated with plant roots. This expertise allowed me to perform *Pseudomonas brassicacearum* inoculation assays on *A. thaliana* seeds (wild-type and FEH knock-out mutants) and to monitor the effect of inoculation on root morphology and on root colonization by confocal microscopy. Before this research internship, I checked the homozygosity of the T-DNA insertion mutants obtained at the Nottingham Arabidopsis Stock Centre (NASC, Nottingham UK. In addition, I had the opportunity of a short technical training (Feb-2020) on the crossing of *A. thaliana* by Dr. Magalie Uyttewall at the Jean-Pierre Bourgin Institute (IJPB, Versailles) to be able to generate double mutant lines.

The agronomic perspective of this work is to provide new insights on the role of the fructan degrading enzymes FEHs in non-fructan accumulating species in particular and in plants in general, which could lead to the development of innovative strategies for crop protection. This manuscript is organized into five chapters:

- A "**literature review**" on the plant defense mechanisms involving the Root Extracellular Trap (RET) model and on the metabolism of fructans in plants. This chapter is

completed by the presentation of the detailed objectives of this thesis and the different techniques used to achieve them.

- A chapter on "**materials and methods**" introduces a detailed description of the biological materials and experimental conditions used in the microscopic analyses, biochemistry and molecular biology techniques.

- The third chapter, organized in four parts, presents the "**results**" obtained during my thesis work and the three first parts are presented in the form of research articles. The first part presents the results on the new anti-fructan antibodies. The second part regroups the work on the characterization of the mucilage secreted and root border cells of perennial ryegrass (*Lolium perenne*). The third part concerns to the assessment of FEH as defense genes. Finally, the fourth part consists on additional promising results obtained at the CEA of Cadarache on the impact of FEHs in root defense *via* the degradation of bacterial fructans.

- The last chapter on " **discussion and perspectives**" presents the key results of this work are compared to data from the literature with the major conclusions of this project and the hypothesis proposed for future work.

I. Literature review

A. Plant cell wall - A constitutive defense barrier in plant immunity

In their natural environment, plants have their own strategy to defend against numerous from biotic and abiotic threats (Panstruga et al., 2009; Miedes et al., 2014). Plant defense responses depend first on the innate immunity of each cell and from the systemic signals deriving from the infection sites (Dangl et al., 2001; Ausubel, 2005). Thus, as the first barrier facing the attacks, the wall that surrounds each plant cell plays an essential role in plant immunity to determine the penetration of the aggressor (Wan et al., 2021). These plant cell walls are mainly rich in polysaccharides but also contain proteins which promote the growth and development of the plant and also the protection from adverse environmental conditions (Fangel et al., 2012; Sakamoto et al., 2018; Calderan-Rodrigues et al., 2019). The composition and architecture of plant cell walls are modified according to developmental environments, plant species, organs, tissues and the stage of development (Showalter, 1993; Knox, 2008; Pattathil et al., 2015; Hofte and Voxeur, 2017). However, the multiplicity of cell walls architecture / composition organization is related to relative proportion and mutual arrangement of fundamental macromolecules such as polysaccharides, including cellulose, hemicelluloses, pectins, and proteins. Basically, plant cell walls are divided into two classes which have their own chemical composition and arrangement of their constituting polymers. The primary cell wall is a thin, dynamic layer developed during cell expansion that is fundamental for plant morphogenesis, and the secondary cell wall is a thicker layer deposited when cells stopped growing and play reinforce functions like forming vessel or fiber cells (Fangel et al., 2012; Miedes et al., 2014).

1. Primary cell walls

Primary cell walls are synthesized during growth and have been formed by three interconnected networks which create thin, pliant, highly hydrated structures (Fig. I-1) (Cosgrove and Jarvis, 2012). The first network contains cellulose microfibrils cross-linked with hemicelluloses (Pauly et al., 2013; Park and Cosgrove, 2015). These microfibrils are tightly interconnected *via* hemicelluloses, this network being embedded in a second network enriched in pectic polysaccharides (Andème-Onzighi et al., 2000; Gibson, 2012; Malinovsky et al., 2014). These pectins are also cross-linked with structural proteins from the hydroxyproline-rich glycoproteins (HRGPs) family such as extensins and arabinogalactan proteins (AGPs) (Carpita and McCann, 2000; Nguema-Ona et al., 2013b; Tan et al., 2010; Miedes et al., 2014). Depending on the plant species, the amounts of each component present in the cell wall might

differ and will be clarified in the following section. Generally, primary cell walls of dicotyledonous plants contain mostly 30–50% pectic polysaccharides, followed by 20–30% hemicelluloses (xyloglucans), 15–40% cellulose (Cosgrove and Jarvis, 2012; Joseleau et Pérez, 2016), and 10-15% proteins (Nguema-Ona et al., 2014). In the monocotyledonous plant species such as grasses, studies have shown that their primary cell walls are composed of approximately 20–40% hemicelluloses including mixed-linkage glucans (MLGs) characteristic of the Poaceae family, 20–30% cellulose, and 5–10% pectins (Cosgrove, 1997; Vogel, 2008; Scheller and Ulvskov, 2010).

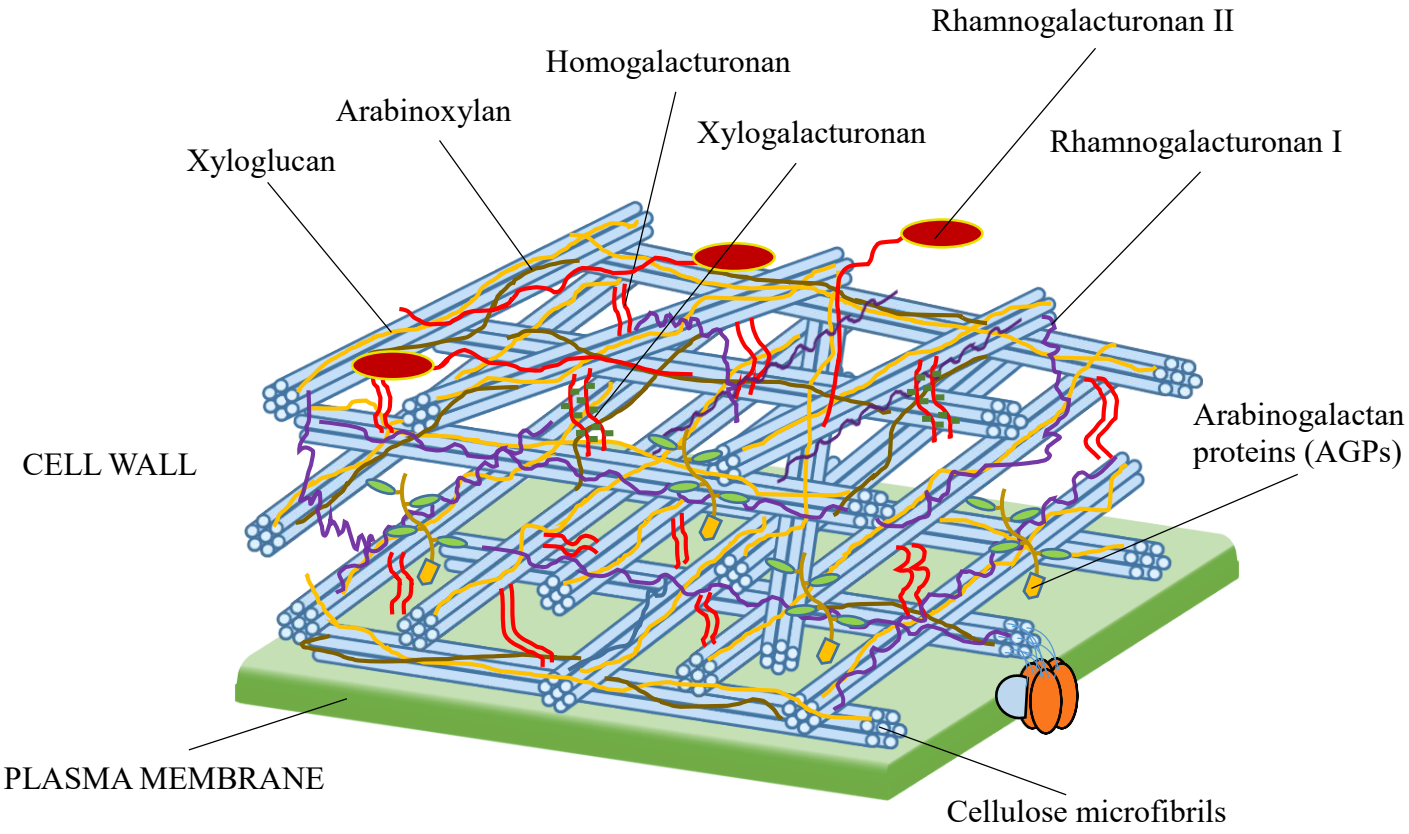

Figure I-1. Structure and composition of the primary wall of plants.

Hemicellulosic compounds including xyloglycan, arabinoxylan and mixed linkage β-glucans, bind to the surface of the cellulose microfibrils. Pectins form a hydrated gel between the cellulose-hemicellulose network and consists of four pectin domains: homogalacturonan (HGA), xylogalacturonan (XGA), rhamnogalacturonan I (RGI), and rhamnogalacturonan II (RGII). Arabinogalactan proteins (AGPs) are interlinked with pectins and can be anchored to the plasma membrane. Modified from Cosgrove (2005) and Lampugnani et al. (2018).

2. Secondary cell walls

Secondary walls are not present in all plant cells. However, in both leaves and stems of grasses, the secondary cell walls comprise at least 50% of the cell wall mass (Jung, 2003).

Secondary cell walls are the additional layers deposited between the primary cell wall and plasmalemma when cells stopped growing (Joseleau and Pérez, 2016). These cell walls are not extensible but provide rigidity and thickness thus allowing plants to grow upright, and transport water efficiently (Dupuy et al., 2010). The major components of these cell walls are cellulose, hemicellulose such as xylan, and lignin (Cosgrove and Jarvis, 2012; Loix et al., 2017). Among all of them, the complex polyphenolic network of lignin plays a principal role to provide strength and rigidity in plant tissues, especially in the walls of the xylem vessels, fiber cells of woody tissues, and sclerenchyma (Alberts et al., 2002; Vogel, 2008; Wang et al., 2013). Like the primary wall, the proportion of these polymers also show variations between cell types and species (Kumar et al., 2016). Typical secondary cell walls are composed of cellulose (40–80%), hemicellulose (10–40%), lignin (5–25%), and cell wall proteins (Kumar et al., 2016). Studies have shown that a higher proportion of cellulose and less pectic polysaccharides are present in the secondary wall as compared to primary wall (Pattathil et al., 2015). Moreover, the major hemicellulose which is xylan has a different structure in dicots and grass secondary cell walls (Vogel, 2008; Gao et al., 2020). In addition, the abundantly distribution of rhamnogalacturonan I (RG I)-associated epitopes, as well as galactan and arabinan epitopes are found over the secondary wall of mature flax fibers (His et al., 2001; Gorshkova and Morvan, 2006).

3. Plant cell wall distinction between eudicots and grasses

Based on the significant compositional differences, primary cell walls of flowering plants have been classified into two types: type I and II (Fig. I-2) (Carpita and Gibeaut, 1993; Carpita, 1996). The main component present in both types of plant cell walls is cellulose microfibrils (Yulia and Yusriana, 2006).

The type I primary wall is present in all dicots, gymnosperms, and non-commelinoid monocot plants such as aroids, alismatids, and lilioids (Carpita and McCann, 2000; Fry, 2004; Yokoyama and Nishitani, 2004; Yulia and Yusriana, 2006; Vogel, 2008). *Arabidopsis thaliana* and *Brassica napus* are perfect representative models for the type I wall. Apart from cellulose, type I wall is predominantly composed of hemicellulose xyloglucan (XyG) with the matrix of pectin and comprises two fundamental polymers, homogalacturonan and rhamnogalacturonan I (RG-I) (Carpita and McCann, 2008). Besides that, some hydroxyproline-rich glycoproteins (HRGPs)

are also present as extensins, proline-rich proteins (PRPs), glycine-rich proteins (GRPs), and arabinogalactan proteins (AGPs) (Carpita and McCann, 2000; Yokoyama and Nishitani, 2004).

The type II primary wall, found only in the commelinoid monocots (e.g. grasses, sedges, rushes, and gingers), contain cellulose microfibrils encased in hemicellulose consisted mostly of glucuronoarabinoxylan (GAX) (Nishitani and Nevins, 1991, Carpita and Gibeaut, 1993), and small proportions of pectin, xyloglucans and structural proteins (Carpita, 1996; Yokoyama and Nishitani, 2004; Harris, 2006). In addition, the cell walls of grasses (family Poaceae – e.g. *Lolium perenne*) and some related families in the order Poales contain significant quantities of β-(1,3),(1,4)-D-glucans (mixed linkage β-glucans - MLG) (Smith and Harris, 1999). Moreover, the GAXs are largely cross-linked by the phenylpropanoid network when cells stop expanding to reinforce the wall into the final shape (Iiyama et al. 1990; Carpita, 1996). The presence of phenolic compounds like ferulic and *p*-coumaric acid esterified with arabinosyl residues of GAX is also reported in grasses cell walls (Ishii, 1997; O'Neil et al., 2004; Penning et al., 2019).

Besides, the plant cell-wall loosening proteins which involve in cell wall expansion and various abiotic stresses including α-expansins and β-expansins have been found but the number of β-expansins in the monocotyledonous is much greater than dicotyledonous plants (Zhu et al., 2014; Han et al., 2019).

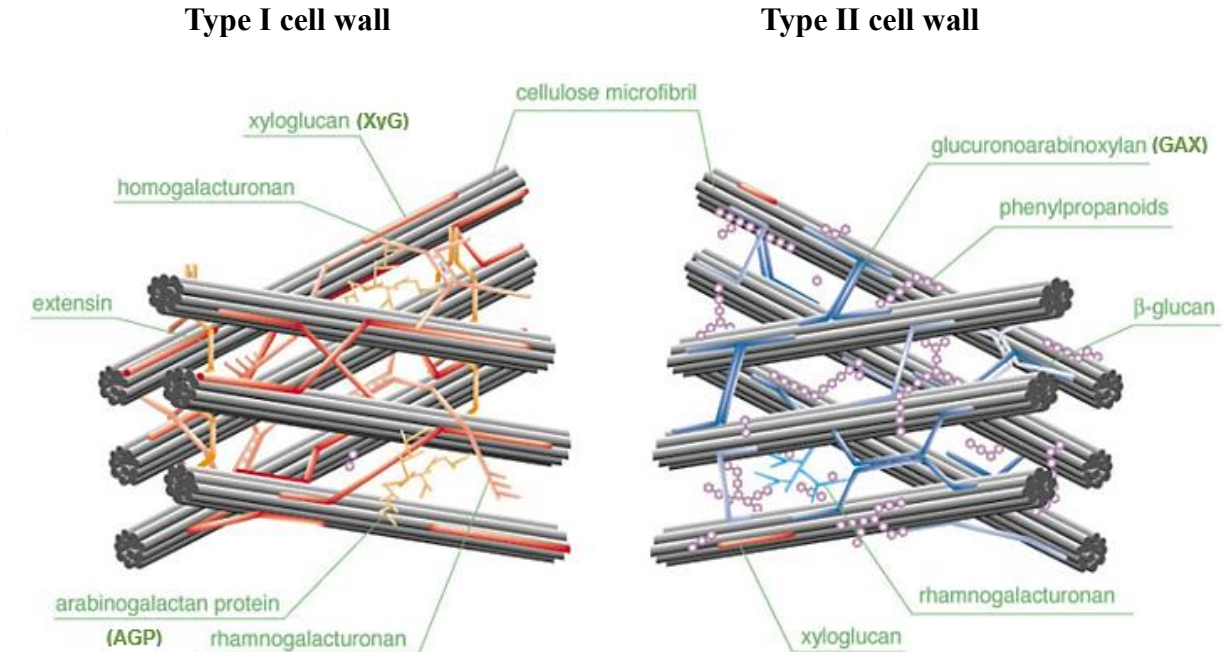

Figure I-2. The model of type I and type II primary walls.

These models are presented in Arabidopsis thaliana and rice (Oryza sativa) cell walls, respectively. From Yokoyama and Nishitani (2004).

As mentioned previously, the secondary walls of dicots and grass are composites mainly of cellulose, xylan, and lignin (Fig. I-3). Interaction of these three polymers occurs mainly through xylans (Kang et al., 2019). Interestingly, further study showed that members from both eudicots and grasses synthesize mannan and glucomannan (Liepman et al., 2007).

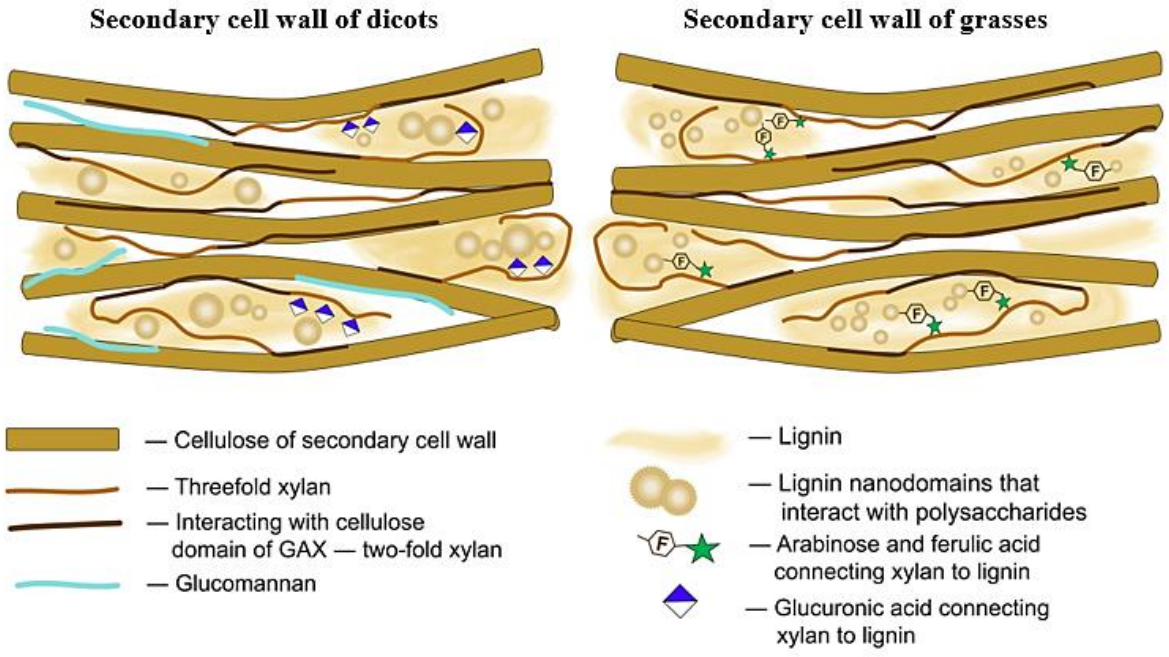

Figure I-3. Composition of secondary cell wall of eudicots and grasses.
Modified from Kozlova et al. (2020).

The approximate composition (% dry weight) of typical eudicot and grass primary and secondary cell walls are resumed in Table I-1.

Table I-1. Approximate composition (% dry weight) of typical eudicot and grass primary and secondary cell walls.

Modified from Vogel (2008).

Cell wall component	Primary wall		Secondary wall	
	Dicot	Grass	Dicot	Grass
Cellulose microfibrils	15–30[c,d,e]	20–30[b,c]	45–50[c]	35–45[c,f]
Hemicelluloses				
Xyloglucan (XyG)	19–25[g,j]	1–5[c,d,g]	Minor [a,k]	Minor [a,k]
Glucuronoarabinoxylan (GAX)	4-5[e,j]	20-40[a,i]	Unknown [i]	40-50[i]
MLG	Absent [a]	10–30[d]	Absent [a]	Minor [a]
Xylans	5[c]	20–40[d]	20–30[c,g]	40–50[c,g]
Mannans and glucomannans	5–10[d]	Minor [a,i]	3–5[g]	Minor [a,i]
Pectins	20–35[d]	5-10[c,h]	0.1[c]	0.1[c]
Structural proteins	10[d,e]	1[d]	Minor [a]	Minor [a]
Ferulic acid and p-coumaric acid	Minor (except order Caryophyllales) [a]	1–5[c,d]	Minor (except order Caryophyllales) [a]	0.5–1.5[c]
Lignin	Minor [a]	Minor [a]	7–10[c]	20[c]

a Numbers in this table were taken from several sources to provide rough approximations of generalized cell wall composition from typical dicots and grasses. Some of the numbers are averages or ranges based on multiple sources (Vogel, 2008).
b (Mitchell et al., 2007)
c (Ishii, 1997)
d (O'Neil and York, 2003)
e (Zablackis et al., 1995)
f (Hatfield et al., 1999)
g (Ebringerová et al., 2005)
h (Scheller and Ulvskov, 2010)
i (Joseleau and Pérez, 2016)
j (Darvill et al., 1980)
k (Carpita and Gibeaut, 1993)

4. Cell wall composition and biosynthesis

As illustrated in Fig. 2 and 3, the plant cell wall is a complex and dynamic structure, where the various components fulfilled a diverse array of functions throughout the plant lifecycle. Here, I will only focus on the main components of dicot and grass cell walls related to my research topic.

(a) Cellulose

Cellulose is the most abundant water-insoluble polymer found in nature. Whether primary or secondary, the plant cell walls are built on the cellulose network organized around the cellulose microfibril units (MF) (Joseleau and Pérez, 2016). Cellulose consists of β-(1,4) linked D-glucose units that make up long and rigid microfibrils, which become interconnected by hemicelluloses and pectins and thus formed the load-bearing structures in the walls (Fig. I-4) (Nishiyama, 2009; Lampugnani et al., 2018). Cellulose accounts for 15–30 % dry weight of the primary cell wall and up to 35-50 % of the secondary walls (Zablackis et al., 1995; Ishii, 1997). This linear polymer is synthesized by the plasma membrane-localized cellulose synthase

complexes (CSCs) consisting of plant cellulose synthase (CESA) proteins organized in a rosette shape either in primary or secondary cell wall (Lerouxel et al., 2006; Gigli-Bisceglia et al., 2020). There are two phases of cellulose present in the plant cell walls: crystalline cellulose which is highly ordered and paracrystalline cellulose which lack high degree of hydrogen bonding, thus giving it a dynamic and malleable structure while facilitating the privileged link with the hemicelluloses (Park and Cosgrove, 2015).

Celluloses from primary cell walls have low degree of crystallinity and less ordered regions (Thomas et al. 2013, Cosgrove, 2014). In contrast, celluloses from secondary cell walls have much higher crystallinity and may aggregate into larger ordered structures (Park and Cosgrove, 2015).

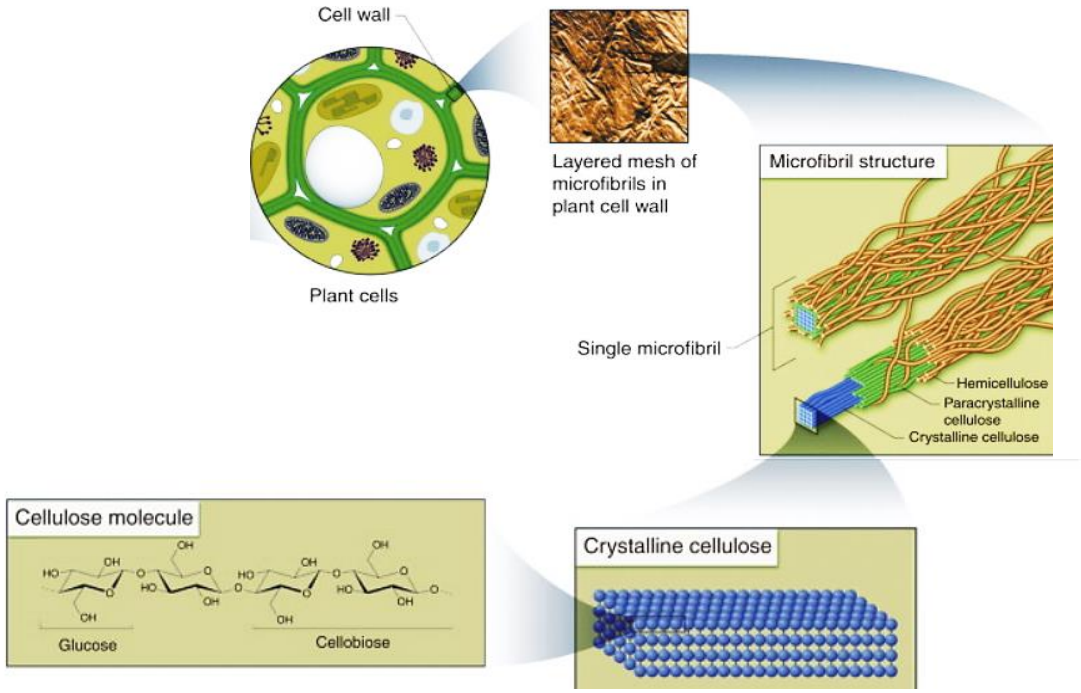

Figure I-4. Association of cellulose molecules in the plant cell wall. .
From Heinze and Liebert (2012).

(b) Hemicelluloses

Unlike cellulose which is a homogeneous polysaccharide, hemicelluloses are heterogeneous branched polysaccharides composed of β-(1,4) linked sugar backbones in an equatorial configuration (Scheller and Ulvskov, 2010). While CESA proteins are involved in cellulose biosynthesis, the family of cellulose synthase like (CSL), which includes eight other gene families, named CslA to CslH, are considered to be good candidates for the synthesis of the

backbone of hemicellulose that is localized in Golgi apparatus. Hemicellulosic polymers are synthetized in Golgi stacks and then delivered to the cell wall by exocytosis (Richmond and Sommerville, 2000; Cosgrove, 2005; Lampugnani et al., 2018).

Studies show that the CslF and CslH families are unique to the grasses whereas CslB and CslG are unique to the dicots (Vogel, 2008). This specialization leads to produce different classes of hemicelluloses including xyloglucans, xylans, mannans, and glucomannans, and β-(1,3),(1,4)-glucans (Scheller and Ulvskov, 2010). The presence and proportion of each class vary according to species, organs, and even cell types (Pauly et al., 2001; Schultink et al, 2014).

The major hemicelluloses in dicot species are the xyloglucans (XyGs) (Fig. I-5), composed of β-(1,4)-linked glucose residues that have α (1,6)-linked xylosyl side chains (Lampugnani et al., 2018). Recent data have shown that xyloglucan plays an important role in the interaction with cellulose, which allows conveying biomechanical stability to the wall, especially on the distinct regions along the microfibril, referred to as hotspots (Park and Cosgrove, 2015). The biosynthesis of xyloglucan requires glycosyltransferases including α-1,6-xylosyltransferase, β-1,2-galactosyltransferase and α-1,2-fucosyltransferase activities responsible for the addition of xylose, galactose and fucose residues to the side chains within the Golgi compartments (Chevalier et al., 2010).

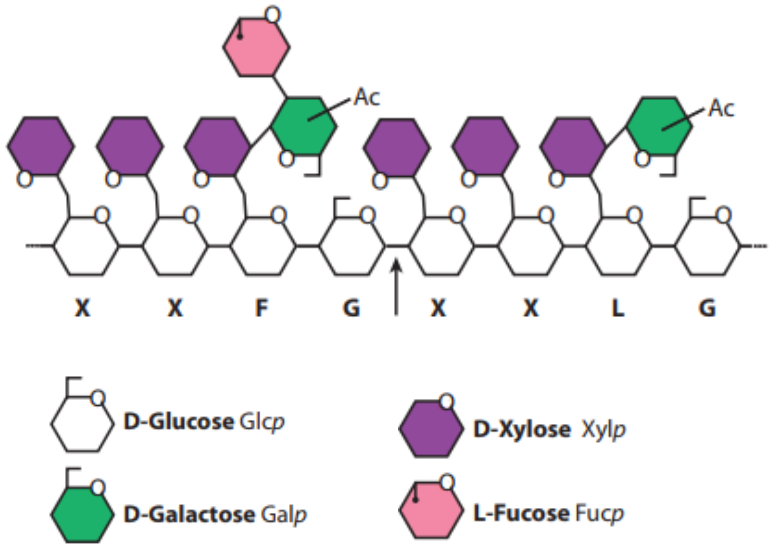

Figure I-5. Xyloglucan [β-D-Glcp-(1 4)]n backbone substituted with side chains as seen in pea and Arabidopsis. .

The arrow indicates the typical β-glucanase cleavage site. "Ac" stands for acetyl groups. From Scheller and Ulvskov (2010).

In addition, xylans are major noncellulosic polysaccharides of plant cell walls after cellulose and are mostly present in secondary cell walls. The backbone of xylan is composed of β-(1,4)-linked xylose residues which can be decorated with, for example, glucuronic acid to produce glucuroxylan (Pauly et al., 2013). Their role is similar to XyGs in primary walls, can also cross-link cellulose microfibrils (Simmons et al., 2016). Xylan biosynthesis seems to also occur in the Golgi based on localization data for the family of GT43 glycosyltransferases (Saulnier et al., 1995). The GT43 proteins have been implicated in the synthesis of xylan backbones during secondary cell wall formation in *Arabidopsis* (Faik, 2010).

In grass cell walls, glucuronoarabinoxylan (GAX) is the major hemicellulose and is composed of a β-(1,4)-linked xylose backbone with single arabinose (Ara*f*) and glucuronic acid (GlcA*p*) or methylglucuronic acid (MeGlcA*p*) side chains primarily attached at the O-3 and O-2 positions, respectively (Fig. I-6) (Vogel, 2008; Scheller and Ulvskov, 2010). The Ara*f* residues of GAX in Poaceae primary and secondary cells walls are often esterified with ferulic or coumaric acids (Buanafina, 2009). Like XyG, GAX is synthesized within Golgi stacks and transported to the cell surface in secretory vesicles (Yulia and Yusriana, 2006).

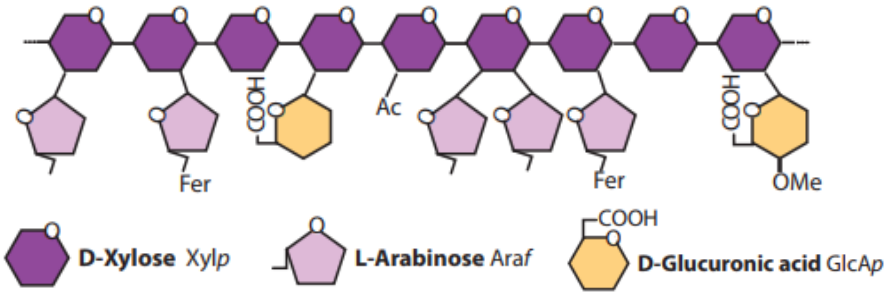

Figure I-6. Glucuronoarabinoxylan (GAX) typical of commelinid monocots.

"Ac" stands for acetyl groups; "Fer" represents esterification with ferulic acid (3-methoxy-4-hydroxycinnamic acid), which is characteristic of xylans in commelinid monocots and "OMe" represents the O- methyl group. From Scheller and Ulvskov (2010).

Moreover, β-(1,4)-linked glucans with interspersed β-(1,3)-glucosyl linkages are well known in grasses (Fig. I-7). In general, MLGs are dominated by cellotriosyl (DP3) and cellotetrasyl (DP4) units linked by β-(1,3) linkages, but longer β-(1,4)-linked segments also occur (Stone and Clarke, 1992; Scheller and Ulvskov, 2010). The MLGs are a key distinguishing feature of the grasses in which they are distributed almost exclusively within the Poaceae since they have not been found in dicots (Fry et al., 2008; Fincher, 2009). CslF and CslH family members are the groups of proteins that synthesize this polymer (Burton et al., 2006; Doblin et al., 2009). In fact, the expressing rice CslF6 can target the plasma membrane (PM) suggests a PM location for the synthesis of MLG by CslF6 (Wilson et al., 2015). Their presence extensively in primary walls of coleoptiles and found in the secondary walls of mature stems of rice, suggesting that they may have a structural and mechanical role (Vega-Sanchez et al., 2013; Joseleau and Pérez, 2016).

Besides that, the mannans and the glucomannans have been found in dicot cell walls. The skeleton of mannans is formed by a succession of β-(1,4)-linked mannose residues, whereas the glucomannans are organized into a β-(1,4)-linked D-glucose and D-mannose backbone. Mannans and glucomannans are often acetylated (Scheller and Ulvskov, 2010). Mannans have been studied mainly for their role as reserve polysaccharides in seeds (Dhugga et al., 2004), but they are also present in varying amounts throughout the cell wall (Schröder et al., 2009; Ropitaux et al. 2020). Glucomannans are presented in minor quantities in the primary walls of dicots and grasses (Joseleau and Pérez, 2016).

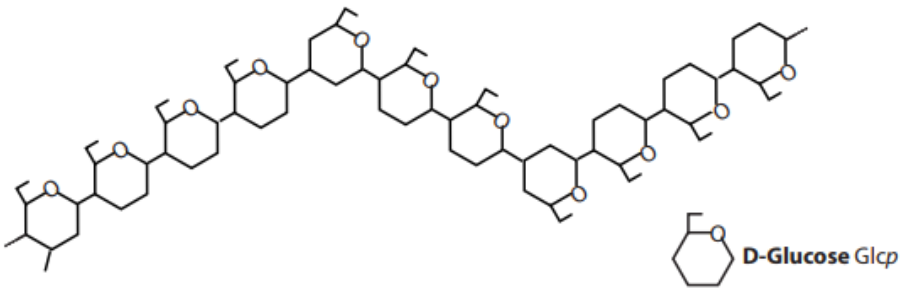

Figure I-7. Mixed linkage β-glucan.

[β-D-Glcp-(1 4)]n-β-D-Glcp-(1 3)-[β-D-Glcp-(1 4)]m, where n and m are 3 or 4; typical of Poales. From Scheller and Ulvskov (2010).

(c) Pectins

Pectins are heterogeneous group of complex polysaccharides in plant cell walls (Scheller and Ulvskov, 2010). They are rich in galacturonic acid (GalA), approximately 70%, that can form a gel-like configuration. All the pectic polysaccharides contain galacturonic acid linked at the O-1 and the O-4 position (Mohnen, 2008; Palin and Geitmann, 2012). They are synthesized in the Golgi and inserted into the extracellular matrix by vesicle-mediated exocytosis (Yulia and Yusriana, 2006). Pectins are negatively charged, and can bind to Ca^{2+}, forming a hydrogel network that stabilizes the cell wall (Tan et al., 2013). Pectins consist of four polysaccharide domains: homogalacturonan (HG), xylogalacturonan (XGA), rhamnogalacturonan I (RGI), and rhamnogalacturonan II (RGII) (Fig. I-8). Approximately 67 glycosyltransferase, methyltransferase, and acetyltransferase activities might be required for pectin synthesis (Mohnen, 2008).

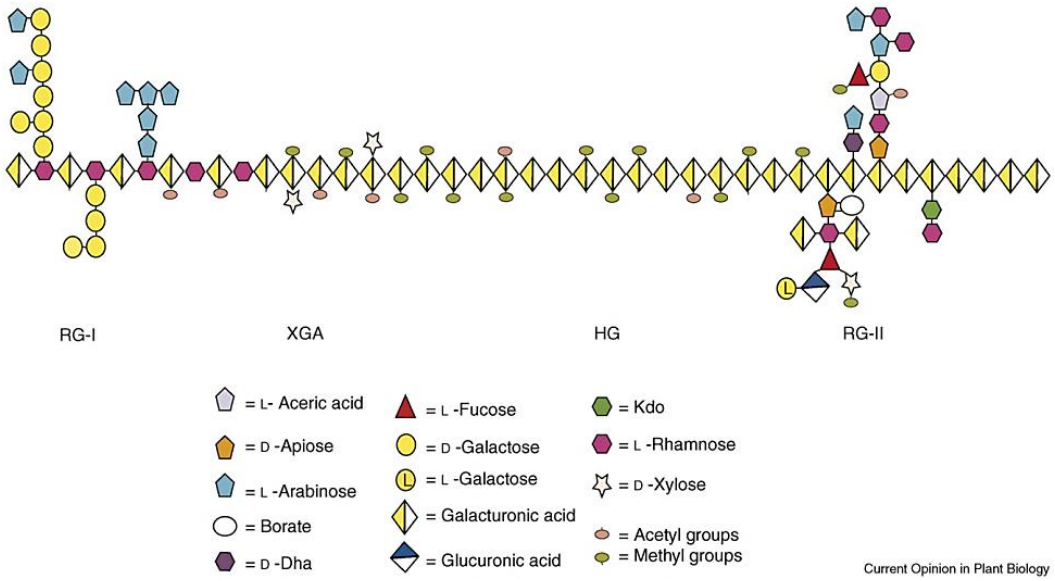

Figure I-8. Schematic structure of pectin showing the four pectic polysaccharides.

Homogalacturonan (HG), xylogalacturonan (XGA), rhamnogalacturonan I (RG-I) and rhamnogalacturonan II (RG-II) linked to each other. The representative pectin structure shown is not quantitatively accurate, HG should be increased 12.5-fold and RG-I increased 2.5-fold to approximate the amounts of these polysaccharides in walls. From Mohnen (2008).

Homogalacturonans (HGs) are the most abundant pectic polysaccharide of primary walls, formed by agalacturonic acid (GalA) chains linked in α-(1,4) with a degree of polymerization of 100/150 residues and form the main backbone of pectins (Coenen et al., 2007). The homogalacturonan parts of the polymer are referred to as 'smooth' regions of pectin (Pérez et al., 2000). Several GalA residues within the backbone may have their carboxyl group at C-6

methyl esterified and may be acetyl esterified at O-2 and/or O-3 positions, depending on the plant origin (O'Neill et al., 1990). HGs with more than 50% methyl esterified residues are known as high methyl-esterified HGs (Joseleau and Pérez, 2016). The carboxyl groups of the HGs chains vary in their degree of methyl esterification which influences their ability to form a gel upon addition of gelling agents such as Ca^{2+} (Proseus and Boyer, 2007). HGs with low degree of methyl esterification can be crosslinked by these ions, resulting in a matrix with increased rigidity (Palin and Geitmann, 2012).

Xylogalacturonan (XGA) is a polymer of α-D-galacturonic acid, highly substituted with *O*-3-β-D-xylose (Jensen et al. 2008). XGA is found in seeds, root cap cells and mucilage of *A. thaliana* root (Zandleven et al., 2007; Durand et al., 2009; Mravec et al., 2017). XGA was reported to confer enhanced resistance to degradation by endopolygalacturonases produced during pathogen attack (Jensen et al., 2008).

Rhamnogalacturonan-I (RG-I) consists of alternating residues of galacturonic acid and rhamnose, has additional side chains containing individual, linear, or branched α-L-Araf and β-D-Galp residues (Fig. I-8) (Mohnen, 2008; Palin and Geitmann, 2012). RG-I represents 20–35% of pectin. The 10% of pectin makes up of rhamnogalacturonan-II (RG-II) which is a complex pectin domain that contains 11 different sugar residues and forms dimers through borate esters (Fig. 9) (Caffall and Mohnen, 2009; Jarvis, 1984). Data indicated that mutations causing even minor modifications to RG-II structure will lead to reduced RG-II dimer formation and severe growth defects such as dwarfism, suggests that the dimerization of RG-II in the wall is crucial for normal plant growth and development (Mohnen, 2008).

(d) The HRGPs (Hydroxyprolin Rich GlycoProteins)

In addition to other polysaccharides, plant cell walls are also composed of proteins and glycoproteins, which generally comprise less than 10% of the dry weight of the primary wall (Bacic et al., 1988). These complex components are known to be implicated in the maintenance of the physical and biological functions of the plant extracellular matrix, and have been suggested to be involved in recognition and signaling (Showalter, 1993; Johnson et al., 2003). as arabinogalactan proteins (AGPs), proline-rich proteins (PRPs), hydroxyproline-rich glycoproteins (HRGPs), or extensins have been identified (Showalter, 1993).

In this manuscript, I will focus on hydroxyproline-rich glycoproteins (HRGPs) belonging to the group of cell wall glycoproteins, including arabinogalactan proteins (AGPs) and extensins (EXTs). AGPs are known as a large heterogeneous family of HRGPs found both within the cell

and on the surface of plant cells (Fincher et al., 1983; Nguema-Ona et al., 2012). They typically bound to the plasma membrane through a glycosylphosphatidylinositol (GPI) anchor (Marzec et al., 2015). In general, AGPs are soluble and highly glycosylated (Showalter and Varner, 1989).

These proteins are characterized by being rich in proline/hydroxyproline residues in their backbone with the surrounding amino acids such as alanine (A), serine (S), threonine (T), and the large branched-glycan chains accounting for about 90% of their total mass (Fig. I-9) (Ellis et al., 2010; Nguema-Ona et al., 2013b; Ma et al., 2018). Glycosyl residue analysis showed that the glycan part mainly included β-(1,3)-galactose, but also of β-(1,6)-galactose and α-(1,3)-linked, α-(1,5)-linked, or β-(1,3)-linked arabinoses (Nothnagel, 1997; Showalter, 2001; Nguema-Ona et al., 2013b).

AGP glycosylation is initiated by the action of hydroxyproline O-β-galactosyltransferase (GalT), which places the first galactose residue onto hydroxyproline residues in AGP protein backbone. Eight genes encoding this activity are known including GALT2, GALT3, GALT4, GALT5, and GALT6 (Basu et al., 2013, 2015a, b). The other three Hyp-*O*-galactosyltransferase (HPGT) genes were found by sequencing proteins selected by affinity chromatography with an AGP peptide and by heterologous expression coupled with an enzyme assay and by genetic mutant analysis, named HPGT1, HPGT2, and HPGT3 (Ogawa-Ohnishi and Matsubayashi, 2015). These genes form two small gene families within GT31 (Tan et al., 2012; Showalter and Basu, 2016).

Specific sets of hydroxyproline *O*-β-Gal-T such as β-(1,3), β-(1,6)- galactosyltransferase; α-(1,3),α-(1,5)-arabinosyltransferase (Ara-T), β-glucuronosyltransferase (GlcAT), and α-(1,2)-fucosyltransferase (Fuc-T) would be also required for the glycosylation of AGPs (Wu et al., 2010; Nguema-Ona et al., 2014; Showalter and Basu, 2016). It was reported that AGP glycosylation mainly occurs in Golgi (Oka et al., 2010; Basu et al., 2013; Showalter and Basu, 2016).

AGPs are synthesized in almost all root cell types including epidermal, cortical, absorptive hair cells of all species studied, but also in the living root border cells/border-like cells (BCs/BLCs). AGPs are present in the root cap mucilage, root exudates and are secreted into the rhizosphere (Hawes et al., 1998, 2000; Durand et al., 2009; Cannesan et al., 2012; Nguema-Ona et al.,

2013b). However, the structure and composition of AGPs vary among species and conditions, reflecting the diversity of their functions including embryogenesis, pollen tube orientation, cell growth, cell proliferation, pattern formation, and reproduction (Showalter, 2001; Borderies et al., 2004; Seifert and Roberts, 2007; Ellis et al., 2010; Goellner et al., 2013; Duchow et al., 2016). In addition, AGPs have been implicated in defense response to various biotic and abiotic stresses (Nguema-Ona et al., 2012; 2013b; Pereira et al., 2015). The detection of AGPs in tissues has been facilitated by using the specific monoclonal antibodies (mAbs) and the β-D-glucosyl Yariv reagent (β-Glc Yariv), which specifically binds and precipitates AGPs (Yariv et al., 1967; Kitazawa et al., 2013).

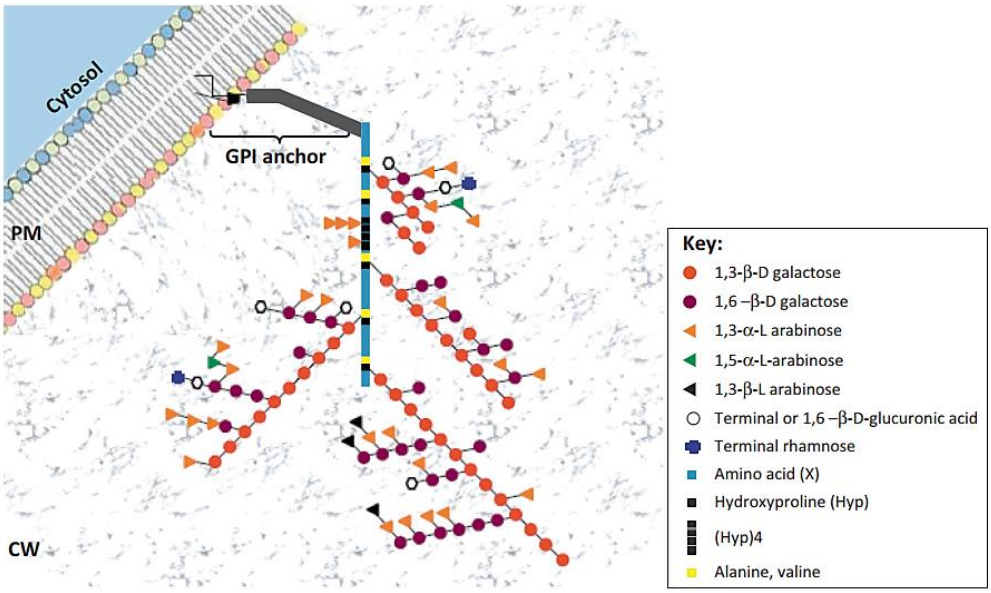

Figure I-9. Structure of arabinogalactan proteins (AGPs) .

They are heavily glycosylated cell wall proteins and their glycans predominantly consist of arabinose and galactose. Minor sugars, such as glucuronic acid or rhamnose, are also present. The backbone of the protein is enriched in hydroxyproline residues. AGPs can be anchored to the plasma membrane via a glycosylphosphatidylinositol (GPI) anchor. Note the high heterogeneity in the structure of the glycan chains. From Nguema-Ona et al. (2013b).

As mentioned previously, extensins (EXTs) also belong to HRGPs found in the cell walls of higher plants. Their structure is rich in hydroxyproline and serine with the repeating of pentapeptide sequences characteristic of a serine followed by hydoxyproline $Ser(Hyp)_4$ then are O-glycosylated with one to four arabinosyl residues and with a single galactose unit (Kieliszewski and Lamport, 1994; Velasquez et al., 2015; Hijazi et al., 2014; Showalter and Basu, 2016; Dehors et al., 2019). The hydrophobic part, on the other hand, will be characterized by the combination of the amino acids such as Valine-Tyrosine-Lysine or Tyrosine-X-Tyrosine sequences (X = Tyrosine, Lysine) which will be the site of "cross-linking" (Fig. I-10) (Showalter et al., 1993; Lamport et al., 2011; Velasquez et al., 2012).

EXTs synthesis starts in the ER and continues in the Golgi (Basu et al., 2013; Knoch et al., 2014) (Figure 11). In the ER, proline residues are hydroxylated to hydroxyprolines (HyP) by prolyl-4- hydroxylases (P4Hs) (Velasquez et al., 2011; Fragkostefanakis et al., 2014), followed by the insertion of a galactose residue as an α-(1,4) on a serine by serine galactosyltransferase 1 (SGT1) (Saito et al., 2014). Subsequently, in the Golgi apparatus, several arabinoses will be successively grafted onto the Hyp residues using the enzymes shown in Figure 11. In the cell wall, EXTs play an important role in development, and cross-linking of EXTs is generally associated with cell expansion and growth since several studies show that EXT-related mutants have shorter root hairs (Cannon et al., 2008; Ringli, 2010; Lamport et al., 2011; Velasquez et al., 2011; Johnson et al., 2017).

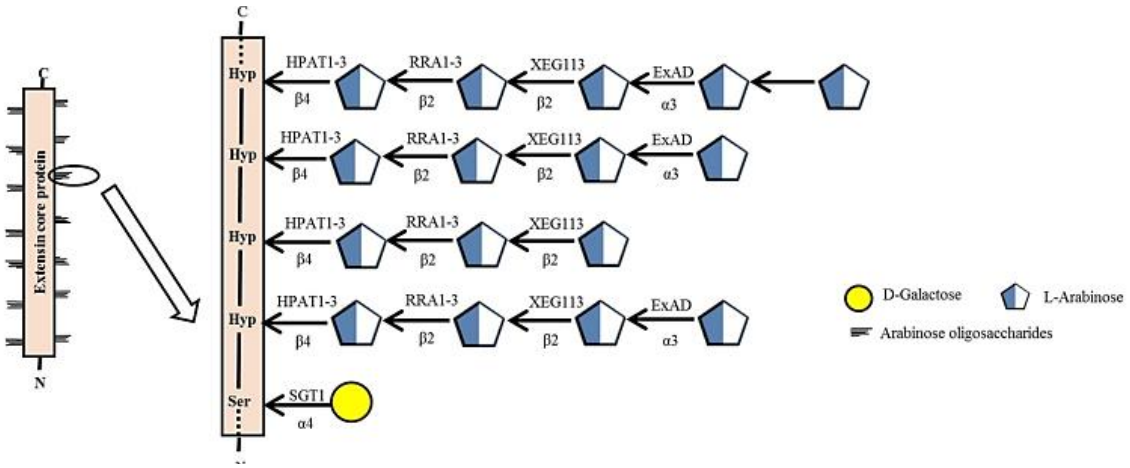

Figure I-10. Classical structure of extensins complemented by the enzymes responsible of their formation.

Proline (Pro) residues are first hydroxylated to hydroxyprolines (Hyp) by Prolyl-4-Hydroxylases (P4Hs). A D-galactose unit is then transferred to the serine residue (Ser) and several arabinosyl residues are transferred to the Hyp residues. The type of binding and enzymes involved in the glycosylation of extensin are indicated. SGT1: Serine GalactosylTransferase 1; HPAT1-3: Hydroxyproline ArabinosylTransferase 1 to 3; RRA1-3: Reduced Residual Arabinose 1 to 3; XEG113: XyloEndoGlucanase 113; ExAD: Extensin Arabinose Deficient transferase. From Showalter and Basu (2016).

5. Role of the cell wall in root defense

The plant cell wall is a natural barrier whose composition and organization vary significantly due to its essential functions at the levels of the cell and of the whole plant. At first, it plays a morphological role providing a physical barrier to maintain cell shape, resists internal turgor pressure, regulates cell differentiation and growth, and mediates bio-molecule transit (Knox, 2008; Collinge, 2009; Xia et al., 2014).

In addition, the cell wall is the first cell structure on which interactions between plants and a wide range of other organisms, including insects, nematodes, pathogenic or symbiotic micro-organisms. It is highly dynamic and can be the source of oligosaccharide fragments that have hormone-like action, especially in defense mechanism against pathogen infection, inducing reaction against the attack (Bellincampi et al., 2014).

Most of researches are dedicated to defense mechanisms involving leaf-pathogen interaction. Due to the general inaccessibility of root, the role of root cell wall components during root-infecting pathogen invasion still needs to be elucidated (Chuberre et al., 2018). The inducible defenses were evoked by wounding, elicitors, and pathogens which lead to the transcriptional activation of genes encoding proteins involved in defense mechanism (Lamb et al., 1989; Bradley et al., 1992).

The presence of an extracellular glycoprotein was found in the intercellular spaces of legume roots and nodules, and nodule-infection threads (Vandenbosch et al., 1989). Since, several studies have reported the potential involvement of EXTs in the attachment of *Rhizobium leguminosarum* to legume root nodules which were detected by the presence of LM1 epitopes (associated with extensins) in infected nodules (Reguera et al., 2010; Sujkowska-Rybkowska and Borucki, 2014). EXTs were also shown to accumulate in roots interacting with pathogenic microbes (Velasquez et al., 2011, 2012; Xie et al., 2011; Hirao et al., 2012). In roots of *A. thaliana* and *Linum usitatissimum* (flax), following elicitation by bacterial flagellin 22 (flg22), LM1 labeling almost completely disappeared which could be explained by a significant reorganization of EXTs containing LM1 epitopes, making them inaccessible to the antibody in cell-wall (Plancot et al., 2013; Castilleux et al., 2018). This result proposed that extensins have a role in strengthening the cell wall during infection in order to limit pathogen invasion.

AGPs have also been shown to play a prominent role at the root surface during root colonization by pathogenic and symbiotic microbes (Vicré et al., 2005; Gaspar et al., 2004; Xie et al., 2012). Interestingly, pretreatment of Arabidopsis roots with β-Glc Yariv reagent caused the disruption of *Agrobacterium* attachment, which can be explained by the physical barrier built from the crosslinking of many different AGPs by β-Glc Yariv at the cell surface. This system helps to prevent the binding of the bacterium and/or entry of the T-DNA into the cell (Gaspar et al., 2004). AGPs extracted from pea root cap and root cap cells prevent *in vitro* zoospores germination of *Aphanomyces euteiches* through their “decoy” function which could attract and immobilize the oomycete. This could explain the reduced infection that is perceptible on the root cap compared to other root zones (Cannesan et al., 2012).

B. Concepts of plant immunity

Plants have developed their own way of defending pathogenic attacks which is adaptable to their lack of adaptive immune system (Henry et al., 2012). Facing potentially infectious agents, plants often rely on the innate immunity of each cell by using their physicochemical barriers of the cell wall, the first line of defense that prevents the penetration of the microorganisms or at least reduce and slow down their progression.

This is done by a rigidification of cell wall with the deposition of structural molecules such as callose or lignin (Underwood, 2012) but also the intervention of other molecules such as EXTs or AGPs as mentioned previously.

If a microorganism manages to cross these constitutive physical barriers, the second line of defense will be induced. For preventing the aggressor from growing and proliferating in infected plant tissue, the first strategy relies the recognition of elicitors by transmembrane receptors known as Pattern Recognition Receptors (PRRs). These elicitors are conserved molecular pattern originated from pathogenic microorganisms for Pathogen-Associated Molecular Patterns (PAMPs) (Dodds and Rathjen, 2010; Arraño-Salinas et al., 2018), or from various microorganisms for Microbe-Associated Molecular Pattern (MAMPs) (Boller and Felix, 2009; Newman et al., 2013). In some cases, the plant cell is also able to produce endogenous elicitors released from the degradation caused by microbes. The so-called Damage-Associated Molecular Pattern (DAMPs) includes plant cell wall fragments, oligogalacturonides (OGs), ATP, and nicotinamide adenine dinucleotide (NAD) (Darvill and Albersheim, 1984; Davidsson et al., 2013; Ferrari et al., 2013; Tanaka et al., 2014; Gust et al., 2017). Plant PRRs are often receptor-like kinases (RLKs) or receptor-like proteins (RLPs) (Boller and Felix, 2009; Schwessinger and Ronald, 2012; Böhm et al., 2014).

Several PAMPs/MAMPs/DAMPs have been widely characterized including polysaccharides such as fungal chitin (Felix et al., 1993) and oomycete glucans (Zipfel, 2008), peptides like bacterial flg22 (Gómez-Gómez and Boller, 2002); elf18 epitope of the bacterial elongation factor-Tu (EF-Tu) (Kunze et al., 2004) and peptidoglycan (PGN), lipopolysaccharide (LPS) from gram-negative bacteria (Boller and Felix, 2009), glycoproteins (Boller and Felix, 2009) and even DNA (Duran-Flores and Heil, 2017).

After detection through PRR receptors, the information is transmitted through signal transduction (Fig. I-11). This will allow the establishment of an early immune response called

PAMP-triggered immunity (PTI) or MAMP-triggered immunity (also called pattern-triggered immunity-PTI) (Jones and Dangl, 2006; Jourdan et al., 2008; Yazawa et al., 2013).

PTI includes immediate events such as the production of reactive forms of oxygen, or ROS (Reactive Oxygen Species), which play a role in both signal transduction and the early immune response (Apel and Hirt, 2004; O'Brien et al., 2012) (Fig. I-11). The oxidative burst triggers several complex mechanisms in order to act as signal molecules, enhance genes regulation or to reinforce the cell wall integrity (Durrant and Dong, 2004; Nicaise et al., 2009). Nitric oxide (NO) production, calcium Ca^{2+} influx, and induction of different protein kinases, namely MAP kinases (MAPKs) and calcium-dependent protein kinases (CDPKs) are also part of the early events of the PTI (Jones and Dangl, 2006; Ingle et al., 2006; Zhang and Zhou, 2010; Henry et al., 2012).

These defense reactions also include the synthesis of defense compounds such as low-molecular-weight secondary metabolites (phytoalexins; Hammerschmidt, 1999) and pathogenesis-related (PR) proteins including pathogen wall degrading enzymes or proteins with antimicrobial activity (van Loon et al. 2006) (Fig. I-11). Many research has shown that P/M/DAMPs activate a signaling network that includes the accumulation of defense-related phytohormones such as salicylic acid (SA), jasmonic acid (JA), and ethylene (ET) (Persello-Cartieaux et al., 2003; An and Mou, 2011; Thakur and Sohal, 2013; Caarls et al., 2015; Ramirez-Prado et al., 2018). These signaling molecules can induce systemic protection and increase the expression of PR genes in a variety of dicotyledonous and monocotyledonous plants (Shah and Klessig, 1999; Mayers et al., 2005; Atsumi et al., 2009; Makandar et al., 2010). For example, the LPS purified from *Burkholderia cepacia* inoculated on tobacco leaves (*Nicotianae tabacum*) induced an accumulation of various PR proteins and contribute to an enhanced defensive capacity in the *Nicotianae tabacum* - *Phytophthora nicotianae* interaction (Coventry and Dubery, 2001). A recent study showed that the well-known SA-responsive genes such as PR1 and WRKY70 were upregulated in rutabaga (*Brassica napus* subsp. *Napobrassica*) and rapeseed (*Brassica napus*) inoculated with *Plasmodiophora brassicae* (Galindo-González et al., 2020).

Nevertheless, PTI can in some cases be defeated by pathogens through the release of highly specific effectors activating Effector-Triggered Susceptibility (ETS). In return, the cell will not be helpless since it can recognize and counteract these effectors thanks to intracellular receptors: cytoplasmic resistance (R) proteins. This response constitutes the second strategy of the immune system by producing effector-triggered immunity (ETI) (Fig. I-11), which is similar

to PTI but faster and more specific (Pieterse et al., 2009; Jones and Dangl, 2006; Katagiri and Tsuda, 2010). By using resistance (R) proteins, ETI detect effectors called avirulence factors (Avr) from some pathogenic microorganisms (Dangl and Jones, 2001; Jones and Dangl, 2006; Henry et al., 2012). This process takes place largely inside the cell and intracellular effectors are perceived by nucleotide binding with leucine rich repeat receptors (NLRs) (Jones and Dangl, 2006; Zhou and Zhang, 2020).

ETI might lead to a hypersensitive response (HR) that is characterized by programmed cell death (Jones and Dangl, 2006; Ramirez-Prado et al., 2018; Nguyen et al., 2021) (Fig. I-11). The compatibility of the effectors and these R-proteins results from the coevolution of the plant and pathogen (Jones and Dangl, 2006; Katagiri and Tsuda, 2010; Gouveia et al., 2017).

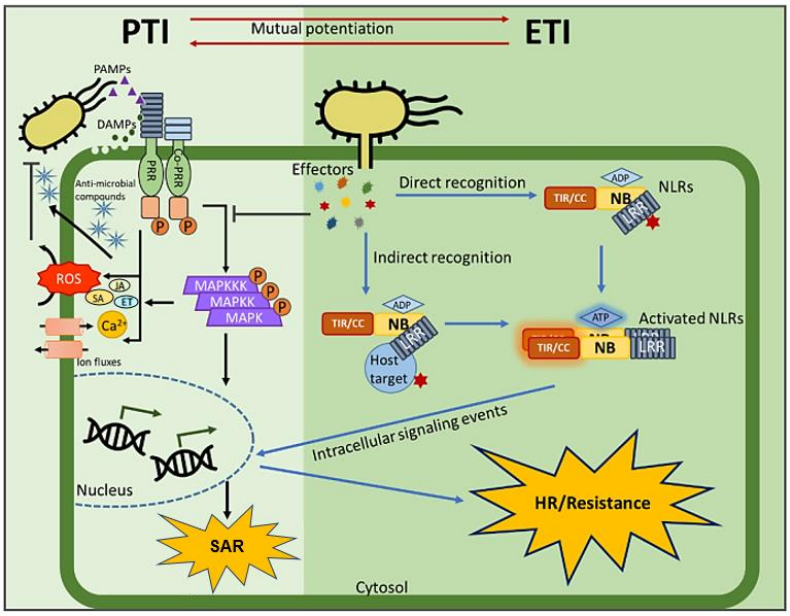

Figure I-11. Schematic view of plant defense signaling.

The first layer of induced immunity, called PTI (indicated by black arrows), is activated by the recognition of PAMPs/MAMPs or DAMPs through pattern recognition receptors (PRRs). Several PTI signaling events occur, such as activation of the mitogen-activated protein kinases (MAPK) kinase cascades, an influx of Ca2+ into the cytosol, and production of reactive oxygen species (ROS). Antimicrobial compounds are produced and the defense genes are activated. Endogenous phytohormone synthesis, such as that of salicylic acid (SA), jasmonic acid (JA), and ethylene (ET), is also induced and contributes to plant immunity. However, to suppress PTI, the pathogens deploy effectors. When they are recognized by nucleotide-binding (NB) and leucine-rich-repeat (LRR)- containing receptors (NLRs), the second immune layer, called ETI (indicated by blue arrows), takes place. NLRs directly or indirectly perceive pathogenic effectors, leading to a conformational change, which together with several intracellular signaling events, ultimately trigger the hypersensitive response (HR) and systemic acquired resistance (SAR). Surprisingly, the most recent studies reported that PTI and ETI are mutually linked and together potentiate the immune response (indicated by red arrows). Modified from Nguyen et al. (2021) and Ramirez-Prado et al. (2018).

Interestingly, recent studies revealed crosstalk and cooperation between ETI and PTI through a substantial linkage between PRR-mediated PTI and NLR-mediated ETI (Fig. I-12) (Ngou et al., 2021; Yuan et al., 2021; Nguyen et al., 2021). In two separate *Arabidopsis* mutants which lack PRR or PRR co-receptor challenged with *Pseudomonas syrinage*, it was shown that the secreted bacterial effector protein AvrRpt2 did not elicit effective ETI and a lesser leaf tissue collapse associated with hypersensitive-response7h after bacterial infiltration was observed. In contrast, in Col-0, AvrRpt2-triggered immunity was increased in response to flg22 (Yuan et al., 2021). Moreover, the absence of PRR co-receptors leads to the inactivation by phosphorylation of PTI components such as Respiratory Burst Oxidase Homologue D (RBOHD), which causes the lack of ROS production and defective ETI. Additionally, Ngou et al. (2021) found a higher accumulation of ROS in plants with co-activation of PTI and ETI compared to those with activation of PTI alone enabling a stronger immune response. These findings revealed that ETI signals through PTI and increases the accumulation of PTI signaling components such as ROS and callose production. Simultaneously, PTI also enhances ETI and is functionally essential for the ETI response (Fig. I-12A; Nguyen et al., 2021). The synergistic cooperation of PTI and ETI provides a robust immunity to confront pathogenic invasion and updates the "zig-zag" model proposed by Jones & Dangl (2006) (Fig. I-12B; Ngou et al., 2021).

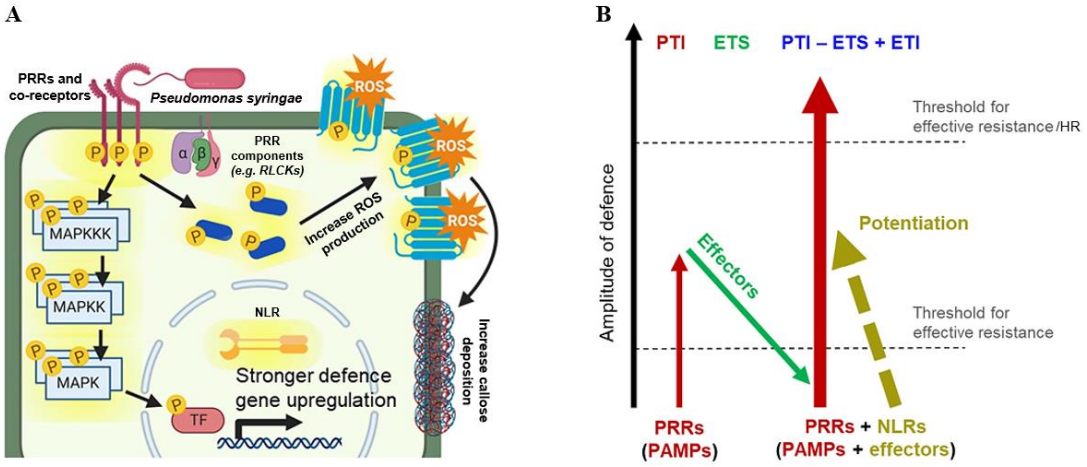

Figure I-12. Model of crosstalk and cooperation between ETI and PTI .

(A) Co-activation of both PTI and ETI (PRR and NLR) increases the accumulation of PTI signaling components (ROS production and callose deposition), enabling a stronger immune response. (B) Updated version of the 'zig-zag' model of Jones and Dangl (2006). In this scheme, the ultimate amplitude of disease resistance or susceptibility is proportional to [PTI – ETS+ETI]. In phase 1, plants detect microbial/pathogen-associated molecular patterns (MAMPs/PAMPs) via PRRs to trigger PAMP-triggered immunity (PTI) (indicated by red arrows). In phase 2, successful pathogens deliver effectors that interfere with PTI, or otherwise enable pathogen nutrition and dispersal, resulting in effector-triggered susceptibility (ETS) (indicated by green arrow). In phase 3, when one effector is recognized by an NB-LRR protein, activating effector-triggered immunity (ETI), an amplified version of PTI that often passes a threshold for induction of hypersensitive response (HR). ETI enhances PTI (indicated by yellow arrow) to produce a robust immune response. Modified from Ngou et al. (2021).

C. Plant roots: A specialized underground defense system

As the underground part of the plant, roots play a vital role in maintaining plant survival in their natural environment. Their main functions are to provide anchorage, mineral nutrition, and water uptake (Petricka et al., 2012). Moreover, the root system is the privileged zone in constant interaction with a multitude of microorganisms which play a crucial role in plant health (Berendsen et al., 2012).

Besides the beneficial microorganisms in the rhizosphere, telluric pathogens are a real threat to the plant and major actors in agricultural production losses. The fact that the roots are underground makes disease more difficult to control as compared to the aerial parts of the plant (Raaijmakers et al., 2008). Thus, the question about the defense mechanisms against pathogens has been largely investigated regarding the aerial parts whereas the knowledge regarding the root system is still scarce (Chuberre et al., 2018).

1. Specificity of root defense: Organ-specific and tissue-specific responses

Differences in plant immune responses were reported between leaves and roots and it is speculative to extrapolate data from the aerial part to the below-ground system (Balmer and Mauch-Mani, 2013). Indeed, the inoculation of the oomycete *Hyaloperonospora parasitica* at the *Arabidopsis* leaf level induces various defense responses such as an oxidative burst and a hypersensitive response (HR), whereas these responses are not detected at the root level which is inoculated with the same pathogen (Hermanns et al., 2003). A difference in transcription level between leaves and roots was also found to occur in maize attacked by *Spodoptera littoralis* on the leaves (Erb et al., 2009) and in rice after inoculation with the fungus *Magnaporthe oryzae* (Marcel et al., 2010). Furthermore, in response to *Phytophthora citrocola*, genes were shown to be differently activated between roots and leaves (Schlink, 2009).

In leaves, it has been demonstrated that the change from biotrophy to necrotrophy is followed by a switch from SA- to JA-mediated responses during infection (Glazebrook, 2005). However, the transcription level of SA- and JA- marker genes have shown a temporary accumulation during penetration of *Phytophthora parasitica* and fungus *Fusarium oxysporum* in *Arabidopsis* roots (Berrocal-Lobo and Molina, 2008; Attard et al., 2010). This difference in the antagonistic interactions of the two hormones SA and MeJA has been also reported in leaves and roots by applying the signaling compounds SA and MeJA exogenously in *A. thaliana* and the two other plants *Brassica oleracera* and *Brassica rapa* (Badri et al., 2008; Tytgat et al., 2013; Papadopoulou et al., 2018). Balmer et al. (2013) showed a late and continuous overexpression

of PR1 in leaves of maize infected by the ascomycete *Colletotrichum graminicola* while the reponse is brief and precoce in roots. The same result has been shown in rice root and leaf tissues upon *Magnaporthe oryzae* infection (Marcel et al., 2010).

Additionally, numerous studies show that plant immune response is not only organ-specific but also tissue-specific in roots (Chuberre et al., 2018). Since 2010, Millet et al. revealed that *A. thaliana* root elicited with flg22 and peptidoglycan produces a strong response with callose deposits at the elongation zone (EZ) while chitin triggers the callose deposition at the differentiation zone (DZ). At the root level, it has been shown that the elongation zone is often the preferred entry zone for pathogens such as *Arabidopsis thaliana - Phytophthora parasitica* (Attard et al., 2010) or *Pisum sativum - Aphanomyces euteiches* pathosystems (Cannesan et al., 2011). Following *A. euteiches* infection a high concentration of a phytoalexin, pisatin, in the DZ were recorded compared to other root zones (Cannesan et al., 2011).

After flg22 treatment, Ca^{2+} signals were induced in the EZ of the root and further spread across root tissues in *A. thaliana* (Keinath et al., 2015; Stanley et al., 2018). Besides that, microscopic analysis of root developmental zones by using YFP (yellow fluorescent protein) marker lines showed that early MAMP-signalling marker (*WRKY11*), ET/JA signaling marker (*HEL/PR4*), and ROS markers (*ZAT12*, *PER5*) were induced in the transition zone (TZ) and DZ of *Arabidopsis* root treated with flg22 and a plant-derived PTI elicitor AtPep1 (Poncini et al., 2017; Rich-Griffin et al., 2020).

All of these results pointed out that the strategy of invading pathogen by choosing the EZ as the major entrance site (Gunawardena and Hawes, 2002; Wen et al., 2006). Interestingly the root tip is often deprived of early infection, probably due to the presence of a defense role created by border cells (BCs) and border-like cells (BLCs) surrounding the root cap periphery and the thick mucilage at this level.

2. Root Associated, Cap-Derived Cells (AC-DCs) – The population of root border cells (BCs) and border-like cells (BLCs)

(a) Origin of BCs and BLCs in plant roots

One on the particularity of the root system is the presence of special cells at the interface between root and soil. Sloughed root cap cells release in the rhizosphere was first reported as desquamation of dead cells from the root allowing a passive release of carbon by the process of rhizodeposition (Hawes and Pueppke, 1986; Haberlandt, 1914; Lynch and Whipps, 1990).

However, their function has been revisited and these cells were renamed “root border cells” (BCs) by Hawes and Lin in 1990.

Root border cells are defined as detached cells that are released individually into the rhizosphere from the periphery of the root cap (RC) in the presence of water (Hawes et al., 2003) (Fig. I-13A). To date, the presence of BCs has been reported in more than 35 species belonging to 11 different families, with the number of BCs varying from approximately fifty in the Solanaceae to more than 11,000 in the Pinaceae (Hawes and Pueppke, 1986; Hawes et al, 2003). The production and detachment of BCs are finely regulated by both endogenous and environmental signals (Brigham et al., 1995; Gunawardena and Hawes, 2002; Driouich et al., 2007). These cells are viable and have an active metabolism with the presence of many intracellular organelles such as mitochondria, numerous Golgi stacks, vacuoles, and others, testifying to their important metabolic activity (Cannesan et al., 2011; Wang et al., 2017) (Fig. I-13B, C). However, their viability also varies according to plant species and families with more than 95% viable BCs in the Fabaceae and the Gramineae, whereas in the Solanaceae they are only between 50 and 70% viable. The BCs can remain alive for several days after detachment (Hawes and Pueppke, 1986; Plancot et al., 2013).

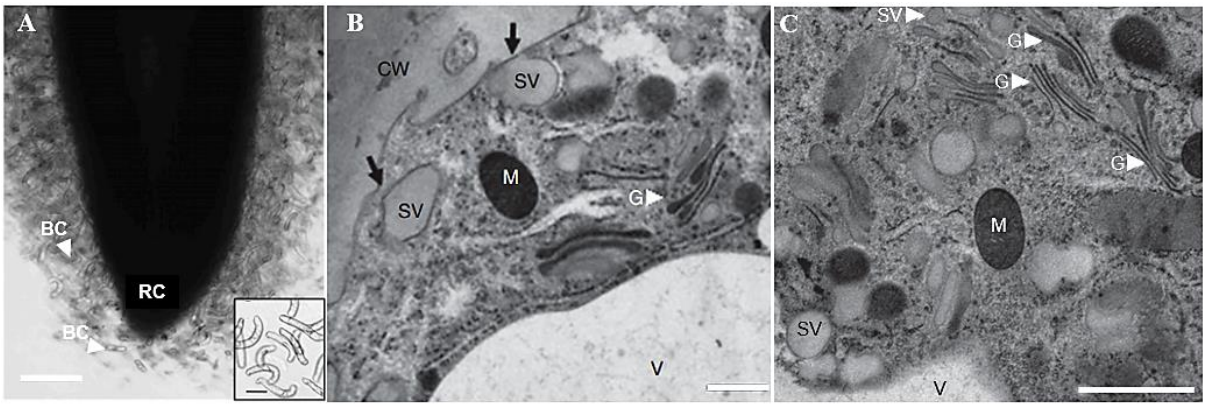

Figure I-13. Microscopical characterization of pea (P. sativum) border cells.

(A) Root border cells (BCs) are released from the root cap as individual cells. (B, C) Observations by transmission electron microscopy of isolated border cells released from pea root; in (B) the presence of large secretory vesicles in close vicinity to the cell wall, some of which appear to fuse with the plasma membrane (indicated by black arrows) and in (C) numerous Golgi stacks and secretory vesicles in the cytoplasm. BC, border cells; CW, cell wall; G, Golgi stack; M, mitochondria; RC, root cap; SV, secretory vesicles; V, vacuole. Scale bars: (A) = 50 µm; (B, C) = 0.7 µm. Modified from Cannesan et al. (2011, 2012).

Moreover, different populations of BCs were found to be released by the root tip of pea (*Pisum sativum*) and soybean (*Glycine Max*) including small spherical cells, intermediate-size cells, and elongated cells (Cannesan et al., 2011; Ropitaux et al., 2020) (Fig. I-14).

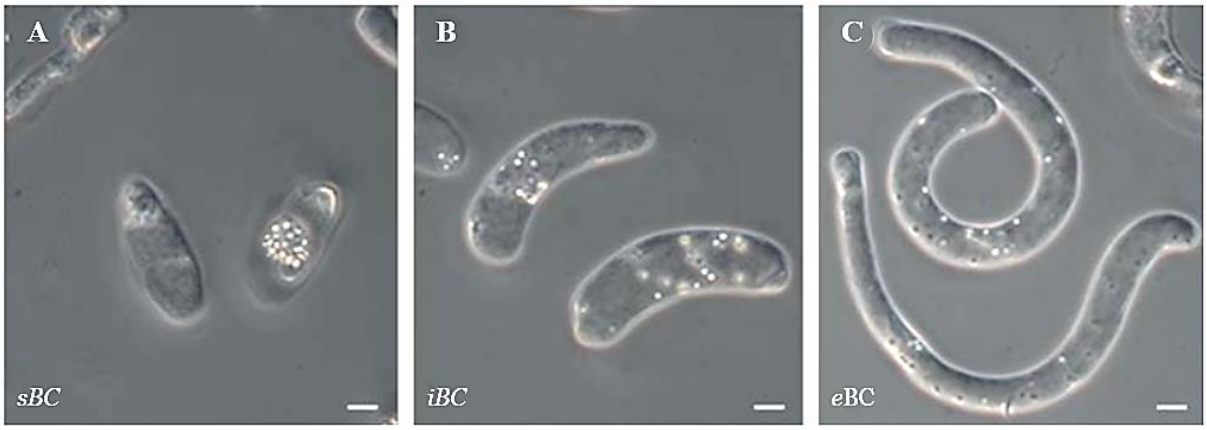

Figure I-14. Root border cell morphotypes from pea (P. sativum) root tip.

Three morphotypes were released and defined as (A) small spherical cells, (B) intermediate-size cells and (C) elongated cells. Scale bars = 5 µm. From Cannesan et al. (2011).

Interestingly, BCs were reported to be absent in several Brassicaceae species including *A. thaliana* (Hawes and Pueppke, 1986; Brigham et al. in 1998; Hawes et al, 2003). Vicré et al. (2005) described for the first time the presence of BC with different properties detaching from the root cap in *A. thaliana* (Fig. I-15A), and later in other species such as rapeseed (*Brassica napus*), Brussels sprout (*Brassica oleraceae*), mustard (*Sinapis alba*), and radish (*Raphanus sativus*) (Driouich et al., 2007, 2010, 2012). These cells are atypical as they remain associated together into small groups of cells and organized in a sheath-like pattern after release from the root tip and adhere to the root apex unlike BCs (Vicré et al., 2005; Durand et al., 2009; Driouich et al., 2007). Based on their organization pattern and their detachment, they were named "border-like cells" or BLCs. The root tip of some plant species from Linaceae and Fabaceae families was also found to produce BLCs such as flax (*Linum usitatissimum*) and *Acacia mangium* (Endo et al., 2011; Plancot et al., 2013). BLCs can reach very impressive sizes, ranging from 1 to 3 mm in the roots of *Acacia mangium* (Endo et al., 2011). By using vital dyes and cell imaging techniques, Vicré et al. (2005) showed the viability of these BLCs as well as an important metabolic activity revealed by the abundant presence of mitochondria and Golgi stacks in their cytoplasm (Fig. I-15B, C).

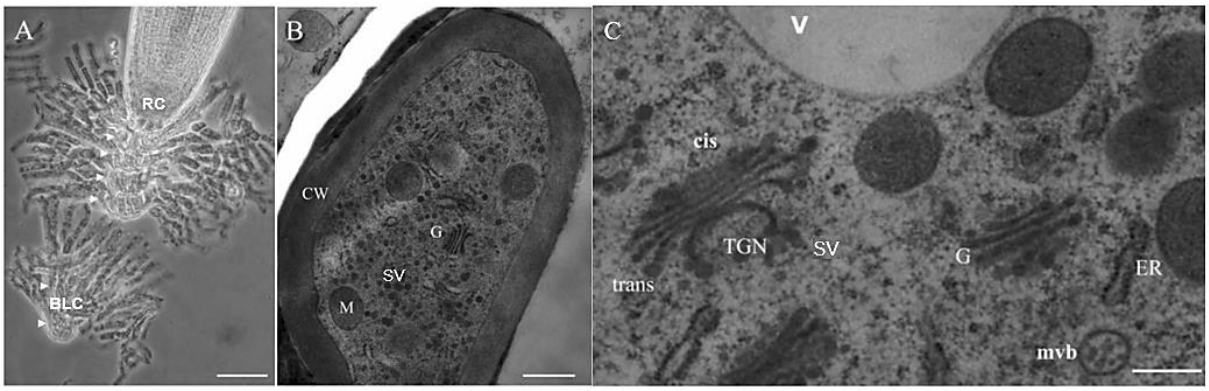

Figure I-15. Microscopical characterization of Arabidopsis root border-like cells.

(A) Root border-like cells (BLCs) are released from the root cap of 2-week-old seedlings. Arrowheads indicate the cell layers where border cell files came from. (B, C) Micrograph illustrating in (B) the general morphology of a BLC from a root prepared by HPF and FS. Note the abundance of Golgi-derived vesicles filled with opaque electron material and in (C) the high magnification view of cytoplasmic content of a BLC prepared HPF/FS. BLC, border-like cells; CW, Cell wall; ER, endoplasmic reticulum; G, Golgi stack; M, mitochondria; mvb, multi-vesicular bodies; TGN, trans golgi network; SV, secretory vesicles; V, vacuole. Scale bars: (A)=100 µm; (B)=1 µm; and (C)=300 nm. Modified from Vicré et al. (2005).

Three morphotypes of BLCs have been observed in flax (*Linum usitatissimum*) root tip including spherical border-like cells (sBLC), elongated border-like cells (eBLC), and filamentous border-like cells (fBLC) (Plancot et al., 2013) (Fig. I-16). Since 2019, BCs and BLCs have been renamed in a simplified term as root-associated, cap-derived cells (AC-DCs) by Driouich et al.

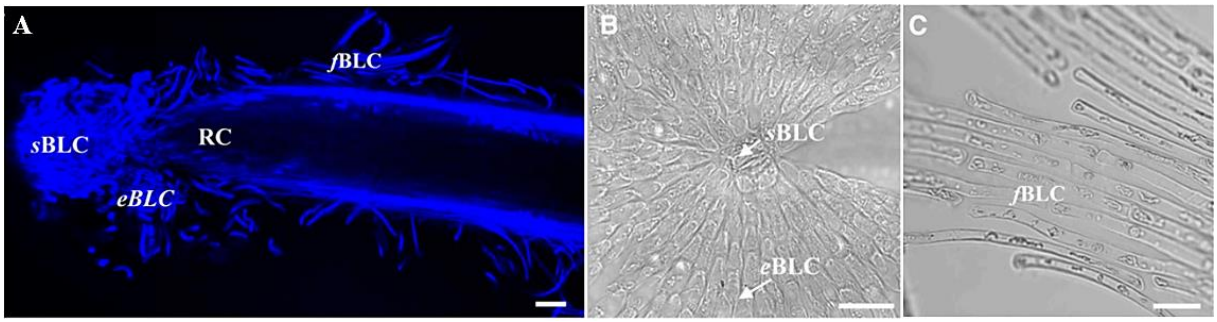

Figure I-16. Microscopical characterization of root border-like cells (BLCs) from flax (L. usitatissimum)

(A) Calcofluor staining of the root tip shows BLC organization in flax with three distinct populations of root BLCs occur: spherical border-like cells (sBLC), elongated border-like cells (eBLC), and filamentous border-like cells (fBLC). (B) Micrographs showing the morphology of the spherical border-like cells and the elongated border-like cells released from the root tip and (C) the filamentous border-like cells along the root surface. RC, Root cap. Scale bars: (A)= 100 µm; (B)=20 µm; and (C)=40 µm. Modified from Plancot et al. (2013).

A recent study of three Sahelian woody species in northern Senegal (*Balanites aegyptiaca, Acacia raddiana*, and *Tamarindus indica*) by optical and transmission electron microscopies

show that plant species *Acacia raddiana* and *Tamarindus indica* release both BCs and BLCs (Carreras et al., 2020).

(b) Production of AC-DCs in plant roots

AC-DCs (BCs/BLCs) production and their mode of detachment from the root tip are dependent on the type of root apical meristem (RAM). This is the region within the root tip from which all primary root tissues and the root cap are derived (Hamamoto et al., 2006).

More precisely, AC-DCs cells come from the central and lateral initials forming the cap meristem (Woo and Hawes, 1997; Arnaud et al., 2010). After several divisions, these cells will form the columella (COL) and lateral root cap (LRC) cells, whose primary function is to protect the RAM during growth. The cells will progress within the cap and differentiate into cells with specific functions (Brigham et al., 1998; Kumpf and Nowack, 2015) (Fig. I-17). The last differentiation that takes place is the detachment of the outermost layer of the root cap which will release the AC-DCs (Hawes et al., 2003).

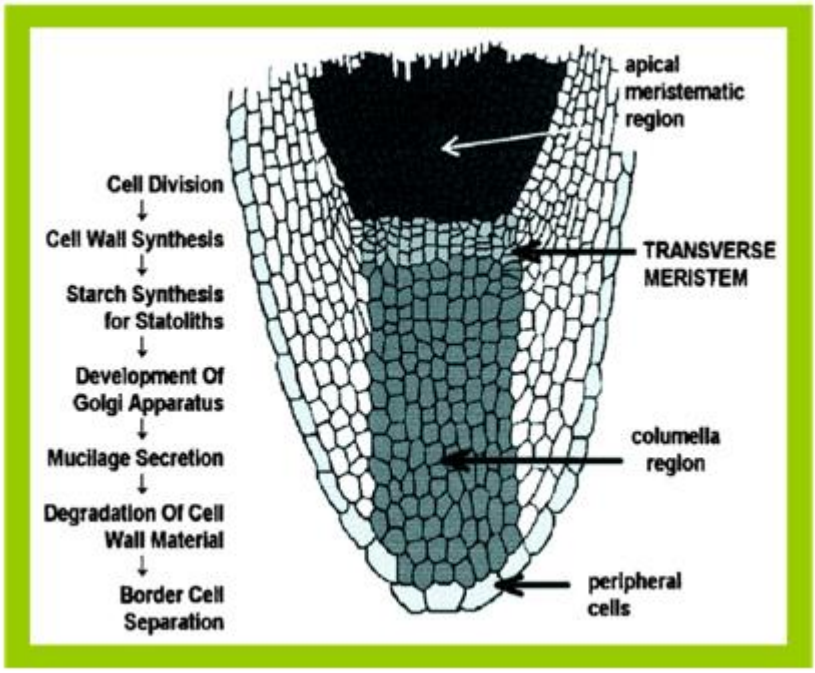

Figure I-17. Root cap structure and development.

As cell division occurs in the meristem of the root cap, cell tiers are displaced toward the periphery of the cap. In the columella region, cell tiers exhibit distinct morphologies reflecting their specialized physiological functions. As each cell tier is displaced, previous functions cease and new functions are initiated within the progressively differentiating cells. From Brigham et al. (1998).

Border cells production and detachment are finely regulated by both endogenous and environmental signals (Brigham et al. 1995; Gunawardena and Hawes 2002; Driouich et al. 2007). The production and of these cells is variable depending on the species (from zero to several thousand per root), but remain constant for related plant species within the same family (Groot et al., 2004; Hawes et al., 2003; Hamamoto et al., 2006) (Fig. I-18).

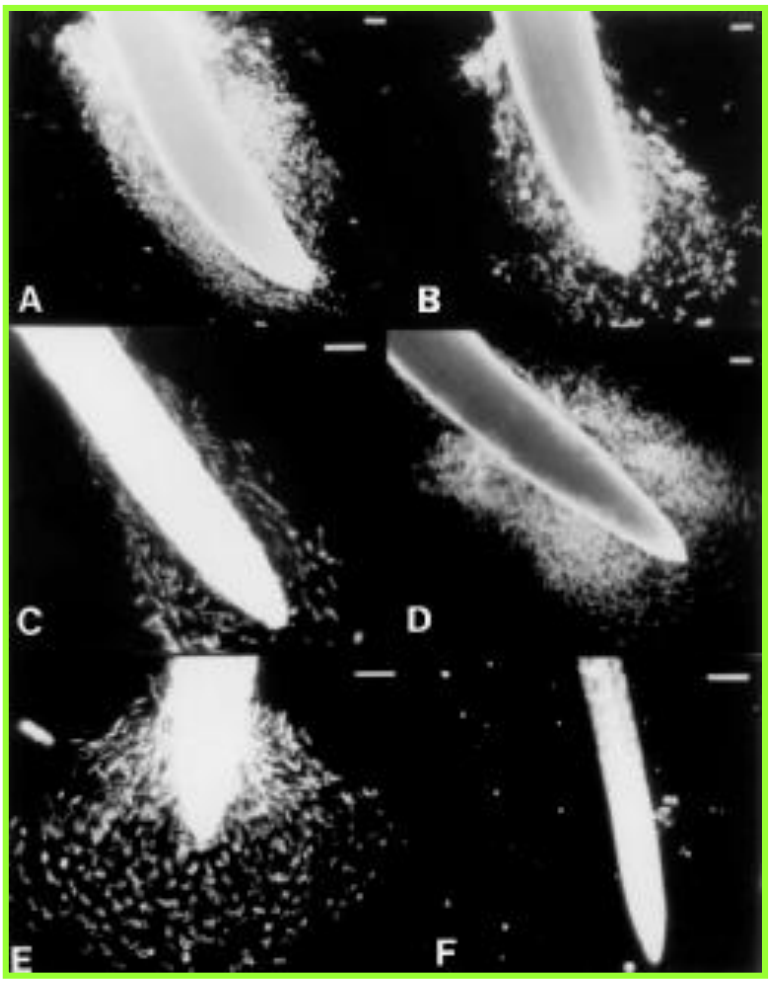

Plants	Number of BCs
Daucus carota	2300-2500
Glycin max	3000-4000
Zea mays	2500-4000
Pisum sativum	3000-5000
Gossypium hirsutum	8000-10000
Arabidopsis thaliana	0

Figure I-18. Evidence of border cells in several plant species.

The number of border cells (BC) produced varies between plant species. A) BC of Carrot, B) Soybean, C) Maize, D) Pea, E) Cotton, and F) Arabidopsis. From Hawes et al. (2003).

The RAM is described as a key player in the production of these cells since, depending on the RAM organization, the type and the number of border cells vary between plant species but conserve at the family level (Driouich et al., 2007, 2012).

In eudicotyledonous angiosperms three types of RAMs have been observed: closed, open and intermediate RAMs (Fig. I-19) (Groot et al., 2004; Rost, 2011). It has been described that species with open RAM release significantly more BCs than species with closed RAM (Groot et al., 2004; Hamamoto et al., 2006). For example, the open RAM observed in pea (*P. sativum*) produces about 4500 BCs per day. In carrot (*Daucus carota*), approximately 2500 BCs per day are produced (Hawes et al., 2003; Groot et al., 2004). About 5000 BCs per day have been

released from wheat (*Triticum aestivum*) root tip while the number of BCs discharged from rice (*Oryza sativa*) is 2100 BCs per day and 4000 BCs per day from maize (*Zea mays*) root tip (Hawes et al., 2003).

In contrast to open and intermediate RAMs that produce and release BCs, closed RAMs in Brassicaceae such as rapeseed, mustard and *A. thaliana* release border cell-like cells (BLCs) (Vicré et al. al., 2005; Driouich et al., 2007).

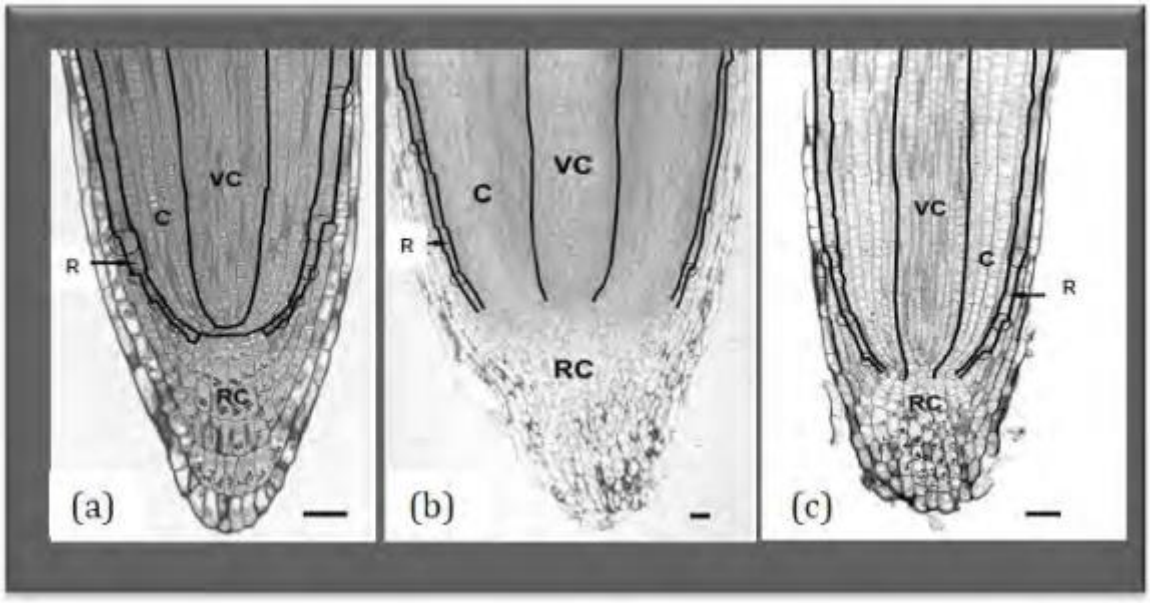

Figure I-19. Organization of the root apex of eudicotyledonous angiosperm plants.

(a) Longitudinal section of a root apex of Linum grandiflorum (flax). The RAM shows a closed organization. b) Longitudinal section of a root apex of Pisum sativum (pea). The RAM shows an open organization. c) Longitudinal section of a root apex of Daucus carota (carrot). The RAM shows an intermediate organization. C: cortex, R: rhizodermis, RAM: root apical meristem, RC: root cap, VC: vascular cylinder. Scale bars: 50 µm (a, b and c). From Groot et al. (2004).

It has been demonstrated that some cell wall polysaccharides such as pectin homogalacturonan (HG) could involve in BLC detachment of *A. thaliana* root (Bouton et al., 2002; Durand et al., 2009; Mravec et al., 2014) or the inhibition of pectin methylesterase (PME) expression also alters BC release in pea (Wen et al., 1999). Moreover, Mravec et al. (2017) highlighted the involvement of HRGPs families, such as EXTs, in the process of BC detachment. In this study, the signal observed in the walls of BCs from the pea root cap is oriented towards the outside of the root. This result is similar to the signal observed for xyloglucan (XyG)-associated epitopes. After the BCs detachment, this signal in the cell wall decreases significantly.

In *A. thaliana* RAM, numerous specific transcription factors are involved in border cells release (Fig. I-20) such as WUSCHEL-RELATED HOMEOBOX 5 (WOX5) or CYCLING DOF (DNA-binding One Zinc Finger) FACTOR 4 (CDF4), whose opposing concentration gradients sculpt the RAM (Pi et al., 2015; Ruta et al., 2020). WOX5 is an additional element required in the QC to maintain columella stem cells by maintaining the initial cells in a proliferating and undifferentiated state (Perilli et al., 2012). WOX5 expression is maintained by SCARECROW (SCR) (Sarkar et al., 2007). The WOX5 gradient decreases when the cells derived from the initials move away from the QC and allows the expression of CDF4 that drives cell differentiation (Rahni et al., 2016).

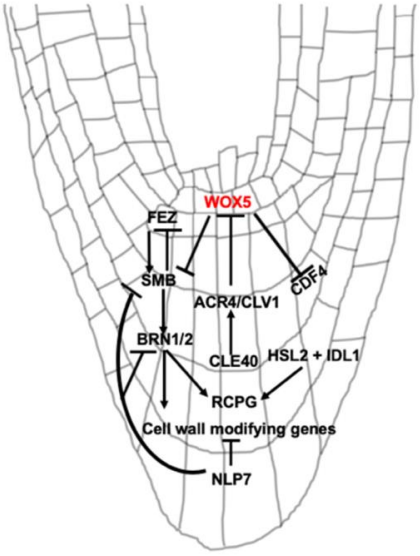

Figure I-20. Involvement of different transcription factors and signaling peptides in Arabidopsis root cap development and BLC release.

Arrows and barred lines indicate positive and negative regulation, respectively. From Kumar and Pascuzzi (2020).

Other players are involved in this columella differentiation, such as the small signaling peptide CLAVATA3 (CLV3)/EMBRYO SURROUNDING REGION 40 (CLE40) (Stahl et al., 2009; Stahl and Simon, 2009; Berckmans et al., 2020). CLE40 inhibits WOX5 expression and promotes columella cell differentiation and the position of the QC through receptor kinases ARABIDOPSIS CRINKLY4 (ACR4) and CLAVATA1 (CLV1) (Perilli et al., 2012; Stahl et al., 2013; Rahni et al., 2016; Berckmans et al., 2020). Besides that, three transcription factors, BEARSKIN 1 (BRN1) and BEARSKIN 2 (BRN2) with SOMBRERO (SMB) are involved in cell differentiation, promoting cap cell maturation while allowing border cell separation (Bennett and Scheres, 2010; Shi et al., 2018; Kumar and Pascuzzi, 2020). BRN1 and BRN2 are also involved in mucilage accumulation (Maeda et al., 2019) and can activate a gene encoding a polygalacturonase, named ROOT CAP POLYGALACTURONANSE (RCPG) which promote the separation of the outermost layer of the columella and the lateral cap through individual detachment of these cells (Bennett et al., 2014; Kamiya et al., 2016).

In addition, a new transcription factor called NIN-LIKE PROTEIN7 (NPL7) was discovered by Karve et al. (2016) playing a role in border cell release. The root of Arabidopsis *npl7* mutant releases BCs rather than BLCs (Karve et al., 2016). These different studies have highlighted the importance of wall components in the genesis and release of AC-DCs.

3. Root mucilage

The root mucilage is revealed using India ink staining showing the presence of a white halo surrounding the root tip (Fig. I-21A) and the AC-DCs (Fig. I-21B-F) (Wen et al., 2007a; Cai et al., 2013; York et al., 2016; Ropitaux et al., 2020). This mucilage is mainly composed of polysaccharides, glycoproteins, and proteoglycans (Vicré et al., 1998; Bais et al., 2006; Badri and Vivanco, 2009; Driouich et al., 2013; Baetz and Martinoia, 2014; Bacic et al. 1986; Chaboud 1983; Chaboud and Rougier 1984; Moody et al. 1988).

Since 1981, a study by Rougier highlighted the carbohydrate nature of the high molecular weight compounds coating the AC-DCs of maize. These results are confirmed latterly in rice, maize, and soybean with the abundant presence of glucose, galactose, xylose, arabinose, fucose, and mannose (Bacic et al., 1986; Moody et al., 1988; Knee et al., 2001; Timotiwu and Sakurai, 2002; Dennis et al., 2010).

The polysaccharides are usually synthesized and transported through Golgi stacks and Golgi-derived secretory vesicles to the cell wall (Battey and Blackbourn, 1993; Bertin et al. 2003; Badri and Vivanco, 2009; Driouich et al., 2012), which scatter throughout the cytoplasm of AC-DCs from the cap of *A. thaliana*, pea, and alfalfa (*Medicago sativa*) (Vicré et al., 2005; Cannesan et al., 2011; Wang et al., 2017). Moreover, this secretory activity in the AC-DCs of root cap is significantly more frequent compared to the cells of the apical meristem and columella (Wang et al., 2017) suggesting the intense activity of these cells.

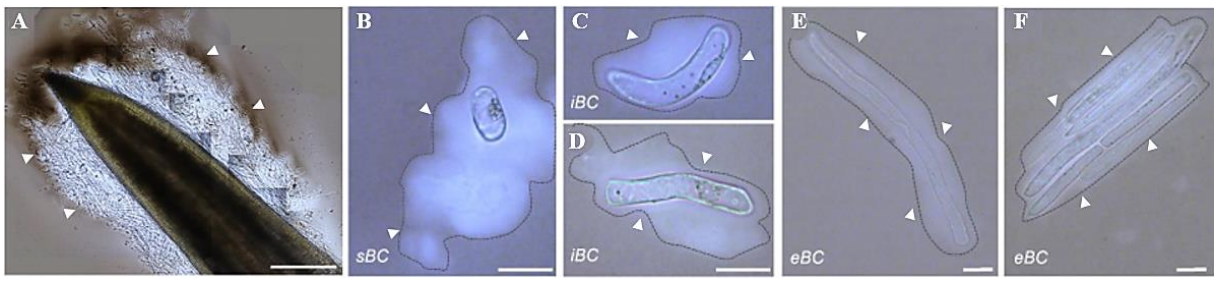

Figure I-21. Visualization of secreted mucilage using India ink staining.

(A) Light microscopy images showing an abundant slimy mucilage present around the root tip and embedding border cells (indicated by white arrows). (B-F) images showing different cell types and their secreted mucilage (stained with India ink and delimited by a dashed line). sBC, spherical border cells; iBC, intermediate border cells; eBC, elongated border cells. Scale bars: (A)=300 µm; (B-F) = 40 µm. Modified from Ropitaux et al. (2020).

During their detachment from the root cap, AC-DCs excrete complex pectic-type polysaccharides such as HGs (Vicré et al., 2005; Durand et al., 2009; Mravec et al., 2017), XGAs (Jensen et al., 2008; Mravec et al., 2017; Wang et al., 2017) or RG-I (Mravec et al.,

2017). Furthermore, numerous parietal glycoproteins belonging to the HRGPs family have also been described by other works such as AGPs in pea mucilage (Knee et al., 2001; Durand et al., 2009; Cannesan et al., 2012; Koroney et al., 2016) or Fasciclin-like AGPs (FLAs) in maize mucilage (Ma et al., 2010). More recently, EXTs have been identified in potato and pea mucilage (Koroney et al., 2016; Castilleux et al., 2018).

In maize mucilage, the protein content has been estimated in the range of 1-6% but about 2848 unique proteins have been identified (Ma et al., 2010). Interestingly, the mucilage proteome has been highly conserved between monocot and dicot species such as rapeseed, *A. thaliana*, pea, and maize with the presence of many protein homologs (Basu et al., 2006; Wen et al., 2007b; Ma et al., 2010).

Furthermore, some proteins involved in carbohydrates and enzymes metabolism such as endoxyloglucan transferases, invertases, β-galactosidases, cellulases, α-mannosidases, and oligosaccharyl transferase have been identified (Wen et al., 2007b; Ma et al., 2010; Rocha et al., 2015). Other research also found the presence of well-known peptides and antimicrobial proteins, e.g. defensins, PR proteins, chitinases, peptidases, and glucanases (Basu et al., 2006; Wen et al., 2007b; De-la-Peña et al., 2008; Badri and Vivanco, 2009; Driouich et al., 2013; Weiller et al., 2016).

Interestingly, the data also show that mucilage in pea root contained extracellular DNA (exDNA) and H4-type histones (Wen et al., 2007b; 2009). This result has been confirmed in soybean mucilage with the presence of pectin, cellulose, exDNA, histones, and two hemicellulosic polysaccharides, xyloglucan, and heteromannan (Ropitaux et al., 2020).

4. Action of border cells and root mucilage in root defense

(a) Role of AC-DCs

As mentioned previously, it has been shown that over half of the root exudates are produced by the root AC-DCs (Griffin et al. 1976; Hawes et al. 2011). Together, their activity is influenced positively or negatively in interactions with microbial communities within the rhizosphere (Pierret et al., 2007; Badri and Vivanco, 2009; Dennis et al., 2010; Galloway et al., 2017).

In response to these various stresses, the AC-DCs have a suitable adaptation for the number of cells produced, their morphology, and their biological activity depending on the plant species (Hawes et al., 2003; Driouich et al., 2007; 2012; Endo et al., 2011; Plancot et al., 2013). The different morphotypes of AC-DCs have been found to play the specific roles, e.g. the spherical

cells and intermediate-size cells have a strong secretory activity, releasing mucilaginous molecules that would allow the root lubrication against abrasion by soil particles (Iijima et al., 2000; 2003; 2004), and would have a role as a trap against pathogenic microorganisms. The number of spherical morphotypes AC-DCs in pea root tip increased in presence of *A. euteiches* compared to the intermediate and elongated morphotypes (Cannesan et al., 2012). In addition, the elongated cells (isolated or attached as a stack), is reminiscent of the "fibrous tissue" of AC-DCs observed in *Acacia mangium* (Endo et al., 2011) and which are more viable than other morphotypes of AC-DCs, would form a physical barrier that could reduce the mechanical stress between the root and the soil particles to promote root elongation.

The AC-DCs play a considerable role in root protection against abiotic and biotic stresses (Hawes et al., 2000; 2003) since they are specialized in the production of antimicrobial molecules such as anthocyanins with antioxidant properties or phytoalexins with antibiotic properties, and enzymes intended to destroy pathogens (Wen et al., 2007b; 2009; Cannesan et al., 2011; 2012). Recent studies highlight the importance of these cells in interactions with beneficial and/or pathogenic microorganisms (Gunawardena et al., 2005; Xie et al., 2012; Cannesan et al., 2012). A study by Zhao et al. (2000a) found that in atmospheres containing increased carbon dioxide, more than twice as many AC-DCs accumulate from pea root. These AC-DCs could attract and induce quiescence of the root-knot nematode *Meloidogyne incognita* (Hawes et al., 2000; Zhao et al.,2000b). After 30 minutes in contact with the AC-DCs, the nematodes stop moving and become rigid (Fig. I-22A, B, C).

Similarly, when pea root tip is inoculated with the fungal pathogen *Nectria haematococca*, the AC-DCs are rapidly covered with a mantle of hyphae and detached from the rest of the root, leaving the root tip free of infection (Hawes et al., 1998). These observations suggest that the AC-DCs function specifically as a host to inhibit *N. haematococca* and protect the root cap and root meristem from infection (Wen et al., 2007b). More recently studies have revealed that the increase of AC-DCs produced as well as increased production of pisatin, an isoflavonoid known to inhibit *in vitro* pathogen growth, in response to *A. euteiches* infection could prevent anchorage of encysted zoospores at the pea root cap surface (Cannesan et al., 2011). Furthermore, in response to *Pseudomonas aeruginosa* and *Fusarium solani* f. *sp. pisi* (Fsp), AC-DCs from pea root cap have been found to produce more mucilage (Driouich et al., 2013) (Fig. I-22D, E, F).

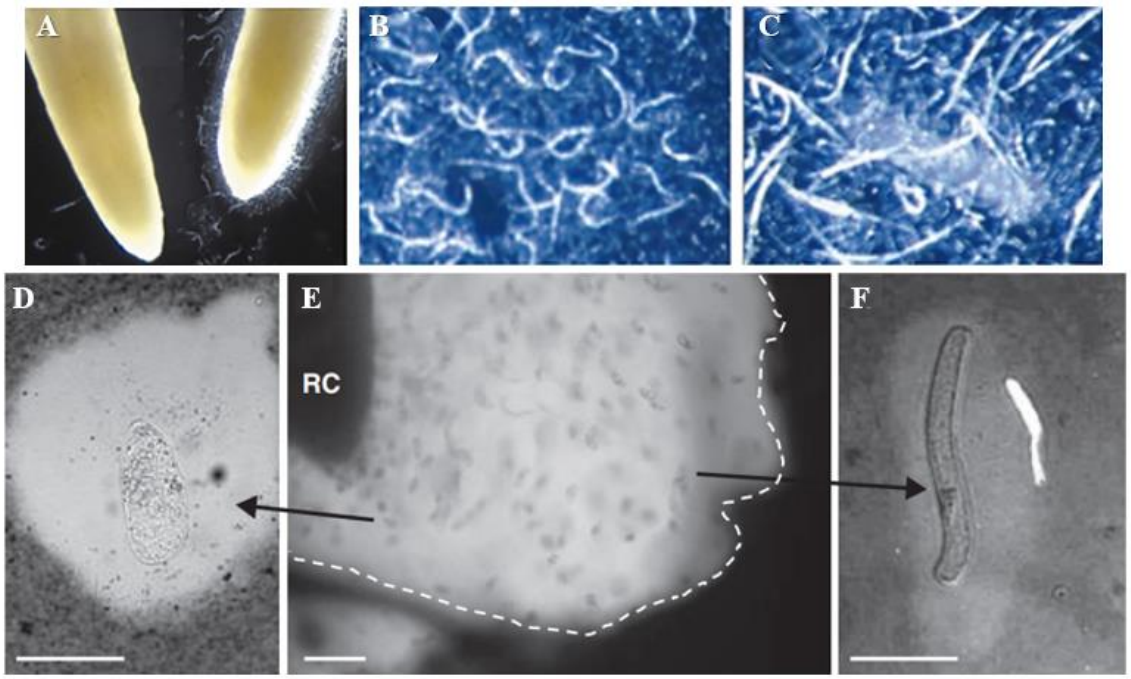

Figure I-22. Role of root AC-DCs in the various stresses.

(A) Attraction and immobilization of the root knot nematode in pea roots. No accumulation of nematodes occurred in the roots with AC-DCs removed prior (left) but within 5 min, an accumulation of nematodes was apparent at the root tip periphery of roots with AC-DCs present (right). (B) High concentration of actively motile nematodes were found to be associated with clumps of detached AC-DCs. (C) Within 30 min, most of the nematodes within clumps of detached border cells had assumed a rigid, stick-like posture and had ceased movement. (E) Visualization of AC-DCs and their mucilage surrounding the root cap using India ink (dashed lines). Increased mucilage production (D) of maize AC-DC (black arrows) in response to Pseudomonas aeruginosa and (F) of pea AC-DC to the presence of germinating spore of Fusarium solani f. sp. pisi. BC, border cell; RC, root cap; Bars: 20 µm. Modified from Hawes et al. (2000) and Driouich et al. (2013).

(b) Role of root mucilage

As mentioned previously, the AC-DCs are coated by dense mucilage and various high and low molecular weight compounds, which together form a structure of their own (Driouich et al, 2013). Studies indicated that root mucilage can stabilize soil aggregates by adhering to soil particles and sticking them together (Guckert et al., 1975; Morel et al., 1991; Watt et al., 1993; McCully, 1995; Traoré et al., 2000). It has been suggested that mucilage might transfer gravitropism signaling from the root cap to the root tip (Moore et al. 1990).

Along with the AC-DCs, the mucilage also contributes to the protection of the root apex against abiotic stresses by lubricating the apex to limit soil abrasion (Iijima et al., 2004; Rabbi et al., 2018), promote soil aggregation (McCully, 1999; Galloway et al., 2017) and limit the toxicity of some heavy metals such as aluminum, cadmium, and copper (Deiana et al., 2003; Cai et al.,

2013). Moreover, AC-DCs with their high and low molecular weight secretions have a key role in root defense. Indeed, high molecular weight compounds, including many antimicrobial proteins such as peptidases, chitinases, peroxidases, glucanases, and 14-3-3 proteins have also been shown to be involved in root defense (Grudkowska and Zagdańska, 2004; Gohel et al., 2005; Ma et al., 2010). A study by Wen et al., (2007b) found that blocking the 14-3-3 protein with a specific antibody considerably increases the severity of disease and suppresses the resistance of the plant to fungal attacks. Besides that, defensins have been described in the mucilage of *Heliophila coronopifolia* (L.) (Weiller et al., 2016) and *Arabidopsis halleri* (L.), are known for their antifungal properties, for example, to limit infection by *Botrytis cinerea* (Pers.) (Nguyen et al., 2014).

For the major compounds of mucilage like polysaccharides, which play not only a structuring role but are also thought to be involved in root defense. For example, the action of polygalacturonases produced by some plant pathogens would be limited by the presence of xylose substitutions (Jensen et al., 2008). In addition, xylogalacturonan (XGA) which is secreted abundantly by AC-DCs and by the root, resisted to degradation by pathogens (Jensen et al., 2008; Mravec et al., 2017).

Among the molecules present in the mucilage, AGPs are also involved in the regulation of plant- microorganism interactions (Cannesan et al. 2012; Nguema-Ona et al. 2013b; Koroney et al. 2016). It has been shown that AGPs purified from the root cap of pea will be able to attract *A. euteiches* zoospores by chemotaxis, accelerate encystment and prevent their germination (Cannesan et al., 2012). AGPs have also been found in root exudates of several plants such as pea (Xie et al., 2012; Knee et al., 2001; Laloum et al., 2021), soybean (*Glycine max* L.) (Timotiwu and Sakurai, 2002), *Arabidopsis* (Vicré et al., 2005; Durand et al., 2009) and maize (Ma et al., 2010).

By studying the *rat1* (*resistant to agrobacterium transformation 1*) mutant of *A. thaliana* deficient in AGP17, Gaspar et al. (2004) showed that AGPs influence root interactions with microbes since the absence of *AtAGP17/RAT1* expression in the mutant suppresses the colonization of Arabidopsis root by *Agrobacterium tumefaciens.* To colonize the root, several soil microorganisms can hydrolyze and metabolize AGPs, thus providing them a source of nutrients for their growth in the rhizosphere (Knee et al., 2001).

Recently, the action of exDNA and H4-type histones (Wen et al., 2007b) in root defense has been reported (Wen et al., 2009; Ropitaux et al., 2020). Enzymatic degradation of exDNA

structure would increase root colonization by the soil-borne fungus *Nectria haematococca* (Berk. & Broome) (Wen et al., 2009). A significant increase in the amount of exDNA after treatment with several elicitors, such as flg22, and following infection with the soil-borne pathogen *Ralstonia solanacearum* (Tran et al., 2016) were also described.

Some low molecular weight compounds secreted into the rhizosphere, terpenes and phenolic compounds such as flavonoids, also have a role in plant defense. For example, pisatin which is well known for its antifungal activity has been found as a major metabolite in pea root exudates (Dewick, 2009; Evidente et al, 2010; Cannesan et al., 2011). At the root level, the monoterpene 1,8-cineole (Eucalyptol) is a plant-derived volatile compound secreted by *A. thaliana* roots could help defense against multiple phytopathogens, such as *Pseudomonas syringae pv tomato DC3000* (Steeghs et al., 2004; Chen et al., 2004; Baetz and Martinoia, 2014).

5. The Root Extracellular Trap (RET) model

The studies on the role of AC-DCs and their secretions in root defense has led to a model named the Root Extracellular Trap (RET) (Driouich et al., 2013) (Fig. I-23), by comparison with the Neutrophil Extracellular Trap (NET) model of mammals (Brinkmann et al., 2004). Many similarities in composition and function have been highlighted between these two models, such as the presence of exDNA forms filamentous structures within pea mucilage (Wen et al., 2009; Hawes et al., 2016; Wen et al., 2017), comparable to those of neutrophils (Von Köckritz-Blickwede and Nizet, 2009; Halverson et al., 2015). It has also been described the presence of antimicrobial peptides, such as defensins (Weiller et al., 2016), glycoproteins and proteoglycans (Bacic et al., 1986; Knee et al., 2001), H4-type histones (Wen et al., 2007b), reactive oxygen species (ROS) (Plancot et al., 2013), and various antimicrobial proteins and enzymes in AC-DCs secretions (Ma et al., 2010), bringing RET closer to NET (Bowdish et al., 2005; Urban et al., 2009).

As explained previously, the RET is probably part of root immunity which functions as an immune defense mechanism through repulsion and killing of microbial pathogens (Driouich et al., 2013; 2019). The RET regulate generally the positive and negative interactions around the root. A large number of studies have clarified the effect of RET on the mobility, germination, and growth of pathogenic oomycete *Aphanomyces euteiches* (Cannesan et al. 2012) or the bacterium *Pectobacterium astrosepticum* (Koroney et al. 2016). Recently, Ropitaux et al. (2020) showed that the soybean RET prevented zoospores of *Phytophthora parasitica* from reaching and colonizing root tissues or inducing their lysis.

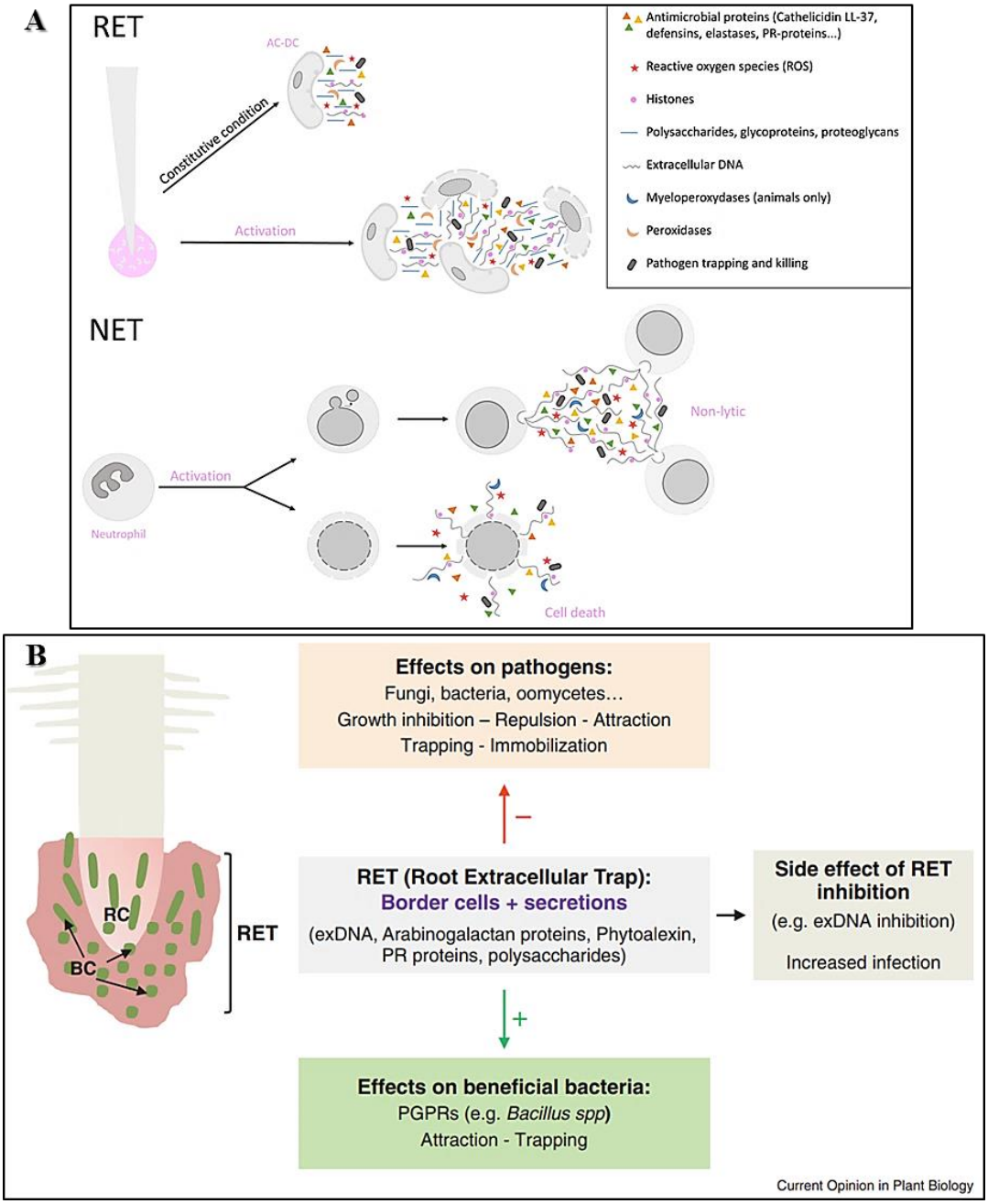

Figure I-23. Schematic model of RET.

(A) Comparison model of Neutrophil extracellular traps (NETs) and root extracellular traps (RETs) formation and function. Formation and release of both NETs and RETs are stimulated by pathogens, via pathogen-associated molecular patterns (PAMP) and damage-associated molecular patterns (DAMPs). RETs can also be released constitutively. Both traps contain anti-microbial proteins and exDNA and are able to trap and neutralize pathogens. (B) Functional model of the RET (Root Extracellular Trap). The RET is formed by border cells and secreted antimicrobial components, arabinogalactan proteins, exDNA, etc. Experiments have shown that RET is able to alter the aggression of various pathogens (-), while promoting exchanges with beneficial soil bacteria (+) and generally ensures root protection. AC-DCs, border cells; exDNA, extracellular DNA; PR proteins, pathogenesis-related proteins; PGPR, plant growth promoting rhizobacteria; RC, root cap. From Driouich et al. (2013; 2019).

D. Fructans and the concept of "Sweet Immunity"

The secreted components of RETs including cell wall-derived polysaccharides, various classes of anti-microbial compounds, and glycoproteins have been proved to play a fundamental role in root immunity (Driouich et al., 2013; 2019; 2021; Hawes et al., 2016).

In addition, researchers proposed recently a new concept consisting the role of plant- or microbial-derived carbohydrates in plant immunity. This concept is called "sweet immunity" or "sugar-enhanced defence" which suggests that sugar metabolism and signaling pathways involved in plant immunity are interconnected (Bolouri Moghaddam and Van den Ende, 2013; Trouvelot et al., 2014; Tarkowski et al., 2019; Svara et al., 2020). This concept postulates that the soluble carbohydrates that come directly from microorganisms, plant metabolism, or that are released during the degradation of extracellular compounds of microorganisms and plants are part of the MAMPs/PAMPs/DAMPs and contribute to the PTI response of plant defense.

Among these soluble carbohydrates, fructans which are water-soluble fructosyl polymers synthesized by certains plants and microorganisms (Hendry, 1993; Velázquez-Hernández al., 2009) could play a particular role.

1. Fructans in microorganisms and plants

In living organisms, the carbohydrate reserves accumulate under various biochemical forms. Some organisms synthesize, in addition to the two most common carbohydrate reserves which are glycogen or starch (Ball et al., 2011), another form of carbohydrate reserve polymers, the fructans. Fructans are water-soluble polymers of fructosyl residues linked by β-(2,1) and/or β-(2,6) linkages with one external or internal glucosyl residue (Vijn and Smeekens, 1999; Ritsema and Smeekens, 2003).

The presence of fructans in plants was discovered in the root of *Inula helenium* as a white material that was distinct from starch (Rose, 1804). Since then, fructans have been found in some bacteria, fungi, algae, land plants (Hendry, 1993). These polymers have been found present in more than 15% of Angiosperms (Hendry, 1993) and in microorganisms, such as beneficial (*Gluconacetobacter diazotrophicus*; Hernández et al., 2000) or pathogenic bacteria (*Erwinia amylovora*; Öner et al., 2016) and fungi (*Aspergillus* and *Rhodotorula*; Trollope et al., 2015). More recently they were found in some Archaea (Kirtel et al., 2019). Thus, some bacteria and fungi accumulate both glycogen and fructans while some green algae and land plants accumulate both starch and fructans. This suggests that in the living kingdom fructans can be synthesized independently of that of starch and glycogen.

(a) Structure of fructans

Different types of fructans are distinguished according to the nature of the linkage connecting the fructosyl residues, the position of the glucosyl residue (internal or external), the presence or absence of branches, and the chain lengths (Pollock and Cairns, 1991; Cochrane, 2000; Peukert et al., 2016). Fructan types are formed by the lengthening of the fructosyl residue chain from the three tri-saccharides of DP3, i.e. 1-kestotriose (or 1-kestose) in which the fructosyl residue is β-(2,1)-linked to the fructosyl residue of sucrose; 6-kestotriose (or 6-kestose) in which the fructosyl residue is β-(2,6)-linked to the fructosyl residue of sucrose; and 6G-kestotriose (or neokestose) in which the fructosyl residue is bound to the C6 position of the glucosyl residue of sucrose (Vijn and Smeekens, 1999; Ritsema and Smeekens, 2003; Cimini et al., 2015; Peukert et al., 2016; Fig. I-24

Four distinct types of fructans ca be distinguished (Fig. I-24) (Cimini et al., 2015):

- Inulin-type fructans: linear chain synthesized from 1-kestotriose in which the fructosyl residues are linked together by β-(2,1) linkages.
- Levan (or phlein) type fructans: linear chain synthesized from 6-kestotriose in which the fructosyl residues are linked together by β-(2,6) linkages.
- Neoserie-type fructans: linear chain synthesized from 6G-kestotriose in which the glucosyl residue is in the internal position and the fructosyl residues are linked together by β-(2,1) linkages (neo-inulin type) or β-(2,6) linkages (neo-levan type). In *Agave* species, another class of highly branched neofructans with β-(2,1) and β-(2,6) linkages, named agavins, has been proposed (Mancilla-Margalli and López, 2006; Mellado-Mojica et al., 2017).
- Graminan-type fructans: branched-chain synthesized from 1,6-kestotetraose (bifurcose) containing both β-(2,1) and β-(2,6) linkages.

Fructans can also be distinguished by their degree of polymerization (DP) into high DP fructans (generally higher than DP10) and low DP fructans (generally less than DP10; called fructooligosaccharides (FOS).

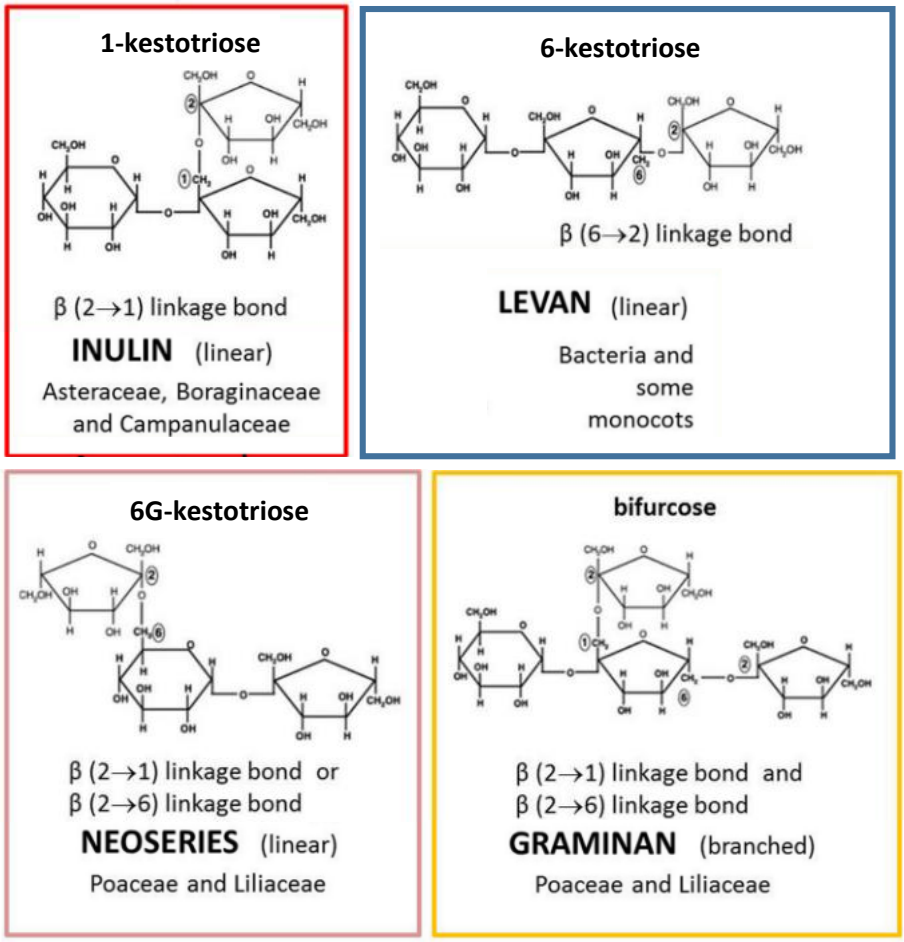

Figure I-24. Schematic representation of the different types of fructans.

Fructans are synthesized starting from sucrose. They are linear or branched polysaccharides. In higher plants, fructans are classified into four structurally distinct major categories depending on the position of the glucosyl unit and on the type of glycosidic linkage between fructosyl residues: inulin, levan, graminan and neoseries fructan can be discerned. From Cimini et al. (2015).

In microorganisms, the DP of fructans can be above 100 and up to 10000, although FOS may also occur (Velázquez-Hernández et al., 2009; Van den Ende, 2013). The levan-type fructans are synthesized in both Gram-positive and Gram-negative bacteria (Sarilmiser et al., 2015; Öner et al., 2016). Some Gram-positive bacteria, including species of the genera *Streptococcus, Leuconostoc* and *Lactobacillus*, synthesize inulin-type fructans (Chambert et al., 1974; Homann et al., 2007; Song and Jacques, 1999; Velázquez-Hernández et al., 2009).

Fungi contain inulin-type FOS with generally DPs between 3 and 8 (Trollope et al., 2015). Fructans are found in many genera including *Aspergillus, Penicillium, Claviceps, Fusarium* (Van Balken et al., 1991; Yun et al., 1997; Heyer et al., 1998; Banguela and Hernández, 2006).

In plants, the DP of fructans is usually between 30 and 150, but in some cases can reach 300 (Van den Ende, 2013). Inulin-type fructans are present mainly in Asteraceae (such as *Cichorium intybus* and *Taxaracum officinalis;* Van Laere and Van den Ende, 2002; Van den Ende et al., 2000) and in other eudicots such as in Boraginaceae (*Myosotis secunda*) and Campanulaceae (*Campanula rotundifolia L.*) (Brocklebank and Henry, 1989). Levan-type fructans have been found in the Poaceae family such as *Phleum pratense* (Cairns and Ashton, 1993; Cairns et al., 1999) and *Dactylis glomarata* (Chatterton et al., 1993; Hendry, 1993). In the Liliaceae family, *Asparagus officinalis* and *Allium cepa* contain neoserie-type fructans (Suzuki and Cutcliffe, 1989; Shiomi, 1989; Vijn et al., 1997). These neo-types occur also in *Agave* species (Mancilla-Margalli and López, 2006; Mellado-Mojica et al., 2017; Pérez-López et al., 2021). Moreover, some plants can contain a mixture of several types of fructans such as *Triticum aestivum* (graminans and inulins; Kawakami et al., 2005) and *Lolium perenne* (neoseries, levans and inulins; Pavis et al., 2001). Some other examples of the presence of different types of fructans in plants and microorganisms are resumed in Table I-2.

Table I-2. Examples of occurrence found in literature of different types of fructans in plants and microorganisms.

	Species	Family/Genus	*Inulins*	*Levans*	*Graminans*	*Neoseries*	References
Monocotyledon plants	*Allium cepa*	Liliaceae				+	Shiomi, 1989; Vijn et al., 1997
	Asparagus officinalis	Asparagaceae				+	Shiomi, 1989
	Dactylis glomarata	Poaceae		+			Chatterton *et al.*,1993
	Phleum pratense	Poaceae		+			Suzuki, 1968; Cairns et Ashton, 1993
	Lolium perenne	Poaceae	+	+		+	Pavis et al., 2001
	Triticum aestivum	Poaceae	+		+		Carpita et al., 1989
Dicotyledon plants	*Campanula rotundifolia*	Campanulaceae	+				Meier et Reid, 1982; Brocklebank et Hendry, 1989
	Cichorium intybus	Asteraceae	+				Meier et Reid, 1982; Van Laere et Van den Ende, 2002
	Helianthus tuberosus	Asteraceae	+				Marx et al., 1997
	Myosotis secunda	Boraginaceae	+				Meier et Reid, 1982; Brocklebank et Hendry, 1989
	Taxaracum officinalis	Asteraceae	+				Van den Ende et al., 2000
Bacteria	*Bacillus subtilis*	Bacillus		+			Wu et al., 2013; Öner et al., 2016
	Erwinia herbicola	Erwinia		+			Tajima et al., 1997; Öner et al., 2016
	Halomonas smyrnensis	Halomonas		+			Ateş et al., 2013; Kazak Sarilmiser et al., 2015
	Lactobacillus reuteri	Lactobacillus	+				Velázquez-Hernández et al., 2009
	Leuconostoc citreum	Leuconostoc	+				Velázquez-Hernández et al., 2009
	Streptococcus mutans	Streptococcus	+	+			Song and Jacques, 1999; Velázquez-Hernández et al., 2009
	Pseudomonas syringae	Pseudomonas		+			Jathore et al., 2012; Öner et al., 2016
	Zymomonas mobilis	Zymomonas		+			Dawes and Ribbons, 1966; Silbir et al., 2014
Fungi	*Aspergillus sydowii*	Aspergillus	+				Heyer et Wendenburg, 2001; Trollope, 2015
	Claviceps africana	Claviceps	+				Yun, 1996; Trollope, 2015
	Fusarium oxysporum	Fusarium	+				Patel et al., 1994; Banguela et Hernández, 2006
	Penicillium chrysogenum	Penicillium	+				Oláh et al., 1993; Trollope, 2015

(b) Roles of fructans

Fructans are multifunctional molecules in plants and microorganisms. They are not only a form of carbon storage in the plant but also contribute to the resistance to abiotic stresses such as cold, drought and salinity (Parvanova et al., 2004; Livingston et al., 2009; Bie et al., 2012; Van den Ende, 2013). The role of fructans in tolerance to these abiotic stresses is due to their water solubility that allows them to contribute to the regulation of osmotic potential, and their ability to insert and stabilize membranes (Hincha et al., 2007). These abilities improve plant endurance during freezing or drought-related dehydration (Livingston et al., 2009). Fructans are also able to control reactive oxygen species (ROS) produced in excess during stress (Stoyanova et al., 2011; Matros et al., 2015).

In addition, as part of the concept of "sweet immunity", some studies shown that the pre-application of plant-derived FOS extracted from *Arctium lappa* (BFOs: Burdock Fructo-Oligosaccharides) reduced the infection of plants by pathogens. A pre-treatment with BFOs on *Lactuca sativa* leaves reduced the infection caused by *Botrytis cinerea* (Tarkowski et al., 2019) (Fig. I-25A). The use of 1-methylcylopropene, a well-known inhibitor of the ethylene signaling pathway, has shown that the induction of the immune response following exposure to BFOs was dependant to ethylene (Tarkowski et al., 2019). Pre-treatment with BFOs on *Cucumis sativus* leaves prior inoculation with *Colletotrichum orbiculare* (the agent of anthracnose of Cucurbitaceae) reduced disease impact and increased SA levels (Zhang et al., 2009) (Fig. I-25B).

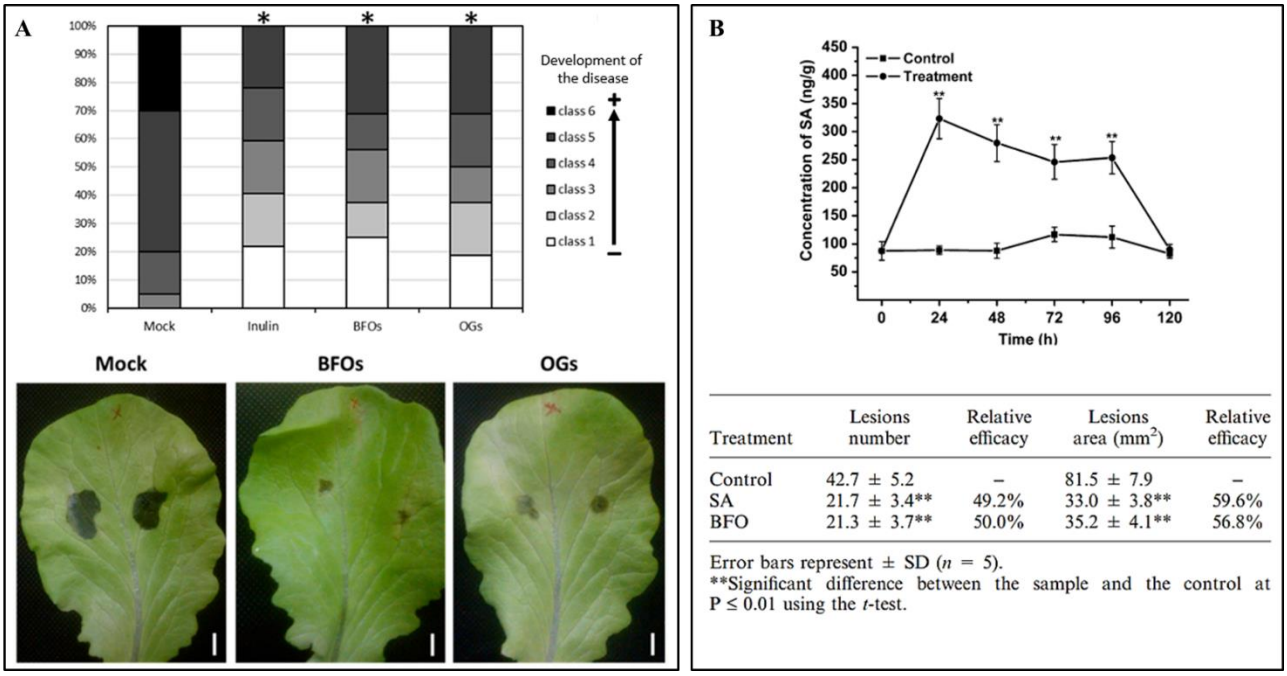

Treatment	Lesions number	Relative efficacy	Lesions area (mm^2)	Relative efficacy
Control	42.7 ± 5.2	–	81.5 ± 7.9	–
SA	21.7 ± 3.4**	49.2%	33.0 ± 3.8**	59.6%
BFO	21.3 ± 3.7**	50.0%	35.2 ± 4.1**	56.8%

Error bars represent ± SD (n = 5).
**Significant difference between the sample and the control at $P \leq 0.01$ using the t-test.

Figure I-25. Role of fructans in plant immunity.

(A) Comparison of the effect of spraying water ("mock", negative control), Burdock Fructo-Oligosaccharides (BFOs) (5 g/L), Cichorium intybus inulin ("Inulin") (5 g/L) and Oligogalacturonides (OGs) (positive control) (0,5 g/L) at 3 days post inoculation with Botrytis cinerea, on reducing development of the disease and Botrytis lesions area on 45-day-old lettuce leaves (bars = 1cm). Asterisks indicate significance against mock (water) at p < 0,01 according to non-parametrical, two-tailed, Mann–Whitney u-test (n=3). From Tarkowski et al. (2019).

(B) BFO (5 g / L) induced changes in the amounts of SA in local cucumber leaves and reduced the lesions area on the treated cucumber leaves. Error bars represent ±SD (n = 3), asterisks denote a significant difference from the control at p ≤ 0,05 and p ≤ 0,01 using the t-test. From Zhang et al. (2009).

Recently, a study by Svara et al. (2020) showed that the application of *Dactylis glomarata* levans by spraying on apple leaves limits the development of the fungal pathogen *Venturia inaequalis* at a level similar to that of treatment with the inorganic compound fosetyl-aluminum (F-Al).

In bacteria, fructans play also an important role in the resistance to abiotic stresses by increasing water availability during water deficit (Bogino et al., 2013). They are involved in adhesion mechanisms by participating in the formation of biofilms (Morris and Monier, 2003) and interactions between bacteria (Velázquez-Hernández et al., 2009). They also contribute to bacterial pathogenicity. Pathogenic bacteria of the genera *Erwinia* and *Pseudomonas* secrete levans that form layers separating the bacteria from the plant cell wall during the early phase of infection, resulting in an inability for the plant to recognize the pathogen (Hettwer et al., 1995). Indeed, the disruption of the gene encoding the fructan-synthesizing enzyme in *Erwinia amylovora* (fire blight agent of the Pomoideae) increases the incubation period for symptom

onset in pear compared to plants treated with untransformed strains (Geier and Geider, 1993). In addition, their degradation products could have signaling functions in pathogenic or symbiotic interactions between plants and microorganisms (Versluys et al., 2017).

2. Fructan metabolism in plant and microorganisms

Based on the Carbohydrate-Active Enzymes database (CAZy), the fructan metabolizing enzymes belong to the Glycoside hydrolase (GH) family which hydrolyze the glycosidic bond between two or more carbohydrates or between a carbohydrate and a non-carbohydrate moiety (Yuan et al., 2012; http://www.cazy.org).

(a) Fructan synthesis and localization

In plants, the fructan metabolizing enzymes belong to the glycoside hydrolase family 32 enzymes (GH32) (Van den Ende et al. 2002; Cantarel et al., 2009; Lombard et al. 2014) (Table I-3).

Table I-3. The occurrence of GH32 enzymes in plants.

*The preferential donor and acceptor substrates are indicated. For more details and side activities see Vijn and Smeekens (1999) and Van Laere and Van den Ende (2002) and references therein. *6G-FFT transfers the fructose unit to the glucose moiety of sucrose/fructan. FBE: fructan biosynthetic enzymes; NA: not allocated. From Lammens et al. (2009).*

	Plant GH32 enzymes	Fructosyl donor	Fructosyl acceptor	EC number
Hydrolase	Acid invertases (vacuolar and cell wall invertase)	Sucrose	Water	3.2.1.26
	Fructan 1-exohydrolase (1-FEH)	Inulin	Water	3.2.1.153
	Fructan 6-exohydrolase (6-FEH)	Levan	Water	3.2.1.154
	Fructan 6&1-exohydrolase (6&1-FEH)	Inulin/Levan	Water	NA
FBE	Sucrose:sucrose 1-fructosyltransferase (1-SST)	Sucrose	Sucrose	2.4.1.99
	Fructan:fructan 1-fructosyltransferase (1-FFT)	Fructan	Sucrose/Fructan	2.4.1.100
	Sucrose:fructan 6-fructosyltransferase (6-SFT)	Sucrose	(Sucrose)/Fructan	2.4.1.10
	Fructan:fructan 6^G-fructosyltransferase* (6^G-FFT)	1-Kestose	Sucrose/Fructan	2.4.1.243

The synthesis of inulin or levan type requires the action of at least two fructosyltransferases (FTs), and three or four FTs are needed to synthesize more complex mixtures of fructans. (Lammens et al., 2009; Van Arkel et al., 2013; Fig. I-26):

- The sucrose: sucrose 1-fructosyl transferase (1-SST) (EC 2.4.1.99) catalyses the transfer of a fructosyl residue from one donor sucrose to the C1 of fructosyl residue of acceptor sucrose, producing 1-kestotriose and a glucose molecule (Van Laere and Van Den Ende, 2002; Van den Ende et al., 2005).

- The fructan: fructan 1-fructosyltransferase (1-FFT) (EC 2.4.1.100): is responsible for the elongation of 1-kestotriose to higher DP inulin. The 1-kestotriose serves as both donor and acceptor for inulin synthesis (Van den Ende et al., 2006).

- The sucrose: fructan 6-fructosyl transferase (6-SFT) (EC 2.4.1.1 0): transfers the fructosyl residue of donor sucrose to the C6 of fructosyl residue of acceptor sucrose (6-SST activity), producing 6-kestotriose. The 6-kestotriose can then be polymerized by 6-SFT leading to the levan synthesis. In addition, 6-SFT activity in the presence of a donor sucrose and an acceptor 1-kestotriose will form 1,6-kestotetraose (or bifurcose). The bifurcose can then be extended by 6-SFT and 1-FFT leading to the synthesis of graminan-type (branched) fructans (Duchateau et al., 1995; Sprenger et al., 1995; Lasseur et al., 2011).

- The fructan: fructan 6G-fructosyl transferase (6G-FFT) (EC 2.4.1.243): transfers the fructosyl residue of a donor 1-kestotriose to the glucosyl residue of an acceptor sucrose, producing 6G-kestotriose (also called neokestose). From 6G-kestotriose, the formation of neo-inulin type fructans can be produced by the action of 1- FFT or neo-levan type fructans by 6-SFT activity (Shiomi, 1989).

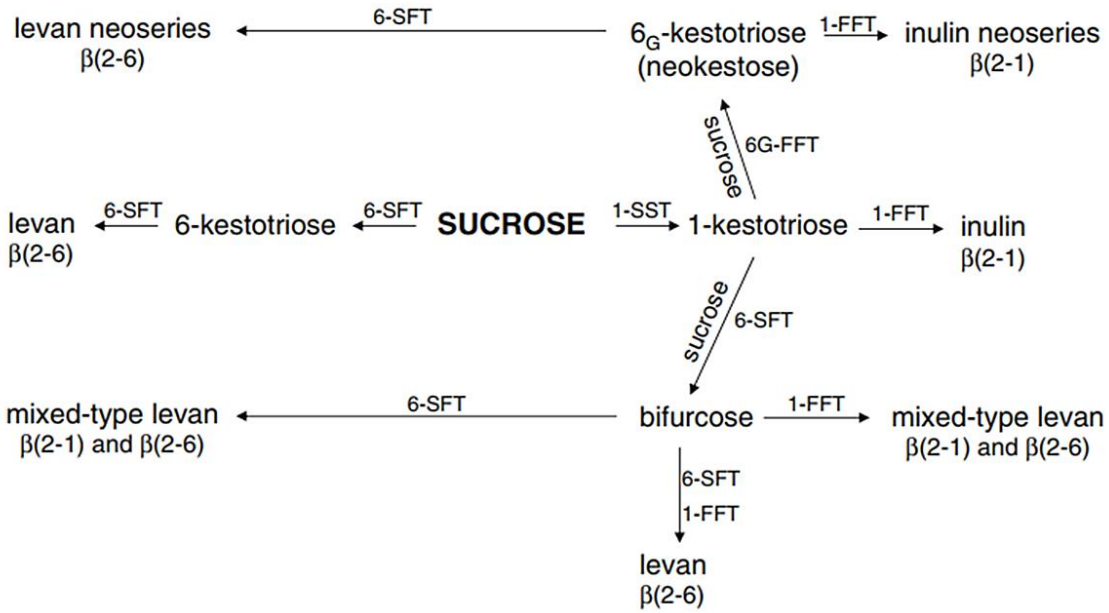

Figure I-26. Model of fructan biosynthesis in plants.

Starting from sucrose (Suc), structurally different fructan molecules can be produced by the concerted action of different fructosyltransferases. From Livingston et al. (2009).

At the tissue level, the accumulation of fructans occurs in specialized storage organs of many plant species such as tubers, corms, or bulbs (Hendry, 1993). Fructans can also be found in leaves, stems, roots, and other non-reserve organs in case where the supply of substrates

exceeds the demand of sucrose (Stumpf and Conn, 1980; Peukert et al., 2014; Cimini et al., 2015). In *Agave* species, fructans are found in all tissues including roots, rhizomes, leaves, and flowers although they accumulate to the highest levels in the oversized stem (Wang and Nobel, 1998; Mellado-Mojica et al., 2017; Pérez-López et al., 2021). In temperate Poaceae such as perennial ryegrass (*Lolium perenne*), fructans accumulate during the vegetative phase, especially at the base of the aerial parts consisting of the sheaths of mature leaves and the base of growing leaves, preferentially at the elongating zones (Pavis et al., 2001). FT activities were also highest in these tissues with a spatial correlation between enzyme activities and fructan storage (Pavis et al., 2001). Fructan stored in the leaf elongation zone serve as short-term storage for use in the development of the secondary wall (Allard and Nelson, 1991; Pollock and Cairns, 1991) and are used for regrowth after defoliation (Morvan-Bertrand et al., 2001). In wheat and barley, fructans are also stored in the stems during flower development and are hydrolyzed to provide carbon for grain filling (Bonnett and Incoll, 1993; Schnyder, 1993).

At the subcellular level, fructans are synthesized in the vacuole (Vijn and Smeekens, 1999; Ritsema and Smeekens, 2003) (Fig. I-27). Pollock and Chatterton (1988), citing Molisch (1921), reported the presence of inulin spherocrystals in the vacuole after precipitation with ethanol. This vacuolar localization of fructans and fructan synthesis has been confirmed later (Wagner et al., 1983). Vacuolar fructan synthesis leads to a decrease in cellular sucrose concentration and prevents sugar-induced feedback inhibition of photosynthesis (Vijn and Smeekens, 1999). However, some authors also mention an apoplastic localization of fructans. Fructan and its hydrolysis products have been localized in the apoplast in crown tissue and in leaf guttated liquid of oat after cold hardening (Livingston and Henson, 1998). The hypothesis regarding their apoplastic localisation is that fructans once synthesized in the vacuole could be transported *via* a vesicle-mediated mechanism, leading to apoplastic localization (Valluru et al., 2008). Fructans have also been found in the phloem of *Agave deserti* (Wang and Nobel, 1998)

and 6-kestotriose has also been found in the phloem of transgenic in potato expressing a yeast-derived invertase (Zuther et al. 2004).

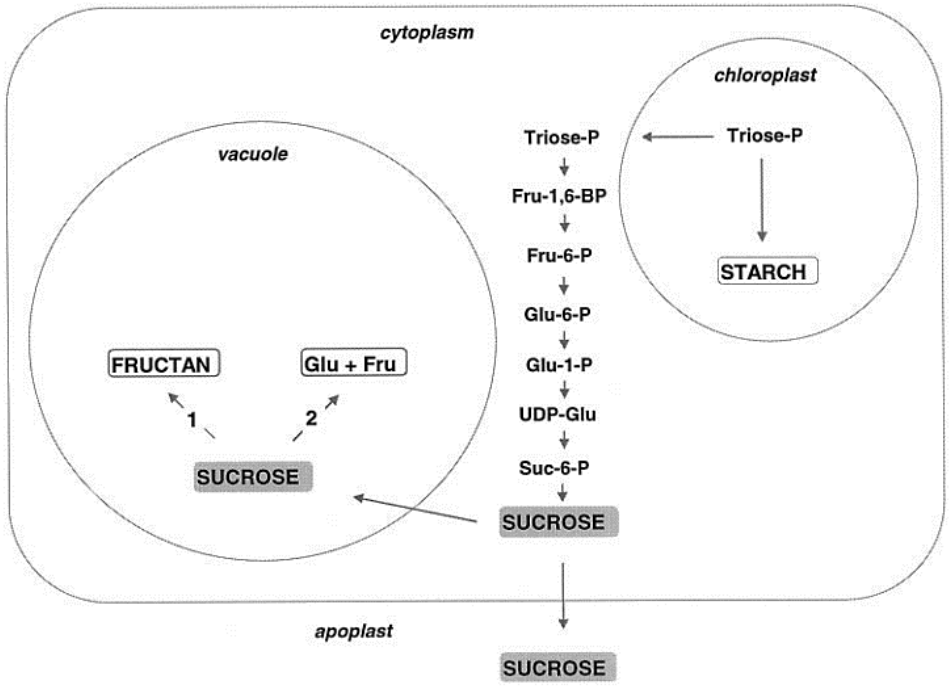

Figure I-27. Schematic representation of carbohydrate metabolism in a plant cell.

High photosynthetic activity is associated with high rates of carbon export from the chloroplast to the cytoplasm, resulting in an increase of intermediates for Suc synthesis. The synthesized Suc is either distributed to the vacuole (storage) or to the apoplast (export). In the vacuole, Suc can be converted into fructans by fructosyltransferases (1) or hydrolyzed into Glu and Fru by invertase (2). From Vijn and Smeekens (1999).

In bacteria, fructans can be synthesized by three classes of extracellular enzymes which belong to the GH68 family (Cantarel et al. 2009; Lammens et al., 2009). Bacterial levans are produced extracellularly from sucrose by the action of levansucrase (EC 2.4.1.10) which catalyzes different reactions including the hydrolysis of sucrose, the synthesis of 6-kestotriose from sucrose, and the polymerization of levans using sucrose as a fructosyl donor (Martínez-Fleites et al., 2005). Levans can also be synthesized by fructosyltransferase that belongs to the same class of enzymes as levansucrase (EC 2.4.1.10; Srikanth et al., 2015) and bacterial inulins are synthesized by inulinosucrase (EC 2.4.1.9) which are only present in lactic acid bacteria (Velázquez-Hernández et al., 2009;).

In bacteria fructans and their synthetic enzymes are extracellularly localized (Velázquez-Hernández et al., 2009; Dogsa et al., 2013). Bacterial fructans are thus part of the exopolysaccharides (EPS) that contribute to biofilm formation, an assembly of microorganisms adhering to each other and/or to a surface and embedded in an EPS matrix (Morris and Monier,

2003; Lembre et al., 2012). In fungi, similarly to bacteria, FOS are produced from sucrose by the action of a single enzyme which may be a β-fructofuranosidase (EC 3.2.1.26) or a fructosyltransferase (EC 2.4.1.9) (Trollope, 2015).

(b) Fructan degradation

In plants, fructan degradation is carried out by fructan exohydrolases (FEHs) that hydrolyze the *O*-glycosidic linkage of the fructosyl unit at the end of fructan to release fructose according to the reaction formula below (Simpson and Bonnett, 1993; De Roover et al., 1999; Lothier et al., 2007; Yoshida, 2021).

$$\text{G-F-Fn} \rightarrow \text{G-F-F}\ (n-1) + \text{F}\ (n \geq 1)$$

As FTs, they are glycoproteins which belong to the GH32 family (Lammens et al., 2009). Two main types of FEHs can be distinguished, the 1-fructan exohydrolases (1-FEHs) and 6-fructan exohydrolases (6-FEHs) which preferentially hydrolyze the β-(2,1) and β-(2,6) linkages, respectively (De Coninck et al., 2007). The FEHs *sensus strictus* are strictly specific to fructans and do not hydrolyze sucrose. However, sucrose acts as an inhibitor on some FEH isoforms (De Roover et al., 1999; Van Riet et al., 2008).

1-FEHs have been characterized in wheat (1-FEHw1, w2 and w3; Bancal et al., 1991; Van den Ende et al., 2003a; Van Riet et al., 2008), barley (Henson and Livingston, 1998), chicory (1-FEH I; 1-FEH IIa and 1- FEH IIb; De Roover et al., 1999; Van den Ende et al., 2001), Jerusalem artichoke (Marx et al., 1997b), perennial ryegrass (Lothier et al., 2007), *Bromus pictus*, a cold-tolerant Patagonian Poaceae (Del Viso et al., 2009) and *Arctium lappa*, an Asteraceae (Ueno et al., 2011).

6-FEHs, which preferentially hydrolyze β-(2,6) linkages, have been characterized in barley (Henson and Livingston, 1996), perennial ryegrass (Marx et al., 1997a; Lothier et al., 2014), wheat (Van Riet et al., 2006), and timothy (Tamura et al., 2011).

In addition, 6&1-FEHs that can hydrolyze both β-(2,1) and β-(2,6) linkages have been identified in cocksfoot (Yamamoto and Mino, 1985), annual ryegrass *Lolium rigidum* (Bonnett and Simpson, 1995), and wheat (Kawakami et al., 2005). More specific FEHs preferentially degrading kestotrioses (KEHs) have been identified in onion (1-KEH; Benkeblia et al., 2005) and wheat (6-KEH; Van den Ende et al., 2005).

As FTs, FEHs activities have been observed in vacuoles isolated from Jerusalem artichoke (*Helianthus tuberosus L.*) protoplasts, so the vacuolar compartment is considered to be the site

of both fructan synthesis and degradation (Frehner et al., 1984). However, as fructans, the presence of FEH activity has been also demonstrated in the apoplast in oat after cold hardening (Livingston and Henson, 1998). Phylogenetic proximity between FEHs and cell-wall invertases (Cw-INVs).

In bacteria, fructans can be degraded by levansucrases when they use water as a fructosyl acceptor and thus act as hydrolases. In addition, bacteria possess levanases (exo- and endo-levanase) and inulinases (exo- and endo-inulinase) which belong to the GH32 family, as well as non-specific β-fructosidases which can also hydrolyze fructans (Fuchs et al., 1985; Vijn and Smeekens, 1999; Lammens et al., 2009). Similarly, endo-inulinases are also present in fungi (Vijn and Smeekens, 1999). While plant FEHs are unifunctional enzymes, degrading fructans but not sucrose (Van Laere and Van den Ende, 2002), microbial exo-inulinases can degrade sucrose as well (Le Roy et al., 2007a).

E. FEHs in non fructan-plants

In a phylogenetic tree based on protein sequences, FTs are grouped with vacuolar invertases (V-INVs) while FEHs are grouped with the cell wall invertases (Cw-INVs) (Fig. I-28). FEHs would derive directly from an ancestral Cw-INV and would subsequently acquire a vacuolar addressing signal peptide (Van den Ende et al., 2002) while the FTs would derive after a few mutations from an ancestral V-INV (Vijn and Smeekens, 1999), which itself would derive from an ancestral Cw-INV (Sturm, 1999).

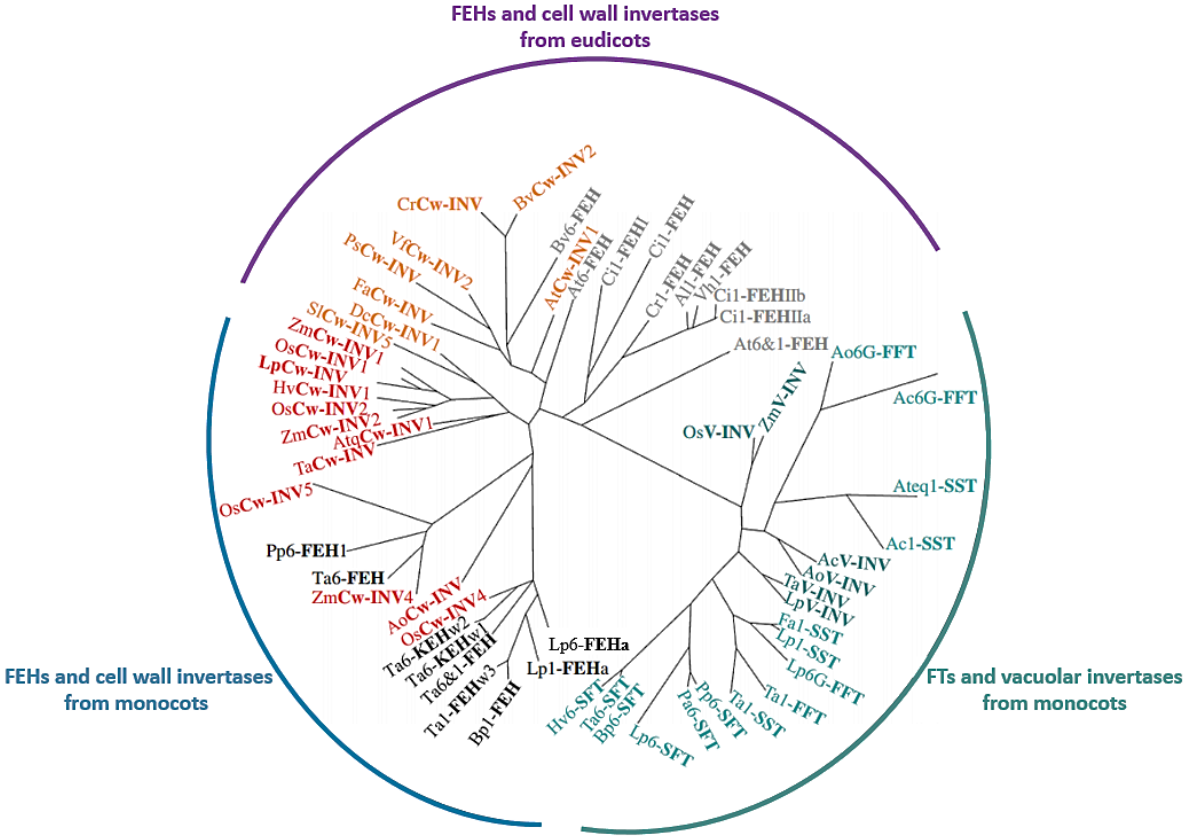

Figure I-28. Phylogenetic tree of FEH, cell wall invertases (Cw-INV), fructosytransferases (FT) and vacuolar invertases (V-INV) of plants based on predicted amino acid sequences (ClustalW/Drawtree).

FEH: Arabidopsis thaliana 6-FEH (AB029310); Arabidopsis thaliana 6&1-FEH (AY060553); Arctium lappa 1-FEH (AB611034); Beta vulgaris 6-FEH (AJ508534); Bromus pictus 1-FEH (GQ247882); Campanula rapunculoides 1-FEH (AJ509808); Cichorium intybus 1-FEH (Y11124); Cichorium intybus 1-FEHI (AJ242538); Cichorium intybus 1-FEHIIa (AJ295033); Cichorium intybus 1-FEHIIb (AJ295034); Lolium perenne 1-FEHa (DQ016297); Lolium perenne 6-FEHa (EU219846); Phleum pratense 6-FEH1 (AB583555); Triticum aestivum 1-FEHw1 (AJ516025); Triticum aestivum 6-FEH (AM075205); Triticum aestivum 6&1-FEH (AB089269); Triticum aestivum 6-KEHw1 (AB089271); Triticum aestivum 6-KEHw2 (AB089270); Vernonia herbacea 1-FEH (AM231149) Cw-INV: Agave tequilana Cw-INV1 (JN790057); Asparagus officinalis Cw-INV (AB244731); Arabidopsis thaliana Cw-INV1 (X74514); Beta vulgaris Cw-INV2 (AJ277458); Chenopodium rubrum Cw-INV (X81792); Daucus carota Cw-INV1 (M58362); Fragaria ananassa Cw-INV (AF000521); Hordeum vulgare Cw-INV1 (AJ534447); Lolium perenne Cw-INV (DQ073969); Oryza sativa Cw-INV1 (AY578158); Oryza sativa Cw-INV2 (AY578159); Oryza sativa Cw-INV4 (AY578161); Oryza sativa Cw-INV5 (AY578162); Pisum sativum Cw-INV (AF063246); Solanum lycopersicum Cw-INV5 (AJ272304); Triticum aestivum CwINV (AF030420); Vicia faba Cw-INV2 (Z35163); Zea mays CwINV2 (AF050128); Zea mays Cw-INV4 (AF043347) FT: Agave tequilana 1-SST (DQ535031); Allium cepa 1-SST (AJ006066); Allium cepa 6G-FFT (Y07838); Asparagus officinalis 6G-FFT (AF084283); Bromus pictus 6-SFT (FJ424612); Festuca arundinacea 1-SST (AJ297369); Hordeum vulgare 6-SFT (X83233); Lolium perenne 1-SST (AY245431); Lolium perenne 6-SFT (AF494041); Lolium perenne 6G-FFT (AF492836); Phleum pratense 6-SFT (BAH30252); Poa ampla 6-SFT (AF192394); Triticum aestivum 1-SST (AB029888); Triticum aestivum 1-FFT (AB088409); Triticum aestivum 6-SFT (AB029887) V-INV: Allium cepa V-INV (AJ006067); Asparagus officinalis V-INV (AF002656); Lolium perenne V-INV (AY082350); Oryza sativa V-INV (AF276703); Triticum aestivum V-INV (AJ635225); Zea mays V-INV (P49175). From Lothier et al. (2014).

To our knowledge, more than ten FEHs have been purified to homogeneity (De Coninck et al., 2007; Ould-Ahmed, 2013) and many genes have been cloned in various eudicot and monocot (Table I-4). For these genes, the FEH activities of the corresponding recombinant proteins produced by heterologous expression in the yeast *Pichia pastoris* have been demonstrated Indeed, because of the phylogenetic proximity, the distinction between FEHs and Cw-INVs based on their protein sequence analysis is not possible.

Therefore, in non-fructan-accumulating species, the genes whose nucleotide sequences show high homologies with Cw-INVs sequences are generally classified by default as genes encoding Cw-INVs. However, functional characterizations of purified proteins and/or corresponding recombinant proteins produced in heterologous systems have shown that some of these genes identified as encoding Cw-INVs actually encode proteins with FEH activity. In *Arabidopsis*, the enzymes originally named AtcwINV3 and AtcwINV6 (*Arabidopsis thaliana* cell wall invertase 3 and 6) have been identified as FEHs that hydrolyse β-(2,6) or both β-(2,1) and β-(2,6) linkages, respectively (De Coninck et al., 2005; Table I-4). They were thus re-named At6-FEH and At6&1FEH, respectively. In addition, the presence of a 6-FEH was discovered in the taproots of the non-fructan plant *Beta vulgaris* (Van den Ende et al., 2003b). Recently, three Cw-INV-related enzymes named *Zm-6&1-FEH1* (Zhao et al., 2019), Zm-6-FEH (Huang et al., 2020) and *Zm-6&1-FEH2* (Wu et al., 2021), displaying FEH activity, were identified in maize (Table I-4).

This discovery has led to the hypothesis that they could act as defense-related proteins in plant-microorganism interactions by hydrolyzing levan-containing slimes surrounding endophytic or phytopathogenic bacteria such as *Pseudomonas* or *Erwinia* (Hettwer et al., 1995; Bereswill et al., 1997). Since levans form a separating layer between bacteria and plant cell wall polymers during the early stages of plant-pathogen interaction, the expression of FEHs might have a crucial role by preventing levan formation and pathogen infection (Hettwer et al., 1995; Van den Ende et al., 2004). Moreover, FEHs have been proposed to be involved in stabilizing the symbiosis between plants such as sugar beet (Tallgren et al., 1999) or sugar cane (Hernández et al., 2000) and fructan-producing beneficial bacteria (Van den Ende et al., 2004).

Furthermore, this hypothesis is supported by the fact that the FEHs identified in maize (*Zm-6&1-FEH1* and *Zm-6&1-FEH2*) are localized in the apoplast, which would allow it to act directly on microbial extracellular fructans (Zhao et al., 2019; Wu et al., 2021). It is also possible that following an injury or pathogen attack that disrupts the plasma membrane and tonoplast, vacuolar FEHs are discharged into the apoplast compartment. The FEHs thus present in the cell wall would be able to degrade the microbial fructans (Fig. I-29), leading to (i) the modification of the properties of the biofilm which could reduce virulence, and (ii) the release of fructose and FOS which could play the role of MAMPs/PAMPs. These MAMPs/PAMPs would be recognized by a PRR triggering PTI as mentioned in section B, which will induce the defense response by signaling cascades involving phytohormones such as SA, JA, and ET (Rejeb et al., 2014). An argument in favor of this hypothesis is that exogenous application of SA and MeJa (Methyl Jasmonate, a JA derivative) leads to increased expression of FEHs in agave (*Agave americana*) which is known as a fructan accumulator plant (Suárez-González et al., 2016). Moreover, the recent discovery of a 6-FEH that degrades microbial levans in *Cichorium intybus*, a plant species that accumulates only β-(2,1)-linked fructans (inulins) strengthens the hypothesis of the role of certain FEHs in plant-microbial interaction (Versluys et al., 2021).

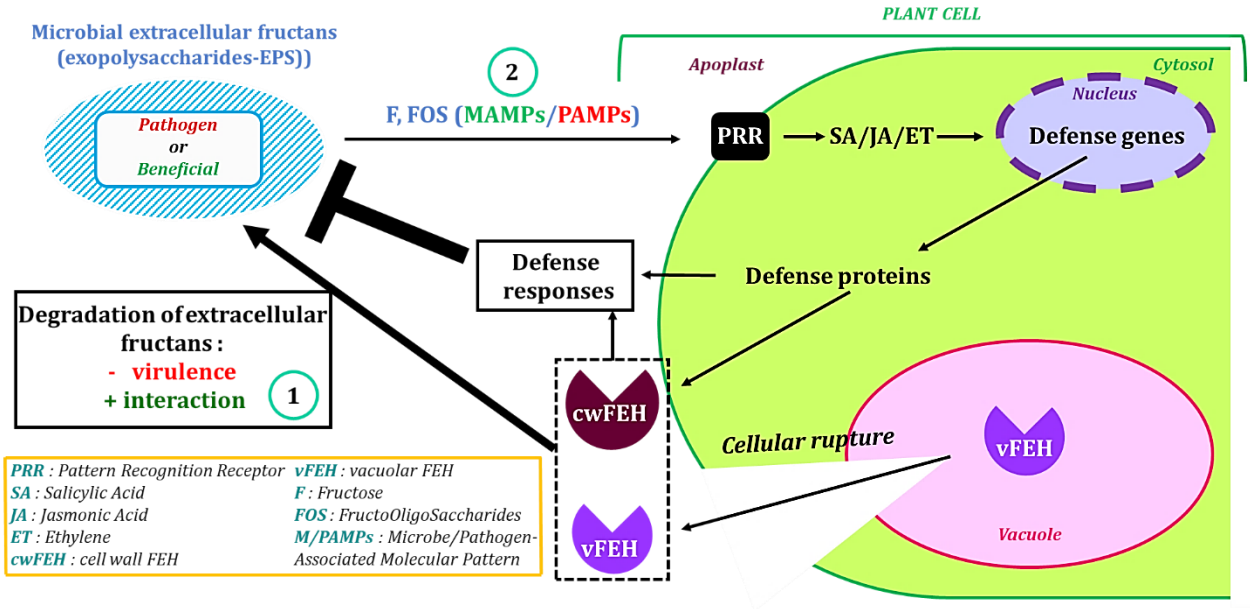

Figure I-29. Schematic representation of FEHs potential roles during biotic stress.

Some FEHs would be apoplastic, others vacuolar and could be released into the apoplast following a rupture of the tonoplast and the plasma membrane. In both cases, these FEHs could degrade the microbial fructans and the consequences would be: 1) to modify the properties of the biofilm, which could reduce virulence; 2) to release FOS that could act as MAMPs/PAMPs whose recognized by a PRR receptor triggering the signal transmission (SA/JA/ET in particular) and the defense response. Modified from Versluys et al. (2017) and Rejeb et al. (2014).

Table I-4. Summary of selected cDNAs from FEHs of plants.

Completed from De Coninck et al. (2007) and Ould-Ahmed (2013).

	Plant species	Enzyme + accession number	*Plant parts tested*	pI (pH)	cDNA derived Mr (kDa)	*Length of ORF*	*Potential glycosylation sides*	*Confirmation heterologous expression*	References
Fructan accumulating plants	*Cichorium intybus*	1-FEH I AJ242538	belgian endive leaves and forced roots	6.5	60.5	568	10	*Solanum tuberosum*	Van den Ende et al., 2000
		1-FEH IIa AJ295033		5.24	61	581	3	*Pichia pastoris*	Van den Ende et al., 2001
		1-FEH IIb AJ295034		5.24	61	581	3	No	Van den Ende et al., 2001
	Phleum pratense	Pp6-FEH1 AB583555	haplocorms	5.5	63.4	601	5	*Pichia pastoris*	Tamura et al., 2011
	Lolium perenne	Lp1-FEHa DQ016297	stubble	5.22	65.4	584	4	*Pichia pastoris*	Lothier et al., 2007
		Lp6-FEHa EU219846		5.5	60.9	580	5	*Pichia pastoris*	Lothier et al., 2014
	Triticum aestivum	Ta1-FEHwl AJ516025	senescing wheat stems	4.79	61.2	597	4	No	Van den Ende el al., 2003a
		Ta1-FEHw2 AJ508387		4.78	61.2	596	4	No	Van den Ende el al., 2003a
		Ta1-FEHw3 AJ564996		4.88	61	596	4	*Pichia pastoris*	Van Riet et al., 2008
		6-FEH AM075205	spike tissue	6.5	65	590	5	*Pichia pastoris*	Van Riet et al., 2006
		6-KEHwl AB089271	wheat crowns, stems and ears at anthesis stage	4.91	61	589	5	*Pichia pastoris*	Van den Ende et al., 2005
		6-KEHw2 AB089270		4.88	61	587	5	*Pichia pastoris*	Van den Ende et al., 2005
		6&1-FEHwl AB089269	wheat crowns	5.2	61	595	5	*Pichia pastoris*	Kawakami et al., 2005
Non-fructan accumulating plants	*Arabidopsis thaliana*	AtcwINV3 (6-FEH) NM104385	all plant	5.52	67	595	4	*Pichia pastoris*	De Coninck et al., 2005
		AtcwINV6 (6&1-FEH) NM121230		4.79	62	551	3	*Pichia pastoris*	De Coninck et al., 2005
	Beta vulgaris	Bv6-FEH AJ508534	roots	5.0	62.9	606	9	*Pichia pastoris*	Van den Ende et al., 2003b
	Zea mays	Zm6&1-FEH1 EU971090	basal part of leaf	9.05	80	595	3	*Pichia pastoris*	Zhao et al., 2019
		Zm6&1-FEH2 BT055913	maize leaf	6.06	80	588	5	*Pichia pastoris*	Wu et al., 2021

F. Objectives

My research work focused on the evaluation of the role of glycomolecules in root defense with particular emphasis on fructans and fructan metabolizing enzymes in two non-fructan Brassicaceae, the model species *Arabidopsis thaliana* and the species of agronomic interest *Brassica napus*, and in a fructan plant, *Lolium perenne*, a *Poaceae* of regional interest due to its role as a grassland fodder plant.

The main objectives were:

- To characterize the RET of perennial ryegrass (*L. perenne*). This work aims to fill the lack of knowledge on the polysaccharide composition of AC-DCs and their associated mucilage in *Lolium perenne* in particular and in fructan plants in general.

- To clarify the roles of FEHs in two non-fructan accumulating plants, rapeseed (*Brassica napus)* and *Arabidopsis thaliana*. The purpose of this work is based on the hypothesis that these FEHs are defense-related proteins that are part of the immune response. To do so, the work was divided into three parts:

The first part concerned the characterization of two new monoclonal antibodies (mAbs) directed against fructans which were produced in collaboration with the company BIOTEM. Antibody specificities have been studied using dot blot on a wide range of carbohydrates. Microscopic observations by immunocytochemistry with the two anti-fructans mAbs were carried out on the surface and on high-pressure frozen sections of root tips of perennial ryegrass and of *A. thaliana* for comparison. The results are presented in the form of a scientific publication corresponding to section II of the "Results" which is entitled: "*Generation and characterization of two monoclonal antibodies that recognized β-(2,1) and β-(2,6)-fructan epitopes: new tools to unravel the functions and subcellular localizations of fructans in plants*".

The second part consisted to examine the occurrence of cell-wall glycomolecules in AC-DCs and mucilage of perennial ryegrass root using immunocytochemistry. The microscopical analysis was done on the root tips of not only perennial ryegrass but also of two other monocots, timothy (*Phleum pratense*) and wheat (*Triticum aestivum*), as well as on the root tips of *A. thaliana* for comparison. The response of the RET of ryegrass to the presence of flagellin22 (flg22) and water stress were also being investigated. The results are presented in the form of a scientific publication corresponding to section I of the "Results" which is entitled:

"*Microscopical characterization of the root extracellular trap (RET) of perennial ryegrass (Lolium perenne), a fructan producing plant".*

The third part contains two subsections. The first subsection corresponds to the study of the expression profiles of defense marker and FEHs genes in *B. napus* and *A. thaliana* treated at the root level with phytohormones involved in defense responses which are SA, MeJA, and precursor of ethylene, the 1-Aminocyclopropane-1carboxylic acid (ACC). Based on the sequences of the two FEH genes of *A. thaliana* (*At6-FEH* and *At6&1-FEH*; De Coninck et al., 2005), four genes encoding a putative 6&1-FEH and two genes encoding a putative 6-FEH were identified in *Brassica napus*. The results are presented in the form of a scientific publication corresponding to section III of the "Results" which is entitled: "*Salicylic acid upregulates fructan exohydrolases (FEH) together with defense-marker genes in non-fructan plants.*

The second subsection aimed to study the involvement of FEHs in root defense by using knock-out mutants of *A. thaliana* lacking FEH genes. Seeds of wild-type and FEH mutant lines were inoculated with two strains (with or without the levansucrase gene encoding the enzyme synthesizing levans) of the non-pathogen root-colonizing bacterium *Pseudomonas brassicacearum*. The preliminary results are presented in section IV of the "Results" which is entitled: "*Involvement of bacterial levans and plant fructan exohydrolases (FEHs) in Arabidopsis thaliana root colonization by Pseudomonas brassicacearum*".

Thus, with regards to fructan plants, my thesis work makes it possible to fill the currently limited knowledge relating to the characterization of the RET and the localization of fructans in the root of perennial ryegrass, and to answer the following questions:

- Is there production of root border cells and mucilage at the root tip of perennial ryegrass? Which types of root border cells are released?

- Which glycomolecules predominate in the RET, root border cells and root sections of perennial ryegrass?

- How does the RET of perennial ryegrass respond to the presence of flagellin22 (flg22)?

With regards to non-fructan producing plants, my thesis work provides answers to the following questions:

- Are the expression profiles of FEH genes similar to those of defense marker genes in response to root treatment with SA, MeJA or ACC?

- Do responses to SA applied at the root level in *B. napus* show genetic variability?

- Are plant FEHs and bacterial extracellular fructans (levans) involved in the plant-bacteria interactions?

II. Materials and methods

A. Seed sterilization and plant growth conditions

1. Seed sterilization

Arabidopsis thaliana ecotype Colombia-0 (Col-0) and timothy (*Phleum pratense* var. Aturo) seeds are placed in a sterile vial under sterile conditions in a horizontal laminar flow hood. A solution of 70% (v/v) ethanol is added to the seeds for 5 min. Then, ethanol is removed and replaced with commercial sodium hypochlorite (9.6 % chlorine bleach) diluted to 0.9% (v/v sterile distilled water) for 2 min. The sodium hypochlorite is then removed and the seeds are rinsed 6 times with sterile distilled water.

Perennial ryegrass (*Lolium perenne* var. Delika) seeds are surface sterilized with commercial sodium hypochlorite (9.6 % chlorine bleach) for 2 min under sterile conditions in horizontal laminar flow hoods (Heath et al., 1998). Then the seeds are washed 6 times with sterile distilled water before sowing.

Wheat (*Triticum aestivum* var. Chevignon) seeds are sterilized with 70% (v/v) ethanol for 10 min in horizontal laminar flow hoods. After removing all of the ethanol, commercial sodium hypochlorite (9.6 % chlorine bleach) diluted to 0.9% (v/v sterile distilled water) is added to the seeds for 10 min. Finally, the seeds are washed 6 times with sterile distilled water before being soaked in sterile distilled water overnight in the dark.

For the *in vitro* root colonization experiments with *Pseudomonas brassicacearum, A. thaliana* seeds (wild-type Col-0 and FEH knock-out mutants) are placed in a 2 mL sterile Eppendorf tube. 2 mL of a sterilization solution containing 1 mL 2.5 % chlorine bleach, 9mL ethanol absolute, and 3 drops of Tween 80 (Sigma-Aldrich-V000749) is added to the seeds for 6 min. Then seeds are washed 4 times with absolute ethanol and dried naturally in a Petri dish under sterile conditions in horizontal laminar flow hoods before sowing.

2. Plant growth

(a) In vitro in square Petri dishes.

- Perennial ryegrass and timothy

Murashige and Skoog (MS) medium (Murashige and Skoog, 1962) (Duchefa Biochemie) is solubilized in distilled water (4.33 g/L) and supplemented with 1% (w/v) agar (European Bacteriological Agar-A01254). The medium (pH 5.8) is autoclaved and then poured into several

square Petri dishes (120x120 mm, Fisher Scientific) with a proportion of 50 mL of medium per dish. After cooling, the sterilized seeds of perennial ryegrass and timothy are placed on the MS medium (10 seeds per plate) (Fig. II-1B, D). The seeds are gently placed into the agar with sterile tweezers to maintain their position when the plates are upright. Also, in this way, the radicle of the seeds will grow downwards. The dishes are then sealed with surgical tape (Anapore-135321), wrapped with aluminum foil to maintain darkness, and placed vertically to avoid the loss of border-like cells in a phytotron at 21 °C. After 48h in the dark to synchronize the germination, the seeds are grown for 10 days under a photoperiod of 16h day/8h night at 21°C.

- *Arabidopsis thaliana*

Arabidopsis medium (Duchefa Biochemie) is prepared in distilled water containing 11.82 g/L and 1% (w/v) agar supplemented with 2mL of 1M $Ca(NO_3)_2$. After being autoclaved, 50mL of medium (pH 5.8) is poured into square Petri dishes and cooled before sowing. In each dish, 10 sterilized seeds are sown by using a sterilized pipette tips 10µL (Fig. II-1C). The dishes are then sealed with surgical tape (Anapore-135321), wrapped with aluminum foil to maintain darkness, and placed vertically to avoid the loss of border-like cells in a phytotron at 21 °C. After 48h in the dark to synchronize the germination, the seeds are grown for 10 days under a photoperiod of 16h day/8h night at 21°C for 10 days.

- Wheat

MS medium diluted to 1:2 in distilled water (2.17 g/L) is prepared with 1% (w/v) agar supplemented. The MS ½ medium is autoclaved and poured into square Petri dishes (120x120 mm). For each dish, 6 sterilized seeds are lightly pressed into the agar with sterile tweezers under sterile conditions in a laminar flow hood (Fig. II-1E). Then, the dishes are sealed with

surgical tape and are placed vertically in phytotron at 21°C under a photoperiod of 16h day/8h night for 4 days.

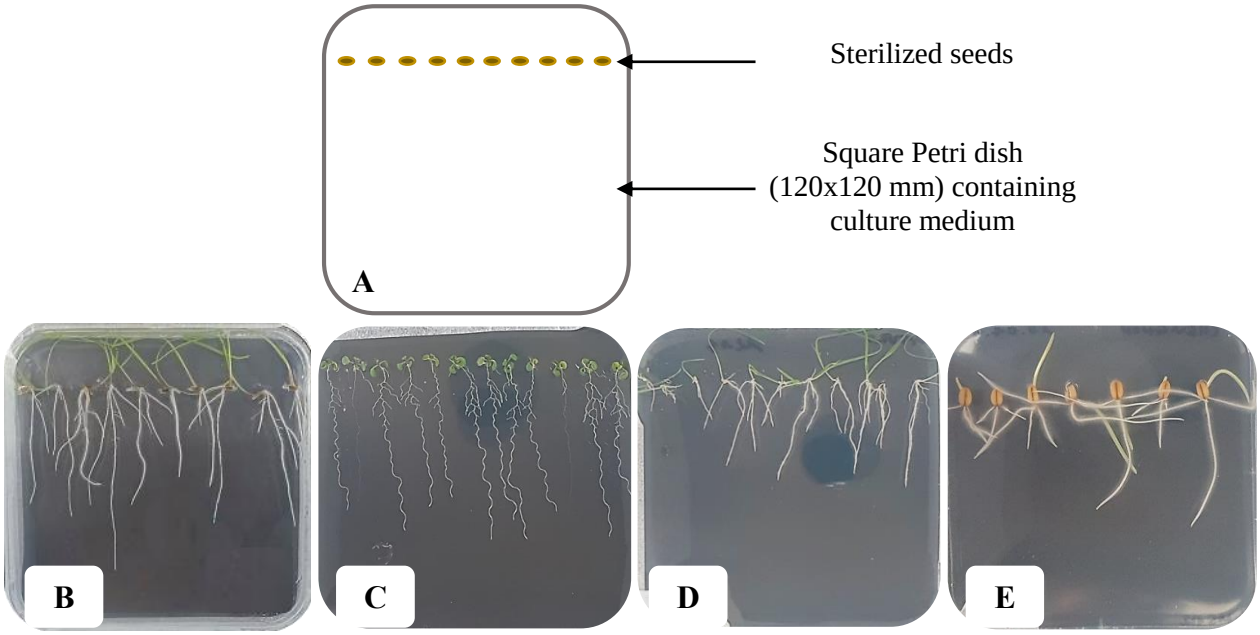

Figure II-1. In vitro plant growth in dishes.

(A) Schematic representation of the culture dish in agar medium. Photographs of 10-d-old perennial ryegrass seedlings (B), 10-d-old Arabidopsis seedlings (C), 10-d-old timothy seedlings (D), 4-d-old wheat seedlings (E).

(b) In hydroponics

- *Arabidopsis thaliana* and *Brassica napus*

Arabidopsis thaliana ecotype Colombia-0 (Col-0) and *Brassica napus* rapeseed (five varieties; 'Aviso', 'Tenor', 'Darmor-*bzh*', 'Yudal', 'Bristol' provided by the BrACySol biological resource center, INRAE Ploudaniel, France) are used. Seeds of both species are soaked in darkness for 48 hours at 4°C in 0.1% (w/v) agar solution to synchronize germination. Each seed is individually sown on the top of a 1.5 mL (*B. napus*) or 0.5 mL (*A. thaliana*) microtube pierced at the bottom and filled with 0.7% (w/v) agarose (Fig. II-2A). Each microtube containing a seedling is transferred to a plastic tank (fifteen plants per tank) containing 10L of Hoagland ¼ nutrient solution. The composition of nutrient solution is detailed in the table. II-1. *A. thaliana* is grown in a plant growth chamber with a PAR (Photosynthetically Active Radiations) of 110 µmol photons·m^{-2}·s^{-1} under a photoperiod of 16 h and a thermoperiod of 20/18°C day/night. *B. napus* is grown weeks in a greenhouse with natural light supplemented by high-pressure sodium lamps (Philips, MASTER GreenPower T400W) with a PAR (Photosynthetically Active Radiations) of 450 µmol photons·m^{-2}·s^{-1} at canopy height with a photoperiod of 16 h and a

thermoperiod of 20/17°C day/night. The nutrient solution is aerated and renewed every 7 days. When the fourth leaf *(B. napus*) or the eighth leaf (*A. thaliana*) has emerged, the microtubes were transferred in 150mL pots (five plants per pot) containing 50 mL of nutrient solution supplied with 0.5 mM SA, 50 µM MeJA, 20 µM ACC (Sigma-Aldrich, Saint-Louis, MO, USA) or without supplement (control) for 3, 6, 12, and 24 h according to the experiment. At the end of the treatment period, plants were collected. The shoot was separated from the root, and each tissue was frozen in liquid nitrogen and stored at -80°C. Before RNA and protein extractions, plant tissue was ground in liquid nitrogen in a precooled mortar and pestle until a fine powder was obtained and the frozen powder was stored at -80°C.

- Perennial ryegrass

Perennial ryegrass (*L. perenne* var. Delika) seeds are soaked in darkness for 48 hours at 4°C in 0.1% (w/v) agar solution to synchronize germination. Each seed is individually sown on the top of a 5 mL microtube pierced at the bottom and filled with 0.7% (w/v) agarose (Fig. II-2B). Each microtube with one seedling is transferred to a plastic pot (two plants per pot) containing 700 mL of 'EVA' nutrient solution (Table II-2). Plants are grown for 7 weeks in a plant growth chamber with high-pressure sodium lamps (Philips, MASTER GreenPower T400W) provide a PAR (Photosynthetically Active Radiations) between 10 and 150 µmol photons·m^{-2}·s^{-1} under a photoperiod of 16 h and a thermoperiod of 21/18°C day/night. The nutrient solution is aerated and renewed every 7 days.

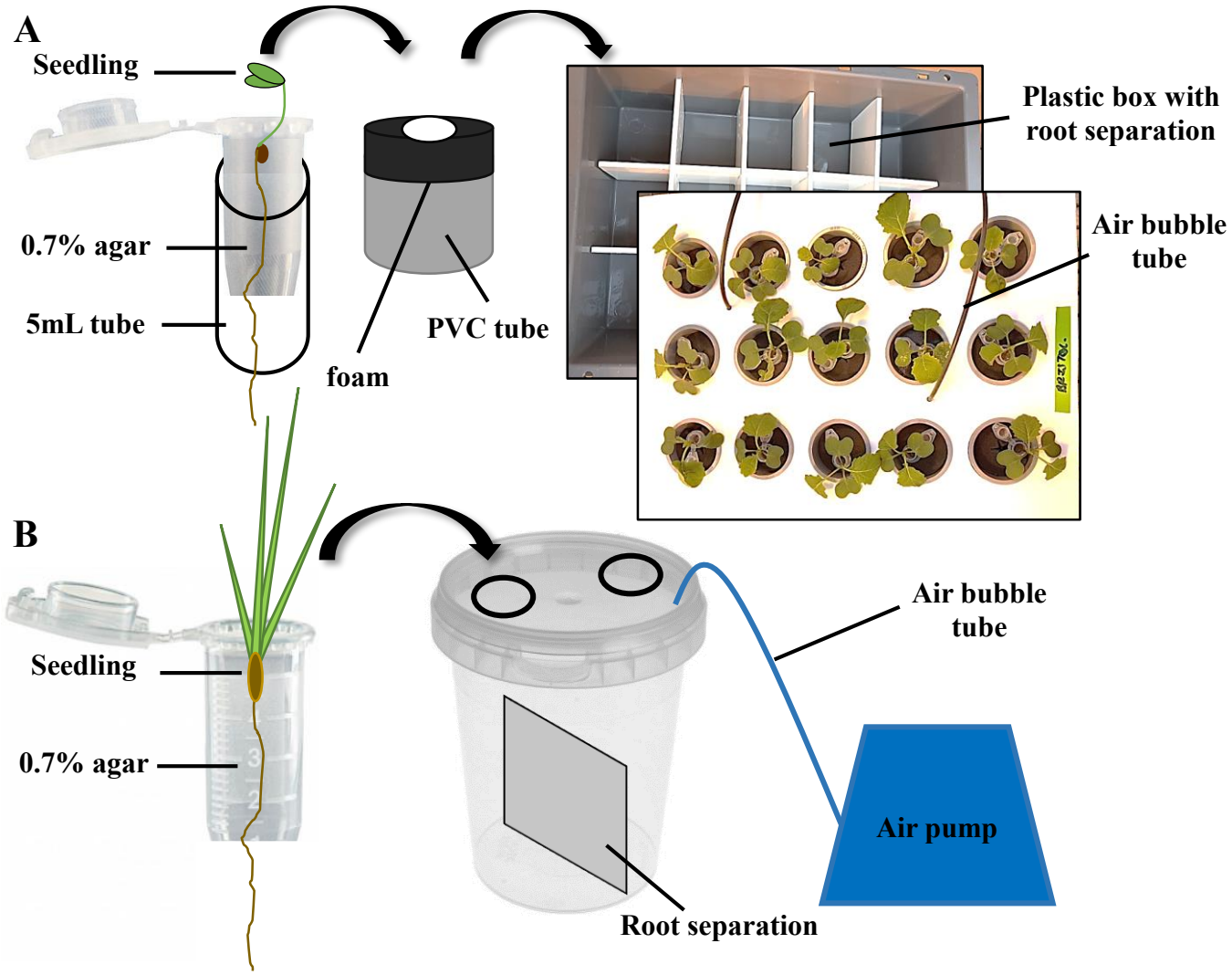

Figure II-2. Experimental design for seedling production.

After being soaked for 48 hours at 4°C in 0.1% (w/v) agar solution. (A) Rapeseed (Brassica napus) and Arabidopsis thaliana seedlings are grown for 2.5 - 4 weeks in a hydroponic system at 20°C under a photoperiod of 16h day/8h night. (B) Perennial ryegrass (Lolium perenne) seedlings are grown for 7 weeks in a hydroponic system at 21°C under a photoperiod of 16h day/8h night.

Table II-1. Composition of the Hoagland ¼ nutrient solution used for the culture in hydroponics of Arabidopsis and rapeseed (Brassica napus).

Salts	Molar mass	[final conc] mM	[stock conc] $mol.L^{-1}$	[stock conc] $g.L^{-1}$	vol. stock solution (mL/ 20 L)
$Ca(NO_3)_2.4H_2O$	236.1	1.25	1.25	295.13	20
KNO_3	101.1	1.25	0.5	50.55	50
KH_2PO_4	136.1	0.25	0.5	68.05	10
$MgSO_4.7H_2O$	246.47	0.5	1	246.47	10
$EDTA.NaFe.3H_2O$	421	0.2	0.08	33.68	50
Trace elements	Molar mass	[final conc] µM	[stock conc] $mol.L^{-1}$	[stock conc] $g.L^{-1}$	vol. stock solution (mL/ 20 L)
H_3BO_3	61.83	14	28	1.731	10
$MnSO_4.H_2O$	169.01	5	10	1.69	
$ZnSO_4.7\ H_2O$	287.5	3	6	1.725	
$CuSO_4.5\ H_2O$	249.68	0.7	1.4	0.35	
$(NH_4)_6Mo_7O_{24}$	1235.6	0.7	1.4	1.729	
$CoCl_2$	237.93	0.1	0.2	0.0475	

Table II-2. Composition of the 'EVA' nutrient solution used for the culture in hydroponics of perennial ryegrass (Lolium perenne).

Salts	Molar mass	[final conc] mM	[stock conc] $mol.L^{-1}$	[stock conc] $g.L^{-1}$	vol. stock solution (mL/ 20 L)
K_2SO_4	174.25	1	0.4	69.7	50
NH_4NO_3	80.04	1	2	160.08	10
KH_2PO_4	136.1	0.4	0.8	108.88	10
K_2HPO_4	174.2	0.15	0.3	52.26	10
$CaCl_2.2H_2O$	147.02	3	3	441.06	20
$MgSO_4.7H_2O$	246.47	0.5	1	246.47	10
$EDTA.NaFe.3H_2O$	421	0.2	0.08	33.68	50
$CaCO_3$ (last added)	100.8	0.907	0.36	36.29	50
Trace elements	Molar mass	[final conc] µM	[stock conc] $mol.L^{-1}$	[stock conc] $g.L^{-1}$	vol. stock solution (mL/ 20 L)
H_3BO_3	61.83	14	28	1.731	10
$MnSO_4.H_2O$	169.01	5	10	1.69	
$ZnSO_4.7\ H_2O$	287.5	3	6	1.725	
$CuSO_4.5\ H_2O$	249.68	0.7	1.4	0.35	
$(NH_4)_6Mo_7O_{24}$	1235.6	0.7	1.4	1.729	
$CoCl_2$	237.93	0.1	0.2	0.0475	

B. Study of the RET in perennial ryegrass

1. Selection and collection of root tips

Plant growth and root tip collection collection methods are key steps for RET preservation. Root tips are collected from plants grown in square Petri dishes. In the case of perennial

ryegrass, *Arabidopsis* and timothy, the plants used are those whose roots have developed on the surface of agar without penetrating it and which do not detach from it (Fig. II-3A). For wheat, the roots remained in contact with the culture medium without leaving it. This ensures intact RET with optimal hydration. The selected roots are excised with ultra-fine tweezers and placed on the appropriate surface for observation, without touching other surfaces, in order to limit the loss of RET (Fig. II-3B).

For these observations, roots are removed with ultra-fine tweezers (Fig. II-3A) and placed on Superfrost microscope slides (Thermo Scientific). Then, 30 µL of distilled water are added to the root apex and two deposits of 30 µL are placed at each end of the slide (Fig. II-3).

A coverslip (50x60mm, Thermo Scientific) is placed on the sample and then taped to the slide with anapore tape. The amount of liquid is adjusted by capillary action from the ends towards the center of the sample. The samples are then observed under an inverted bright-field microscope (Leica DMI6000B, Wetzlar, Germany). For this experiment, 24–30 roots are observed to ensure representativity for each set of observations.

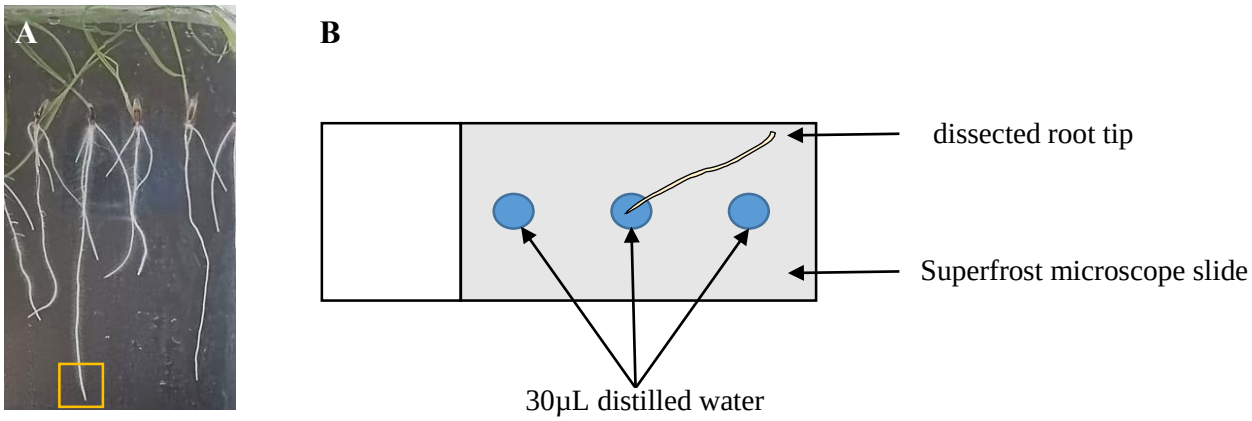

Figure II-3. Schematic representation of root preparation for microscopic observation.
(A) 10-d-old perennial ryegrass grown in dishes (B) The root tip is cut and collected with a ultra-fine tweezer and is deposited in the liquid on the microscope slide 10 min before observation.

2. Water deficit treatment

This experiment is performed by the addition of various amounts of polyethylene glycol (PEG) (molecular weight 8000; Sigma, St Louis, MO) to the growth medium following the protocol described by van der Weele et al. (2000) and Verslues et al. (2006). Initially, 300 g of PEG are added to 1L of autoclaved MS ½ liquid medium (2.17 g/L MS medium, pH 5.7) with stirring. Then, 45mL of MS ½ liquid medium containing PEG is poured on the top of 30mL solidified MS ½ medium with 1% agar prepared previously in a square Petri dish (120x120 mm). During

approximately 12-15h (overnight), the PEG diffuses into the solidified MS ½ medium thus lowering its water potential. After one night the solution on the top of the plate was removed and the dish is used for experiments.

The 6-d-old perennial ryegrass seedlings are transferred on the dish containing 30mL of solidified MS ½ medium mixed with 45mL of liquid MS ½ medium without PEG for the "well-watered" control medium, which gives a water potential of approximately -0.10MPa, whereas other 6-d-old seedlings are transferred on the plate soaked with PEG (300g L^{-1}).

Then, all dishes are sealed with surgical tape and placed vertically in phytotron at 21 °C under a photoperiod of 16-h-day/8-h-night until 12 days. The 12-d-old roots are collected for mucilage observation and immunocytochemistry experiment.

3. Visualization of mucilage by counterstaining with India ink

India ink (Black star Hi-Carb, 1.0 oz) produced from carbon black is used as a negative stain to visualize mucilage (Curlango-Rivera et al., 2013). The root tips are collected and placed on Superfrost microscope slides (Thermo Scientific) (Fig. II-3). Two deposits of 30 µL of distilled water are placed at each end of the slide and then 30 µL are added to the root apex. A coverslip (50x60 mm, Thermo Scientific) is placed on the sample and sealed to the slide with anapore tape. A 0.05% (w/v) India ink solution is added by capillary action between the slide and the coverslip from the ends to the center of the sample. After 10 min, the samples are observed under an inverted bright field microscope (DMI6000B). For this experiment, 4 to 5 technical replicates and 6 biological replicates are performed.

4. MAMPs

The MAMPs used in this study include the synthetic peptide flg22 (Felix et al., 1999) synthesized by Dr. J. Leprince (PRIMACEN platform, University of Rouen). MAMP preparations were made from mycelium extracts of *Fusarium oxysporum* (Hano et al., 2006). Flg22 were used at 1 µM (Millet et al., 2010).

5. Surface immunolabeling of root border cells, mucilage and root tips

In order to label the polysaccharides, glycoproteins, and proteoglycans present in the cell wall of root border cells and in the mucilage, an indirect surface immunolabeling method has been developed. This protocol was recently described by Castilleux et al. (2020).

Roots of 10-d-old seedlings are placed onto sterile 10-welled diagnostic microscope slides (Thermo Scientific, ER-208B-CE24) (Fig. II-4A, II-4B). The wells are then filled up with 30 µL of phosphate-buffered saline (PBS) for 5 min to initiate detachment of root border cells. Next, the liquid is removed using an Eppendorf micropipette (P200), by taking from the severed end of the root (Fig. II-4B). The root samples are fixed for 40 min in 4% (w/v) PFA (paraformaldehyde), in 50 mM PIPES pH 7 (piperazine- N, N'-bis [2-ethanesulfonic acid], Alfa Aesar, A16090) containing 1 mM $CaCl_2$. Roots are washed 4 times for 10 min at room temperature (RT) in PBS 1x containing 1% (w/v) bovine serum albumin (BSA; AURION, Wageningen, The Netherlands) to remove as much PAF as possible and to allow saturation of the non-specific sites in the sample.

After removing the last washing solution, 30 µL of primary antibody solution (Ac.I: PlantProbes, Leeds, UK) diluted to 1:5 in the solution of PBS+1%BSA are added and incubated overnight at 4 °C in a humid chamber (Fig. II-4C). The primary antibody solution is removed (Fig. II-4B) before performing four washes with PBS+1% BSA at RT for 10 min.

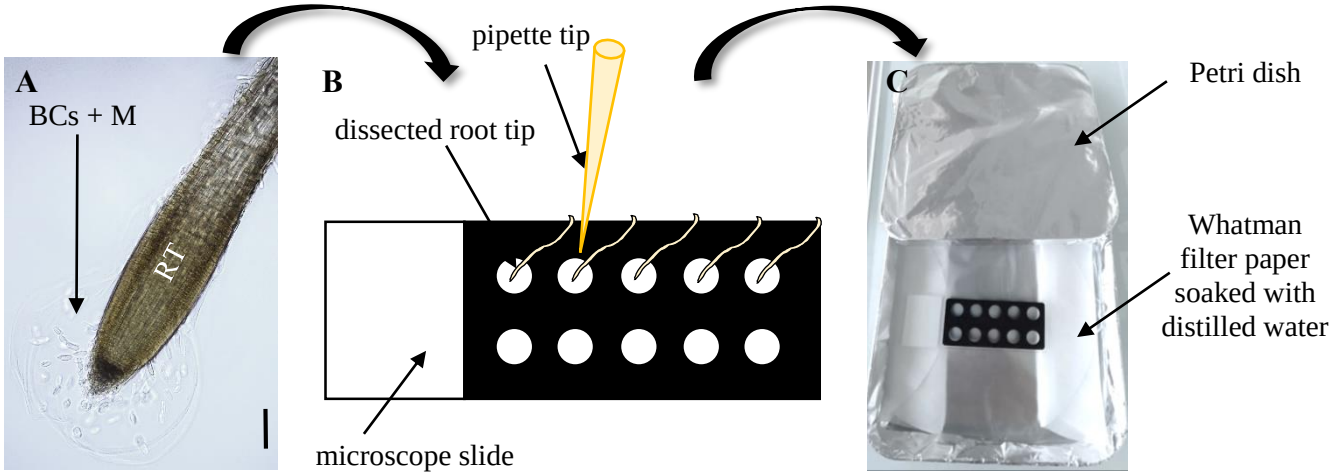

Figure II-4. Schematic representation of root preparation for immunolabeling experiment.

(A) 10-d-old perennial ryegrass roots containing root border cells (BCs) and mucilage (M). (B) The root tip is cut and collected with a ultra-fine tweezer and is deposited in 10-welled diagnostic microscope slide. The liquid is gently and slowly removed from the well with a pipette to avoid disruption of the RET. (C) Photograph of the humid chamber used to maintain sample humidity during the experiment.

The goat anti-rat IgG secondary antibody conjugated to Alexa Fluor 594 (Invitrogen) is diluted to 1:50 in the solution of PBS+1%BSA and incubated with the samples for 2 h at 25°C in the dark. Four washes with PBS+1% BSA are then carried out at RT for 10 min to remove the secondary antibody, followed by a final wash with PBS at RT for 10 min. To avoid

photobleaching, citifluor (Agar scientific, AF2 R1320) is delicately deposited on the sample using a pipette tips 200µL. The slides are then stored in a humid chamber in the dark at 4°C. The samples are observed under an epifluorescence microscope (Leica DMI6000B, Wetzlar, Germany; $\lambda_{Excitation}$: 591 nm; $\lambda_{Emission}$: 614 nm). For this experiment, 3 to 4 technical replicates and 4 to 6 biological replicates are carried out.

6. High-Pressure Freezing/Freeze Substitution (HPF) sample preparation

Dissected 12-d-old root tips of *Arabidopsis* and perennial ryegrass were transferred into the cavity of copper cupules (100 µm depth; 0.6 mm diameter and 200 µm depth; 0.6 mm diameter, respectively). For the perennial ryegrass, the outermost senescent leaf sheaths are discarded from the shoot and a 10-mm long segment is dissected from the basal point of attachment of the leaves including mature leaf sheaths and elongating leaf bases. 0.5mm long sample of leaf bases are dissected from the 10 mm long segments and are also transferred into the cavity of two copper cupules (300 µm depth; 0.6 mm diameter). The cupules are coated with soybean (*Glycine max*) lecithin (100 mg mL^{-1} in chloroform) (Fig. II-5). The excess medium is removed using filter paper. The sample carriers were securely attached to the sample holder pod using a horizontal loading station. Then, samples arre frozen using a high-pressure freezing HPF-EM HPM 100 (Leica Microsystems) with a maximum cooling rate of 20,000°C s^{-1}, an incoming pressure of 7.5 bars, and a working pressure of 4.8 bars. Cupules containing frozen samples are stored in liquid nitrogen until the freeze-substitution procedure is initiated.

After high-pressure freezing, samples are transferred to a freeze-substitution automate (AFS, Leica Microsystems) precooled to −140°C. Samples are substituted in anhydrous acetone with 0.5% uranyl acetate at −90°C for 96 h (Ovide et al., 2018). Using a gradient of +2°C h^{-1}, the temperature is gradually raised from −90 to −15°C with two intermediate steps at −60 and −30°C. Samples are washed twice at RT with fresh anhydrous acetone. Resin infiltration is processed at −15°C in a solution of ethanol/London Resin White (LRW) with successive ratios of 2:1 overday; 1:1 overnight and 1:2 overday followed by a final step in a pure LRW solution renewed twice during 48 h. The LRW is finally polymerized into the AFS apparatus at −15°C under ultraviolet light for 48 h. Using a Leica ultramicrotome EM-UC7 (Leica Microsystems), semithin sections (0.5 µm) were cut and adhered onto 10-welled diagnostic microscope slides (Thermo Scientific, ER-208B-CE24) pre-coated with Poly-L-Lysine (EMS-19320-B, dilution 1:10 in filtered water). The HPF sections are stained with toluidine blue to highlight components.

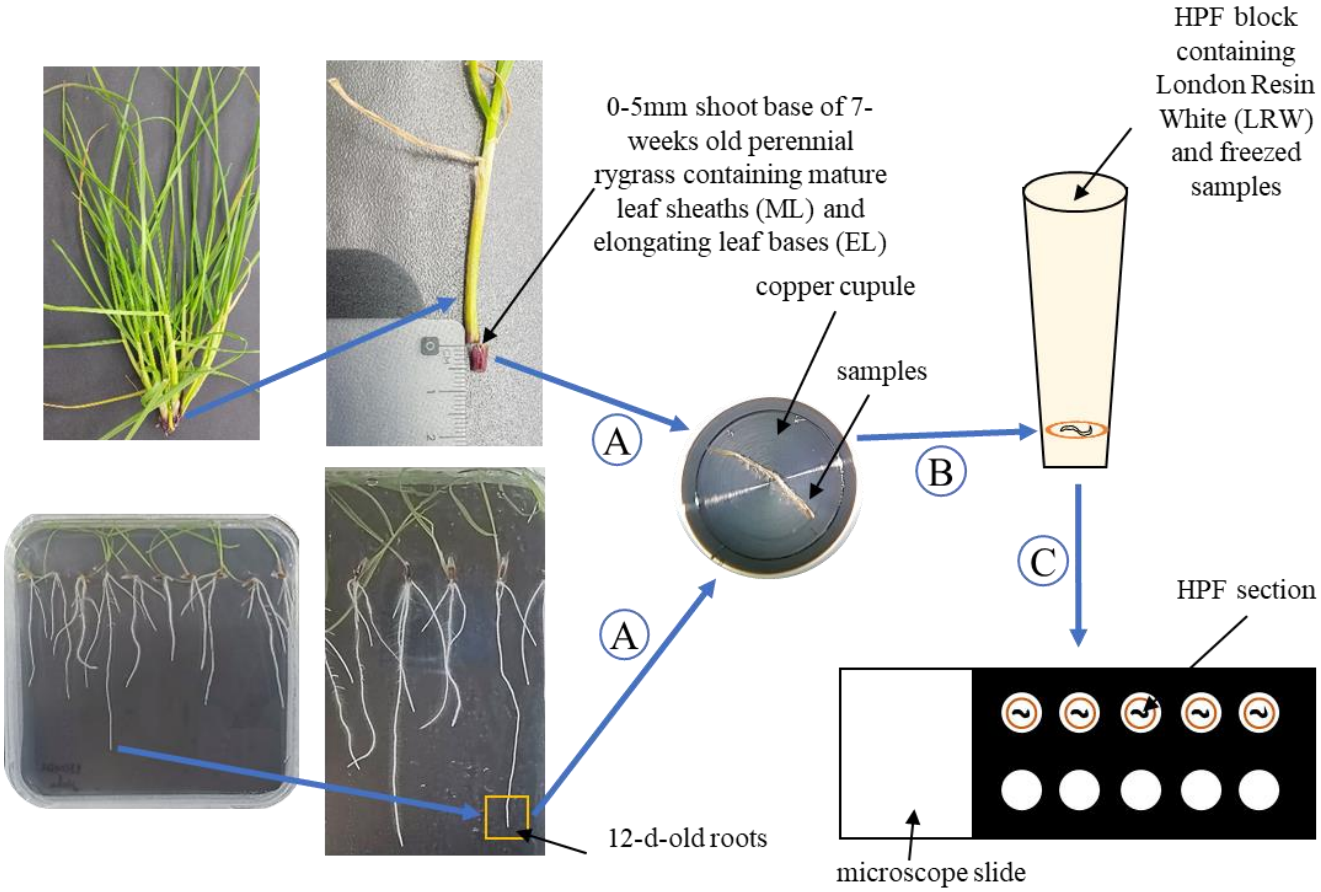

Figure II-5. Schematic representation of high-pressure freezing/freeze substitution (HPF) sample preparation. (A) Sample preparation in the cupule coated with soybean (Glycine max) lecithin. (B) Freezing sample preparation by using a high-pressure freezing HPF-EM PACT I and freeze-substitution automate (AFS). (C) Semithin sections (0.5 µm) are cut off by using a Leica ultramicrotome EM-UC7.

7. Immunolabeling of HPF sections of root border cells, mucilage and root tips

Semithin sections (0.5 µm) of 12-d-old roots and leaf bases on 10-welled Teflon microscope slides coated with Poly-L-Lysine (Fig. II-5) are blocked in PBS 1x with 0.1% (v/v) Tween 20 (PBST) containing 3% (w/v) BSA and normal goat serum (NGS-dilution 1:20) for 30 min at RT. Then, sections are carefully washed 5 times for 5 min with 0.1 % PBST containing 1% BSA. After washing, sections are incubated overnight at 4°C with primary antibody (dilution 1:2 in 0.1% PBST containing 1% BSA and NGS (diluted 1:20)). On the next day, sections are washed 5 times for 5 min with 0.1 % PBST containing 1% BSA before being incubated with secondary goat anti-rat IgG antibody conjugated to Alexa Fluor 594 (Invitrogen) at1:200 dilution in 0.1% PBST containing 1% BSA and NGS (diluted 1:20) for 2 h at 25°C. Sections are rinsed 5 times at RT for 5 min with 0.1 % PBST containing 1% BSA and two final washes

for 5 min at RT with ultrapure water. Then, a droplet of ultrapure water is added to the section in each well. Epifluorescence of the immunostained tissue sections is observed on an epifluorescence microscope (Leica DMI6000B, Wetzlar, Germany; $\lambda_{Excitation}$: 591 nm; $\lambda_{Emission}$: 614 nm). Controls are performed by omission of primary antibodies. For this experiment, 3 technical replicates and 4 biological replicates are performed.

8. Ultrastructural and immunogold analyses using transmission electron microscopy

Ultrathin sections (90 nm; EM UC6 Leica microsystems) of ryegrass root tips from HPF samples prepared previously are collected on nickel formvar-coated grids. For immunogold analysis, sections are blocked in PBS 1X containing 3% BSA for 30 min at RT. Sections are then incubated with the primary antibody (JIM13, PlantProbes, Leeds, UK; dilution 1:2 in PBS 1x containing 0.3% BSA for overnight at 4 °C in a humid chamber. After washing in PBS 1x containing 0.3% BSA, grids are incubated for 1 h at 37 °C with the goat anti-rat secondary antibody conjugated to 10 nm gold particles (dilution 1/20 inPBS 1x containing 0.3% BSA; British Biocell International). Before transmission electron microscopy observation, all sections are stained with classical staining using uranyl acetate (0.2% in methanol) and lead citrate (Delta microscopies, ref: 11.000) and Reynolds lead citrate (Delta microscopies, ref: 11.300). Observations are made with a FEI Tecnai 12 Biotwin transmission electron microscope operating at 80 kV, with ES500W Erlangshen CCD camera (Gatan).

9. Primary antibodies table

Primary antibodies with epitopes associated with different parietal polysaccharides are mainly provided by PlantProbes (University of Leeds, UK) and Biosupplies Australia (http://www.biosupplies.com.au). A summary table of the antibodies used in this project as well as the epitopes recognized by the antibodies and their associated references are presented in table II-3.

10. Statistical and image analysis

Microscope images were acquired by counterstaining with India ink and measurements made using ImageJ 1.53p. The RET surface obtained was determined on by measuring the total surface of the RET containing the root cap and then subtracting the surface of the root cap. Data were analyzed with R software version 4.0.0. Statistical significance was calculated by using the Kruskal–Wallis test and the statistical effect is considered significant with $P<0.05$.

Table II-3. Primary antibodies and associated epitopes of different cell wall polysaccharides used in this project.

	Cell wall polymers	mAbs	Epitopes	References
Hemicelluloses	Xylan	LM10	(1,4)-β-xylosyl residues	McCartney et al., 2005
	Arabinoxylan and low-substituted xylan	LM11	(1,4)-β-xylosyl residues	McCartney et al., 2005
	Grass Heteroxylan	LM27	Unknown	Cornuault et al.,2015
	Glucuronoxylan	LM28	Glucuronosyl residues of xylan	Cornuault et al.,2015
	Feruloylated polymers	LM12	Feruloylated xylan	Pedersen et al., 2012; Bozbuga et al., 2018
	Mixed linkage glucan (MLG)	MLG	(1,3; 1,4)-β-D-glucan	Meıkle et al., 1994; Vega-Sánchez et al., 2013
Pectins	Homogalacturonans (HGs)	LM19	HG with low degree of esterification	Verhertbruggen et al., 2009; Ordaz-Ortiz et al., 2009
		LM20	HG with high degree of esterification	Verhertbruggen et al., 2009; Ordaz-Ortiz et al., 2009
	Galactan chains	LM5	(1,4)-β-D-galactan, Rhamnogalacturonan-I (RG-I)	Jones et al. ,1997; Willats et al., 1998; Ermel et al., 2000
	Arabinan chains	LM6	(1,5)-α-L-highly branched arabinan, RG-I	Willats et al., 1998; Lee et al., 2005; Moller et al., 2007
Extensins	Extensin from rice	LM1	Unknown	Smallwood et al.,1995
	Extensin from carrot	JIM11	Unknown	Smallwood et al.,1994; Yates et Knox, 1994
	Extensin from carrot	JIM12	Unknown	Smallwood et al.,1994
	Extensin from pea	JIM19	Unknown	Knox et al., 1995; Wang et al., 1995
	Extensin from pea	JIM20	Unknown	Smallwood et al.,1994; Pattathil et al., 2010
Arabinogalactan proteins (AGPs)	AGP from rice	LM2	β-D-GlcpA	Smallwood et al.,1996; Yates et al., 1996
	AGP from carrot	JIM13	β-D-GlcA-(1,3)-α-D-GalA-(1,2)-α-L-Rha	Yates and Knox, 1994; Yates et al.,1996
	AGP from carrot	JIM15	Unknown	Yates and Knox, 1994; Yates et al.,1996
	AGP from carrot	JIM16	Unknown	Yates and Knox, 1994; Yates et al.,1996
	AGP from sugar beet	JIM8	Unknown	Pennell et al.,1991

C. Characterization of two new monoclonal antibodies against β-(2,1) and β-(2,6)-plant fructans

1. Antibody generation

The company BIOTEM (Apprieu, France) produced the mAbs by immunising mice with antigenic compounds prepared from two purified plant fructans, inulins from Cichorium intybus and levans from Phleum pratense, both supplied by Megazyme (Wicklow, Irland) under references P-INUL and P-LEV, respectively. After the immunizations, hybridoma preparation and cloning were performed by BIOTEM while we were in charge of screening the hybridoma and sub-clones for the presence of antibodies reacting with inulins and levans by immune-dot blot.

Five mice (Oncins France 1 strain) were injected three times at three-week intervals with inulins and levans conjugated to bovine serum albumin (BSA). The first injection was made subcutaneously and intraperitonealy with complete Freund's adjuvant and the two others intraperitonealy with incomplete Freund's adjuvant. Ten days after the third immunization, the levels of serum immunoglobulins anti-inulins and anti-levans conjugated or not to BSA were tested by indirect competitive ELISA. The mice were injected again three times intraperitonealy the same antigens and incomplete Freund's adjuvant at three-week intervals and ten days after the sixth immunization, the levels of serum immunoglobulins anti-inulins and anti-levans conjugated or not to BSA were again tested. Three month later, the mice were injected again two times intraperitonealy of free inulins and levans and incomplete Freund's adjuvant at two-week intervals and ten days after the eighth immunization, the levels of serum immunoglobulins anti-inulins and anti-levans conjugated or not to BSA were again tested by ELISA and also by immune-dot blot against free inulins and levans. One month after the last injection, a selected mouse was given an intravenous injection of free inulins and levans without adjuvant. Three days after the boost injection, the mouse was sacrificed and the spleen was taken for lymphocytes isolation. The lymphocytes were fused with Sp2/0-Ag14 myeloma cell line using standard hybridoma preparation. The hybridoma supernatants from the fusion were screened for the presence of antibodies reacting with inulins and levans by immune-dot blot. Two hybridomas were selected for subcloning by dilution. Crude hybridoma supernatants were used as the source of two monoclonal antibodies (mAbs) named BTM9H2 and BTM15A6. The

determination of the immunoglobulin isotypes revealed that both antibodies are IgG (IgG1 λ for BTM9H2 antibody and IgG2a κ for BTM15A6).

This study was carried out in strict compliance with French and European animal protection policy. BIOTEM received the approval of the "Direction Départementale de la Protection des Populations de l'Isère (38)" under the number D 38 013 10 001. The animal protocol has been reviewed and approved by the BIOTEM ethics committee.

2. Carbohydrate samples

Commercially available carbohydrates were purchased and prepared as detailed in Table S1.
For preparation of water soluble carbohydrate (WSC) extracts and purification of fructans from perennial ryegrass (*Lolium perenne* var. Bravo; 0-5 cm shoot base), plants were grown hydroponically in green-house for 8 weeks as described in Lothier et al. (2014). WSC extraction and quantification and fructan purification were carried out to the methods described by Benot et al. (2019) and Morvan et al. (1997), respectively

For preparation of WSC extracts of cocksfoot (*Dactylis glomerata*; 0-3 cm shoot base) and dandelion (*Taraxacum officinalis*; roots), tissue was sampled from wild plants taken from the green spaces of the campus of University of Caen. Water soluble carbohydrate (WSC) extracts were prepared and quantified according to the method described by Benot et al. (2019).

3. Immuno-dot blot assay

The immuno-dot blot technique is used to detect the binding capacity of the anti-fructan mAbs on circular deposits of a wide range of carbohydrates to test the specificity of anti-fructan antibodies. The list of the carbohydrate used for this study is given in Appendix 1. The protocol is adapted from Li et al. (2010) and Manceur et al. (2017).

The sheets of Bio-Dot filter paper and nitrocellulose membrane (0.2 µm-Amersham protran-ref.10600006) are pre-wet in TBS 1x (Tris-buffered saline: Tris 20mM and NaCl 500mM), pH 7.5). For each carbohydrate solution, a serial dilution is done with ultrapure water to obtain five quantities of each carbohydrate solution (5, 25, 50, 125, 250 µg) in 50 µL. For each dilution, 50 µL are loaded into the dot-blot wells in duplicate. Ultrapure water is used as a negative control. By suction through the 96-well dot-blotting equipment (DHM96, Scie-Plas), samples were blotted onto the nitrocellulose membrane.

The membrane is then blocked in the TBS 1x containing 0.1% Tween 20 (0.1% TBST) for 2 h at RT with shaking, followed by overnight incubation at 4˚C with 5µg.mL^{-1} anti-fructan

antibodies diluted in 0.1% TBST blocking buffer. After 3 washes 10 min each with 0.1% TBST, the membranes are incubated for 2 h at RT with Horseradish Peroxidase (HRP)-conjugated secondary antibody diluted 1:3000 in 0.1% TBST blocking buffer. Then, three washes 10 min each with 0.1% TBST and one wash 10 min with TBS 1x are performed. Secondary antibodies are detected using a chemiluminescent substrate kit (SuperSignal™ West Pico PLUS-ref. 34580). After 5 min incubation, the image of the blot is captured with VILBER chemiluminescence imaging system (Fusion FX - ref. Imager E-box CX5 EDGE) (Fig. II-6). Control membranes are performed by omission of primary antibodies. Two secondary antibodies are used which are goat anti-mouse IgG (H+L), HRP conjugate (A16078-Invitrogen), and chicken anti-mouse IgG (H+L), HRP conjugate (A15981-Invitrogen). The change in the secondary antibody was due to a significant binding of goat anti-mouse secondary antibody on fructan extracted from perennial ryegrass without the presence of anti-fructans antibodies (control membranes).

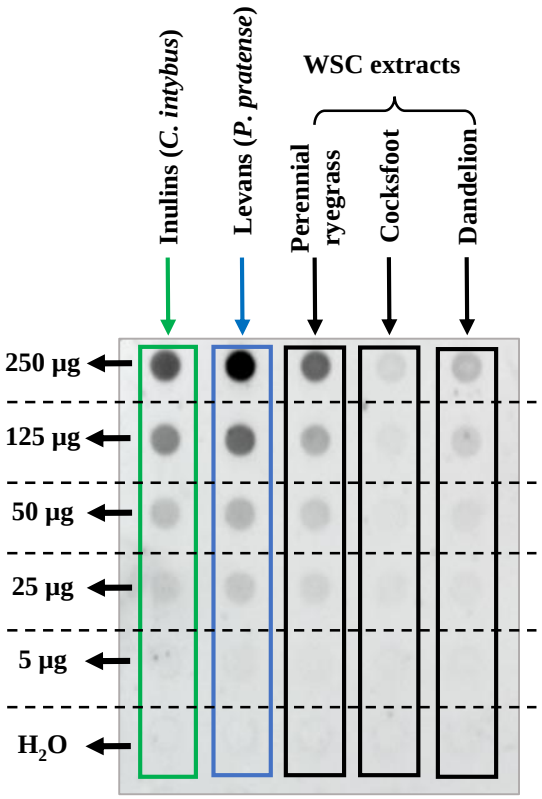

Figure II-6. Illustration of immuno-dot blot assay of the binding of anti-fructan antibodies to a series of fructans and other water soluble carbohydrate (WSC) extracts.

Samples were applied to nitrocellulose membrane (50µL per dots) at concentration allowing to depose from 5 to 250 µg.

4. Immuno-dot blot analysis

The immune-dot blot image analysis were performed using Fiji, an image processing package of ImageJ2 (Schindelin et al., 2012; https://imagej.net/software/fiji/) following the dot-blot analysis method described on the ImageJ website (https://imagej.nih.gov/ij/docs/examples/dot-

blot/index.html). The integrated density of luminescence was determined on each dot by measuring the grey level of the pixels (volume) inside the circular selection of the dot. The integrated density of each dot was normalized against the integrated density obtained with 250 µg of levans from timothy.

5. Localization by immunofluorescence of fructan epitopes

The localization of epitopes recognized by anti-fructan mAbs is performed on root tips according to the protocol described previously in **section B.5** of materials and methods (Fig. II-4). A donkey anti-mouse IgG secondary antibody (Ac. II) conjugated to Alexa Fluor 594 (Invitrogen) (diluted to 1:50 in the solution of PBS+1%BSA) is used for this experiment since two anti-fructan mAbs is produced in mouse.

In addition, immunolabeling on the HPF sections of 12-d-old ryegrass and *Arabidopsis* roots as well as perennial ryegrass leaf bases (Fig. II-5) is also realized by using the protocol corresponding in **section B.7** for the two anti-fructan mAbs. Normal donkey serum (NDS-dilution 1:20) and donkey anti-mouse IgG secondary antibody conjugated to Alexa Fluor 594 (Invitrogen) at 1:100 dilution in 0.1% PBST containing 1% BSA and NDS (diluted 1:20) is used to bind to mouse anti-fructan mAbs.

6. Statistical analysis

All data obtained were analyzed with R software version 4.1.2 using the "Rcmdr" package (R Core Team, 2021). Data are expressed as means ± standard error for three to five biological replicates. The effect of carbohydrate quantity was tested with the Kruskal-Wallis non-parametric test. Statistical significance was set at $P<0.05$. Chi-squared (χ^2) and p-values are detailed in Appendix 2 and 3 for BTM9H2 and BTM15A6 antibodies, respectively.

D. Salicylic acid upregulates fructan exohydrolases (FEH) together with defense-marker genes in non-fructan plants.

1. Plant treatment with phytohormones

When the fourth leaf (*B. napus*) or the eighth leaf (*A. thaliana*) has emerged, the microtubes are transferred in 150mL pots (five plants per pot) containing 50 mL of Hoagland ¼ nutrient solution supplied with 0.5 mM SA, 50 µM MeJA, 20 µM ACC (Sigma-Aldrich, Saint-Louis, MO, USA) or without supplement (control) for 3, 6, 12, and 24 h according to the experiment (Fig. II-7). At the end of the treatment period, plants are collected. The shoot is separated from the root, and each tissue is frozen in liquid nitrogen and stored at -80°C. Before RNA and

protein extractions, plant tissue is ground in liquid nitrogen in a precooled mortar and pestle until a fine powder was obtained and the frozen powder was stored at -80°C.

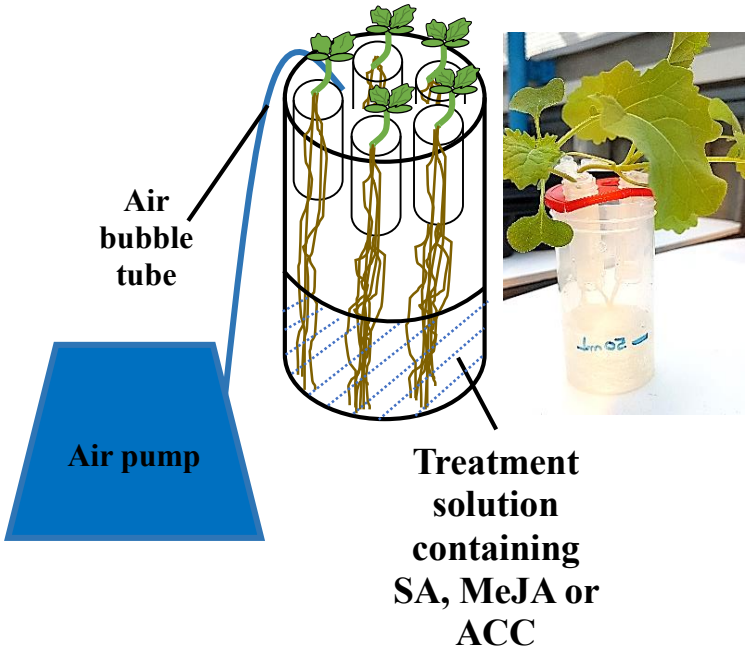

Figure II-7. Experimental design for exogenous supply of phytohormones at the root level.

Plants are treated in 150mL pots (five plants per pot) containing 50 mL of nutrient solution supplemented with phytohormone: 0,5 mM salicylic acid (SA), 50 µM methyl jasmonate (MeJA) or 20 µM 1-Aminocyclopropane-1-carboxylic acid (ACC) for 3, 6, 12, and 24 h. The shoots and the roots were harvested separately, stored at -80°C before RNA or protein extraction.

2. RNA extraction

The frozen powder (approx. 200 mg) was transferred to a tube containing 750 µL extraction buffer (0.1 M LiCl, 0.1 M Tris-HCl, 0.01 M EDTA, 1% (w/v) SDS, pH 8.0) mixed with 750 µL of hot phenol (80°C, pH 4.3), which was reheated to 80°C. After vortexing for 40s, 750µL chloroform/isoamyl alcohol (24:1 v/v) was added. The tube was mixed vigorously and centrifuged at 20 888 g for 5 min at 4°C. The supernatant was transferred into 750 µL LiCl 4M and incubated overnight at 4°C. A white pellet containing RNA was visible after centrifuging for 20 min at 20 888 g at 4°C. Then, the supernatant was removed and the pellet was suspended in 100 µL RNase free water.

Purification of RNAs including a step of DNA digestion by DNAse treatment was performed using RNeasy mini kit according to the manufacturer's protocol (Qiagen, Courtaboeuf, France). Purified RNA was diluted in 20 µl distilled water. Absorbance at 260 nm and the 260/280 nm ratio were measured with an RNA BioPhotometer (Eppendorf, Hamburg, Germany) and used to calculate the total RNA concentration and to check the RNA purity. RNA integrity was visualized by separation of 1 µg of total RNAs on a 1.2% (w/v) standard agarose gel containing ethidium bromide (0.5 $\mu g.ml^{-1}$) (Fig. II-8).

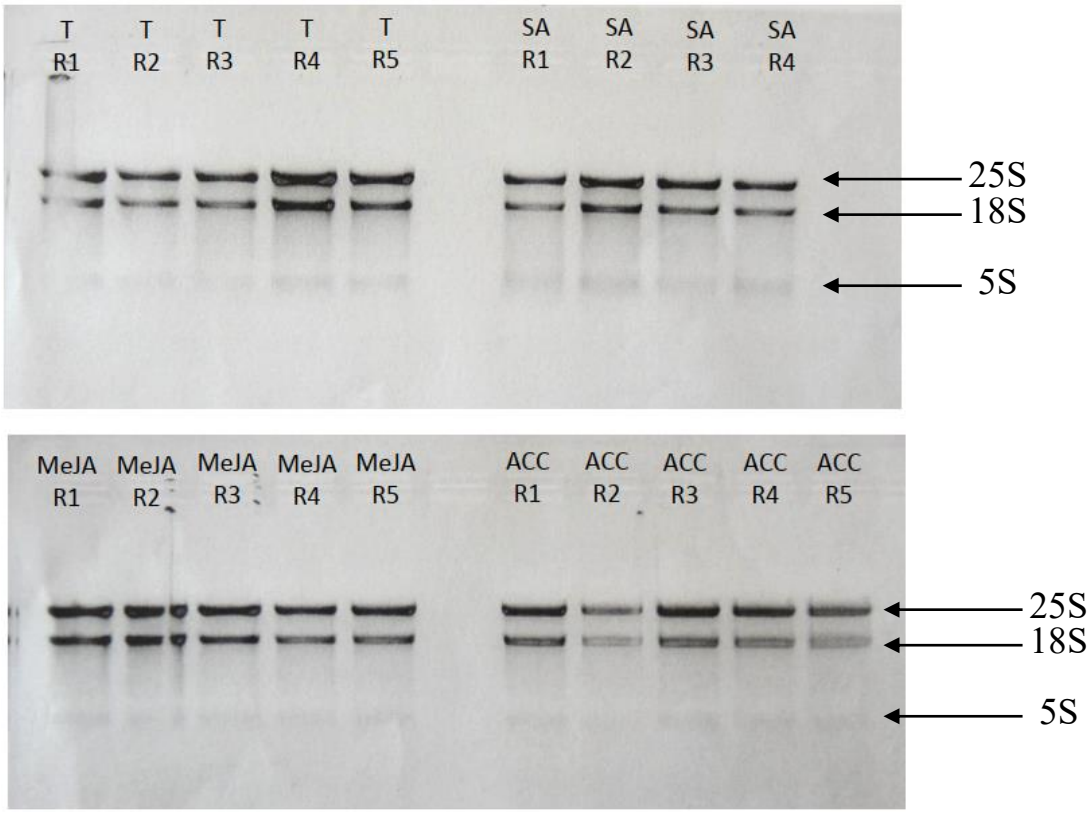

Figure II-8. Separation by 1.2% agarose gel electrophoresis of total RNAs.

1 µg deposited per extract from roots treated with SA (0.5 mM), MeJA (50 µM), ACC (20 µM) and only Hoagland ¼ solution for control plants (T). The quality is controlled by observing the migration of 25S, 18S and 5S RNAs to ensure that the extraction and purification steps are carried out correctly.

3. RT-qPCR analysis

Total RNA was reverse transcribed to cDNA by using iScript™ cDNA Synthesis Kit (Biorad, France) with 2 µL iScript reaction mix (5X) and 0.5 µL iScript reverse transcriptase. Real-Time qPCR experiments were performed using 4 µL of 1:200 dilution of first-strand cDNA on a Biorad CFX96 connect real-time PCR (Chromo4®, Biorad, France). The PCR mix comprised 0.75 µL forward and reverse primers and 7.5 µl of iQ SYBR Green supermix (BioRad, France) in a 15 µL total volume. qPCR was performed using the following program: 95 °C for 3 min followed by 40 cycles of 95 °C for 15 s and 60 °C for 40 s. The description of the gene-specific primers was given in Table II-4. FEHs primer pairs were designed with Primer3 software (https://primer3plus.com/cgi-bin/dev/primer3plus.cgi) from the nucleotide sequences available on the National Center for Biotechnology Information-NCBI and by comparing FEH sequences. Each primer chosen contains about 20 nucleotides with at least 50% GC content and optimal Tm at 60°C, raising to PCR products of 100-300 bp length. For each gene, the

specificity of PCR amplification was validated by monitoring the presence of the single peak in the melting curves and by sequencing the PCR product. For relative transcript level determination, two reference genes were selected (BnGAPDH and BnEF1 for *B. napus* and AtActin and AtEF1α for *A. thaliana*). For each pair of primers, a threshold value and PCR efficiency (%) were determined using a cDNA preparation diluted >10-fold. The PCR efficiency of each pair of primers, ranging from 94.7 to 118.1 %, was used to calculate the relative gene expression using a delta threshold cycle (Ct) method derived from that described by Hellemans et al. (2007). For each target and reference genes of a data series, the relative quantity (RQi) of the corresponding transcript in each sample (i) was calculated as follow:

$$RQi = E^{-\Delta Cti,\ min}$$

where E is (1+ efficacity)/100 and $\Delta Ct_{i,\ min}$ is the difference between Ct_i and the lowest Ct of the series ($Ct_{i,\ min}$). The RQi of the target genes are normalized (NRQi) with the geometric average of the RQi of the two reference genes as follow:

$$NRQ_i = RQ_i / (\sqrt{(RQ_{i,\ ref1} \times RQ_{i,\ ref2})})$$

Then, the NRQ_i are rescaled (rescaled-NRQ_i) by comparison with that of the control sample NRQ_{ctrl} as follow:

$$\text{rescaled-}NRQ_i = NRQ_i / NRQ_{ctrl}$$

Table II-4. Primers used for qRT-PCR in this study.

F: forward; R: reverse. Bn: B. napus genes and At: A. thaliana genes.

Function		Gene name	Protein name	Accession	Primer sequence (5' to 3')	Reference for primers
Reference genes for RT-qPCR		*BnGAPDH*	Glyceraldehyde 3-phosphate dehydrogenase	FJ529182	Forward : CGCTTCCTTCAACATCATTCCCA Reverse : TCAGATTCCTCCTTGATAGCCTT	*Alkooranee et al.*, 2017
		BnEF1	Elongation factor 1	DQ312264	Forward: GCCTGGTATGGTTGTGACCT Reverse: GAAGTTAGCAGCACCCTTGG	*Nicot et al.*, 2005
		AtEF1α	Elongation factor 1- α	AT5G60390	Forward: CTGGAGGTTTTGAGGCTGGTAT Reverse: CCAAGGGTGAAAGCAAGAAGA	*Baud et al., 2003*
		AtActin	Actin constitutively expressed in vegetative tissues	AT3G18780	Forward: GCCATCCAAGCTGTTCTCTC Reverse: CCCTCGTAGATTGGCACAGT	*Pontier et al., 2005*
Defense marker genes	Antimicrobial protein SA responsive	*BnPR1*	Pathogenesis-related 1	AY623008	Forward: ATGCCAACGCTCACAACCA Reverse: CACGGGACCTACGCCTACT	*Wang et al.*, 2012
		AtPR1		AT2G14610	Forward: TTCTTCCCTCGAAAGCTCAA Reverse: AAGGCCCACCAGAGTGTATG	*Zhang et al.*, 2020
	Transcription factor SA responsive	*BnWRKY70*	Proteins with the highly conserve WRKY domain	EV113862	Forward: ACATACATAGGAAACCACACG Reverse : ACTTGGACTATCTTCAGAATGC	*Wang et al.*, 2012
		AtWRKY70		AT3G56400	Forward: CATGGATTCCGAAGATCACA Reverse: CTGGCCACACCAATGACAA	*Li et al.*,2013
	Antimicrobial peptides JA and ET responsive	*BnPDF1.2*	Plant Defensin 1.2	AY884023	Forward : CATCACCCTTCTCTTCGCTGC Reverse : ATGTCCCACTTGACCTCTCGC	*Wang et al.*, 2012
		AtPDF1.2		AT2G26020	Forward: ACCAACAATGGTGGAAGCAC Reverse : CACTTGTGAGCTGGGAAGAC	*Attard et al.*, 2010
	JA biosynthesis gene	*BnAOS*	Allene Oxide Synthase	EV124323	Forward: CGCCACCAAAACAACAAAG Reverse: GGGAGGAAGGAGAGAGGTTG	*Wang et al.*, 2012
		AtAOS		AT5G42650	Forward: ACTACGGTTTACCAATCGTAGGAC Reverse: TCTGTACACCGTGGAGTTGTATTT	*Matsuoka et al.*,2018
	Antimicrobial protein JA and ET responsive	*BnHEL*	Hevein-Like protein	FG577475	Forward : GGAACACAAGGACTAATGC Reverse : TTTCGATAGCCATCACCA	*Wang et al.*, 2012
		AtHEL		AT3G04720	Forward: TAGTGGACCAATGCAGCAAC Reverse : GATCAATGGCCGAAACAAG	*Attard et al.*, 2010
	Ethylene signaling transcription factor	*BnERF2*	Ethylene response transcription factor	FJ788940	Forward: GGAAATTCGCGGCGGAGAT Reverse : GGAACCACGCATCCTAAAAG	*This study*
		AtERF1		AT3G23240	Forward: ATTCTTTCTCATCCTCTTCTTCT Reverse : CGAATCTCTTATCTCCGCCG	*Mao et al.*, 2016
Fructan exohydrolase (FEH) genes	Hydrolysis of both β(2,6) and β(2,1) linkages of fructans	*Bn6&1-FEH_A03*	6&1-FEH	BnaA03G03670D	Forward: CCCTTTAGCTCCAGAGTTCA Reverse: TTCCGGTGTACAAGATCACA	*This study*
		Bn6&1-FEH_A10		BnaA10G20680D	Forward: TAACTTGGCTCCCCGATTCA Reverse: GTCCAGTGTATAGAATTACC	
		Bn6&1-FEH_C03		BnaC03G05170D	Forward: GTACACCGGAAGCGACACCA Reverse : TACTAGGTGGAACCATAACA	
		Bn6&1-FEH_C09		BnaC09G44700D	Forward: CAGTAATTCTCTACACTGGAC Reverse: TGGTAATAGAAACCGGGAAA	
		At 6&1-FEH		AT5G11920	Forward : TTACGGGCCTTTTGGATTGC Reverse : TCGCTGCTGCACATTACAAC	
	Hydrolysis of β(2,6) linkages of fructans	*Bn6-FEH_A06*	6-FEH	BnaA06G00510D	Forward: AAGACTTAACCGGAATGTGG Reverse: AACGTCTCGATCAAACTAAC	
		Bn6-FEH_C06		BnaC06G07120D	Forward: AGGAGTTAACCGGAATGTGG Reverse: AACGTCTCGATCAAACTCAT	
		At 6-FEH		AT1G55120	Forward : ATTGAGAAGGGTTGGTCTGGTC Reverse : TTGCCAGTTGACTTGTTGCC	

4. Statistical analysis

All data obtained were analyzed with R software version 4.0.3 using the "Rcmdr" package (R Core Team, 2021). For each treatment and time, the data correspond to five biological replicates (five individual plants). The comparison of control *versus* treated plants was done using the Wilcoxon nonparametric test (rank-sum test). The comparison of more than two sets of data was done using the Kruskal-Wallis nonparametric test followed by a post-hoc multi-comparison ranking test (with the "pgirmess" and the "multcompView' packages). For each test, the

statistical effect is considered significant with P<0.05. The principal component analysis was performed with the "FactoMinR" package using the relative expression of seven genes in the roots of the five genotypes with five biological replicates for each genotype (n=25).

E. Involvement of bacterial levans and plant fructan exohydrolases (FEHs) in Arabidopsis thaliana root colonization by Pseudomonas brassicacearum

1. Bacterial strains

The strains are red or green fluorescent protein-tagged bacteria corresponding to the reference strain for genome-based analysis (Ortet et al., 2011) which contains the levansucrase gene encoding the levan synthesizing enzyme (NFM421-I::rfp or NFM421-I::gfp; later named NFM421) and the corresponding levansucrase knock-out mutant strain (NFM421-I::Δlev, later named *Δlev*) (Achouak et al., 2004). The levansucrase knock-out mutant strain *Δlev* was obtained by Sylvain Fochesato (Laboratoire d'Écologie Microbienne de la Rhizosphère et de l'Environnement Extrême - LEMiRE, Institut de Biosciences et biotechnologies d'Aix-Marseille – BIAM, CEA, Cadarache).

2. Arabidopsis T-DNA mutant

At6-FEH (At1g55120) and *At6&1-FEH* (At5g11920) *Arabidopsis thaliana* knock-out mutants were selected from the Colombia (Col-0) SALK T-DNA collection of the Nottingham Arabidopsis Stock Centre (NASC, Nottingham UK) (Table II-5). The three *6-feh* mutant lines are N675754-SALK 073323C (further named *6-feh-S073*), N671758-SALK 097556C (further named *6-feh-S097*) and N672154-SALK 134791C (further named *6-feh-S134*). The two *6&1-feh* mutant lines are N655172-SALK 127864C (further named *6&1-feh-S127*) and N655201-SALK 152299C (further named *6&1-feh-S152*).

For mutant genotyping, *A. thaliana* seeds (wild-type Col-0 and FEH knock-out mutants) were stratified for 48 h in 0.1% agar at 4°C in the dark and then sown in pots (9x9x10cm) filled with vermiculite with a 1cm layer of soil on top (Fig. II-9A). The pots were placed in a plastic tank containing Hoagland ¼ nutrient solution which was renewed every 3-4 days. Plants were grown for approximately 8 weeks in a plant growth chamber with a PAR (Photosynthetically Active Radiations) of 110 µmol photons·m^{-2}·s^{-1} under a photoperiod of 16 h and a thermoperiod of 20/18°C day/night.

FEH knock-out mutants were tested by PCR-based genotyping to confirm the T-DNA insertion localization and homozygosity. The PCR primers used for genotyping are listed in Table II-5.

DNA is extracted from 100 mg of fresh young leaves using NucleoSpin™ Plant II kits (Macherey-Nagel, 740770.50). PCR was performed according to a protocol modified from O'Malley et al. (2015) using 3µL of DNA extract. Initial denaturation step at 94°C for 2 min was followed by 40 cycles including a denaturing step at 94°C for 30s, a primer hybridization step at various temperatures according to each pair of primers for 1 min and an amplification step at 72°C for 1 min. Each PCR reaction was finished with a final step at 72°C for 10 min. Then, PCR products were separated by electrophoresis on 1.2% agarose gel in TAE 1X containing 50µL de BET (0.5 mg. mL^{-1}) and revealed by illumination with UV-light using a Gel-Doc TM EZ Scanner (Bio-Rad, Marnes-la-Coquette, France) (Fig. II-9B). In addition, FEH transcript level was also verified by using quantitative RT-PCR on the RNA extracted from leaves. The protocol is detailed in sections D.2 and D.3 of the M&M chapter. Seeds of homozygous plants were collected in 1.5 ml tubes and stored at 12°C.

Table II-5. T-DNA specific primers for SALK insertion mutant collection and primers used for plant genotyping.

Target gene	Primer ID	Primer sequence (5' to 3')
SALK T-DNA	*LB-1.3*	ATTTTGCCGATTTCGGAAC
At 6&1-FEH (At5g11920)	N655172-SALK 127864C *(6&1-feh-S127)*	LP: TATCAGTGGGTTTCTTCCACG RP : TTGCTGTTTGTTGTTGACGTC
	N655201-SALK 152299C *(6&1-feh-S152)*	LP: GACATGGTCAATTGGATCCAG RP: TGGTTTTACTGCATTTACCTCAAG
At 6-FEH (At1g55120)	N675754-SALK 073323C *(6-feh-S073)*	LP: CCTCCTCCACCATAACTCTCC RP : TTTCCGAGGAAAATATGGCTC
	N672154-SALK 134791C *(6-feh-S134)*	LP: ATTGATTGCGTCCAGTTGAAG RP : GGCCTAAACAGAGAATGGTCC
	N671758-SALK 097556C *(6-feh-S097)*	LP: TGTCATTAGAGGATTTTGCGG RP : GGCCTAAACAGAGAATGGTCC

The two *6&1-feh* mutant lines (*6&1-feh-S127* and *6&1-feh-S152*) are homozygote for the T-DNA insertion but *At6&1-FEH* transcript is detected in *6&1-feh-S152* (Table II-6). Two *6-feh* mutant lines are homozygote for the T-DNA insertion (*6-feh-S097* and *6-feh-S134*) while the other is heterozygote (*6-feh-S073*). For the three *6-feh* mutant lines, the *At6-FEH* transcript is not detected (Table II-6).

Table II-6. Characteristics of FEH knockout mutants.

Target gene	SALK insertion mutant	T-DNA insertion		Relative transcript level	
		Position	Homozygotie/ Heterozygotie	*At 6&1-FEH*	*At 6-FEH*
	Col-0	-	-	**1.00**	**1.00**
At 6&1-FEH (At5g11920)	N655172-SALK 127864C *(6&1-feh-S127)*	Intron	Homozygote	nd	**0.53**
	N655201-SALK 152299C *(6&1-feh-S152)*	Intron	Homozygote	**4.32**	**3.68**
At 6-FEH (At1g55120)	N675754-SALK 073323C *(6-feh-S073)*	Intron	Heterozygote	**0.36**	nd
	N672154-SALK 134791C *(6-feh-S134)*	Intron	Homozygote	**0.11**	nd
	N671758-SALK 097556C *(6-feh-S097)*	Exon	Homozygote	**0.13**	nd

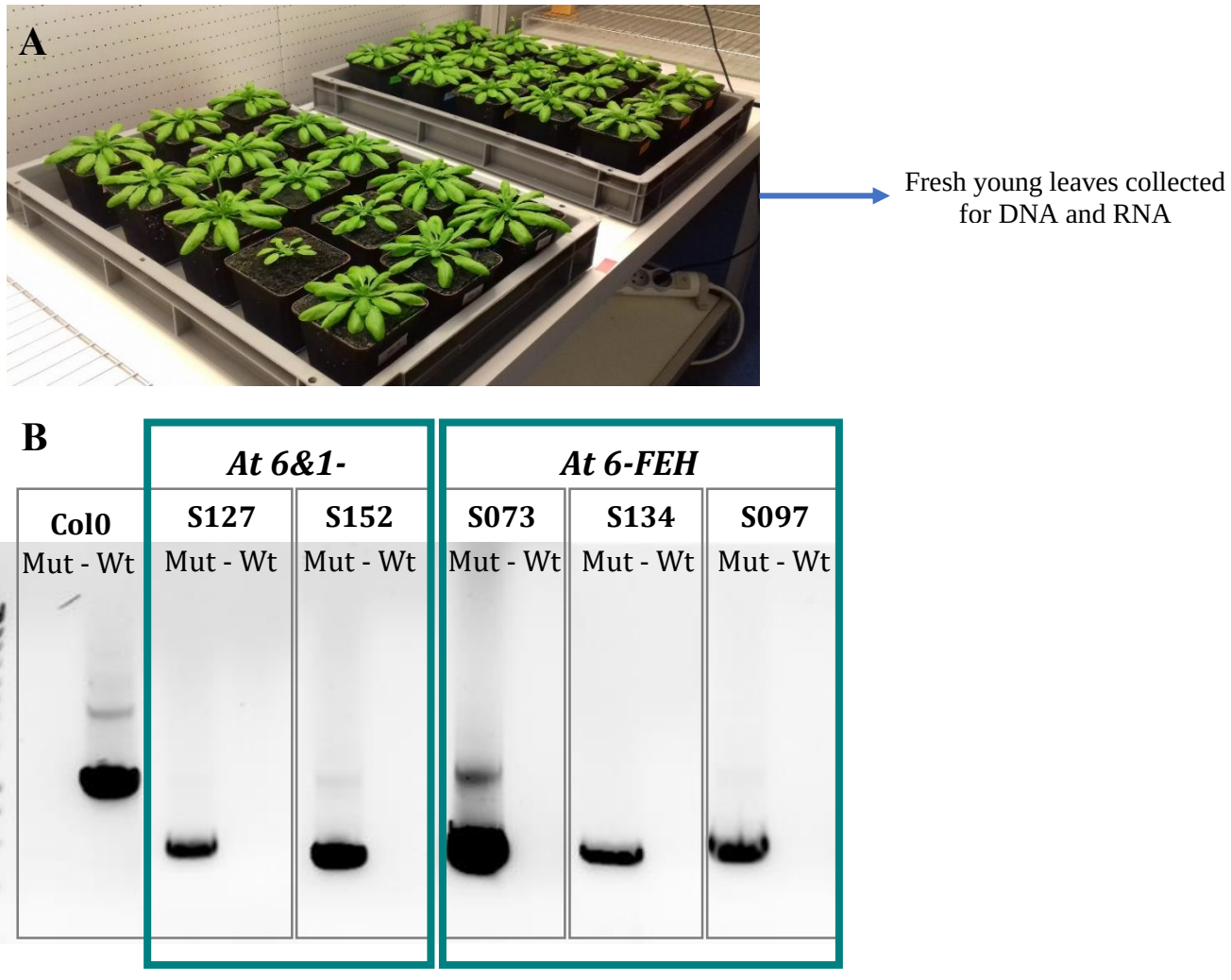

Figure II-9. Arabidopsis T-DNA mutant genotyping.

(A) FEH knock-out A. thaliana mutants growing on plant racks in the growth chamber. (B) Electrophoresis gel after PCR for the genotyping of A. thaliana FEH knock-out mutants to select the homozygous plants. Mut: Mutant primers; Wt: Wild type primers.

3. Bacterial inoculation

For the *in vitro* root colonization experiments with *P. brassicacearum*, *A. thaliana* seeds (wild-type Col-0 and FEH knock-out mutants) were placed in a 2 mL sterile Eppendorf tube. 2 mL of a sterilization solution containing 1 mL 2.5 % chlorine bleach, 9mL ethanol absolute, and 3 drops of Tween 80 (Sigma-Aldrich-V000749) were added to the seeds for 6 min. Then seeds were washed 4 times with absolute ethanol and dried naturally in a Petri dish under sterile conditions in horizontal laminar flow hoods before sowing. Two *P. brassicacearum* strains (NFM421 and *Δlev*) were grown in 10-fold-diluted tryptic soy broth (TSB/10; Difco Laboratories, Detroit) at 30°C for 24h. The optical density (OD) at 600 nm of overnight bacterial cultures was measured before the experiment to obtain approximately 200-1000 bacteria per plate culture. Bacterial suspensions were added to 150mL of half-strength Hoagland (Hoagland ½) medium containing 3.5g agar per liter (Arnon and Hoagland, 1940) and poured as a band where the seeds were sown. 7 sterile seeds were sown in a squared dish (15 x 15 cm) filled with Hoagland ½ medium and 0.4% phytagel (Sigma, St. Louis) (Fig. II-10A). The dishes were sealed with micropore tape (3M, St. Paul, MN, U.S.A.) and incubated vertically at 21°C for 21 days with 16 h of light and 18°C at night (approximately 100 photons m^{-2} s^{-1}). Control experiments were performed by omission of bacteria. For this experiment, 9 technical replicates and 3 biological replicates were performed.

4. Monitoring root colonization by *P. brassicacearum* using bacterial colonies counting

The roots of five 21-d-old plants inoculated with one of the two strains (NFM421 or *Δlev*) were collected and ground in mortar in 1mL of 0.85% potassium chloride (KCl). Then, three dilutions of the ground root were plated on a 10-fold-diluted tryptic soy agar (TSA/10) medium. After 3 days at 25°C in the bacterial incubator, the bacterial colonies of the 3 most diluted points were counted (Fig. II-10B). For this experiment, 5 biological replicates were performed.

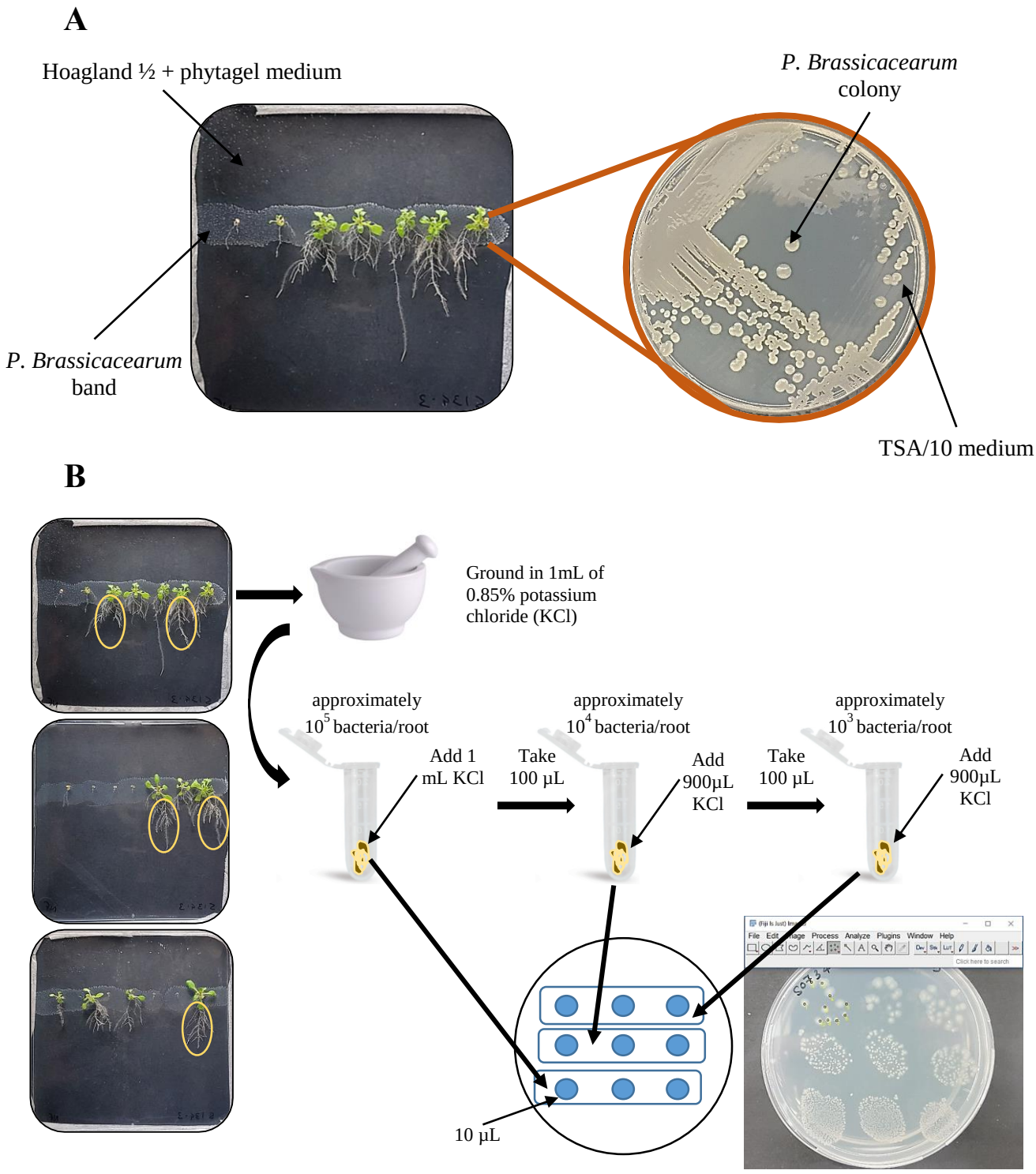

Figure II-10. Schematic representation of the experiments to study the interaction between A. thaliana FEH knock-out mutants and P. brassicacearum.

(A) In vitro root colonization experiments. (B) Quantification of P. brassicacearum colonization (NFrfp and Δlevrfp strains) 21 days after inoculation by counting the colonies on the 3 most dilute points (approximately 10^3 bacteria/root) using ImageJ.

5. Monitoring root colonization by *P. brassicacearum* using fluorescent microscopy

The roots of 14-d-old plants inoculated with one of the two strains (NFM421 or *Δlev*) were observed using a confocal scanning light microscopy (CSLM, Olympus) equipped with a krypton-argon laser, detectors, and filter sets for RFP monitoring. Shadow projections and optical sections were generated using the Fluoview software package. The observation was realized in three compartments of root including the basal part (1.5- to 2-cm), apical part (1-cm), and median part (variable lengths) (Achouak et al., 2004). For this experiment, 4 technical replicates and 3 biological replicates were done.

6. Observations of *P. brassicacearum* exopolysaccharide (EPS) production

Bacterial exopolysaccharide (EPS) production was observed using a fluorescent Concanavalin A probe (ConA, Texas Red™ Conjugate, Molecular Probes- C825, 1 mg/ml). A colony of *P. brassicacearum* NFM421 expressing a plasmid-borne GFP (NFM421-I::gfp) was scraped from the agar surface and deposited on a slide. 100µL of 1 mg/ml ConA was added and the slide was stored 15 min in the dark. The ConA solution was then discarded and the slide is rinsed 2 times with 40 mL of PBS for 15 min. Finally, a droplet of citifluor was delicately deposited on the sample and a coverslip is mounted to the slide before observing by CSLM. In addition, the roots of 14-d-old plants inoculated with the *P. brassicacearum* NFM421-I::gfp strain were removed from the plate and incubated into 100µL of ConA solution for 1h in the dark in the microscope slide. After discarding the ConA solution, roots were washed 2 times with 40 mL of PBS for 15 min. The roots were then observed in a droplet of citifluor after being covered with a coverslip by CSLM equipped with a krypton-argon laser, detectors and filter sets for simultaneous monitoring of GFP and RFP. For this experiment, 3 technical replicates and 2 biological replicates were performed.

7. Analysis of root system morphology

The morphology of root system of at least five plants of each genotype (Col-0 and FEHs knock-out mutant) was studied by analyzing scanned images. WinRHIZO Pro version 2007d (Regent Instruments, Canada) (Fig. II-11B) was used to measure two root traits which are indicators for a potential uptake of water and nutrients (Himmelbauer et al., 2004; Gruber et al., 2013), the total root length (cm) and surface area (cm^2). They were measured in the total root system of each plate and then divided by the number of plants to obtain the root length per plant (cm. $plant^{-1}$) as well as surface area per plant ($cm^2.plant^{-1}$). Moreover, the Fiji (Fiji is Just ImageJ),

an image processing package of ImageJ2 (Schindelin et al., 2012; https://imagej.net/software/fiji/) was used to measure the total primary root length per plate (cm) and the lateral root number (Fig. II-11A, B). Lateral root density (number/cm primary root) was calculated by dividing the total number of visible lateral roots in one plate by the total length of primary root (Lima et al., 2010; Gruber et al., 2013).

A

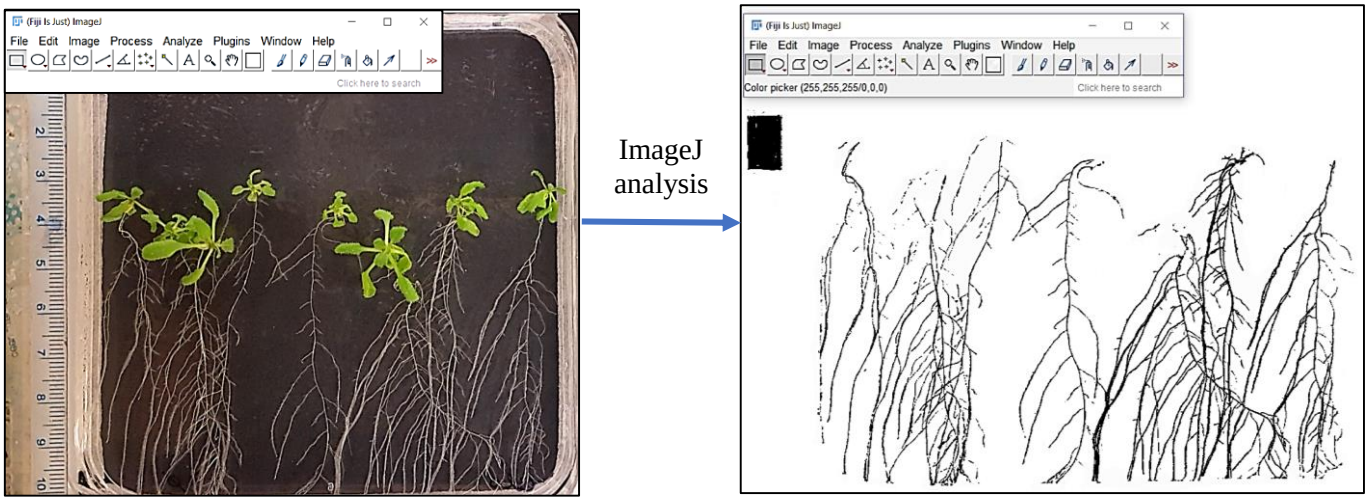

B

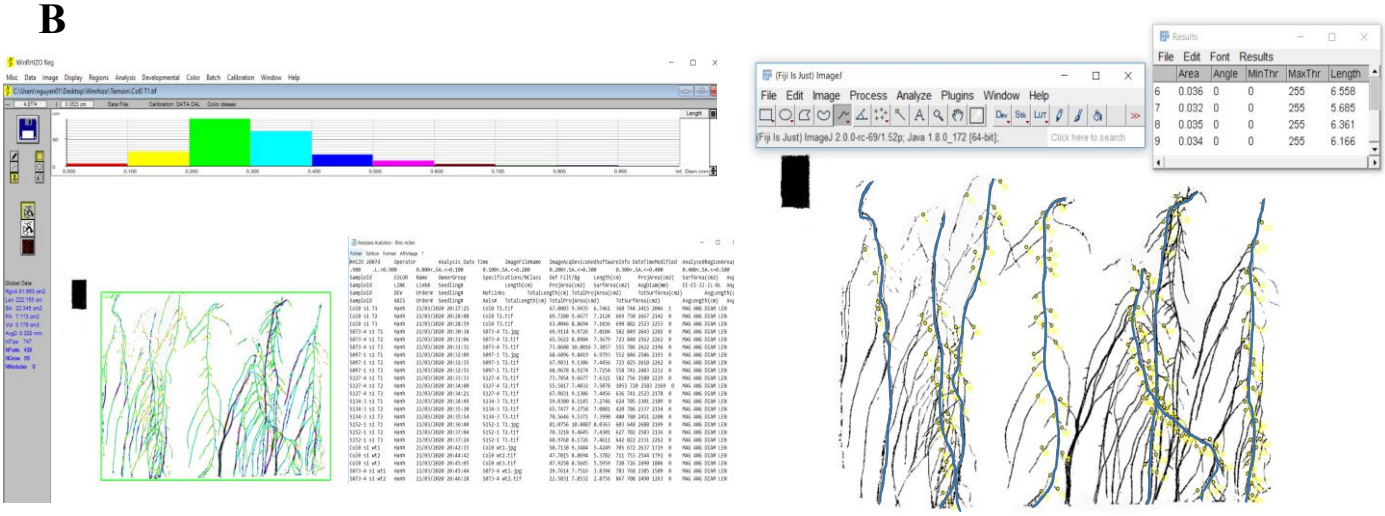

Obtained through WinRHIZO

- *The total root length of the root system (cm)*
- *The surface area (cm ^{2})*

Obtained through ImageJ

- *The total primary root (PR) length (cm)*
- *The lateral root (LR) number*

Figure II-11. Schematic representation of image analysis of root system morphology.

(A) Images obtained are first analyzed using ImageJ to retain only the root system. (B) Two image processing packages 'WinRHIZO' and 'ImageJ' are then used to collect the chosen indicators of root system morphology.

8. Statistical analysis

Data were analyzed with R software version 4.0.3 using the “Rcmdr” package (R Core Team, 2021). For each inoculation, the data correspond to five biological replicates (five individual plants). The comparison of control *versus* inoculated plants was undertaken using a one-way ANOVA with pairwise comparisons made using a Tukey test. Before ANOVA, a Shapiro–Wilk test and a Bartlett test were performed on each set of data to assess data normality and homogeneity of variances, respectively. For each test, the statistical effect is considered significant with $P<0.05$.

III. Results

1. Generation and characterization of two monoclonal antibodies that recognized β-(2,1) and β-(2,6)-fructan epitopes: new tools to unravel the functions and subcellular localizations of fructans in plants

Thi Ngoc Hanh Nguyen[1,2], Didier Goux[3], Marie-Laure Follet-Gueye[2,4], Sophie Bernard[2,4], Laurence Padel[5], Maïté Vicré[2]. Marie-Pascale Prud'homme[1+], Annette Morvan-Bertrand[1*+]. [+]*co-last authors* **corresponding author*

[1]Normandie Univ, UNICAEN, INRAE, EVA Ecophysiologie Végétale, Agronomie & nutritions NCS, FED Normandie Végétale 4277, 14032 Caen, France

[2]Normandie Univ, UNIROUEN, Laboratoire Glyco-MEV EA 4358, FED Normandie Végétale 4277, 76000 Rouen, France

[3]Normandie Univ, UNICAEN, US EMerode, CMAbio[3], 14032 Caen, France

[4]Cell Imaging Platform (PRIMACEN-IRIB), Université de ROUEN Normandie, UFR des Sciences et Techniques, F-76821 Mont-Saint-Aignan, France

[5]Biotem, 38140 Apprieu, France

Abstract

Fructans are water-soluble fructose polymers containing one glucose residue. Fructose residues are bound together by β-(2,1) and/or β-(2,6) linkages. Beside their role as storage carbohydrates in many crop and fodder species, fructans fulfill additional functions and contribute to biotic and abiotic stress resistance. They are synthesized and stored in the vacuole of plant cells but have also been surprisingly reported in the apoplast. Fructan antibodies therefore represent powerful tools to unravel the functions and subcellular localizations of fructans in plants but they are not yet available. Here, we report the production of two monoclonal antibodies (mAbs) using mice immunized with a mixture of antigenic compounds prepared from two fructan plant species, inulins from *Cichorium intybus* and levans from *Phleum pratense*. Their specificity towards β-(2,1) and/or β-(2,6) linkages of fructans was demonstrated by immune-dot blot assays on a wide range of carbohydrates including various oligosaccharides and polysaccharides. The two mAbs were used for *in situ* immunolocalization of fructans by epifluorescence microscopy in three fructan plant species, perennial ryegrass (*Lolium perenne*), timothy (*Phleum pratense*) and wheat (*Triticum aestivum*) and in the non-fructan plant *Arabidopsis thaliana* as a control. Fructans were specifically detected in fructan plants, at the

surface of the root tips or inside the cells of the roots and mature leaf sheaths, suggesting an apoplastic and vacuolar localization, respectively. The two mAbs provide new tools to explore the fructan secretion mechanisms and decipher the fructan involvement in stress resistance and in plant-microorganism interactions.

Introduction

Some organisms including bacteria, fungi, algae and land plants are known to synthesize fructans in addition to the two most common carbohydrate reserves that are glycogen and starch (Hendry, 1993; Ball et al., 2011). Fructans are produced by some beneficial bacteria such as *Gluconacetobacter diazotrophicus* (Hernández et al., 2000), pathogenic bacteria such as *Erwinia amylovora* (Öner et al., 2016), fungi such as *Aspergillus sp.* (Trollope et al., 2015) and some Archaea (Kirtel et al., 2019) and by more than 15% of angiosperms (Hendry, 1993). Fructans are water-soluble polymers of fructose residues linked by β-(2,1) and/or β-(2,6) linkages with one external or internal glucose residue (Ritsema and Smeekens, 2003). Four different fructan types are distinguished according to the nature of the linkage connecting the fructose residues (β-(2,1) or β-(2,6)), the position of the glucose residue (internal or external) and the presence or absence of branches (Ritsema and Smeekens, 2003). Inulins are linear chains with β-(2,1) linkages and an external glucose residue. Levans are linear chain with β-(2,6) linkages and an external glucose residue. Neoserie-type fructans have an internal glucose residue and β-(2,1) (neo-inulin type fructans) or β-(2,6) (neo-levan type fructans) linkages. Graminan-type fructans are branched-chains containing both β-(2,1) and β-(2,6) linkages and an external glucose residue. In plants, the degree of polymerization (DP) is generally between 30 and 150, but in some cases, it can reach 200 (Van den Ende, 2013). In microorganisms, the DP of fructans can be above 100 and up to 10000 (Velázquez-Hernández et al., 2009). Fructans with a DP below 10 are called fructooligosaccharides (FOS). Inulins are mainly found in Asteraceae such as *Cichorium intybus* (Van Laere and Van den Ende, 2002); *Taxaracum officinalis* (Van den Ende et al., 2000) and in other eudicots such as in Boraginaceae (*Myosotis secunda*) and Campanulaceae (*Campanula rotundifolia* L.) (Brocklebank and Henry, 1989). Levans are found in Poaceae such as *Phleum pratense* (Cairns and Ashton, 1993; Cairns et al., 1999) and *Dactylis glomarata* (Chatterton et al., 1993; Hendry, 1993). Neoserie-type fructans are found in monocots such as *Asparagus officinalis*, *Allium cepa* (Shiomi, 1989) and *Agave sp*. (Mancilla-Margalli and López, 2006). Some plants contain a mixture of several types of fructans such as *Triticum aestivum* (graminans and inulins; Kawakami et al., 2005) and *Lolium perenne* (neo-inulin type, neo-levan type and inulins; Pavis et al., 2001). In bacteria, fructans

are mainly of the levan type while some bacteria, specifically in species from the three genera *Streptococcus*, *Leuconostoc* and *Lactobacillus*, synthesize inulins (Öner et al., 2016).

At the subcellular level, plant fructans are synthesized and stored in the vacuole (Wagner et al., 1983). However, some studies also mention an apoplastic localization, in crown tissues of oat after cold hardening (Livingston and Henson, 1998) and in the phloem of *Agave deserti* (Wang and Nobel, 1998). In bacteria, fructans and their synthetic enzymes (levan- and inulosucrases) are extracellular so that fructans are part of the exopolysaccharides (EPS) that contribute to biofilm formation, an assembly of microorganisms adhering to each other and/or to a surface and embedded in an EPS matrix (Öner et al., 2016).

In plants, fructans are not only a form of carbon storage but also contribute to the resistance to abiotic stresses such as cold, drought, and salinity (Parvanova et al., 2004; Livingston et al., 2009; Bie et al., 2012; Van den Ende, 2013). The role of fructans in tolerance to abiotic stresses is due to their water solubility that allows them to contribute to the regulation of osmotic potential, and to their ability to stabilize membranes (Hincha et al., 2007). These abilities improve plant endurance during freezing or drought-related dehydration (Livingston et al., 2009). Fructans are also able to control reactive oxygen species (ROS) produced in excess during stress (Stoyanova et al., 2011; Matros et al., 2015). In addition, fructans are involved in plant immunity as signaling molecules (Bolouri Moghaddam and Van den Ende, 2013) as shown by the reduction of plant infection following the pre-application of exogenous plant fructans (Zhang et al., 2009; Tarkowski et al., 2019; Svara et al., 2020). However, it is not clear if the involvement of fructans as membrane protector during dehydration and as signaling molecules in the defense responses relies on their active secretion or on passive leakage from the vacuole to the apoplast (Valluru et al., 2008; Versluys et al., 2017). Thus, to deepen the understanding of the mechanisms of action of fructans in the resistance of plants against abiotic and biotic stresses, their precise localization at tissue and cellular level in various environmental conditions need to be elucidated. Monoclonal antibodies (mAbs) such as those developed against various cell-wall polysaccharides (Knox, 2008) are thus essential.

Only two studies reported the use of anti-fructan antibodies to localize fructans in plant tissues (Röber et al., 1996; Pilon-Smits et al., 1996). In these two cases, antibodies were used for the immunolocalization of levans produced in transgenic potatoes through the expression of a bacterial levansucrase gene. Pilon-Smits et al. (1996) used mAbs produced in mouse (2-l-3mAb; Hall et al., 1990) while Röber et al. (1996) did not mention the provenance of the anti-levan antibody. In both cases, the cellular localization of fructans was investigated *via* immunofluorescence and showed the presence of fructans in the intercellular space instead of

the expected vacuolar compartment. To our knowledge, apart from these two studies which focused on transgenic plant producing fructans, the immunolocalization of fructans has not been reported, either in transgenic or in native fructan plant species. Moreover, no anti-fructan antibodies are commercially available.

Thus, we produced mAbs using mice immunized with a mixture of antigenic compounds prepared from two fructan-plant species, inulins from *Cichorium intybus* and levans from *Phleum pratense*. Two new anti-fructan mAbs, named BTM15A6 and BTM9H2, were selected because of their binding to inulins and levans used for the antigenic preparation. We demonstrated their specificity towards fructans by immune-dot blot assays on a wide range of carbohydrates including various oligosaccharides and polysaccharides. The two mAbs were used for *in situ* immunolocalization of fructans by epifluorescence microscopy in three fructan plant species perennial ryegrass (*Lolium perenne*), timothy (*Phleum pratense*) and wheat (*Triticum aestivum*) and in the non-fructan plant model *Arabidopsis thaliana*.

Materials and Methods

Antibody generation

The company BIOTEM (Apprieu, France) produced the mAbs by immunising mice with antigenic compounds prepared from two purified plant fructans, inulins from Cichorium intybus and levans from Phleum pratense, both supplied by Megazyme (Wicklow, Irland) under references P-INUL and P-LEV, respectively. After the immunizations, hybridoma preparation and cloning were performed by BIOTEM while we were in charge of screening the hybridoma and sub-clones for the presence of antibodies reacting with inulins and levans by immune-dot blot.

Five mice (Oncins France 1 strain) were injected three times at three-week intervals with inulins and levans conjugated to bovine serum albumin (BSA). The first injection was made subcutaneously and intraperitonealy with complete Freund's adjuvant and the two others intraperitonealy with incomplete Freund's adjuvant. Ten days after the third immunization, the levels of serum immunoglobulins anti-inulins and anti-levans conjugated or not to BSA were tested by indirect competitive ELISA. The mice were injected again three times intraperitonealy the same antigens and incomplete Freund's adjuvant at three-week intervals and ten days after the sixth immunization, the levels of serum immunoglobulins anti-inulins and anti-levans conjugated or not to BSA were again tested. Three month later, the mice were injected again two times intraperitonealy of free inulins and levans and incomplete Freund's adjuvant at two-week intervals and ten days after the eighth immunization, the levels of serum immunoglobulins

anti-inulins and anti-levans conjugated or not to BSA were again tested by ELISA and also by immune-dot blot against free inulins and levans. One month after the last injection, a selected mouse was given an intravenous injection of free inulins and levans without adjuvant. Three days after the boost injection, the mouse was sacrificed and the spleen was taken for lymphocytes isolation. The lymphocytes were fused with Sp2/0-Ag14 myeloma cell line using standard hybridoma preparation. The hybridoma supernatants from the fusion were screened for the presence of antibodies reacting with inulins and levans by immune-dot blot. Two hybridomas were selected for subcloning by dilution. Crude hybridoma supernatants were used as the source of two monoclonal antibodies (mAbs) named BTM9H2 and BTM15A6. The determination of the immunoglobulin isotypes revealed that both antibodies are IgG (IgG1 λ for BTM9H2 antibody and IgG2a κ for BTM15A6).

This study was carried out in strict compliance with French and European animal protection policy. BIOTEM received the approval of the "Direction Départementale de la Protection des Populations de l'Isère (38)" under the number D 38 013 10 001. The animal protocol has been reviewed and approved by the BIOTEM ethics committee.

Plant material

Arabidopsis thaliana (ecotype Columbia) seeds were surface sterilized with 70% (v/v) ethanol (5 min), then with 0.9% (v/v) sodium hypochlorite (2 min), washed 6 times in sterile water before being sown onto Arabidopsis medium (Duchefa Biochemie) containing 1% (w/v) Bacto Agar (ref. A01254) (Durand et al., 2009). Timothy (*Phleum pratense* var. Aturo) seeds were surface sterilized with 70% (v/v) ethanol (5 min), then with 0.9% (v/v) sodium hypochlorite (2 min), washed 6 times in sterile water before being sown onto Murashige and Skoog (MS - Duchefa Biochemie) medium containing 1% (w/v) Bacto Agar. Perennial ryegrass (*L. perenne* var. Delika) seeds were surface sterilized with 9.6% as active chlorine (2 min), washed 6 times in sterile water before being sown onto Murashige and Skoog medium containing 1% (w/v) Bacto Agar (ref. A01254). Wheat (*T. aestivum* var. Chevignon) seeds were sterilized with 70% (v/v) ethanol 10 min), then with 0.9% (v/v) sodium hypochlorite (10 min), washed 6 times in sterile water before being sown onto ½ Murashige and Skoog medium containing 1% (w/v) Bacto Agar. Petri dishes with seeds were placed vertically to avoid the roots penetrating the agar and the subsequent loss of border and border-like cells and grown in continuous light (120 $\mu E\ m^{-2}\ s^{-1}$) at 21°C in 16-h-day/8-h-night as described by Vicré et al. (2005). Freshly root tips were harvested from 10-d-old seedlings of Arabidopsis, perennial ryegrass, timothy, and wheat

for testing. The root sections for immunocytochemistry and HPAEC-PAD profile were collected from 12-d-old Arabidopsis and perennial ryegrass seedlings.

Leaves were collected from mature plants grown in hydroponic conditions. Seeds from perennial ryegrass (*L. perenne* var. Delika) were soaked in darkness for 48 hours at 4°C in 0.1% (w/v) agar solution individually sown on the top of a 5 mL microtube pierced at the bottom and filled with 0.7% (w/v) agarose. Each microtube was transferred to a plastic pot (two plants per pot) containing 700 mL of nutrient solution: K_2SO_4 (1mM), NH_4NO_3 (1mM), KH_2PO_4 (0.4 mM), K_2HPO_4 (0.15 mM), $CaCl_2.2H_2O$ (3mM), $MgSO_4.7H_2O$ (0.5 mM), EDTA-2NaFe.$3H_2O$ (0.2 mM), H_3BO_3 (14 µM), $MnSO_4.H_2O$ (5 µM), $ZnSO_4.7H_2O$ (3 µM), $CuSO_4.5H_2O$ (0.7 µM), $(NH_4)_6Mo_7O_{24}$ (0.7 µM), $CoCl_2$ (0.1 µM). Nutrient solution was aerated continuously and replaced every week. Plants were grown for 7 weeks in a plant growth chamber with a PAR (Photosynthetically Active Radiations) between 10 and 150 µmol photons·m^{-2}·s^{-1} provided by high-pressure sodium lamps (Philips, MASTER GreenPower T400W) under a photoperiod of 16 h and a thermoperiod of 21/18°C day/night. The outermost senescent leaf sheaths were discarded. A 10-mm long segment was dissected from the basal point of tiller attachment and included mature leaf sheaths and elongating leaf bases.

Wild plants of cocksfoot (*Dactylis glomerata*) and dandelion (*Taraxacum officinalis*) were collected on the green space of the University of Caen Normandie.

Carbohydrate samples

Various sources of carbohydrates and plant cell wall polysaccharides were used for the characterization of BTM9H2 and BTM15A6 mAbs specificity using dot blot analysis. Commercially available carbohydrates were purchased and prepared as described in Table S1. Fructans from *L. perenne* were purified from the 0-5 cm shoot base according to the method of Morvan et al. (1997). Water soluble carbohydrate (WSC) extracts of perennial ryegrass (*Lolium perenne;* 0-5 cm shoot base), cocksfoot (*Dactylis glomerata* ; 0-3 cm shoot base) and dandelion (*Taraxacum officinalis* ; roots) were prepared according to the method described by Benot et al. (2019).

Immunodot blot assays

Immuno-dot blot assays were performed to screen serum, hybridoma supernatants and mAbs for their specificity towards a wide range of carbohydrates listed in Appendix 1. The protocol was adapted from Li et al. (2010) and Manceur et al. (2017). Sheets of Bio-Dot filter paper and nitrocellulose membrane (0.2 µm-Amersham Protran- ref.10600006) were pre-moistered in

TBS 1x (Tris-buffered saline with 20 mM Tris and 500 mM NaCl at pH 7.5). For each carbohydrate solution, a serial dilution was done with ultrapure water to obtain five quantities in the 50µL deposited (5, 25, 50, 125, 250 µg). For each concentration, 50 µL was loaded into the dot-blot wells in duplicate, along with the two antigens, inulins from chicory and levans from timothy. Ultrapure water was used as a negative control for each carbohydrate. By suction through the 96-well dot-blotting equipment (DHM96, Scie-Plas, Cambridge, UK), samples were blotted onto nitrocellulose membrane. The membrane was then blocked in the TBS 1x containing 0.1% Tween 20 (0.1% TBST) for 2 h at room temperature with shaking, followed by overnight incubation with 5µg.mL^{-1} anti-fructan mAbs diluted in 0.1% TBST blocking buffer at 4˚C. After three washes of 10 min each with 0.1% TBST, the membranes were incubated for 2 h at room temperature with Horseradish Peroxidase (HRP)-conjugated secondary antibody diluted (1:3000) in 0.1% TBST blocking buffer. Next, three washes of 10 min each with 0.1% TBST and one wash of 10 min with TBS 1x were performed after incubation periods. Secondary antibodies were detected using a chemiluminescent substrate kit (SuperSignal™ West Pico PLUS-ref. 34580, Thermo Fischer Scientific, Waltham, USA). After 5 min incubation, the image of the blot was captured with VILBER (Marne-La-Vallée, France) chemiluminescence imaging system (Fusion FX - Imager E-box CX5 EDGE) (see Supplemental Fig. SIII-3). Control membranes were performed by omission of primary antibodies. Two secondary antibodies were used, namely goat anti-mouse IgG (H+L), HRP conjugate Invitrogen, Thermo Fischer Scientific, Waltham, USA), and chicken anti-mouse IgG (H+L), HRP conjugate, respectively reference A16078 and A15981 (Invitrogen, Thermo Fischer Scientific, Waltham, USA).

Immuno-dot blot image analysis

The immune-dot blot image analysis were performed using Fiji, an image processing package of ImageJ2 (Schindelin et al., 2012; https://imagej.net/software/fiji/) following the dot-blot analysis method described on the ImageJ website (https://imagej.nih.gov/ij/docs/examples/dot-blot/index.html). The integrated density of luminescence was determined on each dot by measuring the grey level of the pixels (volume) inside the circular selection of the dot. The integrated density of each dot was normalized against the integrated density obtained with 250 µg of levans from timothy.

Immunofluorescence localization of fructans epitopes

Roots of 10-d-old seedlings were placed onto sterile 10-welled diagnostic microscope slides (Thermo Scientific, ER-208B-CE24) and fixed for 40 min in 4% (w/v) PFA (paraformaldehyde), in 50 mM PIPES (piperazine- N,N'-bis [2-ethanesulfonic acid]), pH 7, containing 1 mM $CaCl_2$. Roots were washed 4 times for 10 min each wash at room temperature (RT) in phosphate-buffered saline PBS 1x containing 1% (w/v) bovine serum albumin (BSA) (Bovine Serum Albumin; AURION, Wageningen, Holland) and then incubated overnight at 4°C with the primary antibody (dilution 1:5 and 1:20 for 9H2-R2-2B1 and 15A6-R2-3E6, respectively in 1x PBS containing 1% w/v BSA). Roots were carefully washed 4 times at RT with PBS 1× and 1% BSA for 10 min, then were incubated with secondary donkey anti-mouse IgG antibody conjugated to Alexa Fluor 594 (Invitrogen) at 1:50 dilution in PBS 1x and 1% BSA for 2 h at 25°C. After 4 washes at RT in PBS 1x containing 1% w/v BSA and 1 final rinsing with PBS 1x for 10 min, roots were finally mounted in anti-fading solution (Agar scientific, Ref. AF2 R1320) then covered with a coverslip and observed using an epifluorescence microscope (Leica DMI6000B, Wetzlar, Germany; λExcitation: 591 nm; λEmission: 614 nm). Controls were routinely performed by incubation of the roots with the secondary antibody only. For this experiment, 3 to 4 technical replicates and 4 to 6 biological replicates were performed.

Semithin sections (0.5 µm) of 12-d-old roots and leaf bases on 10-welled Teflon microscope slides coated with Poly-L-Lysine were blocked in PBS 1x with 0.1% (v/v) Tween 20 (PBST) containing 3% (w/v) BSA and normal donkey serum (NDS-dilution 1:20) for 30 min at RT. Then, sections were carefully washed 5 times for 5 min with 0.1 % PBST containing 1% BSA. After washing, sections were incubated overnight at 4°C with primary antibody (dilution 1:2 in 0.1% PBST containing 1% BSA and NDS (diluted 1:20) for two anti-fructan mAbs). On the next day, sections were washed 5 times for 5 min with 0.1 % PBST containing 1% BSA before being incubated with secondary donkey anti-mouse IgG antibody conjugated to Alexa Fluor 594 (Invitrogen) at1:100 dilution in 0.1% PBST containing 1% BSA and NDS (diluted 1:20) for 2 h at 25°C. At RT, sections were rinsed 5 times for 5 min with 0.1 % PBST containing 1% BSA and two final washes for 5 min at RT with ultrapure water. Then, a droplet of ultrapure water was added to the section of each well. Epifluorescence of the immunostained tissue sections was observed on an epifluorescence microscope (Leica DMI6000B, Wetzlar, Germany; λExcitation: 591 nm; λEmission: 614 nm). Control experiments were performed by omission of primary antibodies. For this experiment, 3 technical replicates and 4 biological replicates were performed.

High-pressure freezing/freeze substitution sample preparation

Dissected 12-d-old root tips of Arabidopsis and perennial ryegrass were transferred into the cavity of copper cupules (100 µm in depth; 0.6 mm in diameter and 200 µm in depth; 0.6 mm in diameter, respectively). For the perennial ryegrass leaf bases, 0.5-mm long samples were dissected from the 10-mm long segment sampled and were transferred into the cavity of two copper cupules (300 µm in depth; 0.6 mm in diameter). All of the cupules were coated with soybean (*Glycine max*) lecithin (100 mg mL^{-1} in chloroform). The excess medium was removed using filter paper. The sample carriers were tightened securely to the pod of sample holder by using a horizontal loading station. Then, samples were frozen using a high-pressure freezing HPF-EM PACT I (Leica Microsystems) according to a maximum cooling rate of 20,000°C s^{-1}, an incoming pressure of 7.5 bars, and a working pressure of 4.8 bars. Cupules containing frozen samples were stored in liquid nitrogen until the freeze-substitution procedure was initiated.

After high-pressure freezing, samples were transferred to a freeze-substitution automate (AFS, Leica Microsystems) precooled to −140°C. Samples were substituted in anhydrous acetone with 0.5% uranyl acetate at −90°C for 96 h (Ovide et al., 2018). Using a gradient of +2°C h^{-1}, the temperature was gradually raised from −90 to −15°C with two intermediate steps at −60 and −30°C. Samples were washed twice at room temperature with fresh anhydrous acetone. Resin infiltration was processed at −15°C in a solution of ethanol/London Resin White (LRW) with successive ratios of 2:1 overday; 1:1 overnight and 1:2 overday followed by a final step in a pure LRW solution renewed twice during 48 h. The LRW was finally polymerized into the AFS apparatus at −15°C under ultraviolet light during 48 h. Using a Leica ultramicrotome EM-UC7 (Leica Microsystems), semithin sections (0.5 µm) were cut and adhered onto 10-welled diagnostic microscope slides (Thermo Scientific, ER-208B-CE24) pre-coated with Poly-L-Lysine (EMS-19320-B, dilution 1:10 in filtered water).

HPAEC-PAD analysis

HPAEC-PAD profiles of 12-day-old Arabidopsis root tips; 12-day-old ryegrass root tips and 30 mm long segments of perennial ryegrass leaf bases (Supplemental Fig. SIII-5) were carried out as described in Volaire et al. (2020).

Statistical analysis

Immuno-dot blot data were analyzed with R software version 4.1.2 using the "Rcmdr" package (R Core Team; 2021). Data are expressed as means ± standard error for three to five independent replicates. The effect of carbohydrate concentration was tested with the Kruskal-Wallis non-parametric test. Statistical significance was accepted at $P < 0.05$.

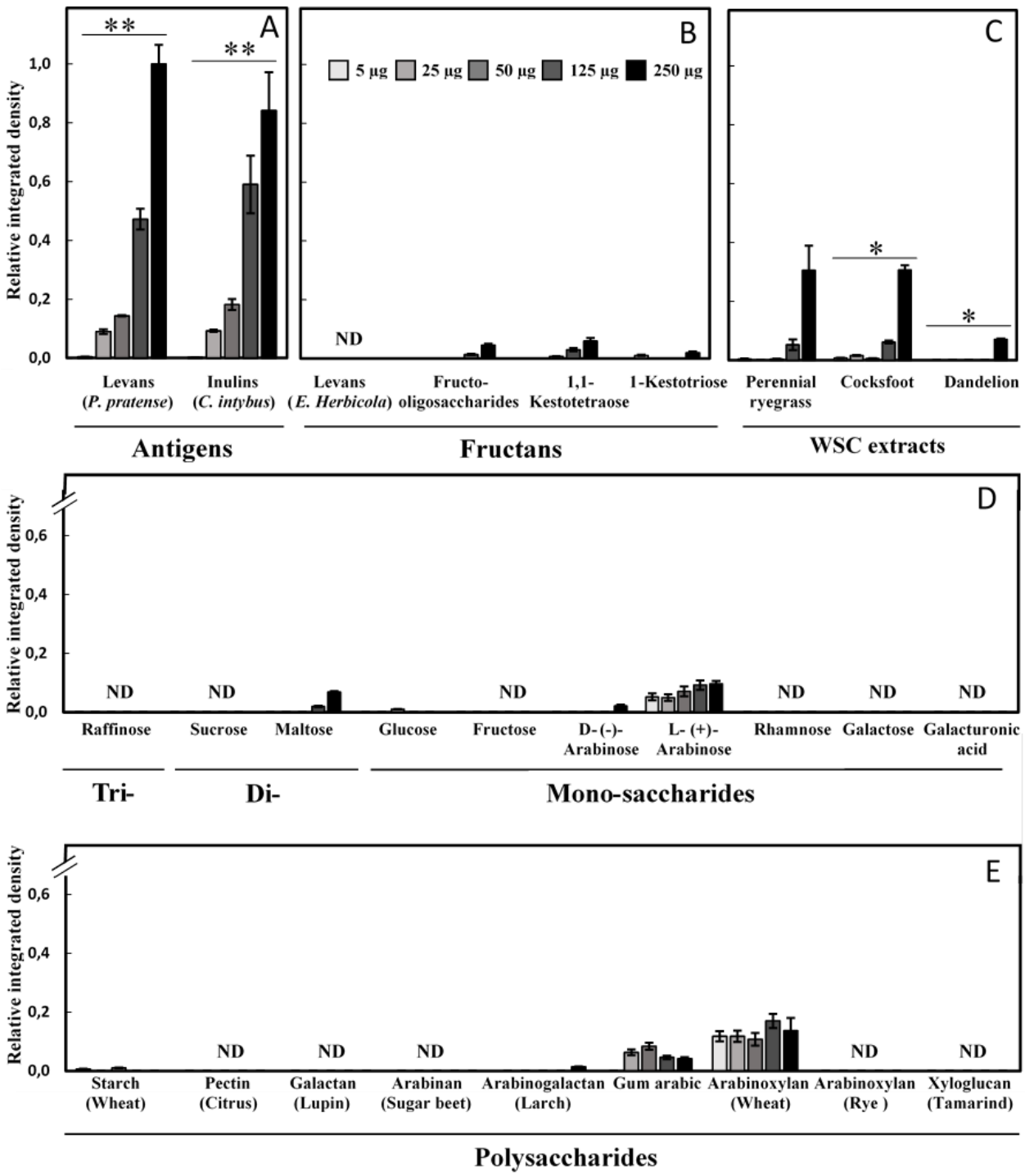

Figure III-1. Immuno-dot blot quantification using BTM9H2 mAb with goat anti-mouse secondary antibody. The assays included antigens used for mouse immunization (A), commercial fructans (B), WSC extracts (C), tri, di and mono-saccharides (D) and polysaccharides (E). The integrated density of each dot was normalized against the integrated density obtained with 250 µg of levans from *Phleum pratense*. Data are expressed as means ± standard error for three to five independent replicates. The effect of carbohydrate concentration was tested with the Kruskal-Wallis non-parametric test. *P < 0.05; **P < 0.01; ND, not detected.

Results

The selection of two mouse hybridoma clones using inulins from *C. intybus* and levans from *P. pratense* led to the purification of two monoclonal antibodies named 9H2-R2-2B1 (named BTM9H2) and 15A6-R2-3E6 (named BTM15A6) for full characterization.

1. BTM9H2 and BTM15A6 epitope characterization

The specificity of BTM9H2 and BTM15A6 was investigated by immune-dot blot assay (Fig. III-1 to III-4, supplemental Fig. SIII-3) against a set of oligosaccharides representing common sub-structures found in fructans as well as water soluble carbohydrate (WSC) extracts of fructan-accumulating plants (see Appendix 1 and Fig. III-1).

BTM9H2 detected 25µg of timothy (*P. pratense*) levans (β-(2,1)-linked-fructans) and 25µg of chicory (*C. intybus*) inulins (β-(2,1)-linked-fructans). The reaction increased with the amount of antigen deposited (25 to 250 µg) (Fig. III-1A). BTM9H2 bound weakly to 250µg of fructo-oligosaccharides (FOS) from chicory (β-(2,1)-linked-fructans from DP3 to 10), 1,1-kestotetraose (DP4) and 1-kestotriose (DP3). No binding was detected to bacterial levans from *Erwinia herbicola* (β-(2,6)-linked fructans from DP100 to 10000) (Fig. III-1B). In addition to commercial purified fructans, WSC extracts from fructan-accumulating plants were also used to assess BTM9H2 binding (Fig. III-1C, Supplemental Fig. SIII-1). BTM9H2 showed a strong reactivity with 250 µg of WSC extracts from perennial ryegrass, cocksfoot, and dandelion. Altogether, these data indicate that BTM9H2 bound strongly to fructans with both β-(2,1) or β-(2,6) linkages from diverse plant species and also, but less strongly, to small purified fructans (DP3-10). Moreover, no binding of BTM9H2 was detected with a wide range of tri-, di- and mono-saccharides except a weak binding to 250 µg of maltose and D-arabinose (Fig. III-1D). Weak binding of BTM9H2 to L-arabinose was observed but was independent of the amount deposited.

BTM9H2 binding was also investigated towards starch and cell wall polysaccharides which do not contain the two consecutive fructose residues that characterize fructans (Fig. III-1E). BTM9H2 did not bind to compounds containing β-(1,4) linkages like citrus pectin, lupin seed galactan, rye arabinoxylan and xyloglucan from tamarind seed, when deposited at up to 250µg per dot. No reaction was detected either with arabinan (α-1,5 linked-arabinose units) from sugar beet pulp. A very low binding to wheat starch and larch wood arabinogalactan was detected. As for L-arabinose, BTM9H2 bound weakly to gum arabic and wheat arabinoxylan but the binding was independent of the amount deposited.

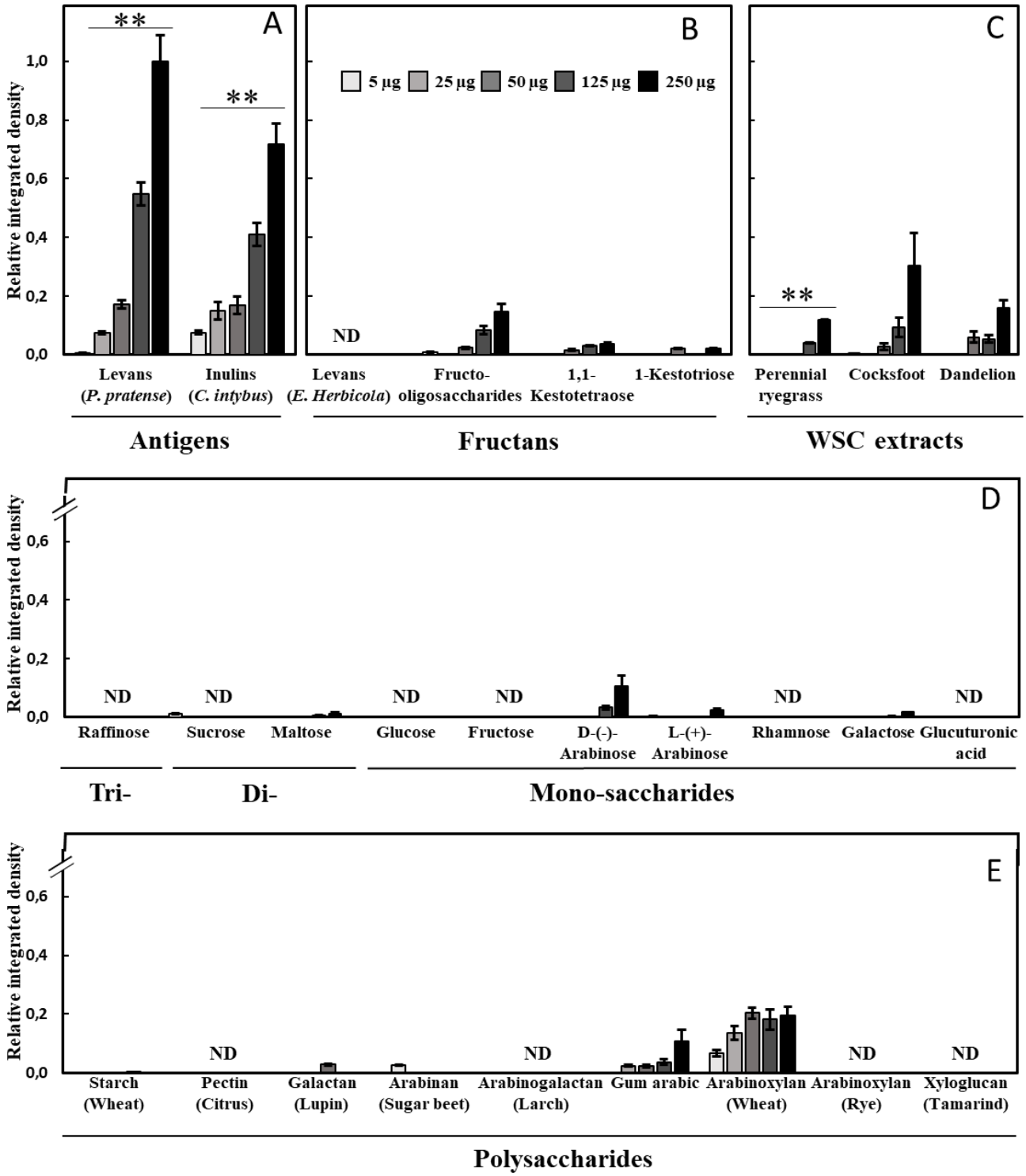

Figure III-2. Immuno-dot blot quantification using BTM15A6 mAb with goat anti-mouse secondary antibody. The assays included antigens used for mouse immunization (A), commercial fructans (B), WSC extracts (C), tri, di and mono-saccharides (D) and polysaccharides (E). The integrated density of each dot was normalized against the integrated density obtained with 250 µg of levans from Phleum pratense. Data are expressed as means ± standard error for three to five independent replicates. The effect of carbohydrate concentration was tested with the Kruskal-Wallis non-parametric test. *P < 0.05; **P < 0.01; ND, not detected.

As shown in Figure III-2A, BTM15A6 detected approximately 25 µg of timothy levans and 5 µg of chicory inulins. This reaction increased according to the concentration of the antigen which confirms that the epitope recognized by BTM15A6 includes β-(2,1) and β-(2,6) linkages in fructans. In addition, BTM15A6 also bound weakly to diverse fructans from plants such as chicory FOS, 1,1-kestotetraose, and 1-kestotriose, but not to bacterial levans from *Erwinia herbicola* (Fig. III-2B). BTM15A6 bound strongly to WSC extracts from perennial ryegrass, cocksfoot, and dandelion (Fig. III-2C). These data confirmed that BTM15A6 binds strongly to β-(2,1) and β-(2,6) linkages of fructans from diverse plant species. Further immuno-dot blot assays were realized with a range of tri-, di- and mono-saccharides and with major polysaccharide classes found in plants including pectins and hemicellulosic polysaccharides which contains β-(1,4)-linked backbones. The results showed that BTM15A6 did not detect any of tri-, di- and mono-saccharides except a weak reaction with 250 µg of maltose, galactose, D-arabinose, and L-arabinose (Fig. III-2D). No reaction of BTM15A6 with citrus pectin, rye arabinoxylan and tamarind xyloglucan was observed (Fig. III-2E), supporting the notion that the epitopes recognized by BTM15A6 do not include β-(1,4)-linkages. BTM15A6 showed no reaction with 250 µg larch wood arabinogalactan. Moreover, the binding obtained with wheat starch, lupin galactan, and sugar beet arabinan was extremely weak and was not proportional to the amount deposited. As illustrated in figure III-2E, BTM15A6 was found to react slightly with gum arabic and wheat arabinoxylan but the binding was independent of the amount deposited.

Negative controls were performed using the secondary antibody (goat anti-mouse IgG-alexa) without the presence of primary anti-fructans antibodies (see Supplementary Fig. SIII-4). A strong binding was observed between goat anti-mouse secondary antibody and WSC extracted from perennial ryegrass and this binding was all the higher as the amount deposited increased (see Supplementary Fig. SIII-4).

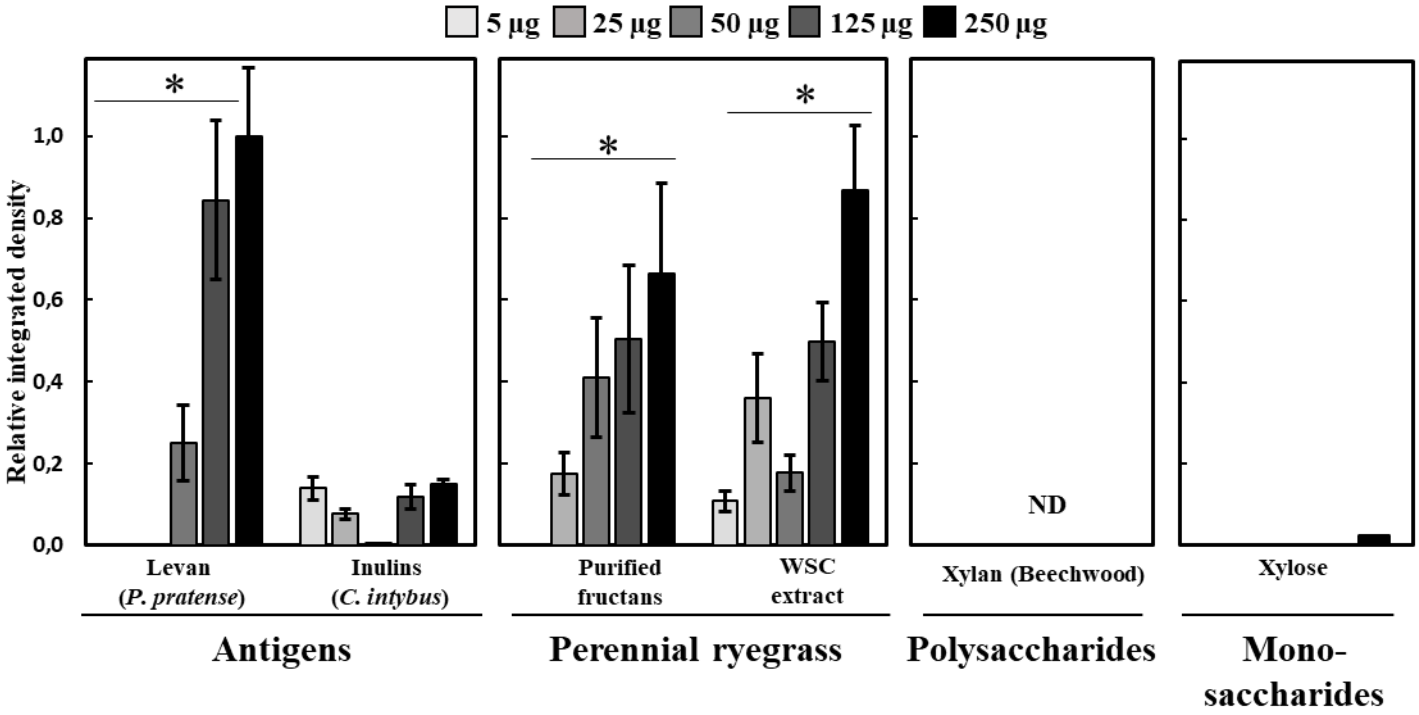

Figure III-3. Immuno-dot blot quantification using BTM9H2 mAb with chicken anti-mouse secondary antibody. The integrated density of each dot was normalized against the integrated density obtained with 250 µg of levans from *Phleum pratense*. Data are expressed as means ± standard error for three to five independent replicates. The effect of carbohydrate concentration was tested with the Kruskal-Wallis non-parametric test. *P < 0.05; **P < 0.01; ND, not detected

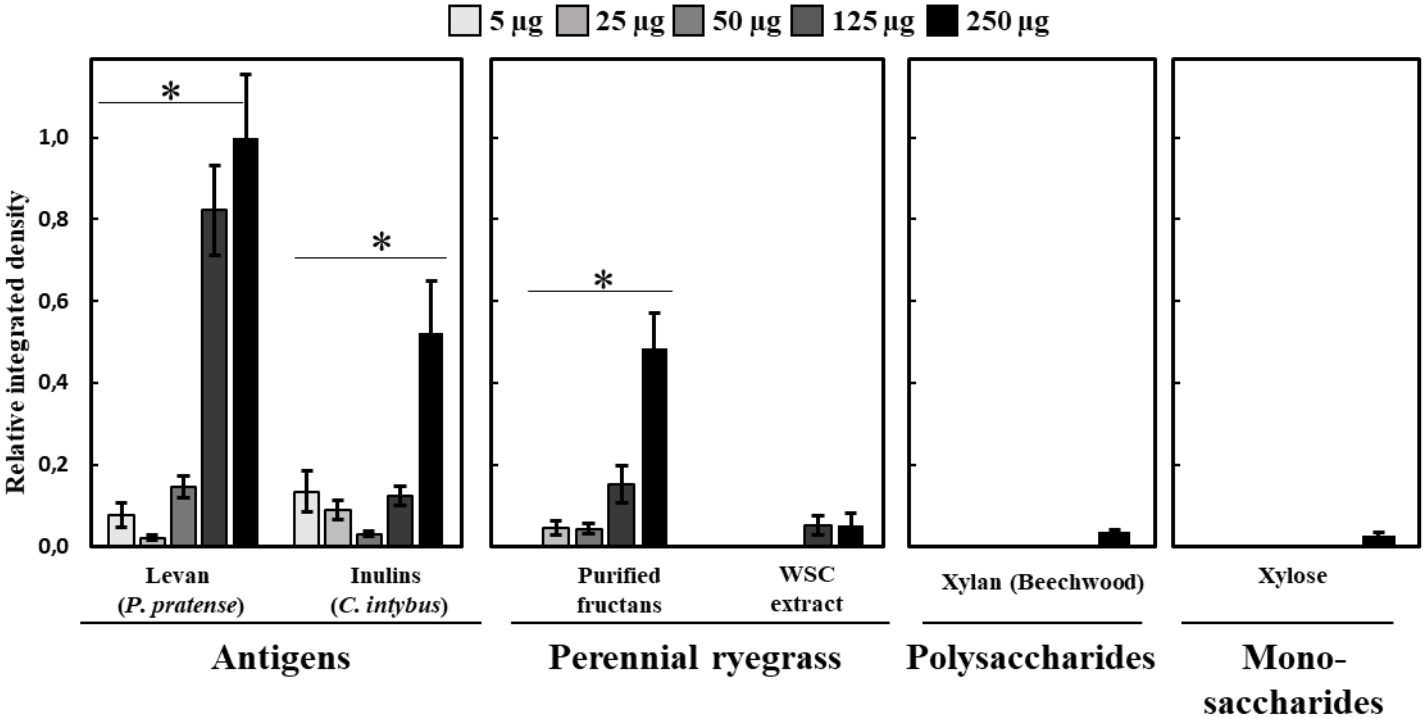

Figure III-4. Immuno-dot blot quantification using BTM15A6 mAb with chicken anti-mouse secondary antibody. The integrated density of each dot was normalized against the integrated density obtained with 250 µg of levans from *Phleum pratense*. Data are expressed as means ± standard error for three to five independent replicates. The effect of carbohydrate concentration was tested with the Kruskal-Wallis non-parametric test. *P < 0.05; **P < 0.01; ND, not detected

Another secondary antibody (chicken anti-mouse secondary antibody) allowing to abolish the non-specific labeling was used for subsequent analyses. It is worth noting that when using chicken anti-mouse secondary antibody, strong binding of BTM9H2 still occured to timothy levans and perennial ryegrass WSC extracts (Fig. III-3) although weakly to chicory inulins. As expected, BTM9H2 reacted strongly with purified fructans and WSC extract from perennial ryegrass, and no reaction was observed with beechwood xylan and xylose. The specificity of BTM15A6 was also clearly confirmed with timothy levans, chicory inulins, and fructans from perennial ryegrass by using chicken anti-mouse secondary antibody (Fig. III-4). A slight binding was detected with 125 µg of perennial ryegrass WSC extract and 250 µg of beechwood xylan. No reaction of BTM15A6 with xylose was observed.

Altogether, these results show the specificity of BTM9H2 and BTM15A6 towards the β-(2,1) and β-(2,6) linkages of fructans and towards diverse fructan types from plant species.

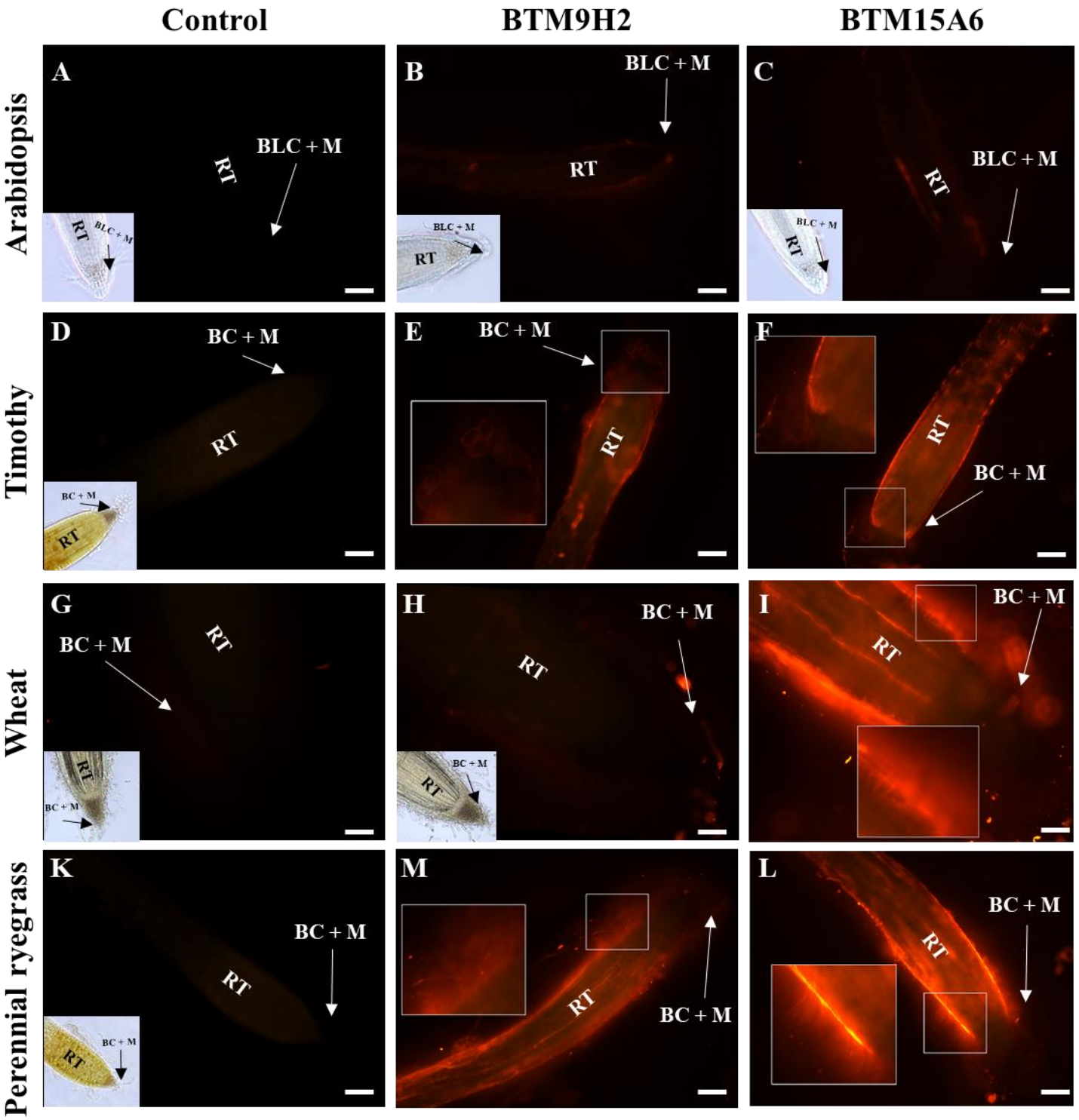

Figure III-5. Immunofluorescence detection of fructans on root tips of A. thaliana, timothy, wheat and perennial ryegrass using the monoclonal antibodies BTM9H2 and BTM15A6.

Observations are made with an epifluorescence microscope (Leica DMI6000B, Wetzlar, Germany; λExcitation: 591 nm; λEmission: 614 nm). (A, D, G, K) control experiments were performed only with secondary antibody. (B, E, H, M) fluorescence images showing labeling with the mAb 9H2 at dilution 1:5. (C, F, I, L) fluorescence images showing labeling with the mAb 15A6 at dilution 1:20. For each plant, 27 to 30 roots were observed. BLC: Border-like cell; BC: Border cell; RT : Root tip ; M: Mucilage. Scale bars = 100 µm.

2. BTM9H2 and BTM15A6 epitope immunolocalization

BTM9H2 and BTM15A6 were further used to look for fructans in the root tips of three fructan-accumulating plants, timothy, wheat and perennial ryegrass. *A. thaliana* root tips were used as control since *A. thaliana* is a non-fructan plant (De Coninck et al., 2005).

Indirect immunofluorescence analysis of BTM9H2 at the root surface indicated a slight signal surrounding the root tip of perennial ryegrass and timothy and a more intense fluorescence at the surface of the meristematic and elongation zones (Fig. III-5E, M). Only a very faint signal was detected at the root surface of wheat (Fig. III-5H). The root surface of perennial ryegrass, timothy and wheat, was specifically and strongly labelled by BTM15A6 mainly at the meristematic and elongation zones (Fig. III-5F, I, L). No labeling was observed at the cell surface of the control root tip without BTM9H2 and BTM15A6 antibodies (Fig. III-5D, G, K). The surface of the root tip of *A. thaliana* were deprive of labeling with both BTM9H2 and BTM15A6 indicating that the epitopes were obviously specific to fructan-accumulating plants (Fig. III-5B, C).

In order to localize mAbs epitopes inside tissues, immunofluorescence labeling with BTM9H2 and BTM15A6 was performed on section of roots and leaves of perennial ryegrass and *A. thaliana* prepared by high pressure frozen/freeze-substituted (HPF) (Supplemental Fig. SIII-2). The analysis of sections of resin-embedded material confirmed the specific recognition of BTM9H2 epitopes in perennial ryegrass root tips as well as in the base of mature leaf sheaths while the labelling was very low in elongating leaf bases (Supplemental Fig. SIII-2G, H). In root tips, the labelling was detected not only in elongation and meristematic area but also in root cap (Supplemental Fig. SIII-2H). At the cellular level, the fluorescence was uniformly distributed inside each cell suggesting cytoplasmic localization of the epitopes (Supplemental Fig. III-2H). In mature leaf sheath section, the labelling was observed in mesophyll and parenchyma bundle sheath cells (Supplemental Fig.SIII-2G). At the cellular level, the fluorescence was not uniformly distributed and appeared to surround and leak from some cells (Supplemental Fig.III-2H). In contrast with perennial ryegrass, BTM9H2 labeling is absent from the Arabidopsis sections (Supplementary Fig.SIII-2I). Analysis of WSC extracts from the same plant materials used for cryofixation confirmed the presence of fructans in perennial ryegrass leaf bases and root tips (Supplemental Fig. SIII-5A, B) while no fructans were detected in Arapidopsis root tips (Supplemental Fig. SIII-5C).

A strong labeling was detected with BTM15A6 on section of root tip and mature leaf sheaths of perennial ryegrass (Supplementary Fig. SIII-2J, K). As for BTM9H2, BTM15A6 epitopes were less detected in the deeper section compared to the shallower section (Supplemental Fig.

SIII-2E, F). Similar to BTM9H2, the fluorescence was uniformly distributed inside each root cell suggesting that the epitopes were localized in cytoplasm (Supplemental Fig. SIII-2K). In mature leaf sheath sections, the labelling was mainly observed in mesophyll and parenchyma bundle sheath cells and appeared to surround and leak from some cells (Supplemental Fig.III-2G, 2J). In contrast, no BTM15A6 epitope was detected in Arabidopsis root tip sections compared to root and leaf tissues of perennial ryegrass (Supplementary Fig.SIII-2K, L).

Discussion

Following hybridoma production, a pre-selection of mAb producing lines was carried out using immuno-dot blot assay. This technique has been proved to be a useful technique in a lot of studies for epitope mapping and allows the screening of antibodies for target specificity across many samples at once (McCartney et al., 2005; Manceur et al., 2017, Cheng et al., 2019). In this study, this leads to the characterization of two new mAbs (BTM15A6 and BTM9H2) with high specificity against β-(2,1) and β-(2,6)-fructans from plants. To our knowledge, this is the first report on the characterization of highly specific anti-fructan mAbs and their application for immunocytochemical analyzes in different types of plant tissues.

The specificity of BTM15A6 and BTM9H2 was demonstrated by a strong binding at low concentration with levans (β-(2,6)-linked fructans) from timothy (*Phleum pratense*) and inulins (β-(2,1)-linked fructans) from chicory (*Cichorium intybus*) as well as with WSC extracts obtained from fructan-accumulating plants grasses (perennial ryegrass, *Lolium perenne* and cocksfoot, *Dactylis glomerata*) and from the Asteraceae dandelion (*Taraxacum officinalis*). Both mAbs did not bind or showed a weak insignificant reaction even at the highest concentration with other carbohydrates representing major mono-, di-, oligo- and polysaccharides found in plants including starch, pectins, proteoglycans and hemicellulosic polysaccharides. The binding profiles are very similar between the two mAbs.

Moreover, the absence of binding with bacterial levans from *Erwinia herbicola* also contribute to confirm the specificity of BTM15A6 and BTM9H2 for β-(2,1) and β-(2,6)-linked fructans from plants. The very high DP of bacterial levans, which is above 100 and up to 10000 (Velázquez-Hernández et al., 2009) compared to the average DP of about 75 for levans from timothy (P-LEVAN, Megazyme) could explain this specificity.

To confirm the specificity of recognition of fructans by the two mAbs, their binding on tissues of fructan- and non-fructan-accumulating plants tissues was tested by fluorescence microscopy. This technique is widely used with anti-glycan antibodies directed against cell-wall polysaccharides to study cell wall structures within complex tissues (Knox, 2008) and also to

analyze the composition of the mucilage produced by root tip (Durand et al., 2009) or seeds (Voiniciuc et al., 2015). Recently, mAbs against starch have been successfully developed and used to localize starch granules in pea root cap (Rydahl et al., 2017). Here, we first used the two anti-fructans mAbs to localize their epitopes on root tip surface as was done to localize other polysaccharides such as xyloglucan, pectic polysaccharides and arabino-galactan-proteins (AGP) at the surface of roots and root border cells and in the root mucilage (Durand et al., 2009).

Our observations showed convincingly that BTM9H2 and BTM15A6 epitopes are present at the surface of the root tips of the fructan-accumulating plants tested, perennial ryegrass, timothy and wheat while they are not detected at the surface of root tips of the non-fructan plant tested, Arabidopsis. In all three species, which accumulate distinct fructan types (Ritsema and Smeekens, 2003), labelling was higher with BTM15A6 than with BTM9H2. The difference was particularly high with wheat which accumulates branched fructans (graminans), suggesting that the two mAbs do not have exactly the same specificity towards fructans of differents types. In addition, the immunofluorescence labeling of both mAbs was found on the cryofixed and freeze-substituted, which are the best techniques for epitope preservation (Chevalier et al., 2010). Labeling was specifically detected on sections of perennial ryegrass root tip and leaf bases but not on root section of Arabidopsis, confirming once again their specificity towards plant fructans.

The fact that BTM15A6 and BTM9H2 epitopes were found at the surface of the elongation and meristematic zones of the root tips indicates that fructans are present outside the cells and suggests that a mechanism of secretion from their synthesis localization (i.e. vacuole; Wagner et al., 1983) to the apoplast operates in these tissues. Apoplastic localization of fructans has been reported in crown tissues of oat after cold hardening (Livingston and Henson, 1998) and in the phloem of *Agave deserti* (Wang and Nobel, 1998) but, to our knowledge, this is the first report of fructans outside the cells at the root level.

In the root and mature leaf sheath sections, the labelling was mainly found inside the cells, consistent with the vacuolar localization of fructans. Their localization in mature leaf sheaths is also consistent with their detection in large amount in leaf sheath water soluble extracts (Lothier et al., 2014) where they serve as carbon storage for regrowth after defoliation (Morvan-Bertrand et al., 2001). The very low labelling detected in elongating leaf bases is unexpected because high fructan levels are usually found in the leaf elongation zone where they serve as short-term storage for use in the secondary cell wall development (Allard and Nelson, 1991; Pollock and Cairns, 1991). This could be due to fructan leakage during tissue fixation, as seen

from some cells in the leaf sheath section, but which could be greater for young cells than for mature cells. This indicate that cryofixation and freeze-substitution protocols need to be improved for these fragile tissues.

In addition to the wide range of techniques used for the characterization and quantification of fructans (Matros et al., 2019), the mAbs BTM15A6 and BTM9H2 provide new tools that will be powerful for the specific localization of fructans in different plant tissues and cells. Their use as fructan probes will deepen the understanding of the mechanisms of fructans involvement in plant metabolism and in their interaction with microorganisms. More broadly, these two mAbs enrich the family of antibodies against structural and non-structural polysaccharides already available for plant research (Rydahl et al., 2017; 2018).

Acknowledgments

We thank Aurelia Lornac (EVA laboratory) for her very valuable technical assistance for preparation of WSC extracts, purification of perennial ryegrass fructans and HPAEC-PAD analysis. We thank Carole Burel and Quentin Arnaudin (GlycoMEV laboratory) for their very valuable technical assistance for immune-dot blot assays, and Bruno Gugi for providing the oligo/polysaccharides used in this study.

Author contributions

TNHN, MV, MPP, MLFG and AMB conceived and designed the experiments; LD managed mAbs production; TNHN performed immune-dot blot and immunocytochemistry; DG performed preparation of perennial ryegrass samples for preliminary microscopical observations; SB performed the high-pressure freezing/freeze substitution sample preparation and MLFG performed their sections; TNHN and AMB analyzed the immune-dot blot data; TNHN wrote the first draft, AMB, MV, LP, MLFG and MPP edited and improved the manuscript.

Funding

This work was supported by the Universities of Caen and Rouen Normandie. The Normandie Council supported the work through the research projects EPURE (Enhancing Plant nutRition and Health, 2017-2019) and Normandy Plant Technologies (2018-2021). The Normandie Council and the European Union (in the framework of the ERDF-ESF operational program 2014-2020) supported the work through the research project BEER (Bactéries, Exsudats, Et Rhizodépots, 2019-2022). Thi Ngoc Hanh Nguyen received a PhD grant (2018-2021) from the Normandie Council.

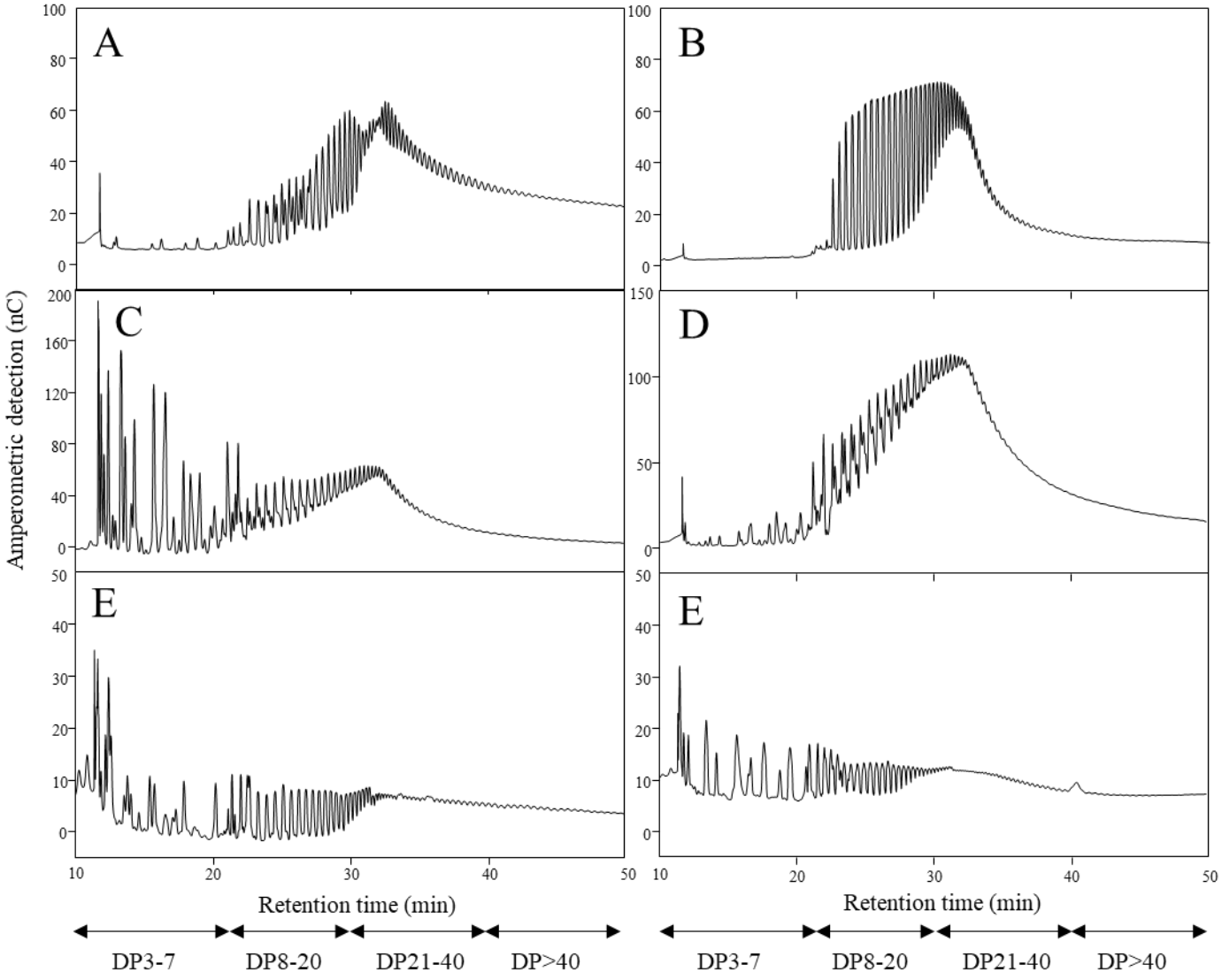

Figure S III-1. HPAEC-PAD profiles of levans from timothy (A; P-LEVAN Megazyme), inulins from chicory (B; P-INUL Megazyme), fructans from WSC extracted from 8-week-old perennial ryegrass 0-5cm-leaf bases (C), purified fructans of high DP from 8-week-old perennial ryegrass 0-3cm-leaf bases (D); fructans from WSC extracted from cocksfoot 0-5cm-leaf bases (E); fructans from WSC extracted from dandelion roots (F). DP3-7, retention time 10-22 min; DP8-20, retention time 22-30 min; DP21-40, retention time 30-40 min; DP>40, retention time 40-50 min.

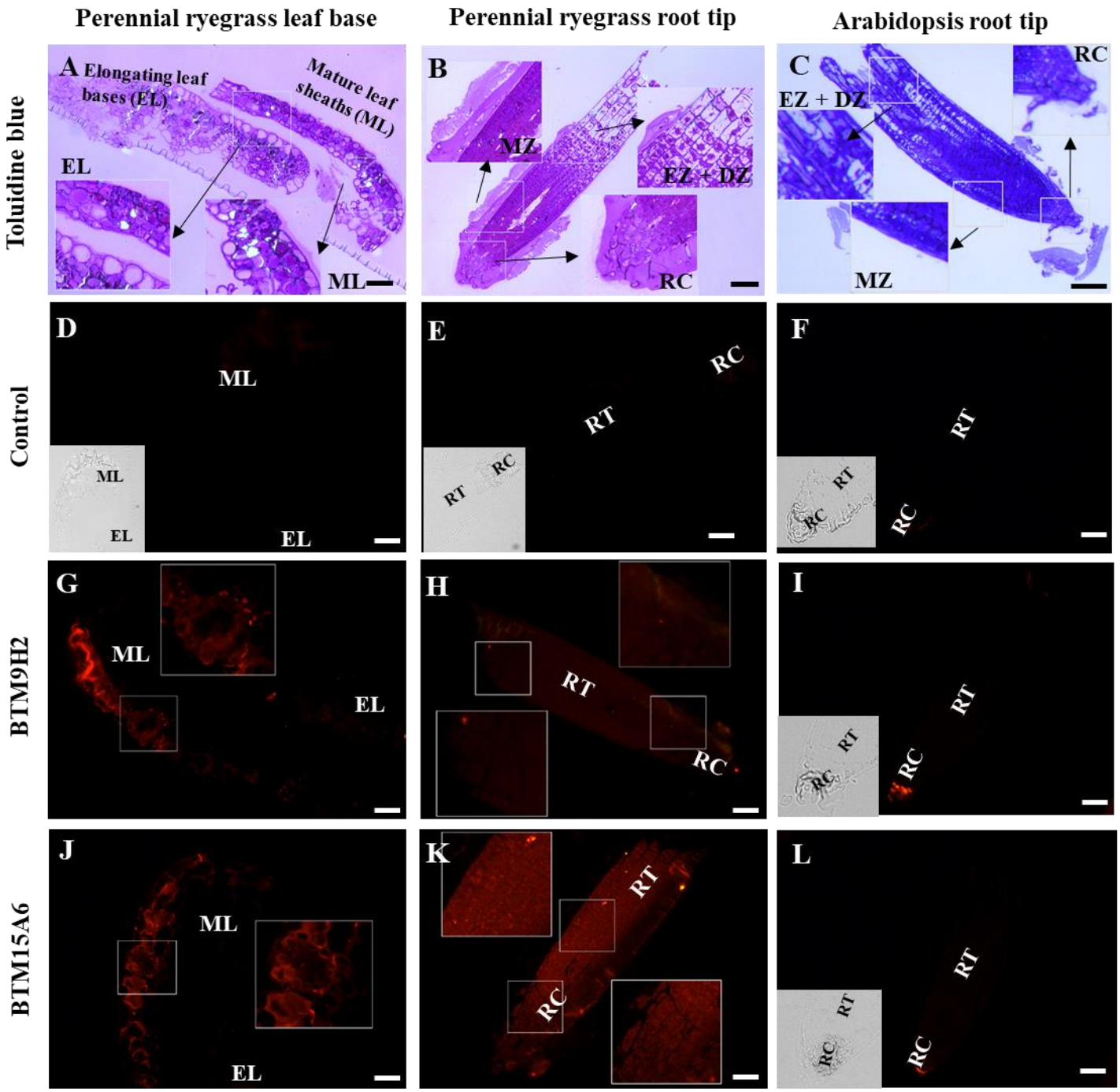

Figure S III-2. Toluidine blue staining (A-C) and immunofluorescence labeling of fructans epitopes of high pressure frozen/freeze-substituted sections of leaf bases of perennial ryegrass grown for 7 weeks (A, D, G, J), root tips of perennial ryegrass grown for 12 days (B, E, H, K), and root tips of *Arabidopsis* grown for 12 days (C, F, I, L) Observations are made with an epifluorescence microscope (Leica DMI6000B, Wetzlar, Germany; λExcitation: 591 nm; λEmission: 614 nm). Detection of fructan epitopes with BTM9H2 (C, G, K) and BTM15A6 (D, H, L). RT: Root tip; RC: Root cap; ML: Mature leaf sheaths; EL: Elongating leaf bases. Scale bars = 100 µm.

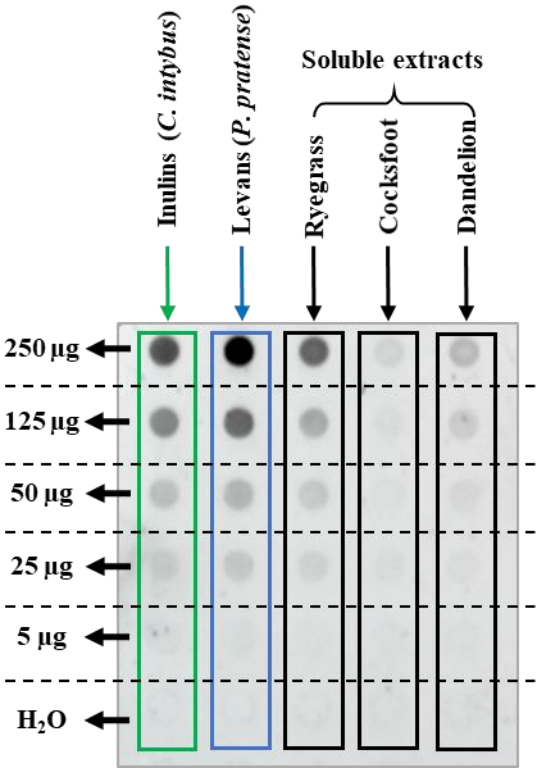

Figure S III-3. Illustration of immunodot blot assay of the binding of anti-fructan antibodies to a series of fructans and other soluble extracts.
Samples were applied to nitrocellulose as 50µL dots from 250µg to 5 µg.

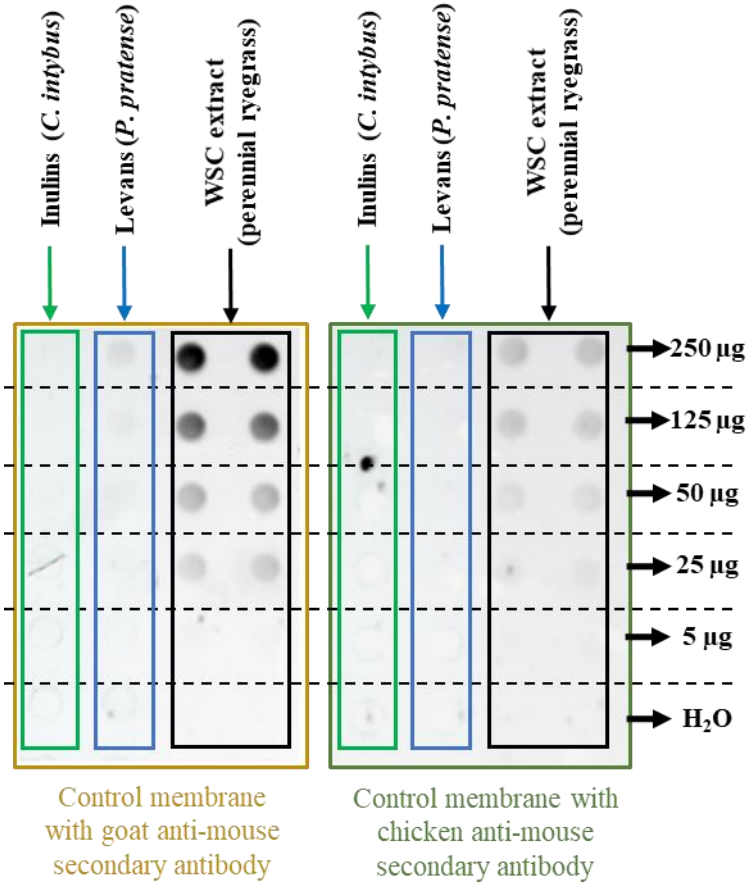

Figure S III-4. Illustration of immunodot blot assay of the binding of secondary antibodies to perennial ryegrass WSC extract.
Samples were applied to nitrocellulose as 50µL dots from 250µg to 5 µg. These membranes were performed with omission of anti-fructan mAbs. The goat anti-mouse secondary antibody (left membrane) binds strongly to perennial ryegrass WSC extract while the chicken anti-mouse secondary antibody (right membrane) shows only a weakly signal.

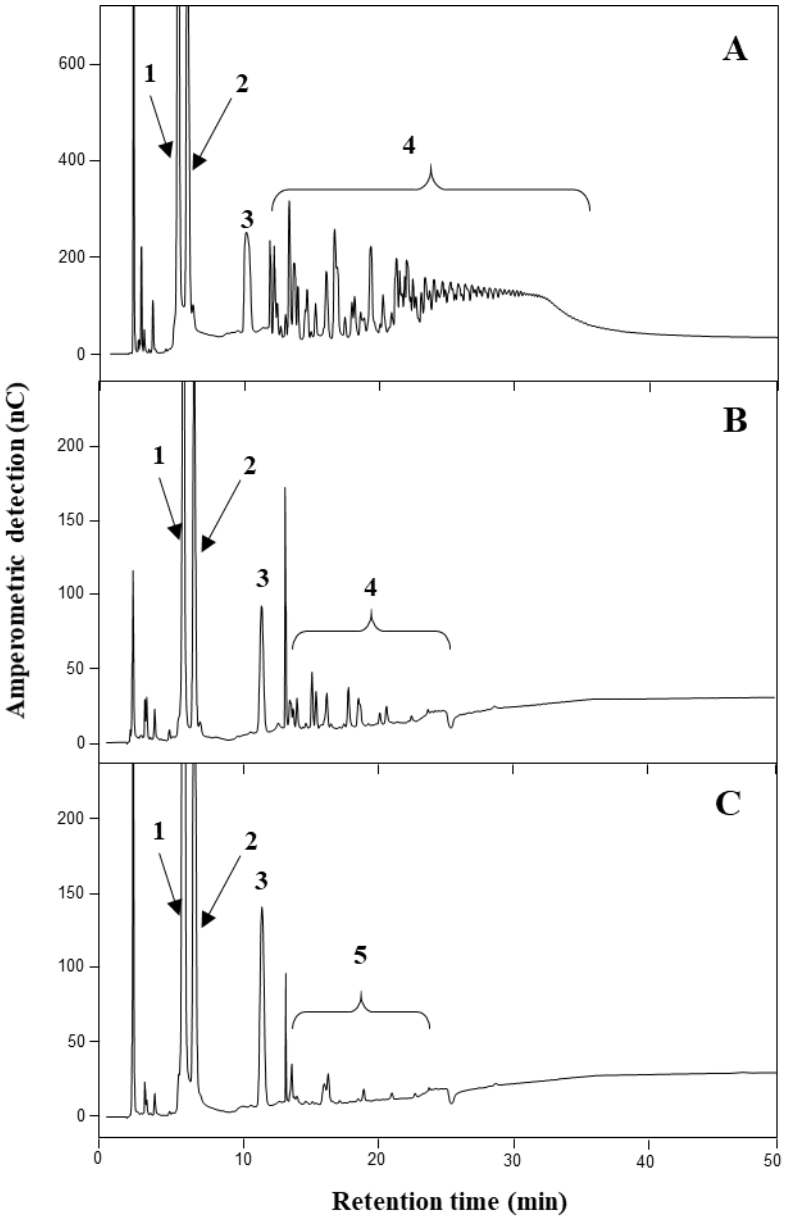

Figure S III-3. HPAEC-PAD profiles of WSC extracted from sub-samples from the samples used for high pressure frozen / freeze substitution fixation of 7-week-old perennial ryegrass 0-3cm-leaf bases (A). 12-day-old perennial ryegrass 0-1cm root tips (B) 12-day-old *Arabidopsis* 0-1cm-root tips (C). 1, glucose; 2, fructose; 3, sucrose; 4, fructans; 5, other oligosacharides. The extracts were injected with an equivalent dry matter mass.

2. Microscopical characterization of the root extracellular trap (RET) of perennial ryegrass (*Lolium perenne*), a fructan producing plant.

Thi Ngoc Hanh Nguyen[1,2], Mélanie Fortier[2], Annette Morvan-Bertrand[1], Marie-Pascale Prud'homme[1], Sophie Bernard[2,3], Azeddine Driouich[2], Marie-Laure Follet-Gueye[2,3], Maïté Vicré[2].

[1]Normandie Univ, UNICAEN, INRA, EVA Ecophysiologie Végétale Agronomie et nutritions N.C.S, FED Normandie Végétale 4277, 14032 Caen, France

[2]Normandie Univ, UNIROUEN, Laboratoire GLyco-MEV EA 4358, FED Normandie Végétale 4277, 76000 Rouen, France

[3]Cell Imaging Platform (PRIMACEN-IRIB), Université de ROUEN Normandie, UFR des Sciences et Techniques, F-76821 Mont-Saint-Aignan, France

Abstract

The root defense remains poorly investigated as compared to the aerial part of the plant. In roots, atypical protection is provided by the « Root Extracellular Trap » or RET specifically dedicated to the root tip defense. The composition of the RET and the structural organization of the different polymers are essential to provide root defense against pathogen attacks. The RET is mainly composed of polysaccharides (pectins, xyloglucan), proteoglycans such as arabinogalactan-proteins (AGPs), extracellular DNA and defense proteins such as defensin. The precise role of the different compounds in root protection remains to be clearly established. Our study aims to characterize the RET composition of perennial ryegrass (*Lolium perenne*) using cell imaging techniques and a wide range of monoclonal antibodies directed against epitopes from cell wall polymers. Moreover, since *L. perenne* produces high level of fructans which constitute the main carbohydrate reserve and which act in plant protection against abiotic and also biotic stresses, we evaluated if fructans are present in the RET. Interestingly, we found that both mucilage and cell wall surface of border cells were enriched in AGPs epitopes. An increase amount of the AGP-containing mucilage was produced by *L. perenne* root tip in response to both elicitor and water stress. Our hypothesis is that AGPs play an essential role in root protection in *L. perenne*. Fructan epitopes were not detected within the RET, but are present at the surface and inside the cells of meristematic and elongation zones and also inside the cap cells. This suggest that these carbohydrates may be also involved in root protection against biotic and/or abiotic stresses.

Introduction

The root system plays a vital role in maintaining plants health and survival in their natural environment. Although their main functions are to provide anchorage, mineral nutrition, and water uptake (Petricka et al., 2012), roots are also an area in constant interaction with a myriad of microorganisms (Berendsen et al., 2012). Soil-borne pathogens pose a real threat to the plant and are often major problems agriculture resulting in sever production losses. Due to their belowground localization, diseases caused by root infecting pathogens are often more difficult to control as compared to the aerial parts of the plant (Raaijmakers et al., 2008). While the defense mechanisms against pathogens have been largely investigated for the aerial parts of the plants, knowledge is still scarce regarding the root system (Chuberre et al., 2018). Differences were reported between immune responses in leaves and roots and it is hazardous to extrapolate data from the aerial part to the below-ground system. It is thus necessary to get a better understanding of the root system defense (Millet et al., 2010; Mauch-Mani et al., 2017; Poncini et al., 2017). Furthermore, it is always a challenge for the root system to discriminate beneficial microbes from harmful pathogens (Yu et al., 2019). Root immune suppression is supposed to be a key event for the establishment of mutualistic relationships with beneficial microbes, including rhizobia and arbuscular mycorrhiza. It is thus an exciting field of research to decipher the defense mechanisms allowing the root system to selectively ward off pathogens (Zhou et al., 2020).

It is now well recognized that a particularity of the root system is to rely on atypical cells termed root "border cells" providing protection specifically dedicated to the root tips. Due to their localization at the interface between root and soil, border cells act in the rhizosphere by either promoting or inhibiting interactions with microbes. BCs are defined as detached cells that are released individually into the rhizosphere from the periphery of the root cap (RC) in the presence of water (Hawes et al., 2003). To date, the presence of BC has been reported in more than 35 species belonging to 11 different families (Hawes et al., 2003; Cannesan et al., 2011). Different populations of BCs are found to be released by the root tip of a single plant species, i.e. pea (*Pisum sativum*) and soybean (*Glycine Max*) including small spherical cells, intermediate-size cells, and elongated cells (Cannesan et al., 2011; Ropitaux et al., 2020).

Vicré et al. (2005) described for the first time the presence of cells that remain associated together into small groups of cells and organized in a sheath-like pattern after release from the root tip in *Arabidopsis thaliana* and which adhere to the root apex unlike BCs. Based on their organization pattern and their detachment, they were named "border-like cells" or BLCs (Vicré

et al., 2005; Durand et al., 2009; Driouich et al., 2007). The presence of BLCs were then discovered in other species belonging to Brassicacea family including rapeseed (*Brassica napus*), Brussels sprout (*Brassica oleraceae*), mustard (*Sinapis alba*), and radish (*Raphanus sativus*) (Driouich et al., 2007, 2010, 2012). This type of BLC organization was also reported in flax (*Linum usitatissimum*) where three morphotypes were described: spherical border-like cells (sBLC), elongated border-like cells (eBLC) and filamentous border-like cells (fBLC) (Plancot et al., 2013). For simplification, the term root-associated, cap-derived cells (AC-DCs) was proposed by Driouich et al. (2019) to include all the different type of cells previously described (Hawes et al., 2000, 2003; Driouich et al., 2007, 2010; Endo et al., 2011; Karve et al., 2016; Wang et al., 2017).

AC-DCs are surrounded by a thick layer of mucilage enriched in cell wall polysaccharides and proteoglycans including homogalacturonan, xylogalacturonan, arabinogalactan-proteins (AGPs) and xyloglucan (Knee et al., 2001; Durand et al 20009; Cannesan et al., 2012; Mravec et al., 2017; Ropitaux et al., 2019). Xyloglucan was reported as an important compound and was shown to be part of the scaffold of this mucilage providing a dense fibrillary network surrounding border cells. This mucilage together with AC-DCs form a protective structure defined as the Root Extracellular Trap (RET) by analogy with the Neutrophil Extracellular Trap (NET) involved in mammalian immunity (Bowdish et al., 2005; Urban et al., 2009; Driouich et al. 2013). The RET is characterized by the presence of diverse anti-microbial molecules such as proteins (Ma et al., 2010; Weiller et al., 2016), glycoproteins, proteoglycans (Bacic et al., 1986; Knee et al., 2001), H4-type histones, extracellular DNA (exDNA) (Wen et al., 2009; Tran et al., 2016) and reactive oxygen species (ROS) (Plancot et al., 2013). The role of the RET in immune defense mechanism is thought to occur through a wide range of mechanisms including either attraction, repulsion or neutralization of microbial pathogens (Driouich et al., 2013; 2019). In the case of the pathogenic oomycete *Aphanomyces euteiches*, the RET from *Pisum sativum* interfere with the mobility of zoospores and cyst germination (Cannesan et al. 2012). Ropitaux et al. (2020) showed that the RET from soybean acts as a physical (or even chemical) barrier preventing zoospores of *Phytophthora parasitica* from reaching and colonizing the root cap. The involvement of RET in the root protection towards abiotic environmental stresses, e.g. toxicity of some heavy metals such as aluminum, cadmium, and copper (Deiana et al., 2003; Cai et al., 2013) or drought, is also studied (Carreras et al., 2020). Although the protective role of the RET is clearly demonstrated, the molecules involved in such mechanisms and providing a correct RET functioning remained to be clearly established.

Lolium perenne or perennial ryegrass is a *Poaceae* of agronomic interest due to its role as a grassland forage plant. In addition, perennial ryegrass is one of the species that accumulate carbon reserves mainly in the form of fructans, which are water-soluble polymers of fructosyl residues linked by β-(2,1) and/or β-(2,6) linkages with one external or internal glucosyl residue (Hendry, 1993, Vijn and Smeekens, 1999; Ritsema and Smeekens, 2003). It was previously reported that fructans could play a particular role in the concept of 'sweet immunity' or 'sugar-enhanced defense' which supports the idea that sugar metabolism and signaling involved in plant immunity are tightly interconnected (Bolouri Moghaddam and Van den Ende, 2013; Trouvelot et al., 2014; Tarkowski et al., 2019; Svara et al., 2020). The RET of perennial ryegrass in particular and more generally the involvement of fructans in the RET has never been investigated. In this article, we provide the first detailed characterization of the occurrence of cell-wall glycomolecules in root BCs and mucilage of perennial ryegrass using immunocytochemistry. The microscopical analysis was done on the root tips of not only perennial ryegrass but also of two other monocotyledonous fructan-accumulating species, timothy (*Phleum pratense*) and wheat (*Triticum aestivum*), as well as on the root tips of *A. thaliana* for comparison. The response of the RET of ryegrass to the presence of the bacterial elicitor flagellin22 (flg22; Millet et al., 2010) was also investigated. The most important findings are: (i) ryegrass root tip released different BC types showing different morphologies and an abundant mucilage production; (ii) mucilage secretions consisted predominantly of cell wall polymers, especially, AGPs that have never been reported previously in perennial ryegrass root secretions; (iii) flg22 elicitation and water deficit by PEG treatment trigger modifications of AGPs epitopes in perennial ryegrass root mucilage.

Materials and Methods

Plant material and growth conditions

Perennial ryegrass (*Lolium perenne* var. Delika) and timothy (*Phleum pratense* var. Aturo) seeds were surface sterilized and sown onto Murashige and Skoog (MS) medium (Murashige and Skoog, 1962) (Duchefa Biochemie) containing 1% (w/v) agar (European Bacteriological Agar-A01254). Wheat (*Triticum aestivum* var. Chevignon) seeds were sown on the MS ½ medium (MS medium diluted 1:2) supplemented with 1% (w/v) agar after being sterilized (6 seeds per plate). For comparison, *Arabidopsis thaliana* (Col0) seeds were sterilized at the same time and sown on Arabidopsis medium (Duchefa Biochemie) containing 1% (w/v) agar supplemented with 2mL $Ca(NO_3)_2$. All of the Petri dishes with seeds were then placed vertically in continuous light (120 µE m^{-2} s^{-1}) at 21°C in 16-h-day/8-h-night, to avoid the roots penetrating

the agar and the subsequent loss of border and border-like cells, as described by Vicré et al. (2005).

Morphotypes and location of root border cells

For this technique, root tips from 10-d-old perennial ryegrass seedlings were selected with ultra-fine tweezers and mounted on microscope slides Superfrost (Thermo Scientific) in a drop of water for examination directly for morphological analyses using an inverted bright-field microscope (Leica DMI6000B, Wetzlar, Germany). For this experiment, 24–30 roots are observed to ensure representativity for each set of observations.

Water deficit treatment

The 6-d-old perennial ryegrass seedlings (with same root length) are transferred on the plate containing 30mL solidified MS ½ medium soaked with 45mL of MS ½ liquid medium containing polyethylene glycol (PEG) (300g L^{-1}) (molecular weight 8000; Sigma, St Louis, MO) prepared approximately 12-15h before the experiment following the protocol described by van der Weele et al. (2000) and Verslues et al. (2006). Other 6-d-old ryegrass seedlings were sown on the 30mL solidified MS ½ medium mixed with 45mL of MS ½ liquid medium without PEG for the "well-watered" control medium. Then, all the plates are sealed with surgical tape and placed vertically in a phytotron at 21 °C under a photoperiod of 16-h-day/8-h-night until 10 days. The 12-d-old roots will be collected lately for visualizing mucilage and for the immunolabeling experiment.

Visualization of mucilage by counterstaining with India ink

India ink (Black star Hi-Carb, 1.0 oz) produced from carbon black, is used as a negative stain to visualize mucilage (Curlango-Rivera et al., 2013). The root tips are collected and placed on microscope slides Superfrost (Thermo Scientific). A 0.05% (w/v) India ink solution is added by capillary action between the slide and the coverslip from the ends to the center of the sample. After 10min, the samples are observed under an inverted bright field microscope (DMI6000B). For this experiment, 4 to 5 technical replicates and 6 biological replicates are performed.

MAMPs

The MAMPs used in this study include the synthetic peptide flg22 (Felix et al., 1999) synthesized by Dr. J. Leprince (PRIMACEN platform, University of Rouen). MAMP

preparations were made from mycelium extracts of *Fusarium oxysporum* (Hano et al., 2006). Flg22 were used at 1 µM (Millet et al., 2010).

Immunolabeling of root border cells and mucilage on the surface of root tips

To label the polysaccharides, glycoproteins, and proteoglycans present in the cell wall of root border cells and the mucilage, an indirect surface immunolabeling has been developed. This protocol was recently described by Castilleux et al. (2018).

Roots of 10-d-old seedlings are placed onto sterile 10-welled diagnostic microscope slides (Thermo Scientific, ER-208B-CE24). The wells are then filled up with 30 µL of phosphate-buffered saline (PBS) for 5 min to initiate detachment of root border cells. Next, the liquid is removed using an Eppendorf micropipette (P200), by taking from the severed end of the root. All of the root tips are fixed for 40 min in 4% (w/v) PFA (paraformaldehyde), in 50 mM PIPES pH 7 (piperazine- N, N'-bis [2-ethanesulfonic acid], Alfa Aesar, A16090) containing 1 mM $CaCl_2$. Roots were washed 4 times for 10 min each wash at room temperature (RT) in PBS 1x containing 1% (w/v) bovine serum albumin (BSA) (AURION, Wageningen, Holland) to eliminate the maximum of PFA, and to allow the saturation of the non-specific sites of the sample. After having eliminated the last wash, 30 µL of a solution of primary antibody (Ac. I: Plant Probes) diluted to 1:5 in the solution of PBS+BSA 1% is added and incubated overnight at 4 °C and in a humid chamber. The primary antibody solution is removed before performing four washes with PBS+1% BSA at RT for 10 min.

The goat anti-rat IgG secondary antibody (Ac. II) conjugated to Alexa Fluor 594 (Invitrogen) is diluted to 1:50 in the solution of PBS+BSA 1 % and incubated with the samples for 2 h at 25°C in the dark. Four washes with PBS+BSA 1% are then carried out at RT for 10 min to eliminate the secondary antibody, followed by a final wash with PBS at RT for 10 min. To avoid photobleaching, citifluor (Agar scientific, AF2 R1320) is delicately deposited on the sample using a pipette tips 200µL. The samples are observed under an epifluorescence microscope (Leica DMI6000B, Wetzlar, Germany; λExcitation: 591 nm; λEmission: 614 nm). For this experiment, 3 to 4 technical replicates and 4 to 6 biological replicates are carried out.

The fluorescence intensity obtained with the monoclonal antibodies was estimated from the epifluorescence microscopy images as described in Supplemental Fig. SIII-6).

High-Pressure Freezing/Freeze Substitution (HPF) sample preparation

For this experiment, in addition to the *in vitro* samples, perennial ryegrass (*L. perenne* var. Delika) seeds grown in hydroponics were added to provide the fresh leaf sample. Ryegrass is

grown for 7 weeks in a plastic pot (two plants per pot) containing 700 mL of EVA nutrient solution (see Materials and Methods Table II-2) in a plant growth chamber with high-pressure sodium lamps (Philips, MASTER GreenPower T400W) provide a PAR (Photosynthetically Active Radiations) between 10 and 150 µmol photons·m^{-2}·s^{-1} under a photoperiod of 16 h and a thermoperiod of 21/18°C day/night. The nutrient solution is aerated and renewed every 7 days. Dissected 12-d-old root tips of Arabidopsis and perennial ryegrass grown *in vitro* were transferred into the cavity of copper cupules (100 µm in depth; 0.6 mm in diameter and 200 µm in depth; 0.6 mm in diameter, respectively). For the perennial ryegrass leaf bases, the 0.5mm long sample of freshly elongating leaf grown in hydroponics were dissected from 10 mm long segments selected and were also transferred into the cavity of two copper cupules with 300 µm in depth; 0.6 mm in diameter. All of the cupules were coated with soybean (*Glycine Max*) lecithin (100 mg mL^{-1} in chloroform). The excess medium was removed using filter paper. The sample carriers were tightened securely to the pod of the sample holder by using a horizontal loading station. Then, samples were frozen using a high-pressure freezing HPF-EM HPM 100 (Leica Microsystems) according to a maximum cooling rate of 20,000°C s^{-1}, an incoming pressure of 7.5 bars, and a working pressure of 4.8 bars. Cupules containing frozen samples were stored in liquid nitrogen until the freeze-substitution procedure was initiated.

After high-pressure freezing, samples were transferred to a freeze-substitution automate (AFS, Leica Microsystems) precooled to −140°C. Samples were substituted in anhydrous acetone with 0.5% uranyl acetate at −90°C for 96 h (Ovide et al., 2018). Using a gradient of +2°C h^{-1}, the temperature was gradually raised from −90 to −15°C with two intermediate steps at −60 and −30°C. Samples were washed twice at room temperature with fresh anhydrous acetone. Resin infiltration was processed at −15°C in a solution of ethanol/London Resin White (LRW) with successive ratios of 2:1 overday; 1:1 overnight and 1:2 overday followed by a final step in a pure LRW solution renewed twice during 48 h. The LRW was finally polymerized into the AFS apparatus at −15°C under ultraviolet light for 48 h. Using a Leica ultramicrotome EM-UC7 (Leica Microsystems), semithin sections (0.5 µm) were cut and adhered onto 10-welled diagnostic microscope slides (Thermo Scientific, ER-208B-CE24) pre-coated with Poly-L-Lysine (EMS-19320-B, dilution 1:10 in filtered water). The HPF sections are stained with toluidine blue to highlight components.

Immunolabeling of root border cells and mucilage on the HPF sections

Semithin sections (0.5 µm) of 12-d-old roots and leaf bases on 10-welled Teflon microscope slides coated with Poly-L-Lysine were blocked in PBS 1x with 0.1% (v/v) Tween 20 (PBST)

containing 3% (w/v) BSA and normal goat serum (NGS-dilution 1:20) for 30 min at RT. Then, sections were carefully washed 5 times for 5 min with 0.1 % PBST containing 1% BSA. After washing, sections were incubated overnight at 4°C with primary antibody (dilution 1:2 in 0.1% PBST containing 1% BSA and NGS (diluted 1:20)). On the next day, sections were washed 5 times for 5 min with 0.1 % PBST containing 1% BSA before being incubated with secondary goat anti-rat IgG antibody conjugated to Alexa Fluor 594 (Invitrogen) at 1:200 dilution in 0.1% PBST containing 1% BSA and NGS (diluted 1:20) for 2 h at 25°C. At RT, sections were rinsed 5 times for 5 min with 0.1 % PBST containing 1% BSA and two final washes for 5 min at RT with ultrapure water. Then, a droplet of ultrapure water was added to the section of each well. Epifluorescence of the immunostained tissue sections was observed on an epifluorescence microscope (Leica DMI6000B, Wetzlar, Germany; λExcitation: 591 nm; λEmission: 614 nm). Control experiments were performed by omission of primary antibodies. For this experiment, 3 technical replicates and 4 biological replicates were performed.

Immunofluorescence localization of fructans epitopes

Roots of 10-d-old seedlings were placed onto sterile 10-welled diagnostic microscope slides (Thermo Scientific, ER-208B-CE24) and fixed for 40 min in 4% (w/v) PFA (paraformaldehyde), in 50 mM PIPES (piperazine- N,N'-bis [2-ethanesulfonic acid]), pH 7, containing 1 mM $CaCl_2$. Roots were washed 4 times for 10 min each wash at room temperature (RT) in phosphate-buffered saline PBS 1x containing 1% (w/v) bovine serum albumin (BSA) (Bovine Serum Albumin; AURION, Wageningen, Holland) and then incubated overnight at 4°C with the primary antibody (dilution 1:5 and 1:20 for 9H2-R2-2B1 and 15A6-R2-3E6, respectively in 1x PBS containing 1% w/v BSA). Roots were carefully washed 4 times at RT with PBS 1× and 1% BSA for 10 min, then were incubated with secondary donkey anti-mouse IgG antibody conjugated to Alexa Fluor 594 (Invitrogen) at 1:50 dilution in PBS 1x and 1% BSA for 2 h at 25°C. After 4 washes at RT in PBS 1x containing 1% w/v BSA and 1 final rinsing with PBS 1x for 10 min, roots were finally mounted in anti-fading solution (Agar scientific, Ref. AF2 R1320) then covered with a coverslip and observed using an epifluorescence microscope (Leica DMI6000B, Wetzlar, Germany; λExcitation: 591 nm; λEmission: 614 nm). Controls were routinely performed by incubation of the roots with the secondary antibody only. For this experiment, 3 to 4 technical replicates and 4 to 6 biological replicates were performed.

Semithin sections (0.5 µm) of 12-d-old roots and leaf bases on 10-welled Teflon microscope slides coated with Poly-L-Lysine were blocked in PBS 1x with 0.1% (v/v) Tween 20 (PBST)

containing 3% (w/v) BSA and normal donkey serum (NDS-dilution 1:20) for 30 min at RT. Then, sections were carefully washed 5 times for 5 min with 0.1 % PBST containing 1% BSA. After washing, sections were incubated overnight at 4°C with primary antibody (dilution 1:2 in 0.1% PBST containing 1% BSA and NDS (diluted 1:20) for two anti-fructan mAbs). On the next day, sections were washed 5 times for 5 min with 0.1 % PBST containing 1% BSA before being incubated with secondary donkey anti-mouse IgG antibody conjugated to Alexa Fluor 594 (Invitrogen) at1:100 dilution in 0.1% PBST containing 1% BSA and NDS (diluted 1:20) for 2 h at 25°C. At RT, sections were rinsed 5 times for 5 min with 0.1 % PBST containing 1% BSA and two final washes for 5 min at RT with ultrapure water. Then, a droplet of ultrapure water was added to the section of each well. Epifluorescence of the immunostained tissue sections was observed on an epifluorescence microscope (Leica DMI6000B, Wetzlar, Germany; λExcitation: 591 nm; λEmission: 614 nm). Control experiments were performed by omission of primary antibodies. For this experiment, 3 technical replicates and 4 biological replicates were performed.

Ultrastructural and immunogold analyses using transmission electron microscopy

Ultrathin sections (90 nm; EM UC6 Leica microsystems) of ryegrass root tips from HPF samples prepared previously are collected on nickel formvar-coated grids. For immunogold analysis, sections are blocked in PBS 1X containing 3% BSA for 30 min at RT. Sections were then incubated with the primary antibody (JIM13, PlantProbes; dilution 1:2 in PBS 1x containing 0.3% BSA overnight at 4 °C in a humid chamber). After washing in PBS 1x containing 0.3% BSA, grids were incubated for 1 h at 37 °C with the goat anti-rat secondary antibody conjugated to 10 nm gold particles (dilution 1/20 in PBS 1x containing 0.3% BSA; British Biocell International). Before transmission electron microscopy observation, all sections were stained with classical staining using uranyl acetate (0.2% in methanol) and and Reynolds lead citrate (Delta microscopies, ref: 11.300). Observations were made with a FEI Tecnai 12 Biotwin transmission electron microscope operating at 80 kV, with ES500W Erlangshen CCD camera (Gatan).

Primary antibodies

Primary antibodies recognizing epitopes associated with different parietal polysaccharides are mainly provided by Plant Probes (University of Leeds, UK) and Biosupplies Australia (http://www.biosupplies.com.au). A summary table of the antibodies used in this project is

presented in Appendix 4 as well as details of the epitopes recognized by the antibodies and their references associated.

Statistical and image analysis

Microscope images were acquired by counterstaining with India ink and measurements made using ImageJ 1.53p. The RET surface obtained was determined on 61 root tips by measuring the total surface of the RET containing the root cap and then subtracting the surface of the root cap. Data were analyzed with R software version 4.0.0. Statistical significance was calculated by using the Kruskal–Wallis test and the statistical effect is considered significant with $P<0.05$.

Results

1. Characteristics of ryegrass RET

Observation of the root tip with a bright-field illumination revealed that ryegrass releases large numbers of individual root BCs from the periphery of the root cap in the presence of water (Fig.III-6A; *all of the figures in this chapter are after the text*). Two cell morphotypes based on their size and shape were observed depending on their localization at the root tip. Spherical border cells (sBC) were the smallest and were abundantly i-6present among of the BC population. sBC were mostly observed in the root cap zone (Fig. III-6C, D). The presence of few elongated border cells (eBC) with an elongated shape and slightly curved (Fig. III-6B), was also found along the meristematic and the elongation zones. The sBC represent around 65%, and the eBC 35%. The negative staining with India ink revealed the presence of an abundant mucilage along the root tip (Fig. III-7A). Most of the mucilage is concentrated at the root cap and meristematic zone (Fig. III-7D), and to a lesser extent in other root zones (Fig. III-7B, C).

2. Cell-wall polymers distribution in ryegrass root tip

Using immunocytochemistry and various anti-cell wall antibodies, we investigated the occurrence of major non-cellulosic polysaccharides of plant cell walls in perennial ryegrass, timothy and wheat in comparison with Arabidopsis root tips. Data related to immunolabeling detected in the RET are summarized in Table III-1.

2.1. Immunolocalization of hemicellulosic epitopes

We found that xylan epitopes recognize by mAb LM10 and arabinoxylan and low-substituted xylan epitopes recognized by mAb LM11 were only slightly detected in the mucilage of the three monocots and Arabidopsis. The mAb LM27, which binds to grass heteroxylan epitope, was found to label the cell wall of all BC morphotypes of perennial ryegrass, timothy and wheat

(Table III-1). This fluorescent labeling on the cell wall of ryegrass BCs is shown in figure III-8C. In addition, we observed that the intensity of LM27 fluorescence was higher in the BLCs of Arabidopsis (Fig. III-8D). This result was confirmed by the observation with LM27 on the HPF sections of perennial ryegrass root (Fig. III-9E,). Immunolabeling on leaf sections were performed as positive control (Fig. III-9F). No labeling was observed in all control roots and control HPF sections omitted primary antibodies (Supplemental Fig. SIII-9, SIII-10).

Interestingly, the LM12 feruloylated epitope (Pedersen et al., 2012) appeared slightly in the mucilage of perennial ryegrass root (Fig. III-9E) but no fluorescence labeling was observed with Arabidopsis root (Fig. III-9F). With MLG, which recognized mixed linked glucans, no labeling was observed neither in the cell wall nor in the mucilage of perennial ryegrass suggesting the absence of the recognized epitope (Table III-1).

2.2. Immunolocalization of pectin epitopes

The distribution of pectic polysaccharides was examined in perennial ryegrass root tips and compared with timothy, wheat, and Arabidopsis. Our data revealed that only LM5 epitopes corresponding to galactan side chains were detected and showed weak fluorescence with the cell wall of perennial ryegrass BCs (Table III-1; Fig. III-10E). The other epitopes corresponding to low and highly methylesterified homogalacturonans (LM19) and arabinan side chains (LM6) were not detected in the RET of perennial ryegrass. However, root surfaces from Arabidopsis used as positive control were heavily labeled with the different mAbs specific to pectic epitopes (Fig. III-10B, D, F, H). However, observations on perennial ryegrass sections revealed that LM20 displayed a very distinct and interesting pattern of cell wall recognition especially in the middle lamella junctions or cell corners in the root tip cells (Supplemental Fig. SIII-7).

2.3. Immunolocalization of extensin (EXTs) epitopes

In addition to hemicelluloses and pectins, we investigated the occurrence of EXT epitopes in the mucilage surrounding border cells using a range of monoclonal antibodies previously described in the literature LM1, JIM11, JIM12, JIM19, and JIM20 (Smallwood et al., 1994, 1995; Knox et al., 1995; Pattathil et al., 2010). The extensin epitopes recognized by these mAbs were mostly present at the surface of the meristematic and the elongation zones in perennial ryegrass (Fig.III-11A, C, E and Table III-1). However, no labeling or only a faint fluorescence was observed at the RET surface of perennial ryegrass (Fig.III-11). Similar data were observed in the HPF root sections (Supplemental Table SIII-1). Only the mAb JIM 20 labelled the mucilage and border cells present at the surface of meristematic zone in perennial ryegrass (Fig.III-11E).

Our data showed that all anti-pectin mAbs stained more or less strongly the cell surface of BLCs in Arabidopsis, except JIM19 (Table III-1). The fluorescence labeling was also detected at the cell surface of BLCs with LM1, JIM11, and JIM20 as shown in figure III-11 (B, D, F).

2.4. Immunolocalization of arabinogalactan protein (AGPs) epitopes

To test whether AGPs epitopes are present in the cell walls of BCs or the mucilage in perennial ryegrass and the two other monocots by comparison with Arabidopsis, we stained roots with a panel of mAbs that have been widely used for immunocytochemical studies of the distribution of these proteoglycans (Appendix 4; Knox et al., 1991; Smallwood et al.,1996; Yates and Knox, 1994; Yates et al., 1996; Pennell et al., 1991).

Interestingly, these mAbs strongly stained the mucilage of perennial ryegrass as well as timothy and wheat root tips, especially the mAbs JIM13 and JIM8 (Table 1). In contrast, JIM13 only showed weak labeling in the BLCs of Arabidopsis, or no labeling was detected with JIM8 on the surface of Arabidopsis root tip (Fig. III-12D, H). As shown in figure 7, fluorescence labeling of JIM13 and JIM8 appeared as a dense structured network surrounding the root cap and the meristematic zone (Fig. III-12C, G). In addition, the LM2 associated epitopes were also detected in the mucilage of all monocot species (Table III-1) and mostly in the BLCs of Arabidopsis (Fig. III-12B, D), whereas JIM16 were restricted to the mucilage of these plants (Table SIII-1) suggesting that AGP structure in the mucilage of root tip varies according to plant species.

Likewise, in the HPF sections, the BCs and the mucilage of perennial ryegrass root were strongly stained with JIM13 and JIM8, particularly at the root cap and the meristematic zone (Fig. III-13C, E). No labeling was observed in leaf sections (Fig. III-13D, F) with these mAbs suggesting that AGPs concentrated mainly in the root in perennial ryegrass. The fluorescence labeling of LM2 was weakly detected in both HPF sections (Fig. III-13A, B). No labeling was observed in control HPF sections when no primary antibody was used (Supplemental Fig. SIII-10).

Considering the strong detection of mAb JIM13 to the mucilage on perennial ryegrass root (Fig. III-12C, III-13C), we were interested to assess the immunogold labeling of AGPs using JIM13 on 12-d-old ryegrass root. As shown in figure III-14, we observed in perennial ryegrass root BC the presence of a large number of Golgi stacks which could be actively secreting materials, such as complex polysaccharides and glycoproteins to their walls and the surrounding medium. It is thus confirmed that the AGP epitopes recognized by JIM13 appear abundant in the mucilage associated with the cell wall of BCs (Fig. III-14).

2.5. Immunolocalization of fructan epitopes

To test whether fructan epitopes are present in the cell walls of BCs or the mucilage in perennial ryegrass, we stained roots with BTM15A6 that recognized specifically to β-(2,6) and β-(2,1) linked fructans from plants (Nguyen *et al.* unpublished). Indirect immunofluorescence analysis with BTM15A6 at the root surface indicated labeling at the surface of the meristematic and elongation zones while no labeling was observed at the cell surface of BC or RET mucilage (Supplemental Fig. SIII-8A). Labeling was also detected with BTM15A6 on root tip section where fluorescence was detected not only in elongation and meristematic area but also in root cap with an uniform distribution inside each root cell (Supplementary Fig. SIII-8B).

2.6. Impact of flg22 and PEG treatments

To investigate the impact of flg22 on AGPs in perennial ryegrass root tip compared with that of Arabidopsis, we used three mAbs to examine the distribution of AGPs including LM2, JIM13, and JIM8.

In non-elicited Arabidopsis and as shown in figure 10, the fluorescence labeling was observed all over the roots, including root BLCs, with the mAb LM2 (Fig. III-15C). Interestingly, the JIM13 labeled only the BLCs (Fig. III-15E) and no labeling was observed with JIM8 (Fig. III-15G). When Arabidopsis roots were elicited with flg22, stronger staining was observed in the mucilage of elicited roots with LM2 and JIM13 (Fig. III-15D, F). Treatment of Arabidopsis roots with flg22 showed no labeling with JIM8 as the non-elicited root (Fig. III-15H).

In perennial ryegrass, all three mAbs strongly labeled the mucilage which forms a densely structured network covering the root cap (Fig. III-16C, E, G). Interestingly, we obtained the same fluorescence labeling with LM2, JIM13, and JIM8 in elicited roots (Fig. III-16D, F, H) but the labeling is more spread out creating a wider mucilage structure until the elongation zone.

To explore the change of AGPs distribution in perennial ryegrass root tip under osmotic stress induced by PEG treatment, we performed immunolabeling on 10-day-old plants using the LM2, JIM13, and JIM8 mAbs (Fig. III-17). Labeling was observed in the mucilage of all the non-treated roots with all the mAbs tested (Fig. III-17C, E, G). In PEG-treated roots, visualization

by counterstaining with India ink shows that the mucilage has dispersed compared to the non-elicited roots (Fig. III-17A, B). The pattern of labeling was similar between treated and non-treated roots but the dispersion surface of the mucilage was wider when the PEG treatment was performed (Fig. III-17D, F, H). This observation was confirmed by measuring the RET surface area on PEG condition compared with the control condition (Fig. III-18).

Discussion

The formation and release of RETs from the root cap to the rhizosphere is essential for protecting the root against biotic and abiotic stresses (Haichar et al., 2014; Driouich et al., 2019). In this study, we provide the first in-depth characterization of the RET in perennial ryegrass (*Lolium perenne*), an important grassland forage plant that accumulate fructans. The RET from *L. perenne* consists of individual root border cells embedded in a thick mucilage. Different populations of BCs were previously found to be released at the root tip of pea (*Pisum sativum*) and soybean (*Glycine max*) including small spherical cells, intermediate-size cells, and elongated cells (Cannesan et al., 2011; Ropitaux et al., 2020). It was reported that small BC were probably the more efficient cells in protecting the root tip against pathogenic oomycetes *A. euteiches* (Cannesan et al., 2012). Here, we found two different morphotypes of border cells in perennial ryegrass with small spherical cells (sBC) and elongated cells (eBC). In other plants belonging to the Poacee family, including barley, spherical and elongated border cells were also reported with a high level of viability (Tamas et al., 2005). In maize only border cells presenting a bell-shape morphology were previously described (Canellas and Olivares, 2017). Interestingly, the number of border cells released in maize was shown to increase upon exposure to humic acid in a dose-dependent manner (Canellas and Olivares, 2017).

It is worth noting that border cells produced by perennial ryegrass were embedded in an abundant mucilage mostly found covering the root cap and the meristematic zone. Such an important mucilage was previously reported to occur in pea (Hawes et al., 2003) or the root tip of rice, another cereal (Xiao and Lang, 2022). In rice, the production of mucilage increased at the root tip in response to both aluminium and silicon exposure (Xiao and Lang, 2022). This result suggests that root mucilage from Poaceae might be involved in protecting the root tip against abiotic stress. The degree of methylesterification of pectins present within the RET of rice was thought to be a key event in such protection against abiotic stress (Xiao and Lang, 2022).

It is thus important to unravel the chemical composition of mucilage in perennial ryegrass. In this species, the presence of pectins were not or only very faintly detected in both mucilage and

cell wall surface of border cells. Such findings were also found in the RET of wheat and timothy, two other species from the Poaceae family. Although pectins (and more especially homogalacturonans) are central elements for border cells detachment and are abundantly reported in the mucilage of eudicots (Durand et al., 2009; Cannesan et al., 2011), they appear to be insignificants in the RET of perennial ryegrass. These findings suggest that other polymers are expected to be present as major components of the thick root mucilage of this species. As xyloglucan epitopes were reported to be part of the scaffold of the RET in eudicots (Ropitaux et al., 2020), we investigated the presence of a wide range of hemicellulosic epitopes usually found in the cell wall of grasses. The labeling of epitopes from xylans, arabinoxylans and mixed linkage glucan (MLG) was scarce in the RET of perennial ryegrass and no difference was observed compared to the RET of *A. thaliana*. These data suggest that pectins and hemicellulosic compounds are not abundant in the RET of perennial ryegrass. The presence of fructan epitopes was thus investigated. However, the presence of fructan epitopes were not detected within the mucilage of perennial ryegrass. These epitopes were found inside the cells and at the surface of elongation and meristematic zone and inside the root cap cells (Supplemental Fig. SIII-8), consistent with the vacuolar localization of fructan synthesis (Wagner et al., 1983). We can speculate that fructans found inside root cap cells could be released in the RET upon abiotic and/or abiotic stresses but are not part of a constitutive defense. One of the major findings is the abundance of AGPs epitopes detected within the RET of perennial ryegrass not only in the mucilage but in the root border cell walls. Although previous findings reported the presence of AGPs in the RET of other plant species such as *A. thaliana* and pea, other glycomolecules were also abundantly recognized which is not the case here with perennial ryegrass (Durand et al., 2009; Plancot et al., 2013; Cannesan et al., 2012; Ropitaux et al., 2019). It appears that the RET of *L. perenne* is particularly enriched in AGP epitopes as compared to other plant species such as *A. thaliana*. AGPs are heterogeneous proteoglycans characterized by a highly complex and diverse carbohydrate moiety, and distinct populations of AGPs are found in the root cap (including root border cells) and in the rest of the root system (Cannesan et al., 2012). It is tempting to hypothesize that AGPs from the RET of perennial ryegrass are highly involved in the RET architecture and cohesion. It was previously reported that heteroxylan epitope from Poaceae (oat) cell walls recognized by the mAbs LM27 are likely to bind AGPs (Cornuault et al., 2015). Such linkages between heteroxylans and AGPs could be involved in the RET of perennial ryegrass and the abundance of AGPs would result in masking hemicellulosic epitopes.

AGPs are involved in response to various biotic and abiotic stresses (Cannesan et al. 2012; Nguema-Ona et al., 2013; Pereira et al., 2015; Koroney et al. 2016). AGPs were shown to play a prominent role at the root surface during root colonization by pathogenic and symbiotic microbes (Vicré et al., 2005; Gaspar et al., 2004; Xie et al., 2012). Previous studies revealed that recognition of MAMPs (Microbe-Associated Molecular Pattern) such as bacterial flagellin 22 (flg22) trigger the innate immune system in roots (Millet et al., 2010). Interestingly, we found that flg22 elicitation increased the quantity of mucilage in perennial ryegrass which forms a larger halo at the root tip until the elongation zone. Although, the pattern of labeling for AGP epitopes is not altered by flg22 treatment, the presence of fluorescence was detected throughout the whole surface of mucilage. It is likely that AGPs from perennial ryegrass contribute to interactions between the root and soil-borne microbes. The alteration of AGPs was found to significantly inhibit the attachment of the rhizobium bacteria to the surface of BLC and Arabidopsis root tip (Vicré et al., 2005). AGPs were also reported to be involved in the susceptibility of root to pathogenic cyst nematode in Arabidopsis (Baum et al., 2000; Bozbuka et al., 2018).

Root tip from perennial ryegrass respond to water stress by producing enhance quantity of mucilage and / or changing the adhesion and structure of the mucilage. AGPs are known as the glycoproteins extremely hydroscopic and have a high water-holding capacity (Fincher et al. 1983; Showalter 2001), the widespread distribution of AGPs epitopes in the mucilage that we found supports the role of these proteins toward the root tip in water deficit condition. Previously, AGPs have been shown to be involved in the salt adaptation processes (Olmos et al. 2017) and low-temperature tolerance (Yan et al. 2015).

In summary, our findings provide evidence that AGPs are major compounds of the RET in perennial ryegrass. This study emphasizes that AGPs could contribute to protect the root tip against water deficit stress and strongly support the hypothesis that AGPs are implicated in the defense response of plant roots. Further research will be necessary to fulfill their function in perennial ryegrass root in microbial interaction.

Acknowledgments

We are grateful to Dr. Isabelle Boulogne (GlycoMEV laboratory, University of Rouen Normandy) for providing the wheat seeds (var. Chevignon) and Carole Plasson GlycoMEV laboratory, University of Rouen Normandy) for excellent technical assistance with plant cultures. Gaelle Lucas (GlycoMEV laboratory, University of Rouen Normandy), Nicolas Ellie

(CMAbio3 University of Caen Normandy) and Didier Goux (CMAbio3 University of Caen Normandy) are thanks for their technical assistance with microscopical analyses.

Author contributions

TNHN, MF, MV, MLFG, MPP, and AMB conceived and designed the experiments; TNHN performed flg22 elicitation and immunocytochemistry experiments; MF performed water deficit treatment and immunocytochemistry for PEG treatment; SB performed the high-pressure freezing/freeze substitution sample preparation and MLFG performed their sections; TNHN, MF, MV and MLFG analyzed the data; TNHN wrote the first draft, AMB, MV, AD, MLFG and MPP edited and improved the manuscript.

Funding

This work was supported by the Universities of Caen and Rouen Normandie. The Normandie Council supported the work through the research projects EPURE (Enhancing Plant nutRition and Health, 2017-2019) and Normandy Plant Technologies (2018-2021). The Normandie Council and the European Union (in the framework of the ERDF-ESF operational program 2014-2020) supported the work through the research project BEER (Bactéries, Exsudats, Et Rhizodépots, 2019-2022). Thi Ngoc Hanh Nguyen received a PhD grant (2018-2021) from the Normandie Council.

Figures

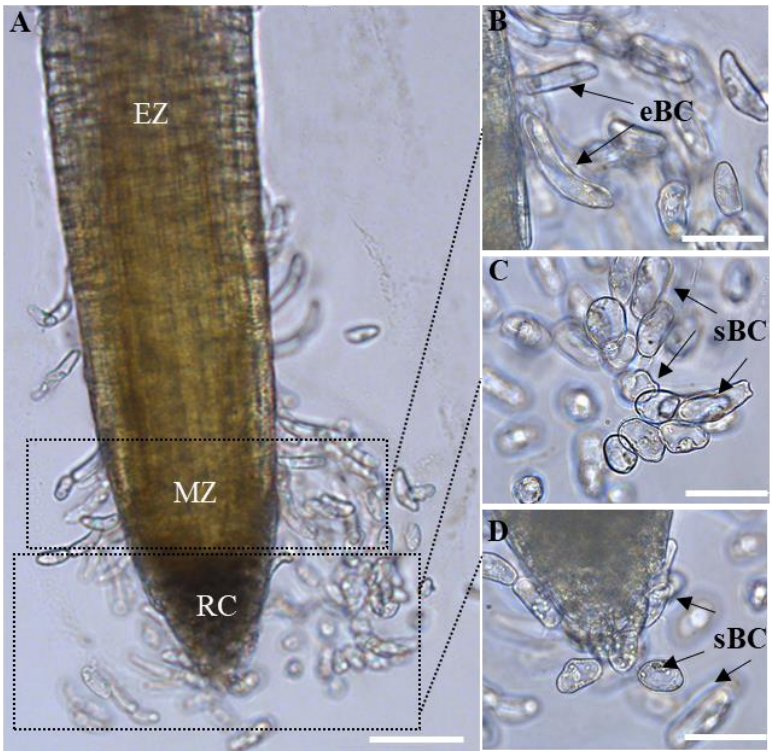

Figure III-6. Root border cell morphotypes. Images showing different cell morphotypes using a bright-field microscope: (A) localization of different cell types along the root tip using a bright-field microscope.

Different root zones are: EZ, elongation zone; MZ, meristematic zone; RC, root cap. (B) elongated or curved border cells: eBC; (C) spherical border cells sBC (D) sBC are mostly present at the root tip. Scale bars: (A) 100 µm; (B–D) 20 µm.

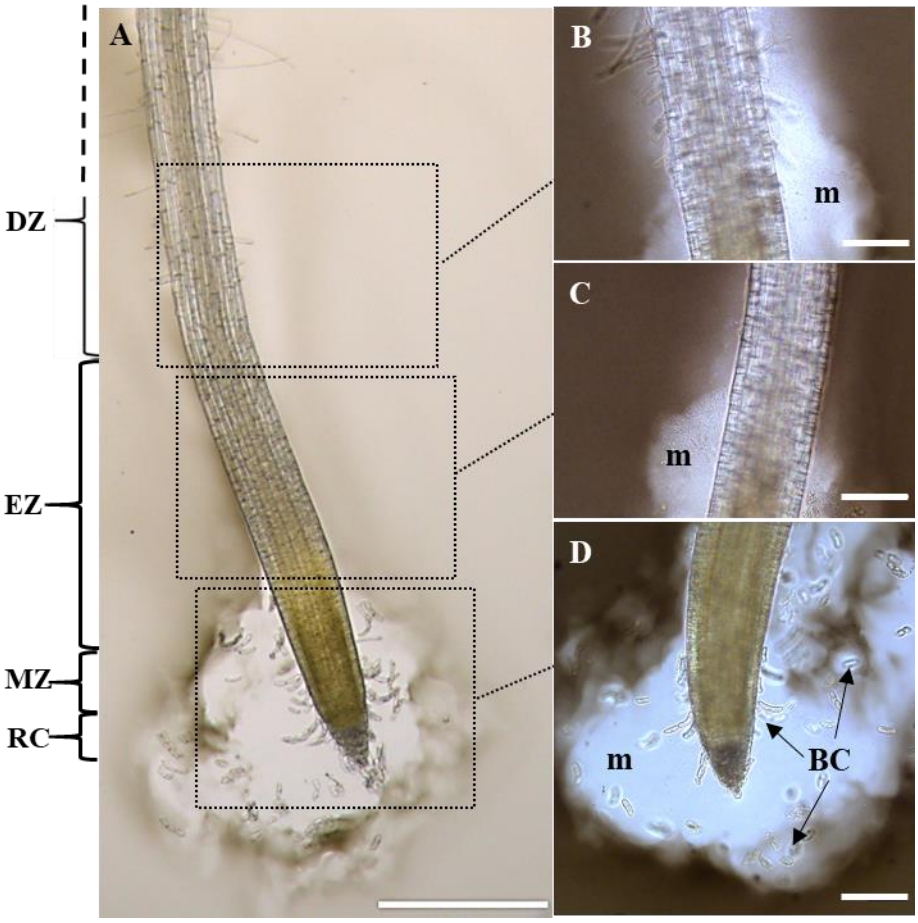

Figure III-7. Visualization of secreted mucilage (m) using India ink staining.

(A) localization of different root zones along the root tip 10-day-old with a stereomicroscope. Different root zones are: (B) DZ, differentiation zone; (C) EZ, elongation zone; (D) MZ, meristematic zone; RC, root cap. (A, D) Light microscopy images showing an abundant slimy mucilage present around the root tip and embedding border cells (BCs). Scale bars: (A) 500 µm; (B, C, D) 100 µm.

Table III-1. Immunolabeling of major glyco-polymer motifs in the RET of perennial ryegrass, timothy, wheat and Arabidopsis using immunofuorescence microscopy.

	CW polymers	mAbs	Epitopes	Perennial ryegrass	Timothy	Wheat	*A. thaliana*
Hemicelluloses	Xylan	LM10	(1,4)-β-xylosyl residues	–	–	–	–
	Arabinoxylan and low-substituted xylan	LM11	(1,4)-β-xylosyl residues	–	–	–	–
	Grass Heteroxylan	LM27	Unknown	++	++	++	++
	Glucuronoxylan	LM28	Glucuronosyl residues of xylan	–	–	–	–
	Feruloylated polymers	LM12	Feruloylated xylan	+	+	+	–
	Mixed linkage glucan (MLG)	MLG	(1,3; 1,4)-β-D-glucan	–	–	–	–
Pectins	Homogalacturonans (HGs)	LM19	HG with low degree of esterification	–	–	–	+++
		LM20	HG with high degree of esterification	–	–	–	+++
	Galactan chains	LM5	(1,4)-β-D-galactan, Rhamnogalacturonan-I (RG-I)	+	+	++	++
	Arabinan chains	LM6	(1,5)-α-L-highly branched arabinan, RG-I	–	–	+	++
Extensins	Extensin from rice	LM1	Unknown	–[(1)]	+	–[(1)]	++
	Extensin from carrot	JIM11	Unknown	–[(1)]	–[(1)]	–[(1)]	++
	Extensin from carrot	JIM12	Unknown	–[(1)]	–	–[(1)]	++
	Extensin from pea	JIM19	Unknown	–	–	–	–
	Extensin from pea	JIM20	Unknown	–[(1)]	++	–[(1)]	+++
Arabinogalactan proteins (AGPs)	AGP from rice	LM2	β-D-GlcpA	+++	+	++	++
	AGP from carrot	JIM13	β-D-GlcA-(1,3)-α-D-GalA-(1,2)-α-L-Rha	+++	+++	++	+
	AGP from carrot	JIM15	Unknown	–	–	–	–
	AGP from carrot	JIM16	Unknown	+	–	+	++
	AGP from sugar beet	JIM8	Unknown	+++	+++	++	–

–Fluorescence labeling not detected; + Fluorescence labeling detected weakly; ++ Fluorescence labeling detected clearly; +++ Fluorescence labeling detected strongly compared to control roots (See Supplementary Figure S2).

[(1)] Fluorescence labelling detected on the meristematic zone and the beginning of the elongation zone but absent from the root cap and the RET.

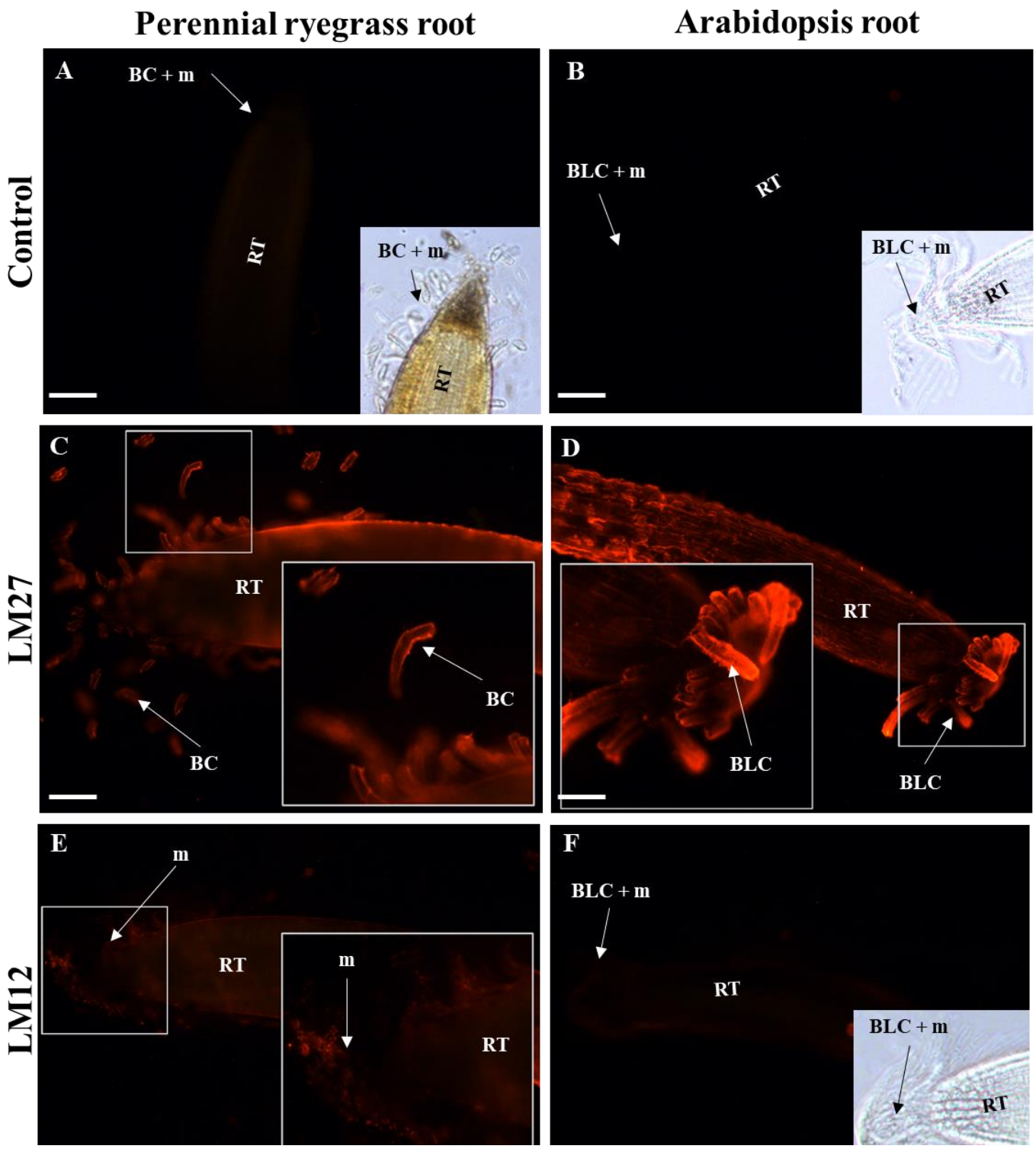

Figure III-8. Immunolocalisation of hemicellulose epitopes on the surface of root tips.

(A, B) Control root tips without primary antibodies. (C, E) Immunofluorescence labeling of the cell wall and extracellular material in 10-d-old ryegrass and (D, F) 10-d-old Arabidopsis root tips. (C, D) the mAbs LM27; and (E, F) LM12. Fluorescence labeling appears around the cells and faintly stained the mucilage of perennial ryegrass root. Observations are made with an epifluorescence microscope (Leica DMI6000B, Wetzlar, Germany; λExcitation: 591 nm; λEmission: 614 nm). BLC: Border-like cell; BC: Border cell; RT : Root tip ; m: mucilage. Scale bars:100 µm.

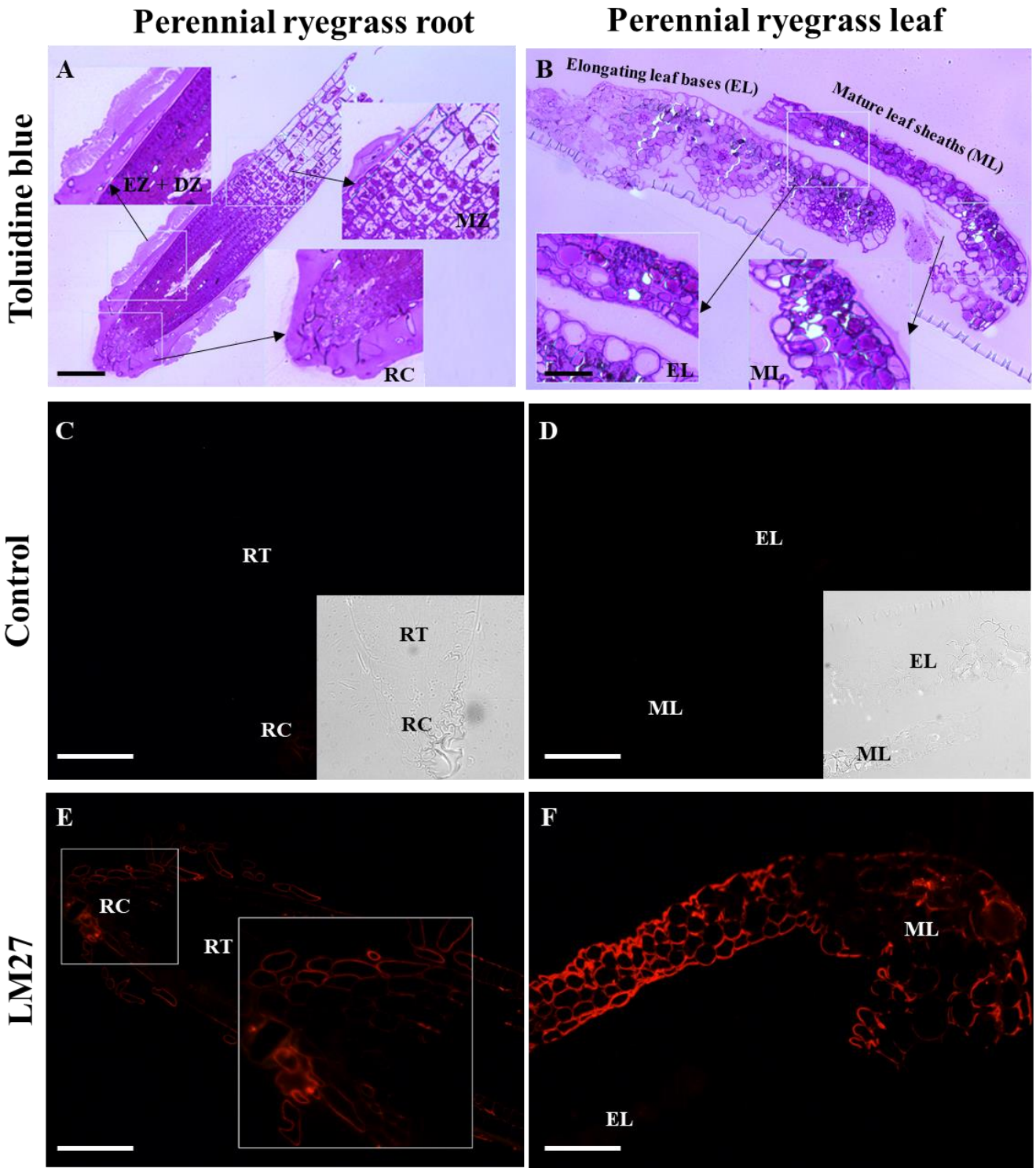

Figure III-9. Immunolocalisation of hemicellulose epitopes on the HPF sections.

Immunofluorescence images showing labeling of the cell wall in (E) 10-d-old ryegrass root section and (F) ryegrass leaf section with the mAb LM27. Fluorescence labeling appears around the cells in both types of section. (C, D) Control experiments without primary antibody LM27. (A, B) Components of HPF sections stained with toluidine blue. Observations are made with an epifluorescence microscope (Leica DMI6000B, Wetzlar, Germany; λExcitation: 591 nm; λEmission: 614 nm). RT: Root tip; RC: Root cap; ML: Mature leaf sheaths; EL: Elongating leaf bases. Scale bars:100 µm.

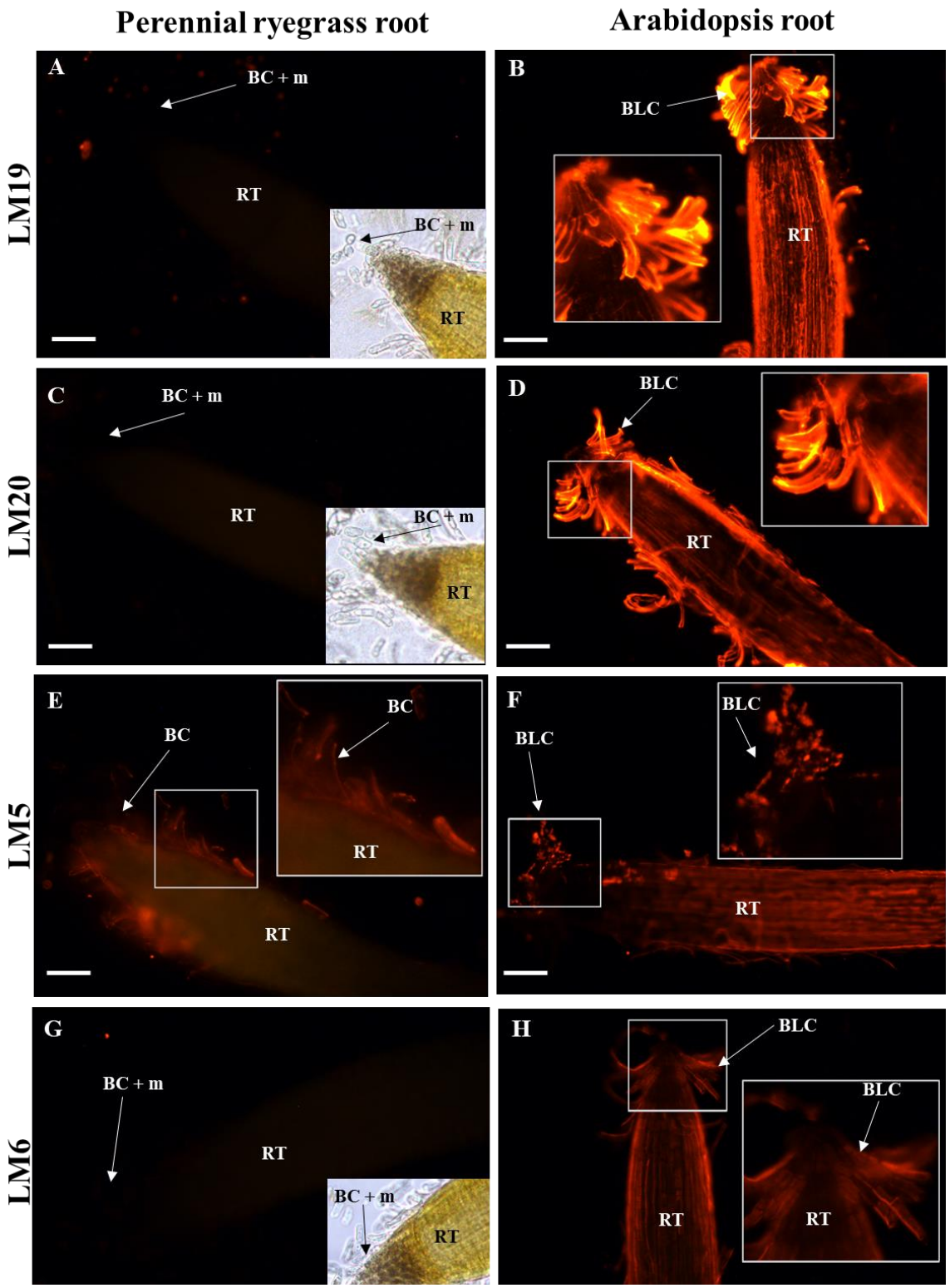

Figure III-10. Immunolocalisation of pectin epitopes on the surface of root tips.

Immunofluorescence images showing labeling of the cell wall and extracellular material in (A, C, E, G) 10-d-old ryegrass and (B, D, F, H) 10-d-old Arabidopsis root tips with (A, B) the mAbs LM19; (C, D) LM20; (E, F) LM5; and (G, H) LM6. Observations are made with an epifluorescence microscope (Leica DMI6000B, Wetzlar, Germany; λExcitation: 591 nm; λEmission: 614 nm). BLC : Border-like cell ; BC : Border cell; RT : Root tip ; m: mucilage. Scale bars:100 µm.

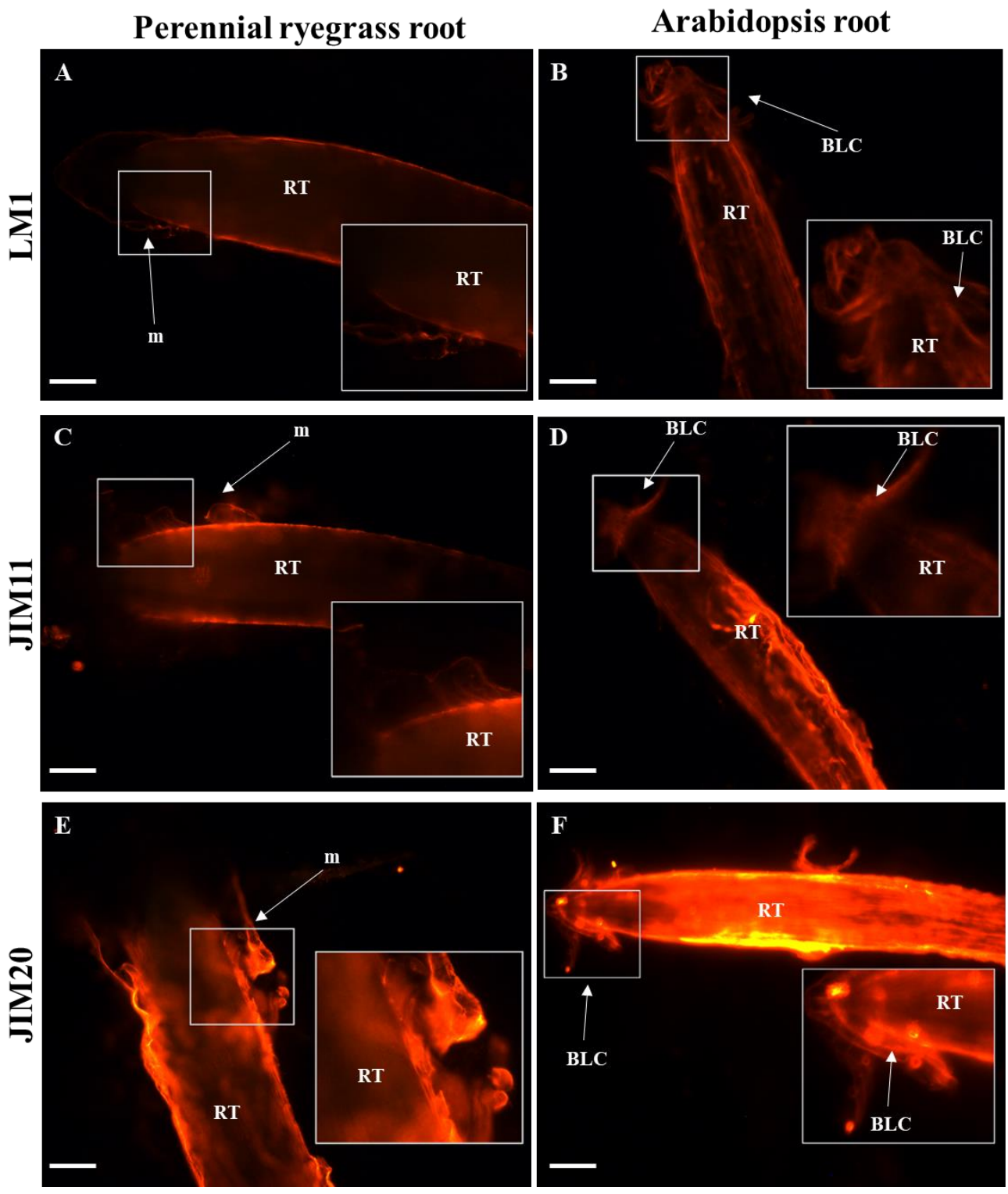

Figure III-11.Immunolocalisation of extensin epitopes on the surface of root tips.

Immunofluorescence images showing labeling of the cell wall and extracellular material in (A, C, E) 10-d-old ryegrass and (B, D, F) 10-d-old Arabidopsis root tips with (A, B) the mAbs LM1; (C, D) JIM11; and (E, F) JIM20. Observations are made with an epifluorescence microscope (Leica DMI6000B, Wetzlar, Germany; λExcitation: 591 nm; λEmission: 614 nm). BLC: Border-like cell; RT : Root tip ; m: mucilage. Scale bars:100 µm.

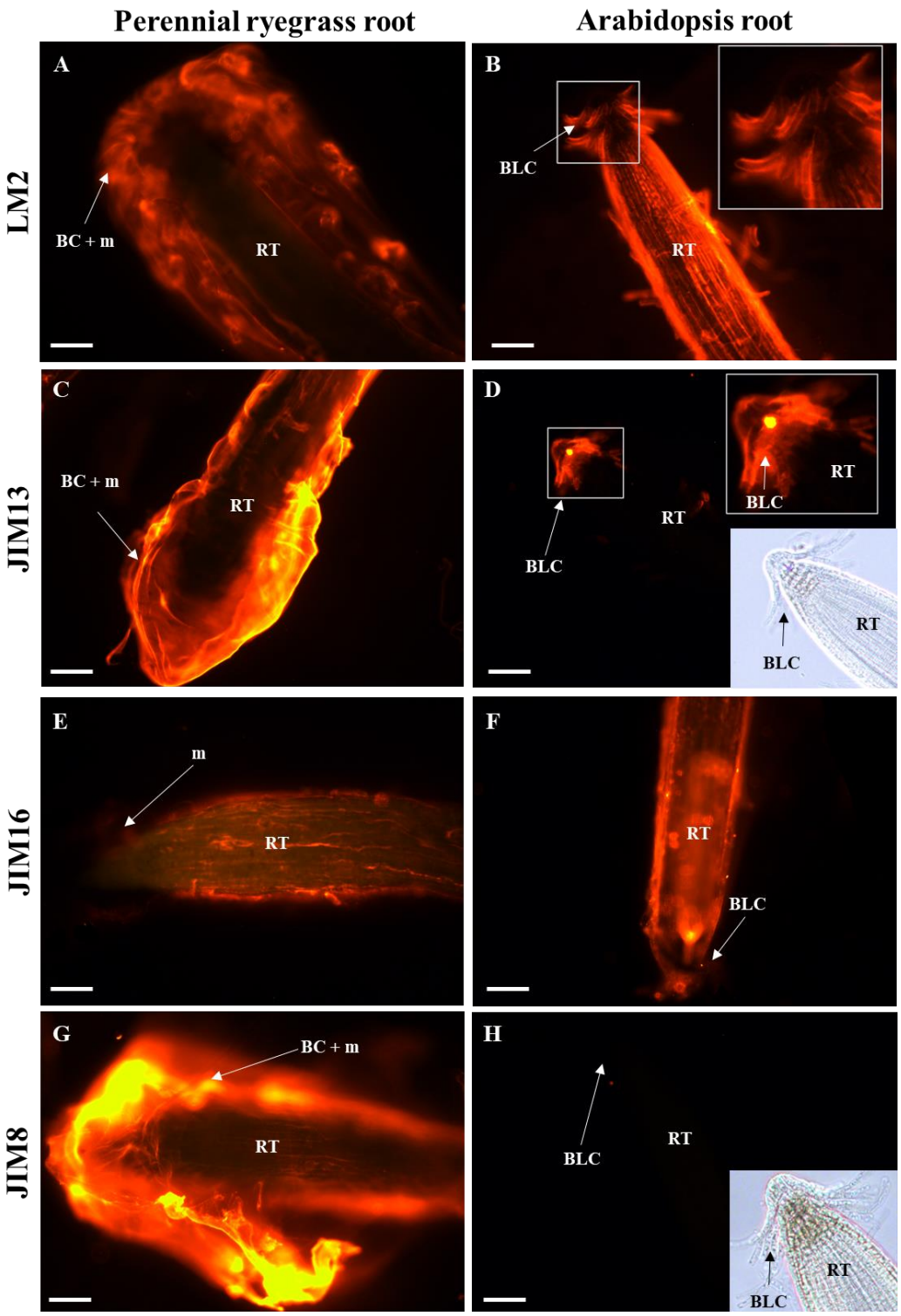

Figure III-12. Immunolocalisation of arabinogalactan proteins (AGPs) epitopes at the surface of root tips.

Immunofluorescence images showing labeling of the cell wall and extracellular material in (A, C, E,G) 10-d-old ryegrass and (B, D, F,H) 10-d-old Arabidopsis root tips with (A, B) the mAbs LM2; (C, D) JIM13; (E, F) JIM16; and (G, H) JIM8. Fluorescence labeling appears as a dense network surrounding the ryegrass root tips. Observations are made with an epifluorescence microscope (Leica DMI6000B, Wetzlar, Germany; λExcitation: 591 nm; λEmission: 614 nm). BLC: Border-like cell; BC : Border cell; RT : Root tip ; m: mucilage. Scale bars:100 µm.

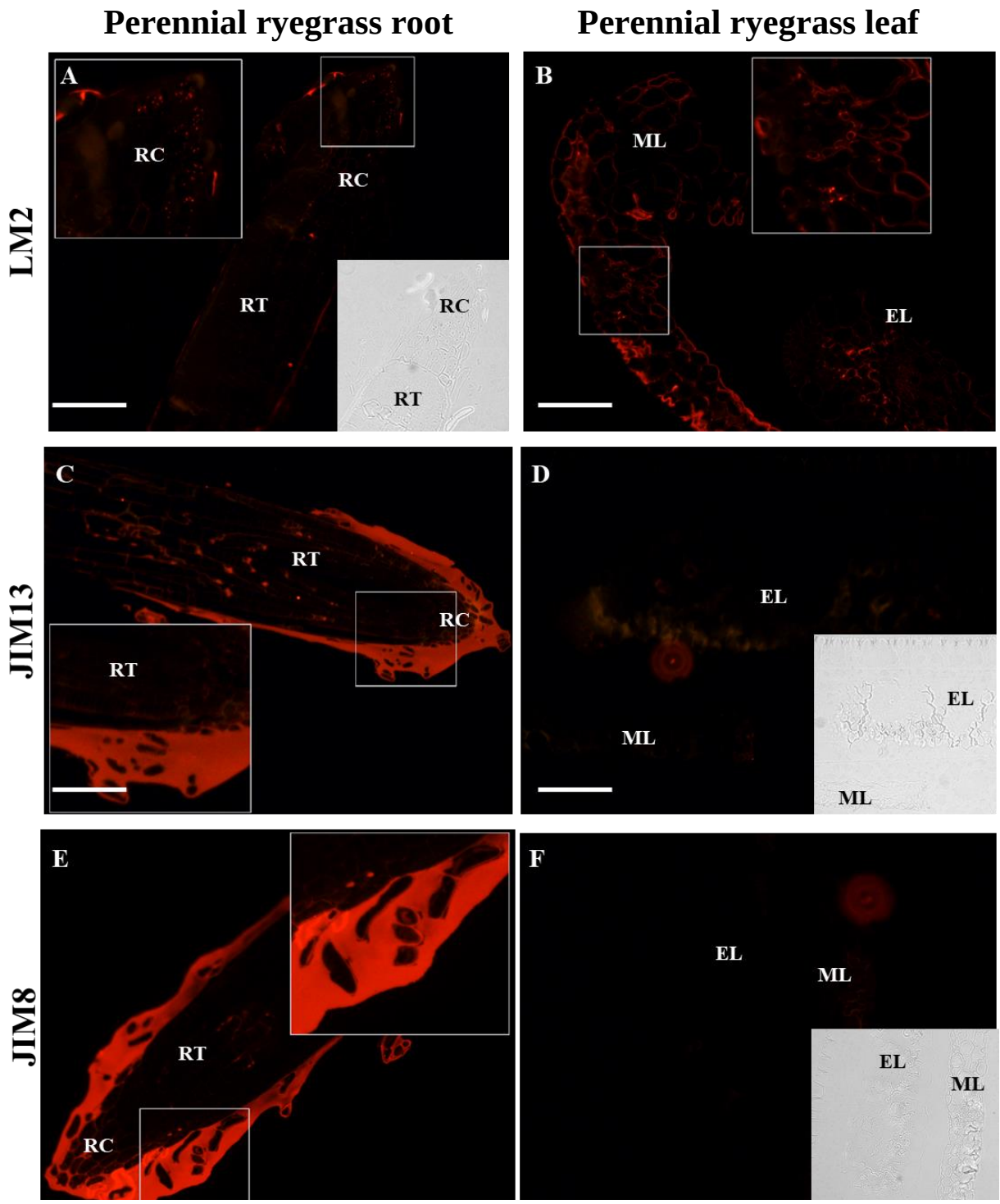

Figure III-13. Immunolocalisation of arabinogalactan proteins (AGPs) epitopes on the HPF sections.

Immunofluorescence images showing labeling of the cell wall and extracellular material in (A, C, E) 10-d-old ryegrass and (B, D, F) ryegrass leaf section with (A, B) the mAbs LM2; (C, D) JIM13; and (E, F) JIM8. Fluorescence labeling of JIM13 and JIM8 appears as a dense network surrounding the BCs and the mucilage in ryegrass root. Observations are made with an epifluorescence microscope (Leica DMI6000B, Wetzlar, Germany; λExcitation: 591 nm; λEmission: 614 nm). RT : Root tip; RC: Root cap; ML: Mature leaf sheaths; EL: Elongating leaf bases. Scale bars:100 µm.

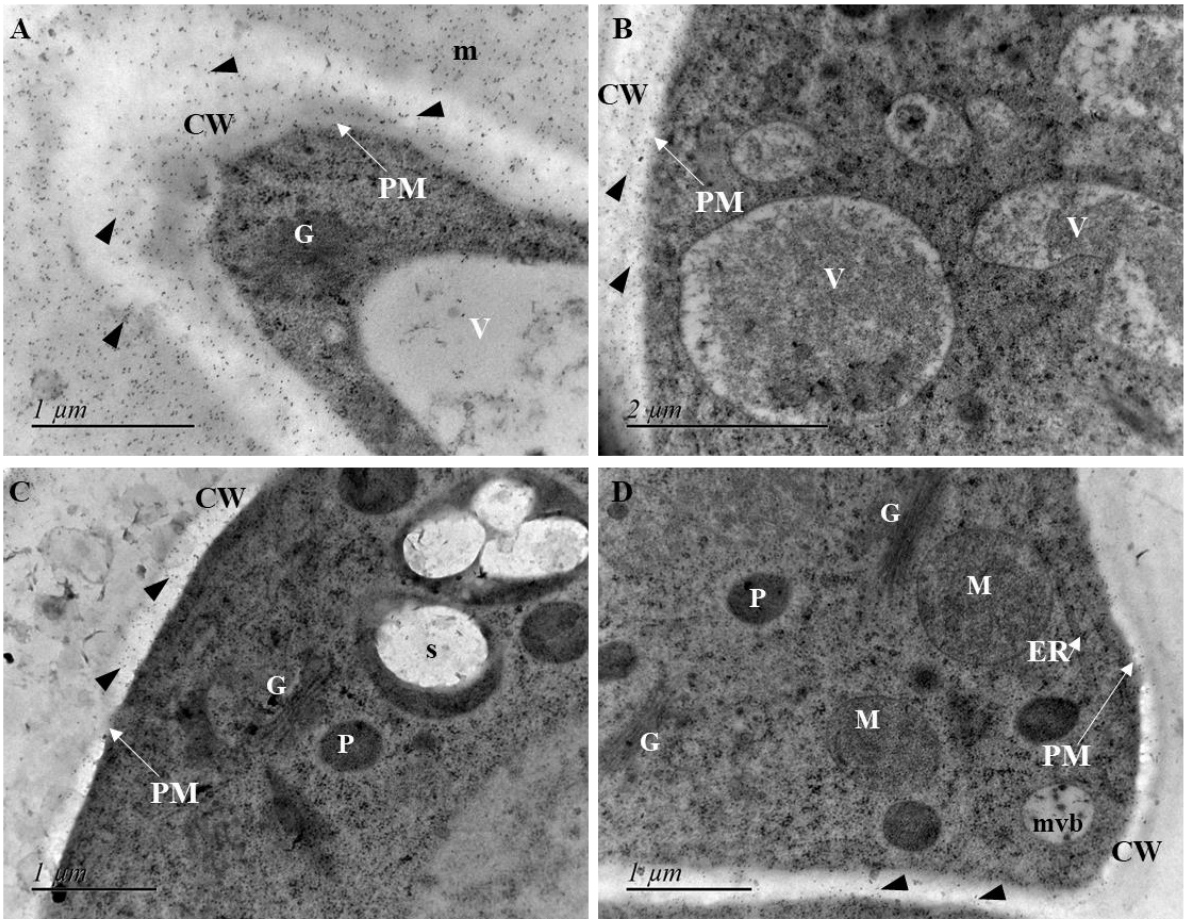

Figure III-14. Immunogold labeling of AGPs using mAb JIM13 on 12-d-old perennial ryegrass root border cells prepared by HPF and FS.

Arrowheads indicate the AGP epitopes recognized by JIM13. m: mucilage; mvb, multivesicular body; ER, endoplasmic reticulum; PM: plasma membrane; V: vacuole; CW: Cell wall; G, Golgi stack; M, mitochondria; P, plastid; s, starch. Scale bars: (A, C, D) 1 µm; (B) 2µm.

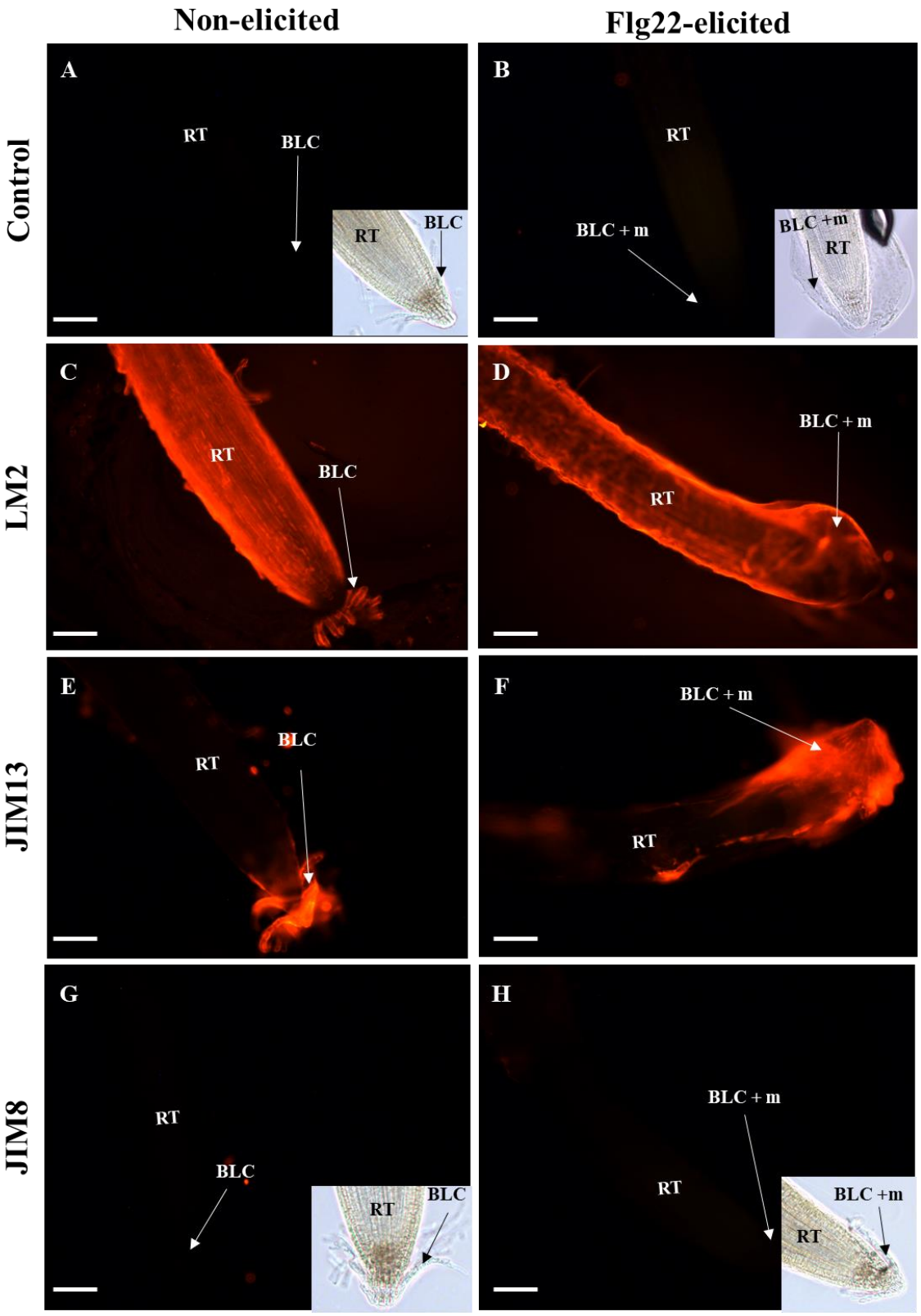

Figure III-15. Immunostaining of AGPs epitopes at the surface of Arabidopsis

With (C, D) the mAbs LM2; (E, F) JIM13; and (G, H) JIM8. Roots of Arabidopsis were treated with sterilized water only (A, C, E, G), or with 1 µM flg22 (B, D, F H). Note the presence of a dense mucilage observed in E and F. Arrows point to BLCs. BLC: Border-like cell; RT : Root tip ; m: mucilage. Scale bars:100 µm.

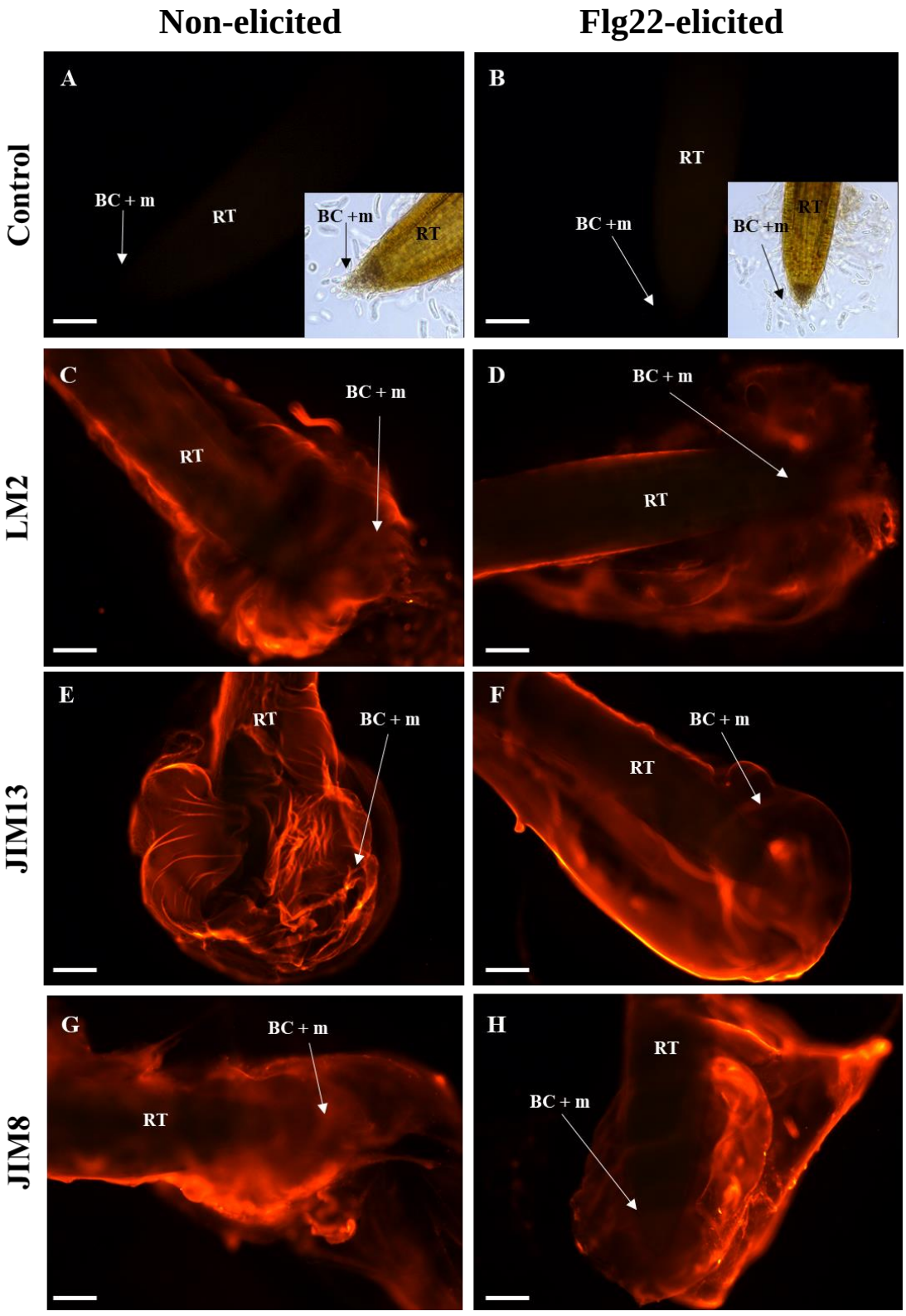

Figure III-16. Immunostaining of AGPs epitopes at the surface of perennial ryegrass With (C, D) the mAbs LM2; (E, F) JIM13; and (G, H) JIM8. Roots of ryegrass were treated with sterilized water only (A, C, E, G), or with 1 µM flg22 (B, D, F H). Note the presence of a dense mucilage observed in the ryegrass root tip. Arrows point to BCs. BC: Border-like cell; RT: Root tip ; m: mucilage. Scale bars:100 µm.

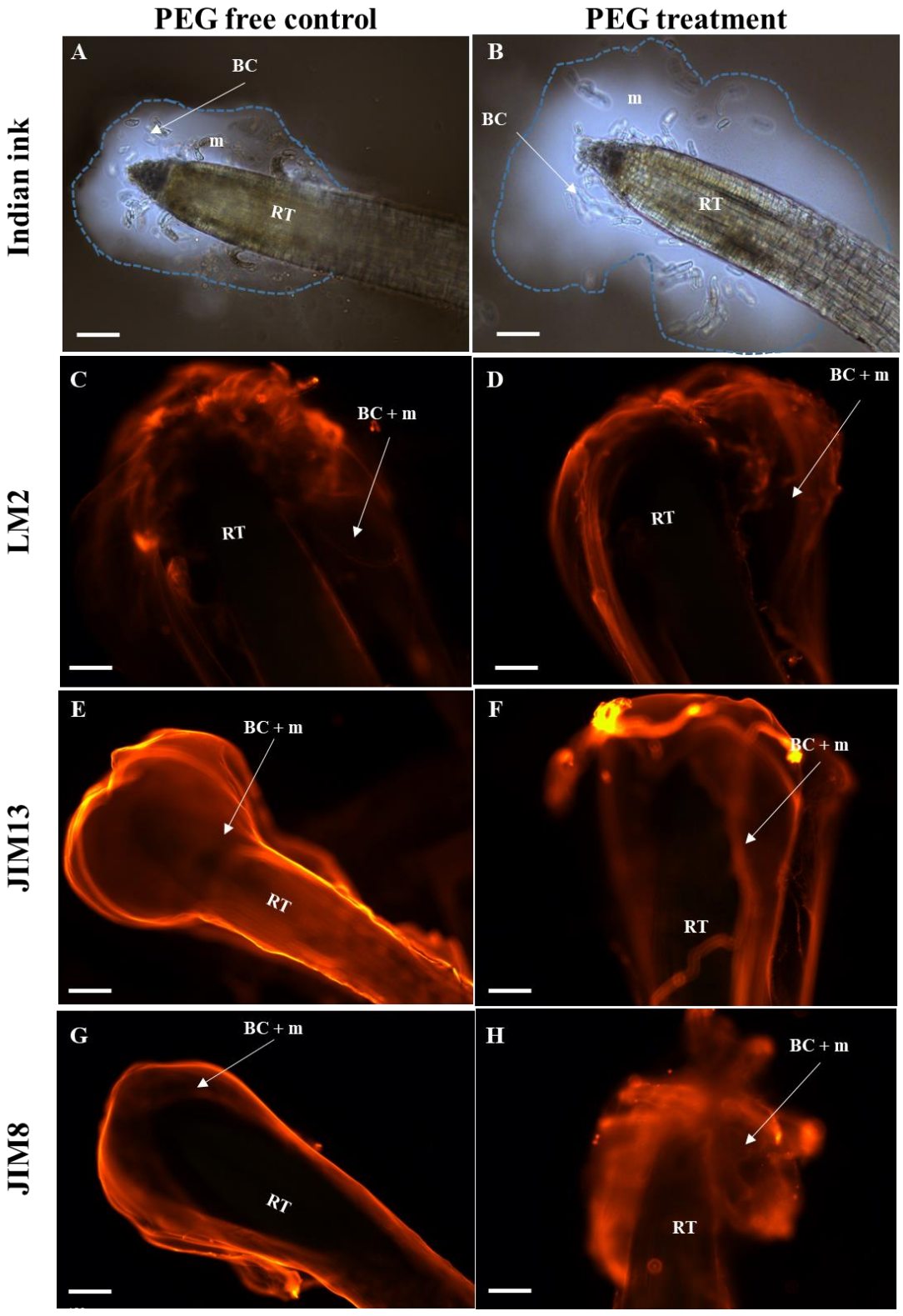

Figure III-17. Immunostaining of AGPs epitopes at the surface of ryegrass

With (C, D) the mAbs LM2; (E, F) JIM13; and (G, H) JIM8. Roots of ryegrass were developed in vitro without PEG (A, C, E, G), or with PEG treated (300g L-1)(B, D, F H). Note the presence of a dense mucilage observed in the ryegrass root tip. Arrows point to BCs and mucilage. BC : Border-like cell ; RT : Root tip ; m: mucilage. Scale bars:100 µm.

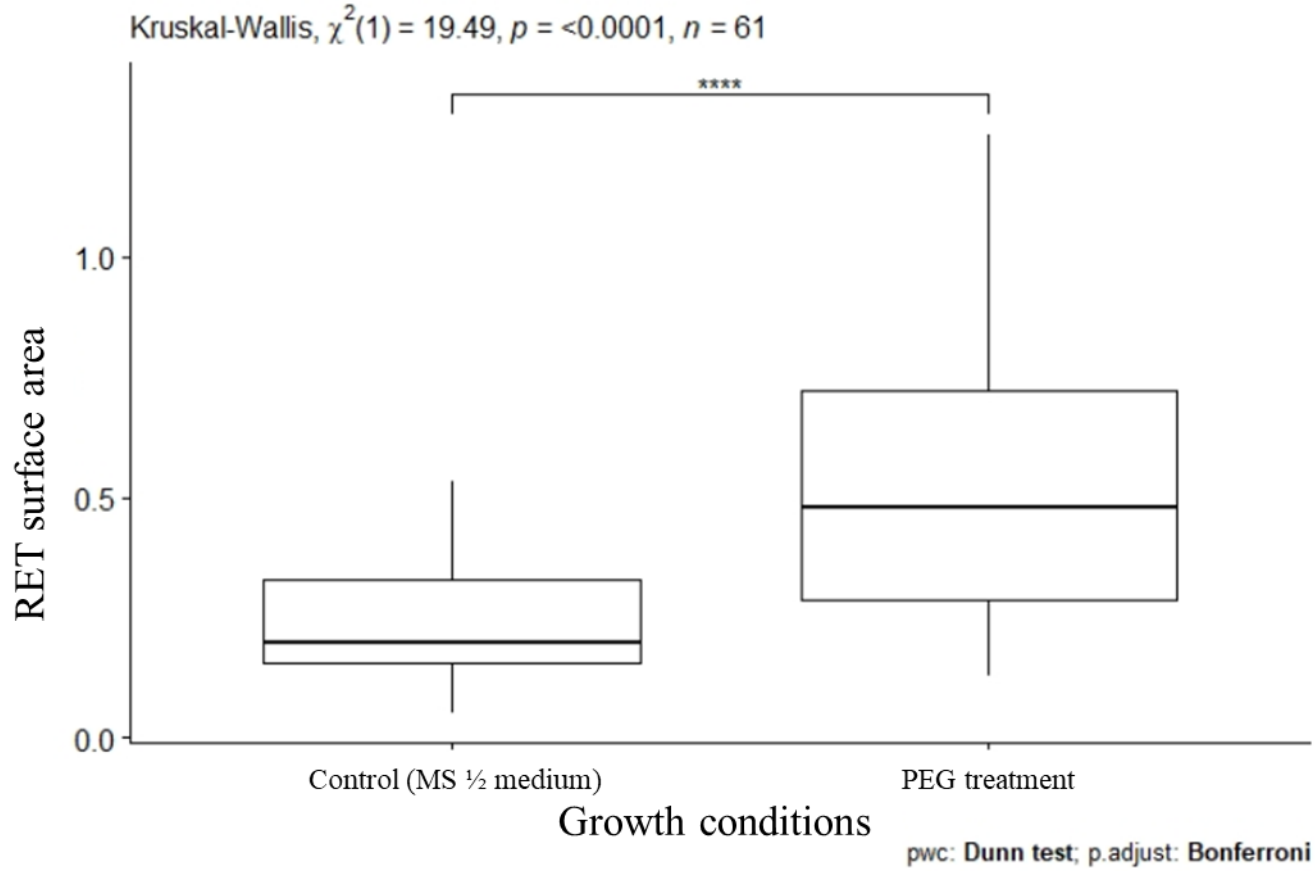

Figure III-18. Histograms represent quantitative data indicating the proportion of RET surface area surrounding the root cap.

*The histogram represents the mesure from 30 roots per condition by counterstaining with India ink. Kruskal–Wallis multiple comparisons test used with Bonferroni's correction. **** $P \leq 0.0001$*

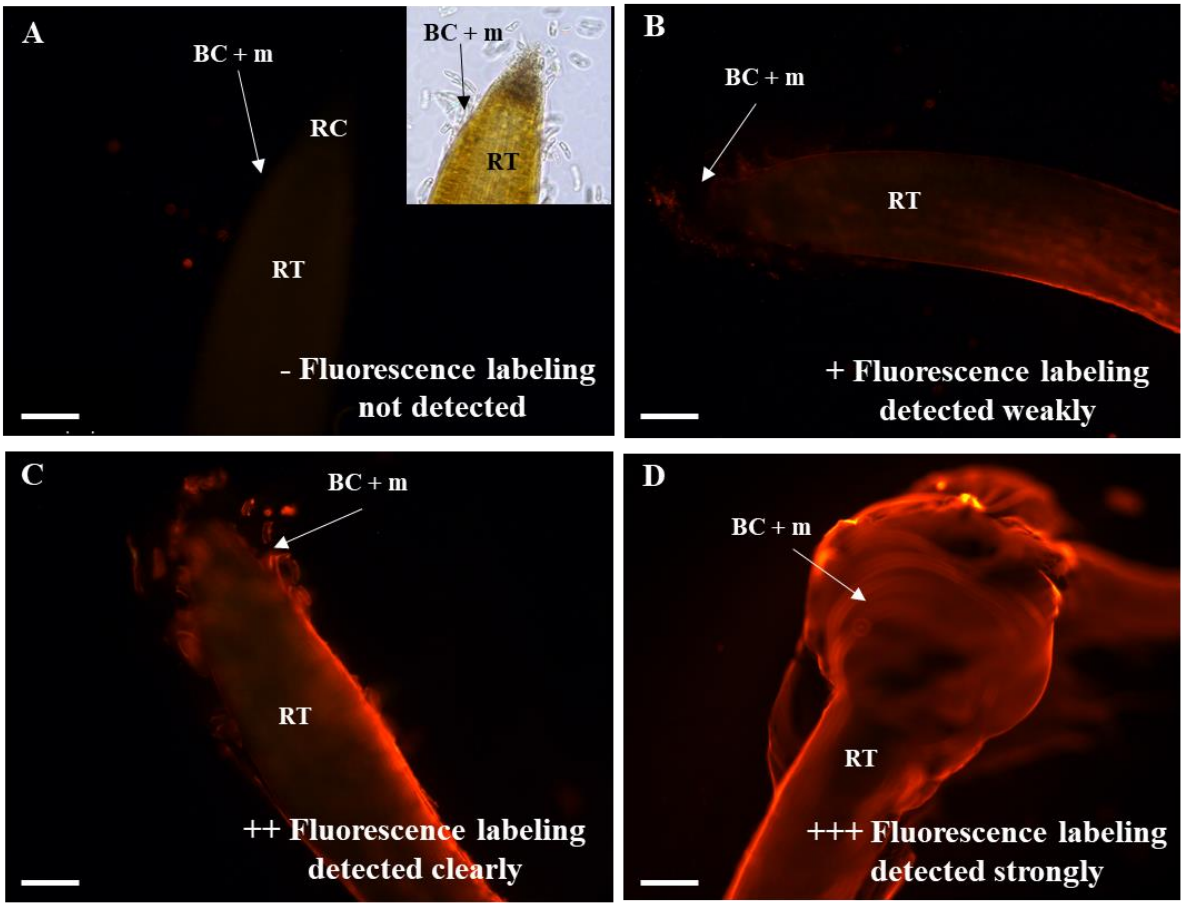

Figure S III-5. Illustration of different fluorescence labeling obtained in ryegrass root tips

Using an epifluorescence microscope (Leica DMI6000B, Wetzlar, Germany; λExcitation: 591 nm; λEmission: 614 nm) with the mAbs (A) JIM19 (B) LM12; (C) LM27; (D) JIM13. BC: Border-like cell; RT : Root tip ; m: mucilage. Scale bars:100 µm.

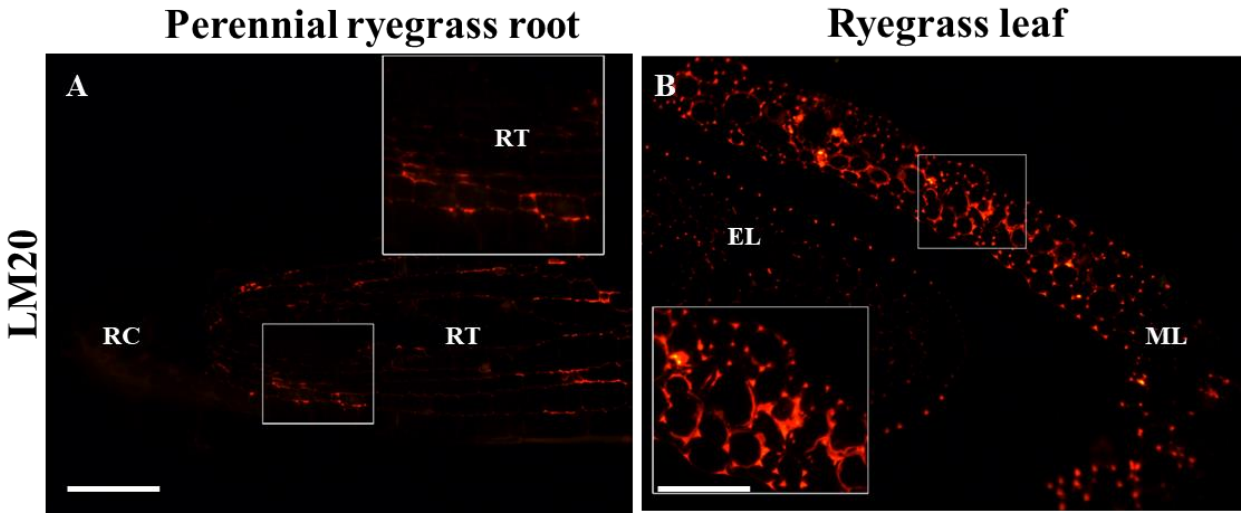

Figure S III-4. Immunolocalisation of pectin epitopes on the HPF sections.

Immunofluorescence images showing labeling of the cell wall in (A) 10-d-old ryegrass root section and (B) ryegrass leaf section with the mAb LM20. Observations are made with an epifluorescence microscope (Leica DMI6000B, Wetzlar, Germany; λExcitation: 591 nm; λEmission: 614 nm). RT: Root tip; RC: Root cap; ML: Mature leaf sheaths; EL: Elongating leaf bases. Scale bars:100 µm.

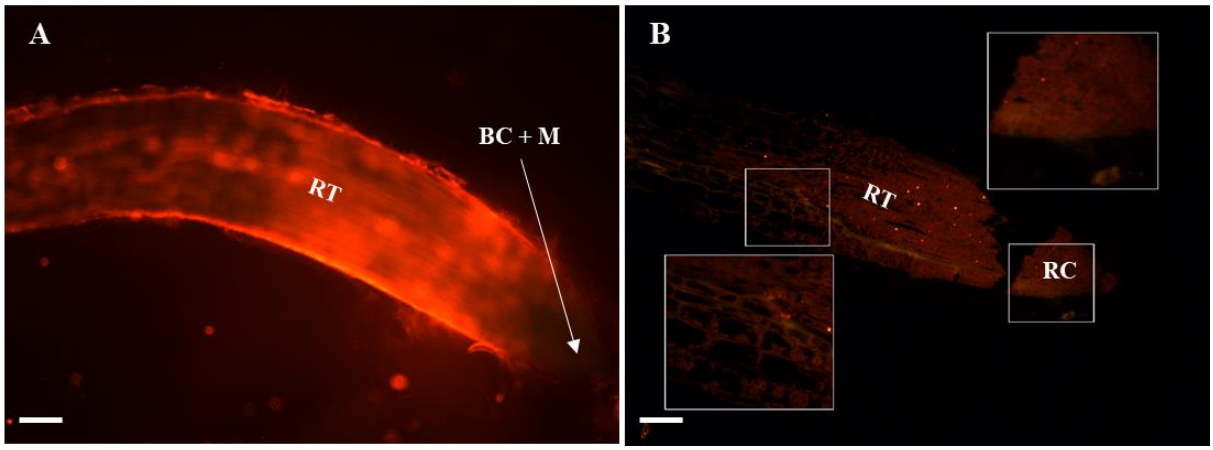

Figure S III-6. Immunofluorescence detection of fructans in perennial ryegrass using the monoclonal antibodies BTM15A6.

Observations are made with an epifluorescence microscope (Leica DMI6000B, Wetzlar, Germany; λExcitation: 591 nm; λEmission: 614 nm). (A) on ryegrass root tips. (B) on the HPF sections. BC: Border cell; RT : Root tip ; M: Mucilage; RC: Root cap . Scale bars = 100 µm.

Table S III-1. Immunolabeling of major glyco-polymer motifs in HPF sections of perennial ryegrass root using immunofuorescence microscopy.

	CW polymers	mAbs	Epitopes	Root section
Hemicelluloses	Xylan	LM10	(1,4)-β-xylosyl residues	–
	Arabinoxylan and low-substituted xylan	LM11	(1,4)-β-xylosyl residues	–
	Grass Heteroxylan	LM27	Unknown	+
	Feruloylated polymers	LM12	Feruloylated xylan	+
	Mixed linkage glucan (MLG)	MLG	(1,3; 1,4)-β-D-glucan	+
Pectins	Homogalacturonans (HGs)	LM19	HG with low degree of esterification	–
		LM20	HG with high degree of esterification	+
	Galactan chains	LM5	(1,4)-β-D-galactan, Rhamnogalacturonan-I (RG-I)	–
Extensins	Extensin from rice	LM1	Unknown	–
	Extensin from carrot	JIM11	Unknown	–
	Extensin from pea	JIM20	Unknown	–
Arabinogalactan proteins (AGPs)	AGP from rice	LM2	β-D-GlcpA	+
	AGP from carrot	JIM13	β-D-GlcA-(1,3)-α-D-GalA-(1,2)-α-L-Rha	+++
	AGP from carrot	JIM15	Unknown	–
	AGP from carrot	JIM16	Unknown	–
	AGP from sugar beet	JIM8	Unknown	+++

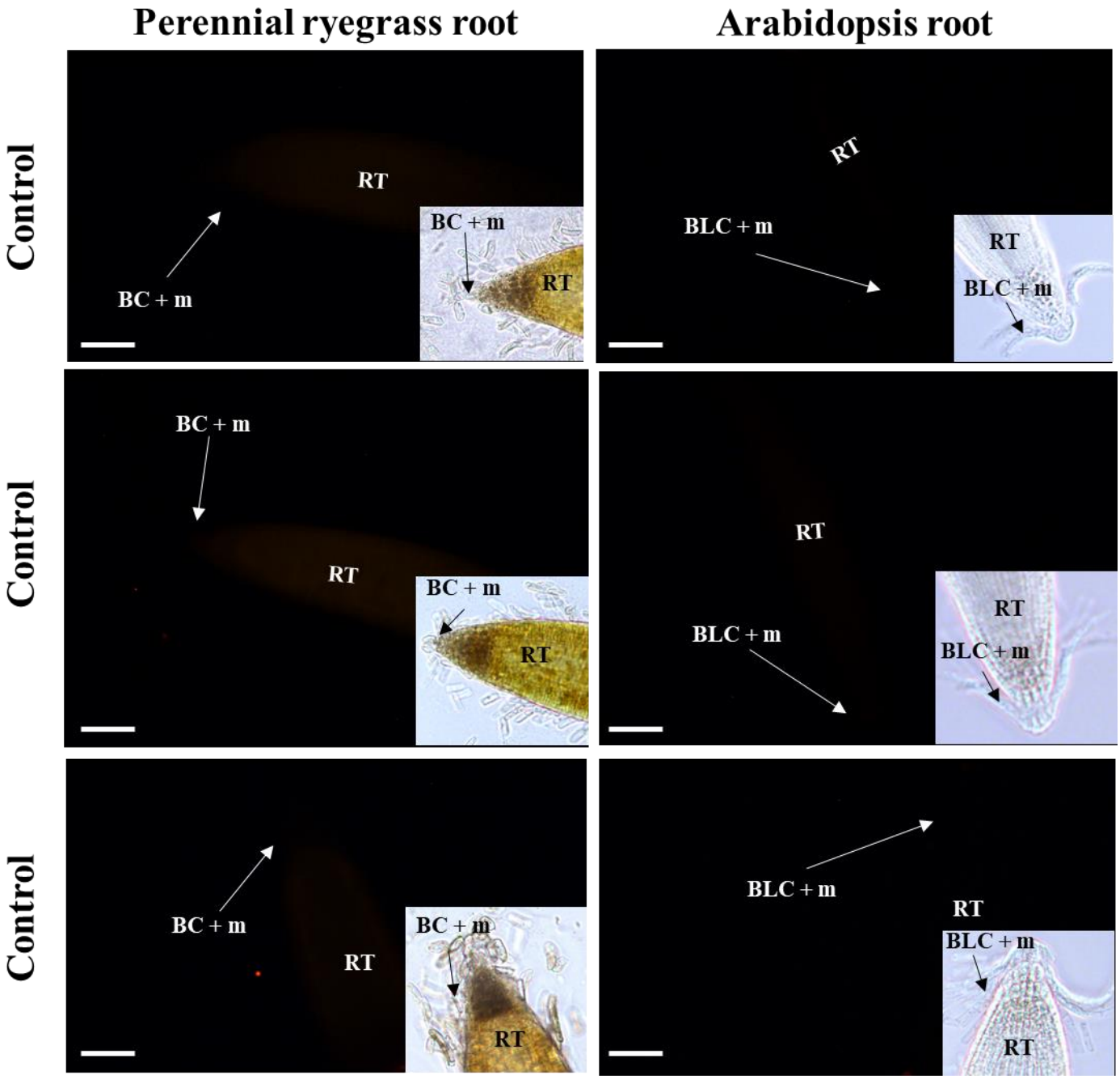

Figure S III-7. Observations of the control roots omitted primary antibodies

With an epifluorescence microscope (Leica DMI6000B, Wetzlar, Germany; λExcitation: 591 nm; λEmission: 614 nm). BLC: Border-like cell ; BC: Border cell; RT : Root tip ; m: mucilage. Scale bars:100 µm.

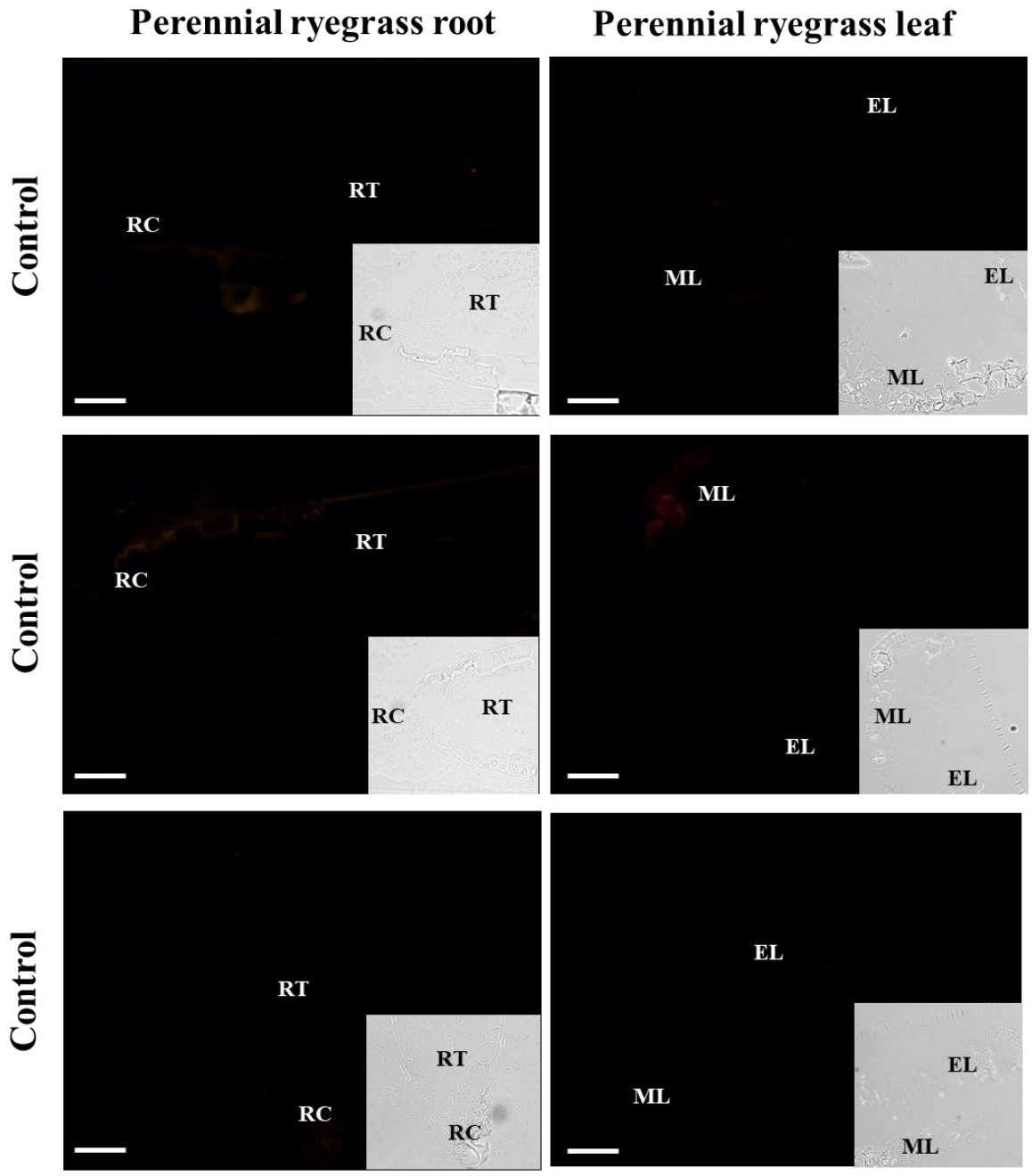

Figure S III-8. Observations of the control roots omitted primary antibodies

With an epifluorescence microscope (Leica DMI6000B, Wetzlar, Germany; λExcitation: 591 nm; λEmission: 614 nm). BLC: Border-like cell; BC: Border cell; RT: Root tip ; m: mucilage. Scale bars:100 µm.

3. Salicylic acid upregulates fructan exohydrolases (FEH) together with defense-marker genes in non-fructan plants.

Thi Ngoc Hanh Nguyen[1,2], Laëtitia Leclerc[1], Maria J. Manzanares-Dauleux[3], Antoine Gravot[3], Maïté Vicré[2], Annette Morvan-Bertrand[1+*], Marie-Pascale Prud'homme[1+]. **corresponding author* *[+]co-last authors*

[1]Normandie Univ, UNICAEN, INRAE, EVA Ecophysiologie Végétale Agronomie et nutritions N.C.S, FED Normandie Végétale 4277, 14032 Caen, France

[2]Normandie Univ, UNIROUEN, Laboratoire GLyco-MEV EA 4358, FED Normandie Végétale 4277, 76000 Rouen, France

[3]Institut Agro, Université Rennes, INRAE, IGEPP, 35653 Le Rheu, France

Abstract

Identification of fructan exohydrolases (FEHs) in non-fructan plants raised the question of their roles. We tested the hypothesis that they are defense-related proteins in the model plant *Arabidopsis thaliana* and the genetically related allopolyploid species *Brassica napus*. By sequence homologies with the two known FEH genes of *A. thaliana*, *At6-FEH* and *At6&1-FEH*, the genes coding for the putative *B. napus* FEHs, *Bn6-FEH* and *Bn6&1-FEH*, were identified. Plants were treated at root level with salicylic acid (SA), methyl jasmonate (MeJA) or 1-aminocyclopropane-1-carboxylic acid (ACC). The transcript levels of defense-marker and FEH genes were measured after 12 h of treatment. The ability of phytohormones to induce a defense response was confirmed by the strong induction of *PR1* and *WRKY70* by SA, *AOS* by MeJA, *PDF1.2* and *ERF1/2* by ACC treatments. *HEL* was up-regulated by the three phytohormones and proposed as a generic marker of root defense response. SA increased the expression of *6-FEH* genes and, to an even higher level, that of *6&1-FEH* genes in both species, clearly supporting their role as defense proteins in non-fructan plants. A genotypic variability of SA-mediated FEH regulation was observed among five *B. napus* varieties, that may have consequences on the susceptibility to fructan synthesizing pathogens.

Introduction

Unlike mammals, plants do not have an adaptive immune system but have their own way of defending themselves against pathogenic attacks (Henry *et al.*, 2012). Facing potential pathogens, plants rely on the innate immunity of each cell to detect the pathogen using constitutive transmembrane pattern recognition receptors (PRRs) which recognized pathogen/microbial/ damage-associated molecular patterns (PAMPs/MAMPs/DAMPs),

resulting in PAMP-triggered immunity (PTI) (Boller and Felix, 2009). PTI constitutes the first layer of plant immunity also called basal resistance (Henry *et al.*, 2012). PAMPs have been characterized widely and include flagellin, peptidoglycans, lipopolysaccharides and proteins from bacteria, chitin from fungi and β-glucans from oomycetes (Newman *et al.*, 2013). PTI responses lead to the accumulation of defense-related phytohormones such as salicylic acid (SA), jasmonic acid (JA), and ethylene (ET) (Penninckx *et al.*, 1998; Caarls *et al.*, 2015). These signaling molecules can induce local and systemic protection through the induction of expression of pathogenesis-related (PR) genes (van Loon *et al*., 2006). A recent study showed that SA-responsive genes such as the genes coding for the transcription factor WRKY70 and the PR protein PR1 were upregulated in two genotypes of *Brassica napus* inoculated with *Plasmodiophora brassicae*, a soil-borne pathogen (Galindo-González *et al.*, 2020), as was also shown in Arabidopsis (Lemarié *et al*., 2015).

Among the large diversity of PAMPs/MAMPs/DAMPs that have been described, the role of carbohydrates in plant immunity has recently been demonstrated (Trouvelot *et al.*, 2014; Bacete *et al.*, 2018). Specifically, based on the fact that the supply of soluble carbohydrates to healthy plants induces defense responses which protect the plant from subsequent infections, the concept of "sweet immunity" also known as “sugar-enhanced defense” has emerged (Bolouri-Moghaddam and Van den Ende, 2012). Among soluble carbohydrates, fructans, which are polymers of fructosyl residues linked by β-2,1 and/or β-2,6 linkages with an external or internal glucosyl residue (Ritsema and Smeekens, 2003), may play a particular role in plant-microorganism interactions since they are synthesized by some plant species (Hendry, 1993) and microorganisms (Velazquez-Hernandez *et al.*, 2009).

In plants, fructans are synthesized and stored in the vacuole (Ritsema and Smeekens, 2003). Their degrees of polymerization (DP) vary generally between 30 and 150, but in some cases can reach 200 (Van den Ende, 2013). Fructans are divided into four types that are distinguished by the nature of the linkage connecting the fructosyl residues, the position of the glucosyl residue (internal or external) and the presence or absence of branches: inulin-type (β-2,1 linkage), levan-type (β-2,6 linkage), graminan-type (β-2,1 and β-2,6 linkages forming branches) and neoseries-types (levan or inulin) for which the glucosyl residue carried by the precursor molecule (sucrose) is in the internal position. Inulin-type fructans are found mainly in *Asteraceae* plant species such as *Cichorium intybus* (Van Laere and Van Den Ende, 2002), levan-type fructans (also called phleins) are found mainly in *Poaceae* such as *Phleum pratense* (Cairns *et al.*, 1999) and neoseries-type fructans in *Amaryllidaceae* such as *Allium cepa* (Shiomi, 1989). Some *Poaceae* produce several types of fructans such as graminan- and inulin-

types in *Triticum aestivum* and inulin- and neoseries-types in *Lolium perenne* (Pavis *et al.*, 2001). In microorganisms, the DP of fructans can be much higher, from 20 to 10,000 residues, and fructans are secreted as exopolysaccharides (Velázquez-Hernández *et al.*, 2009). In bacteria, levan-type fructans predominante and are produced by Gram-positive and Gram-negative bacteria (Öner *et al.*, 2016) while some Gram-positive bacteria synthesize inulin-type fructans (Velázquez-Hernández *et al.*, 2009). In fungi, inulin-type oligofructans known as fructo-oligoaccharides (FOS) with generally DPs between 3 and 8 are found in several genera including *Aspergillus* and *Penicillium* (Trollope *et al.*, 2015). Fructans are multifunctional molecules in plants and microorganisms. In plants, they are not only a form of carbon storage but also contribute to the resistance to abiotic stresses such as freezing, drought, and salinity (Parvanova et al., 2004; Livingston et al., 2009) due to their ability to contribute to the regulation of osmotic potential, to insert and stabilize membranes (Hincha *et al.*, 2007) and to scavenge reactive oxygen species produced in excess during stress (Stoyanova *et al.*, 2011). In bacteria, fructans also play an important role in carbon storage, and abiotic stress resistance by increasing water availability during water deficit (Bogino *et al.*, 2013).

In addition to these roles, there is growing evidence for the role of fructans and their degradation products in pathogenic or beneficial interactions between plants and microorganisms. In presence of sucrose, the plant pathogenic bacteria *Pseudomonas syringae* secrete levan-type fructans that form a layer between bacteria and the plant cell wall during the early phase of infection, preventing the plant to recognize the pathogen (Hettwer *et al.*, 1995). This is confirmed by the fact that the disruption of the gene coding for the fructan-synthesizing enzyme in *Erwinia amylovora* (the fire blight agent of the *Pomoideae*) delayed the onset of symptoms in pear, indicating that the synthesis of levans increases the virulence of the bacteria by the formation of a protective layer which prevents the plant from perceiving the presence of bacteria (Geier and Geider, 1993). Similarly, in the beneficial rhizobacterium *Bacillus subtillis*, sucrose induced the synthesis of levans which increased the thickness and stability of the biofilm (Dogsa *et al.*, 2013) and promoted root colonization (Tian *et al.*, 2021). In addition, several studies using exogenous supplies of fructans have shown that they can act as elicitors in the plants-microorganisms interactions (Versluys *et al.*, 2017), triggering defense-related phytohormones signaling pathways and reducing the infection. For example, the pre-application of plant-derived inulin-type fructans to *Lactuca sativa* leaves reduced the infection caused by *Botrytis cinerea*. The treatment of inulin-treated plant with 1-methylcylopropene (1-MCP), a well-known inhibitor of the ET signaling pathway, cancelled the effect of the pre-application with inulin-type fructans, indicating that a functional ET signaling pathway is needed for the

enhanced defense response induced by fructans (Tarkowski *et al.*, 2019). Similarly, the treatment of cucumber leaves with inulin-type fructo-oligosaccharides before inoculation with *Colletotrichum orbiculare*, a fungus causing anthracnose in *Cucurbitaceae*, reduced disease impact and increased SA levels (Zhang *et al.*, 2009).

The detection of fructan degrading enzymes (fructan exohydrolases, FEH) in plants that do not accumulate fructans, *Beta vulgaris* (Van den Ende *et al.*, 2003), *Arabidopsis thaliana* (De Coninck *et al.*, 2005) and *Zea mays* (Zhao *et al.*, 2019), has led to the hypothesis that these proteins could play a role in plant-microorganism interactions by contributing to the production of the MAMPs from microbial fructans and/or by weakening the bacterial biofilm (Van den Ende *et al.*, 2005). FEHs act by hydrolyzing the *O*-glycosidic linkage of the external fructosyl residue. 1-FEHs and 6-FEHs hydrolyze preferentially the β-2,1 and β-2,6 linkages, respectively, and 6&1-FEHs hydrolyze the two types of linkages (Lammens *et al.*, 2009). In fructan accumulating plants, FEHs activities have been demonstrated in vacuoles (Frehner *et al.*, 1984) but FEH activity has also been detected in the apoplast in response to abiotic stress (cold) in oat (*Avena sativa*; Livingston and Henson, 1998) and wheat (*Triticum aestivum;* Van den Ende *et al.*, 2005). In the non-fructan plant *Zea mays*, the localization of a FEH (Zm-6&1-FEH1) in the apoplast supports the hypothesis of its role in the interaction between plants and microorganisms (Zhao *et al.*, 2019). In the case of vacuolar FEHs, it is possible that following injury or pathogen attack causing disruption of the plasmalemma and tonoplast, vacuolar FEHs are discharged into the apoplast compartment. The FEHs thus present in the cell wall would be able to degrade the microbial fructans, leading to (i) a modification of the properties of the biofilm which could reduce virulence, and (ii) the release of fructose and small fructans (fructo-oligosaccharides, FOS) which could play the role of PAMPs. These PAMPs would be recognized by a PRR receptor triggering the plant PTI defense response through a signaling cascade inducing the biosynthesis of phytohormones such as SA, JA, and ET (Rejeb *et al.*, 2014). An argument in favor of this hypothesis is that exogenous supply of SA and Methyl Jasmonate (MeJA, a JA derivative) led to increased expression of FEHs in agave (*Agave americana)* which is known as a fructan accumulator plant (Suárez-González *et al.*, 2016).

To deepen the understanding of the role of fructans in the plant-microorganism interactions, and more precisely the role of FEHs in defense responses, the objective of this study was to evaluate the regulation of FEH expression by defense-related phytohormones. We hypothesized that the treatment of plants with SA, MeJA, or ACC (1-Aminocyclopropane-1-carboxylic acid, a precursor of ethylene synthesis) will induce the expression of known defense-related marker genes (see Materiels and Methods Table II.4) together with that of FEH genes. The

phytohormone treatments were applied at the root level to investigate defense mechanisms in roots which remain largely underexplored (Chuberre *et al.,* 2018). We hypothesized that the regulations of FEH genes and defense-related marker genes upon phytohormone treatments at the root level differ markedly as compared to plants with leaves treatment. These hypotheses have been tested in two non-fructan plant species, the model plant *Arabidopsis thaliana* and the genetically related species *Brassica napus*. In *A. thaliana*, two FEHs genes (*At6-FEH* and *At6&1-FEH* corresponding to At1g55120 and At5g11920, respectively) have been identified by De Coninck *et al.* (2005) using heterologous expression of two genes initially identified as cell-wall invertase genes (*AtcwINV3* and *AtcwINV6*). By sequence homology with the two *A. thaliana* FEH genes, we looked for genes coding for putative FEHs in the allopolyploid genome of *B. napus* (Chaloub *et al.,* 2014), a species of agronomic interest which is susceptible to several root pathogens (Neik *et al.,* 2020). We identified two genes with complete sequence coding for a putative 6-FEH (named *Bn6-FEH*) and four genes with complete sequence coding for a putative 6&1-FEH (named *Bn6&1-FEH*) (Table 1). Since SA is involved in both plant pathogenic and non-pathogenic interactions (Zhang and Li, 2019; Koo *et al.*, 2020), the variability of responses to SA treatment could help to identify varieties less susceptible to pathogens and/or abler of being colonized by beneficial endophytes. Thus, to test this hypothesis, we evaluated five varieties of oilseed rape ('Aviso', 'Tenor', 'Darmor-*bzh'*, 'Yudal', 'Bristol') harbouring contrasted behaviour in both pathogenic and non-pathogenic interactions (Manzanares-Dauleux *et al.,* 2000; Fopa Fomeju *et al.,* 2015; Daval *et al.,* 2020).

Materials and Methods

Plant material and growth conditions

A. thaliana ecotype Colombia-0 (Col-0) and five varieties of *B. napus* oilseed rape ('Aviso', 'Tenor', 'Darmor-*bzh'*, 'Yudal', 'Bristol') were used in this study. Seeds of both species were soaked in darkness for 48 h at 4°C in 0.1% (w/v) agar solution to synchronize germination. Each seed was individually sown on the top of a 1.5 mL microtube pierced at the bottom and filled with 0.7% (w/v) agarose (Supplementary Fig.SIII-11). The plants were grown in hydroponic conditions. Each microtube was transferred to a plastic tank (fifteen plants per tank) filled with 10 L of nutrient solution containing: $Ca(NO_3)_2$ (1.25 mM), KNO_3 (1.25 mM), KH_2PO_4 (0.25 mM), $MgSO_4$ (0.5 mM), EDTA-2NaFe (0.2 mM), H_3BO_3 (14 µM), $MnSO_4$ (5 µM), $ZnSO_4$ (3 µM), $CuSO_4$ (0.7 µM), $(NH_4)_6Mo_7O_{24}$ (0.7 µM), $CoCl_2$ (0.1 µM). *A. thaliana* was grown for 4 weeks in a plant growth chamber with high-pressure sodium lamps (Philips, MASTER GreenPower T400W) providing a PAR (Photosynthetically Active Radiations)

between 10 and 150 µmol photons·m^{-2}·s^{-1} under a photoperiod of 16 h and a thermoperiod of 20/18°C day/night. *B. napus* was grown for 2.5 weeks in a greenhouse with natural light supplemented by high-pressure sodium lamps (Philips, MASTER GreenPower T400W) with a PAR (Photosynthetically Active Radiations) of 450 µmol photons·m^{-2}·s^{-1} at canopy height with a photoperiod of 16 h and a thermoperiod of 20/17°C day/night. The nutrient solution was aerated and renewed every 7 days. After the emergence of the fourth leaf in *B. napus* and the eighth leaf in *A. thaliana*, the microtubes were transferred in 150 mL pots (five plants per pot) containing 50 mL of nutrient solution supplied with 0.5 mM SA (Wang et al., 2012), 50 µM MeJA (Suárez-González *et al.*, 2016), 20 µM ACC (Liu et al., 2013) (Sigma-Aldrich, Saint-Louis, MO, USA) or without supplement (control) for 12h or 3, 6, 12, and 24 h depending on the experiment. Plants were collected and the shoots were separated from the roots, frozen in liquid nitrogen and stored at -80°C. Before RNA and protein extractions, plant tissue were ground in liquid nitrogen in a precooled mortar and pestle until a fine powder was obtained and the frozen powder was stored at -80°C.

RNA extraction

The frozen powder (approx. 200 mg) was transferred to a tube containing 750 µL extraction buffer (0.1 M LiCl, 0.1 M Tris-HCl, 0.01 M EDTA, 1% (wv) SDS, pH 8.0) mixed with 750 µL of hot phenol (80°C, pH 4.3). After vortexing for 40s, 750 µL chloroform/isoamyl alcohol (24:1 v/v) was added. The tubes were mixed vigorously and centrifuged at 20 000 *g* for 5 min at 4°C. The supernatant was transferred into 750 µL LiCl 4M, and incubated overnight at 4°C. A white pellet containing RNA was visible after centrifuging for 20 min at 20 000 *g* at 4°C. Then, the supernatant was removed and the pellet was suspended in 100 µL RNase free water.

Purification of RNAs including a step of DNA digestion by DNAse treatment was performed using RNeasy mini kit according to the manufacturer's protocol (Qiagen, Courtaboeuf, France). Purified RNA was diluted in 20 µL distilled water. Absorbance at 260 nm and the 260/280 nm ratio were measured with an RNA BioPhotometer (Eppendorf, Hamburg, Germany) and used to calculate the total RNA concentration and to check the RNA purity. RNA integrity was visualized by separation of 1 µg of total RNAs on a 1.2% (w/v) standard agarose gel containing ethidium bromide (0.5 µg.mL^{-1}).

RT-qPCR analysis

Total RNA was reverse transcribed to cDNA by using iScript™ cDNA Synthesis Kit (Biorad, France) with 2 µL iScript reaction mix (5X) and 0.5 µL iScript reverse transcriptase. Real-Time qPCR experiments were performed using 4 µL of 1:200 dilution of first-strand cDNA on a

Biorad CFX96 connect real-time PCR (Chromo4®, Biorad, France). The PCR mix comprised 0.75 µL forward and reverse primers and 7.5 µl of iQ SYBR Green supermix (BioRad, France) in a 15 µL total volume. qPCR was performed using the following program: 95 °C for 3 min followed by 40 cycles of 95 °C for 15 s and 60 °C for 40 s. The description of the gene-specific primers is given in table SIII-3. FEHs primer pairs were designed with Primer3 software (https://primer3plus.com/cgi-bin/dev/primer3plus.cgi) from the nucleotide sequences available on the National Center for Biotechnology Information-NCBI and by comparing FEH sequences. Each primer chosen contains about 20 nucleotides with at least 50% GC content and optimal Tm at 60°C, raising to PCR products of 100-300 bp length. For each gene, the specificity of PCR amplification was validated by monitoring the presence of the single peak in the melting curves and by sequencing the PCR product. For relative transcript level determination, two reference genes were selected (*BnGAPDH* and *BnEF1* for *B. napus*, *AtActin* and *AtEF1α* for *A. thaliana*). For each pair of primers, a threshold value and PCR efficiency (%) were determined using a cDNA preparation diluted >10-fold. The PCR efficiency of each pair of primers, ranging from 94.7 to 118.1 %, was used to calculate the relative gene expression using a delta threshold cycle (Ct) method derived from that described by Hellemans *et al.* (2007). For each target and reference genes of a data series, the relative quantity (RQ_i) of the corresponding transcript in each sample (i) was calculated as follow:

$$RQi = E^{-\Delta Cti,\ min}$$

where E is (1+ efficacity)/100 and $\Delta Ct_{i,\ min}$ is the difference between Ct_i and the lowest Ct of the series ($Ct_{i,min}$). The RQ_i of the target genes are normalized (NRQ_i) with the geometric average of the RQ_i of the two reference genes as follow:

$$NRQ_i = RQ_i / (\sqrt{(RQ_{i,\ ref1} \times RQi_{,\ ref2})})$$

Then, the NRQ_i are rescaled (rescaled-NRQ_i) by comparison with that of the control sample NRQ_{ctrl} as follow:

$$\text{rescaled-}NRQ_i = NRQ_i / NRQ_{ctrl}$$

Statistics

All data obtained were analyzed with R software version 4.0.3 using the "Rcmdr" package. For each treatment and time, the data correspond to five biological replicates (five individual plant). The comparison of control versus treated plants was done using the Wilcoxon nonparametric test (rank sum test). The comparison of more than two sets of data was done using the Kruskal-Wallis nonparametric test followed by a post-hoc multi-comparison ranking test (with the

"pgirmess" and the "multcompView' packages). For each test, the statistical effect is considered significant with P<0.05. The principal component analysis was performed with the "FactoMinR" package using the relative expression of seven genes in the roots of the five genotypes with five biological replicates for each genotype (n=25).

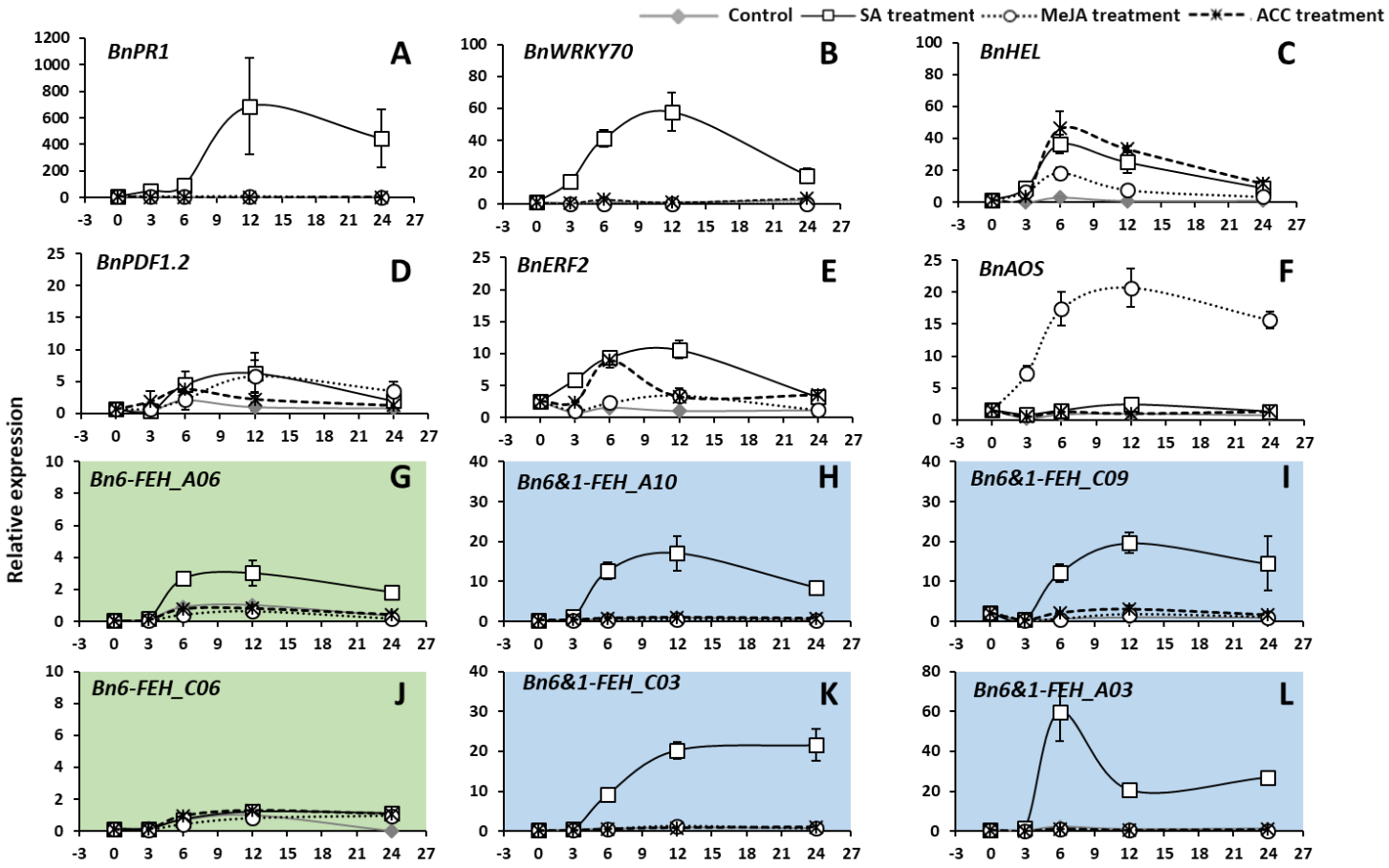

Figure III-19. Phytohormone treatments increased the expression of some defense-marker and FEH genes in B. napus roots.

Relative expression of defense marker genes (BnPR1, BnWRKY70, BnHEL, BnDPF1.2, BnERF2, BnAOS) and FEH genes (Bn6-FEH_A06; Bn6-FEH_C06; Bn6&1-FEH_A10; Bn6&1-FEH_C09; Bn6&1-FEH_C03 and Bn6&1-FEH_A03) in B. napus cv. 'Tenor' roots treated with 0.5 mM salicylic acid (SA), 50 µM methyl jasmonate (MeJA) or 20 µM 1-Aminocyclopropane-1-carboxylic acid (ACC) during 3, 6, 12 and 24h. For each gene, the data were normalized against the control plant sampled after 12 h of treatment. Each data point is the average of five independent biological replicates and the bars indicate the standard errors. The statistical analyses of the difference between the control and the treated plants are presented in Supplementary Table S1.

Results

Expression profiles of defense marker and FEHs *genes in* B. napus 'Tenor' *after root treatment with SA, MeJA or ACC*

Based on gene homologies between the sequences of the two known *A. thaliana* FEH genes (Col-0) and the *B. napus* genome cv. "Darmor-bzh" (Version 4.1; Chalhoub et al., 2014), we idendified two genes with complete sequence coding for a putative 6-FEH (named *Bn6-FEH*) and four genes with complete sequence coding for a putative 6&1-FEH (named *Bn6&1-FEH*) (Table 1).

B. napus seedlings were treated at root level with 0.5 mM SA, 50µM MeJA or 20µM ACC to trigger the activation of SA, JA, and ET signaling pathways. To assess plant responses, the level of expression of genes known to be involved in the corresponding signaling pathways (defense marker genes in table SIII-3) was monitored over 24 h. SA treatment increased the transcript level of genes coding for the WRKY70 and ERF2 transcription factors from the first 3 h of treatment (Fig.III-19B, E, Supplementary Table SIII-3). After a latency time of 6 to 12 h, it increased the transcript level of genes coding for the antimicrobial peptides PR1, HEL, and to a lower extent PDF1.2 (Fig.III-19A, C, D). MeJA treatment increased from the first 3 h of root treatment the transcript level of *BnAOS* which codes for the allene oxide synthase, an enzyme catalyzing a key step of the biosynthesis of jasmonic acid from membrane lipids (Cheong and Choi, 2003) (Fig.III-19F). It also increased the transcript level of the antimicrobial peptides HEL ($p<0.05$) and PDF1.2 ($p=0.06$) (Fig.III-19 C, D). The treatment with ACC increased the transcript level of *BnERF2* and *BnHEL* (Fig.III-19 C, E). Overall, the results indicate that the three treatments applied at the root level were able to elicit defense responses characterized by the induction of genes involved in the signaling or in the synthesis of antimicrobial peptides. The same samples were used to assess whether the treatments were also able to induce the expression of FEH genes.

Following a latency of 3 h, the transcript level of one of the two *Bn6-FEH* genes (*A06;* Fig.III-19G; Supplementary Table SIII-3) was slightly increased after 6 h of SA treatment. With a much stronger effect, the transcript level of the four *Bn6&1-FEH* genes (*A10*, *C09*, *C03* and *A03*) increased in SA-treated roots (Fig.III-19H, I, K, L) with a maximum after 6 h (*A03*) or 12 h (*A10, C09, C03*) of treatment. In contrast, neither MeJA nor ACC treatments altered the transcript level of FEH genes (Fig.III-19). Since the transcript level of the defense marker genes and the FEHs genes were strongly induced after 12 h of root treatment, the following experiments were carried out using plants treated for 12 h. The repetition of this experiment

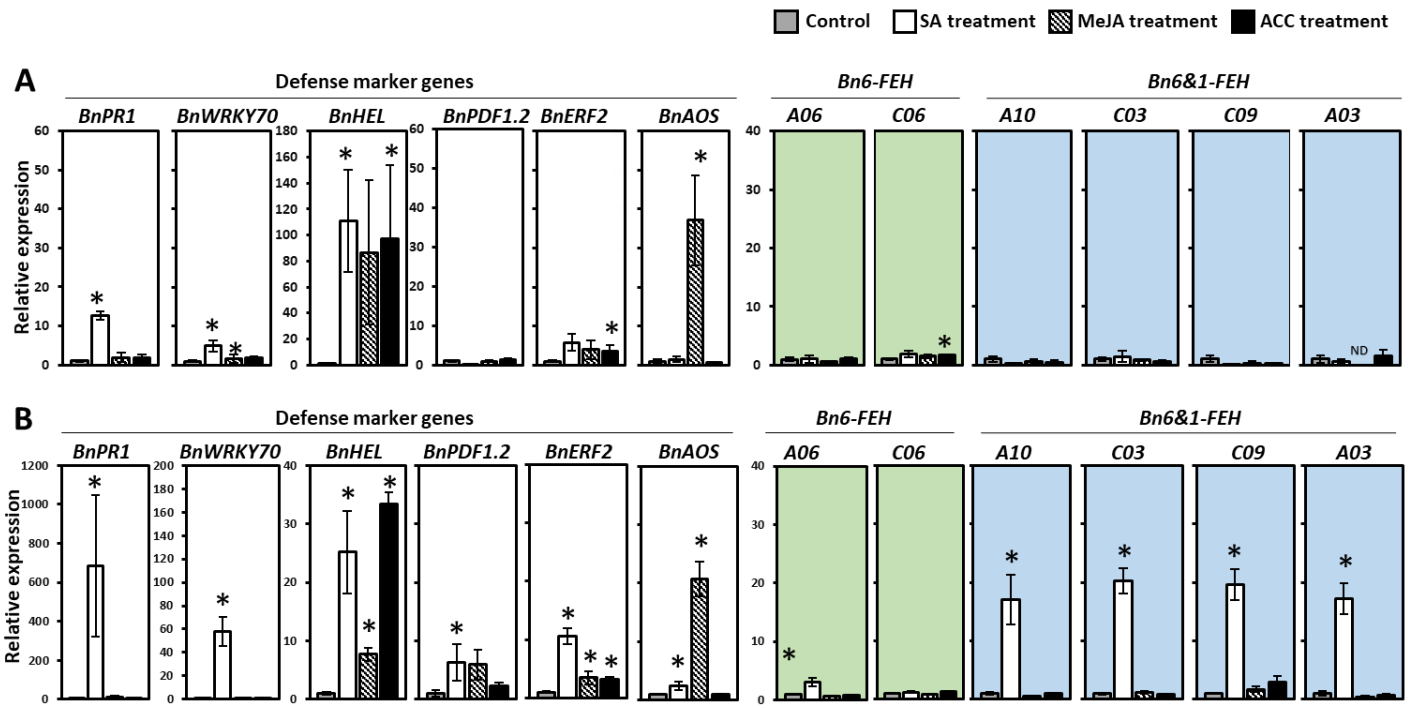

Figure III-20. Phytohormone treatments increased the expression of some defense-marker and FEH genes in B. napus roots and shoots.

Relative expression of defense marker genes (BnPR1, BnWRKY70, BnHEL, BnDPF1.2, BnERF2, BnAOS) an FEH genes (Bn6-FEH_A06; Bn6-FEH_C06; Bn6&1-FEH_A10; Bn6&1-FEH_C09; Bn6&1-FEH_C03 and Bn6&1-FEH_A03) in B. napus cv. 'Tenor' shoots (A) and roots (B) after 12 hours of treatment with 0.5 mM salicylic acid (SA), 50 µM methyl jasmonate (MeJA) or 20 µM 1-Aminocyclopropane-1-carboxylic acid (ACC). For each gene, the data were normalized against the control plant sampled after 12 h of treatment. Each data point is the average of five independent biological replicates and the bars indicate the standard errors. The asterisk indicates a statistically significant difference between the treated plants and the control plants (Wilcoxon rank sum test; $p<0.05$).

with another independent set of plants treated with SA, MeJA, and ACC during 12 h gave similar results (Supplementary Fig.SIII-12).

To assess whether root treatments also altered gene expression in aerial parts of the plants, the transcript levels of the defense maker and the *FEH* genes were measured in both shoots (Fig.III-20A) and roots (Fig.III-20B) after 12 h of treatment with SA, MeJA or ACCh. The treatment of roots with SA increased the transcript level of *BnPR1* (13-fold) and *BnWRKY70* (5-fold) in shoots (Fig.III-20A) but with a much weaker effect than in roots (Fig.III-20B; 686-fold and 58-fold for *BnPR1* and *BnWRKY70*, respectively). In contrast, *BnHEL* expression was much more induced by SA in shoots (110-fold) than in roots (25-fold). The main effect of treating the roots with MeJA was an increase of the transcript level of *BnHEL* (87-fold) and *BnAOS* (37-fold) in shoots. The treatment of roots with ACC mainly increased the transcript level of *BnHEL* in shoots. These results indicate that in *B. napus, PR1* and *WRKY70* are SA-responsive marker genes, *AOS* a MeJA-responsive marker gene, and *HEL* a SA, MeJA and ACC-responsive marker gene. Unlike *PR1, WRKY70* and *HEL*, for which the SA treatment of the roots increased the level of expression in the shoots, the transcript level of the *FEH* genes did increase in response to SA in the shoots (Fig.III-20A). To compare the level of FEH gene expression with that of defense marker genes, the relative expression level of the different genes in the roots and shoots of the SA-treated plants were normalized to that of Bn6&1-FEH_C03 (Supplementary Fig.SIII-12). The data indicate that among defense marker genes, the highest expression level was that of PR1 in shoots and HEL in roots. Among FEH genes, the highest expression level in roots was that of Bn6&1-FEH_A10 which level was similar to that of BnPR1 (Supplementary FigSIII-12).

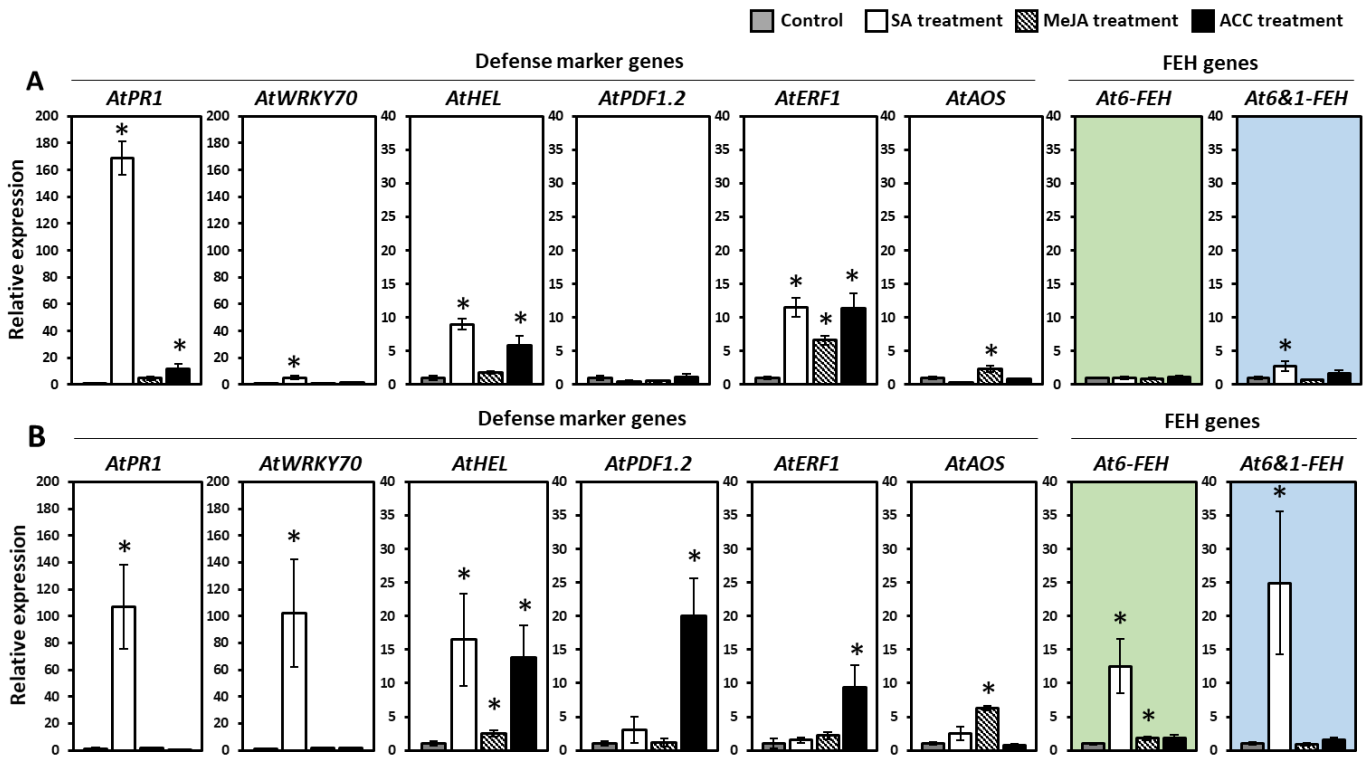

Figure III-21. Phytohormone treatments increased the expression of some defense-marker and FEH genes in A. thaliana roots and shoots.

Relative expression of defense marker genes (AtPR1, AtWRKY70, AtHEL, AtDPF1.2, AtERF1, AtAOS) and FEH genes (At6-FEH and At6&1-FEH) in A. thaliana (Col 0) shoots (A) and roots (B) after 12 hours of treatment with 0.5 mM salicylic acid (SA), 50 µM methyl jasmonate (MeJA) or 20 µM 1-Aminocyclopropane-1-carboxylic acid (ACC). For each gene, the data were normalized against the control plant sampled after 12 h of treatment. Each data point is the average of five independent biological replicates and the bars indicate the standard errors. The asterisk indicates a statistically significant difference between the treated plants and the control plants (Wilcoxon rank sum test; $p<0.05$).

Expression profiles of defense marker genes and FEHs genes in A. thaliana *after root treatment with SA, MeJA or ACC*

In order to determine whether the observed expression profile is species-specific, the expression of the homologous defense marker genes and FEH genes was measured in the shoots and roots of A. thaliana in response to 0.5 mM SA, 50µM MeJA or 20µM ACC applied to the roots (Fig.III-21A-B). As in B. napus, treatment of roots with SA increased the transcript level of AtPR1 (107-fold in roots and 169-fold higher in shoots), AtWRKY70 (102-fold in roots and 5-fold in shoots), and to a lesser extent AtHEL (14-fold in roots and 6-fold in shoots) and AtERF1 (12-fold in shoots) (Fig.III-20 and III-21). The main effect of treating roots with MeJA was an increase of the transcript level of AtERF1 (6.6-fold in shoots) and AtAOS (6.3-fold in roots and 2.4-fold higher in shoots). Unlike in B. napus, treatment with MeJA did not increase HEL expression in shoots, but as in B. napus slightly increased HEL expression in roots (Fig.III-20 and III-21). As in B. napus, treating the roots with ACC increased the transcript level of HEL (14-fold in roots and 5.8-fold in shoots) and ERF1 (9.4-fold in roots and 11-fold in shoots). Unlike in B. napus, treatment with MeJA strongly increased PDF1.2 in roots (20-fold higher) (Fig.III-20 and III-21). Overall, the results indicate that, as in B. napus, the three treatments applied at the root level of A. thaliana were able to elicit defense responses characterized by the induction of genes involved in the defense signaling or in the synthesis of antimicrobial peptides. Moreover, our results indicate that in A. thaliana, as in B. napus, PR1 and WRKY70 are root SA-responsive marker genes, *AOS* a root MeJA-responsive marker gene, and *HEL* a root SA, MeJA, and ACC-responsive marker gene (Fig.III-21).

The same samples were used to assess whether the treatments were able to induce the expression of *FEH* genes. *At6&1-FEH* transcript levels were higher in roots (25-fold) of plants treated with SA than in roots of control plants and to a lesser extent higher in shoots (2.7-fold) (Fig.III-21). *At6-FEH* transcript level was also up-regulated (12.5-fold) in roots of SA-treated plants. Neither of the two *FEHs* genes was affected by the MeJA or ACC treatment. To compare the level of *FEH* gene expression with that of defense marker genes, the relative expression level of the different genes in the roots and shoots of the SA-treated plants were normalized to that of *At6&1-FEH* (Supplementary Fig.SIII-13). The data indicate that among defense marker genes, the highest expression level was that of *PR1* in shoots and *HEL* in roots. Among *FEH* genes, the highest expression level in roots was that of *At6&1-FEH* which level was similar to that of *AtPR1*.

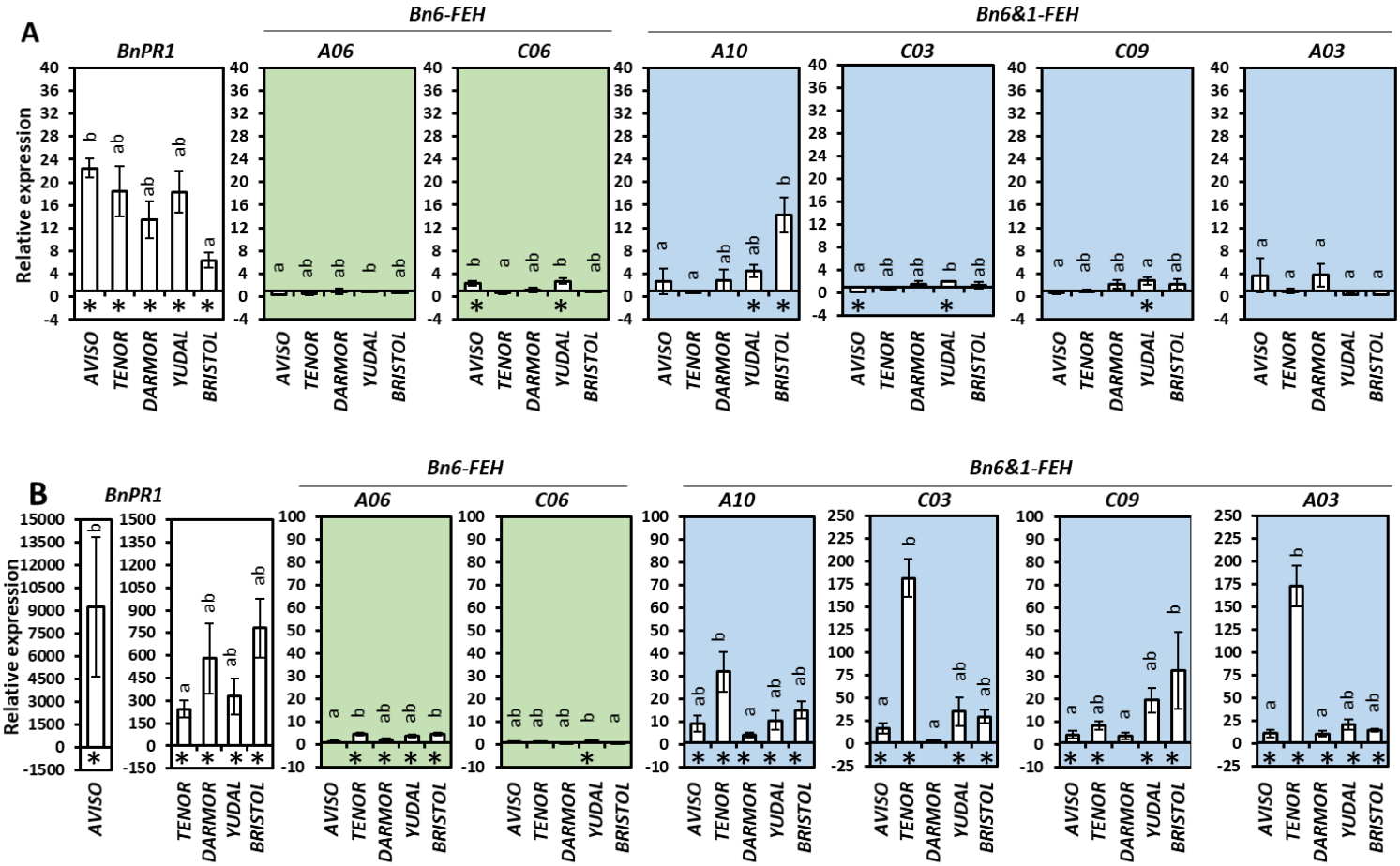

Figure III-22. The expression of defense-marker and FEH genes in B. napus roots after SA treatment differed among genotypes.

Relative expression of the defense marker PR1 and FEH genes (Bn6-FEH_A06; Bn6-FEH_C06; Bn6&1-FEH_A10; Bn6&1-FEH_C09; Bn6&1-FEH_C03 and Bn6&1-FEH_A03) in B. napus shoots (A) and roots (B) of five genotypes ('Aviso'; 'Tenor'; 'Darmor-bzh'; 'Yudal'; 'Bristol') after 12 hours of treatment with 0.5 mM salicylic acid (SA). For each gene, the data of each variety were normalized against the average of the control plant data. A value above 1 indicates an increase of the expression by SA while a value below 1 indicates a decrease of the expression by SA. Each data point is the average of five independent biological replicates and the bars indicate the standard errors. For each gene and genotype, the asterisk indicates a statistically significant difference between the treated plants and the control plants (Wilcoxon rank sum test; $p<0.05$). Different letters indicate statistically significant differences between genotypes (Kruskal-Wallis test followed by a multi-comparison post-hoc rank test; $p<0.05$).

Genetic variability of responses to SA applied at root level in B. napus

Since among the three phytohormones evaluated, only SA had an effect on the expression of *FEHs,* a treatment with SA applied at root level was used to assess the genetic variability of the *B. napus.* The expression profiles of the SA-responsive gene *PR1* and the *FEH* genes were followed in the roots and shoots of the five oilseed rape genotypes ('Aviso', 'Tenor', 'Darmor-*bzh'*, 'Yudal', 'Bristol') (Fig. III-22). Treatment with SA for 12 h led to the induction of *BnPR1* expression in shoots and roots of all genotypes tested, with a much stronger effect in roots (200 to 9000-fold) than in shoots (6 to 22-fold). The most SA-responsive genotype in both shoots and roots was 'Aviso'. The least SA-responsive genotypes were 'Tenor' for roots and 'Bristol' for shoots. However, the extent of the *BnPR1* response to SA was not very large, only the differences between the most reactive ('Aviso') and the least reactive genotype ('Bristol' in shoot and 'Tenor' in root) being statistically significants ($p<0.05$; Fig. III-22).

Bn6-FEH_A06 expression slightly increased in four genotypes ('Tenor', 'Darmo-*bzh'*, 'Yudal', and 'Bristol') in SA-treated roots but not in shoots. The expression of *Bn6-FEH_C06* was also slightly induced in roots of 'Yudal' and in shoots of 'Yudal' and 'Aviso'. Expression of the four genes coding for *Bn6&1-FEH* (*A10, C03, C09,* and *A03*) increased in SA-treated roots of all five genotypes, except *Bn6&1-FEH_ C03* and *C09* in 'Darmor-*bzh'*. Two of these four genes, *Bn6&1-FEH_C03* and *A03*, were strongly induced in the roots of 'Tenor' and showed great genotypic variability in their level of expression in roots, with 'Tenor' as a highly reactive genotype, 'Aviso', 'Yudal' and 'Bristol' as moderately reactive genotypes and 'Darmor-*bzh'* as non-reactive genotype. Similarly to *BnPR1, Bn6&1-FEHs* were much less induced in shoots than in roots. Among the four genes, *Bn6&1-FEH_A10* showed the highest induction by SA in 'Bristol' (14-fold). A principal component analysis (PCA) was performed to assess whether the expression profile could discriminate the five genotypes (Supplementary Fig.SIII-14). The first two axes accounted for 63.8 % of the total variance observed among genotypes. The relative expression in response to SA of *Bn6&1-FEH_A03, C03,* and *A10* were closely correlated with the first axis (Supplementary Fig.SIII-14A) with correlation coefficients of 0.89, 0.87, and 0.86, respectively ($p<10^{-7}$). *Bn6-FEH_A06* and *BnPR1* were also significantly correlated with the first axis but with lower coefficients (0.68 and -0.48 with $p<0.001$ and $<0.0.5$, respectively). Along the first axis, PCA confirms a strong distinction between 'Tenor' and the four other genotypes ('Aviso', 'Darmor-*bzh*,' 'Yudal', 'Bristol') (Supplementary Fig.SIII-14B). Of these four genotypes, 'Aviso' was separated from 'Bristol' along the second axis. This axis was negatively correlated with *Bn6&1-FEH_C09* (correlation coefficient of -0.78; $p<10^{-5}$) and positively correlated with *BnPR1* relative expression (correlation coefficient of 0.53; $p<0.01$).

Overall, the PCA analysis highlights four different expression profiles of *PR1* and *FEH* genes in response to root SA treatment, i) a strong induction of *PR1* associated with a low induction of *FEHs* ('Aviso'), ii) a weak induction of *PR1* associated with a strong induction of *FEHs* ('Tenor'), iii) a strong induction of *Bn6&1FEH_C09* ('Bristol') and iv) a weak induction of *PR1* and *FEH* ('Yudal', 'Darmor-*bzh'*).

Discussion

Identification of root defense marker genes in two Brassicaceae

Over the past decade, many studies reported the induction of plant defense responses against pathogens through the use of exogenous phytohormone application (*i.e.* SA, JA and ET). These studies were mainly based on the changes in the level of expression of defense marker genes after phytohormone application at the leaf level, while data are still scarce after phytohormone application at root level (Papadopoulou *et al.*, 2018). In the present study, roots of *B. napus* and *A. thaliana* were treated with SA, MeJA and a precursor of ET. The expression of defense marker genes was monitored not only in roots but also in shoots in order to assess the systemic response to phytohormone treatments.

As expected, a strong induction of the expression of the well known SA-responsive genes *PR1* and *WRKY70* (Li *et al.*, 2004; van Loon *et al.*, 2006) was observed in *B. napus* and *A. thaliana* roots after 12 h of SA treatment at the root level. Together with the absence of their induction following MeJA and ACC treatments, the results show that *PR1* and *WRKY70* correspond to specific SA-sensitive marker genes in roots of *B. napus* and *A. thaliana*. Similar induction of *PR1* and *WRKY70* was reported in the leaves of *B. napus* (Wang *et al.*, 2012) and *A. thaliana* (Lemarié *et al.*, 2015; Zhang *et al.*, 2020) treated with SA at the leaf level. Here, the fact that treatment of SA at root level also increased the expression of these two genes in shoots reveals a systemic response in distal tissues most likely through a long-distance transport of SA or SA-conjugates (Kawano and Bouteau, 2013).

Exogenous supply of MeJA at root level induced the expression of *AOS*, which codes for the allene oxide synthase involved in JA biosynthesis. The induction was very strong in roots and shoots of *B. napus*. A similar up-regulation of *AOS* expression was reported in *B. napus* MeJA-treated leaves (Wang *et al.*, 2012). An induction of *AOS* expression was also reported in leaves of *A. thaliana* treated with MeJA (Jost *et al.*, 2005). Here, the MeJA treatment of *A. thaliana* at root level increased *AOS* expression in roots and in shoots. *AOS* expression in both species was not induced by ACC and only slightly induced by SA in *B. napus*. All together, these results

demonstrated that *AOS* is a suitable JA-sensitive marker gene in roots of *B. napus* and *A. thaliana*.

ET response factors (ERF) constitute a family of plant-specific transcriptional factors which play important roles in response to biotic and abiotic stresses (Huang *et al.*, 2016). Particularly, ERF1 has been confirmed as a regulator of ET responses after pathogen attack in *A. thaliana* (Berrocal-Lobo *et al.*, 2002). As expected, the treatment at root level with ACC, a precursor of ET synthesis, increased the transcript level of *ERF1* in roots and shoots of *A. thaliana*. A similar increase of *ERF1* expression was reported after ACC treatment at root level in seedlings of *A. thaliana* (Mao *et al.*, 2016) and in roots of *Brassica rapa* treated with ethephon, another ET precursor (Papadopoulou *et al.*, 2018). In *B. napus*, ACC treatment at root level induced the expression of *BnERF2* inroots ans in shoots. These *ERF* genes were also reported to be induced by JA treatment at root level in *B. napus* (*BnERF2*, in roots and in shoots) and in *A. thaliana* (*AtERF1*, in shoots but not in roots) (Lorenzo *et al.*, 2003). However, other experiments have shown that is not always the case. Indeed, MeJA-treatment at leaf level down-regulated *AtERF1* expression in shoots of *A. thaliana* (Caarls *et al.*, 2016) and MeJA-treatment at root level decreased *BrERF1* expression in roots of *B. rapa* (Papadopoulou *et al.*, 2018). Interestingly, these two genes (*BnERF2* and *AtERF1*) were also induced after root treatment by SA. This was not the case in *B. rapa* treated with SA at shoot or root level (Papadopoulou *et al.*, 2018) while similar *AtERF1* induction was observed after SA-treatment at leaf level (Caarls *et al.*, 2016). These contrasting results indicate that the regulation of ERFs by exogenous phytohormones depends not only on the *ERF* gene considered (Caarls *et al.*, 2016) but also on the species and of the treated tissue. Moreover, this induction of *BnERF2* and *AtERF1* by SA, MeJA and ACC support the hypothesis of the role of these ERFs in the cross-talk of SA and ET/JA signaling pathways (Li *et al.*, 2019) in *B. napus* (*BnERF2*) and *A. thaliana* (*AtERF1*).

HEL codes for a protein with antimicrobial activity (Hevein-like protein also known as PR4; Bertini *et al.*, 2012). We observed a strong induction of *BnHEL* and *AtHEL* in roots and shoots following the SA and ACC treatments at root level and also, but to a lesser extent, following the MeJA treatment. Conversely, in the leaves of *A. thaliana*, Norman-Setterblad *et al.* (2000) showed that *HEL* was up-regulated by ET but not by SA or JA, while in *B. napus* leaves, *HEL* expression was induced by MeJA but not by SA (Wang *et al.*, 2012). This suggests that *HEL* regulation depends on the location of signal perception (roots versus shoots). The induction of *HEL* observed in *B. napus* and *A. thaliana* following the supply at root level of each of the three main defense phytohomones indicates that *HEL* can be considered as a generic marker gene of defense response in the roots.

While MeJA treatment of *B. napus* at leaf level strongly increased the expression of the plant defensin *BnPDF1.2* (Wang *et al.*, 2012), MeJA treatment at root level had no significant effect on *BnPDF1.2* expression in roots. Contrary to its down-regulation in leaves by SA treatment at leaf level (Wang *et al.*, 2012), the expression of *BnPDF1.2* in roots was induced by SA treatment at root level. In *A. thaliana*, treatment at root level with ACC but not MeJA strongly increased the expression of *AtPDF1.2* in roots, as already reported by Norman-Setterblad *et al.* (2000). Expression of *AtPDF1.2* was induced by a treatment at leaf level with MeJA and ET (Penninckx *et al.*, 1998) and repressed by SA (Koornneef *et al.*, 2008). Thus, *PDF1.2* regulation seems to depend on the location of signal perception (roots versus shoots) and on the species.

Altogether, our results indicate that the regulation of gene expression by exogeneous phytohormone treatment in the aerial parts of the plants can not be extrapolated to the root system. Only three of the defense marker genes studied (*PR1*, *WRKY70* and *AOS*) displayed similar responses after root treatments (present results) and after leaf treatments (literature data). *PR1* et *WRKY70* can then be considered as specific marker genes of SA signaling pathway and *AOS* as a specific marker of MeJA signaling not only in shoots but also in roots of both *Brassicaceae*. The three other defense marker genes (*ERF1/ERF2*, *HEL* and *PDF1.2)* were differently regulated by phytohomones depending on whether they are applied to the roots (our results) or to the leaves (literature data). *AtPDF1.2* and *AtERF1* can be used as specific marker genes of ET signaling pathway in roots of *A. thaliana. HEL*, which was up-regulated by the three defense phytohormones, seems to be a suitable generic marker of root defense responses in both *Brassicaceae*.

Up-regulation of At6&1FEH *and* Bn6&1FEH *by SA is in favor of their role in plant defense.*

The effect of the phytohormone treatments was assessed by measuring the transcript levels of genes coding for putative FEHs in *B. napus* (four genes coding for *Bn6&1-FEH* and two genes coding for *Bn6-FEH*) and FEHs in *A. thaliana* (*At6&1-FEH* and *At6-FEH*, De Coninck *et al.*, 2005). Among the three phytohormones evaluated, only SA had an effect on the expression of *FEHs*. Its exogenous application to the roots of *B. napus* increased the relative expression of the four genes coding for proteins with putative 6&1-FEH activity and of one of the two genes coding for proteins with putative 6-FEH activity. In *A. thaliana*, *At6&1-FEH* and *At6-FEH* were also specifically induced by SA. Interestingly, the relative amount of *Bn6&1-FEH_A10* transcripts after 12h of root SA treatment was at a similar level to that of *BnPR1* in the roots of *B. napus*. Similarly, after 12 h of treatment with SA, the relative amount of *At6&1-FEH* transcripts was at the same level as that of *AtPR1* in the roots of *A. thaliana*.

The fact that SA treatment at root level strongly up-regulated all *6&1-FEHs* together with *PR1* and *HEL*, two well-known pathogen-induced antimicrobial proteins, and *WKRY70*, a marker of SA-mediated signaling, in the five varieties of *B. napus* and in the model species *A. thaliana*, clearly supports the role of FEHs as defense proteins in non-fructan plants. In *B. napus*, the similarity between the kinetics of induction of genes coding for FEHs and for the defense proteins PR1 and HEL reinforces this hypothesis. As it is generally accepted that SA is involved in resistance to biotrophic pathogens while JA is more specific to the activation of defenses against insect herbivores and necrotrophic pathogens (Caarls *et al.*, 2015), the fact that *6&1FEHs* were up-regulated by SA but not MeJA suggests that 6&1FEHs are involved in interactions with plant pathogens displaying a biotrophic lifestyle. The comparison of *PR1* and *FEH* regulation by SA in five genotypes of *B. napus* ('Aviso', 'Tenor', 'Darmor-*bzh*', 'Yudal', 'Bristol') highlighted different expression profiles. 'Aviso' displayed a strong *PR1* induction associated with a weak *FEH* induction, 'Tenor' a weak PR1 induction associated with a strong FEH induction while in 'Yudal' and 'Darmor-*bzh'* the expression of *PR1* and *FEHs* was almost not affected by SA. This underlines a genotypic variability of FEH regulation in *B. napus* that could lead to different susceptibility to fructan synthesizing pathogens and raise breeding possibilities on this character.

Conclusions

Present results show that the regulation of defense-related genes by exogenous phytohormone supply at the leaf level cannot be generalized to phytohormone treatments at root level confirming that defense signaling differed between roots and shoots (Millet *et al.*, 2010; Mauch-Mani *et al.*, 2017). Furthermore, we demonstrated that in *A. thaliana* and *B. napus* roots, *6-FEH* and *6&1-FEH* genes are SA-responsive genes strongly suggesting that they are involved in defense responses and that the proteins derived from their expression correspond to root defense proteins. Thus, these results support the hypothesis that FEHs identified in non-fructan plants are involved in plant-microorganism interactions and may constitute, together with some cell-wall invertases, a new family of pathogenesis-related (PR) proteins (Roitsch *et al.*, 2003; van Loon *et al.*, 2006). FEHs may play a specific role in these interactions through the production of MAMPs from microbial fructans and/or through the weakening of bacterial biofilm (Van den Ende *et al.*, 2003). Since FEH activity can release fructose and FOS, their role in plant defense suppose that these sugars act as elicitors of defense responses reducing the severity of pathogen attack. This has been demonstrated in different species (Bolouri-Moghaddam and Van den Ende, 2012; Versluys *et al.*, 2017). This hypothesis is also supported by the transient

upregulation of *At6&1FEH* during the early phase of root infection by *Phytophthora parasitica* (Le Berre *et al.*, 2017). The fact that the corresponding knockout mutant did not show a higher susceptibility than the wild type (Le Berre *et al.*, 2017) suggests that At6-FEH could compensate for the absence of 6&1FEH. To properly assess the role of FEHs in plant defense, *At6-FEH_6&1FEH* double knockout mutants will be produced and challenged by fructan-producing rhizospheric microorganisms.

Acknowledgments

We thank the BrACySol biological resource center (INRAE Ploudaniel, France) for providing the seeds used in this study. We also thank Julie Fremont, Anne-Françoise Ameline and Théophile Modéna (EVA laboratory) for their very valuable technical assistance.

Author contributions

TNHN, LL, MV, MPP and AMB conceived and designed the experiments; MMD and AG chose the *B. napus* genotypes; MPP, MMD and AG identified the genes coding putative FEH in *B. napus*, TNHN and LL performed the experiment; TNHN, AMB and MPP analysed the data; TNHN wrote the first draft, AMB, MPP, MMD, and MV edited and improved the manuscript.

Funding

This work was supported by the Universities of Caen and Rouen Normandie and by the Normandie Council through the research project EPURE (Enhancing Plant nutRition and Health, 2017-2019. Hanh Nguyen received a PhD grant (2018-2021) from the Normandie Council.

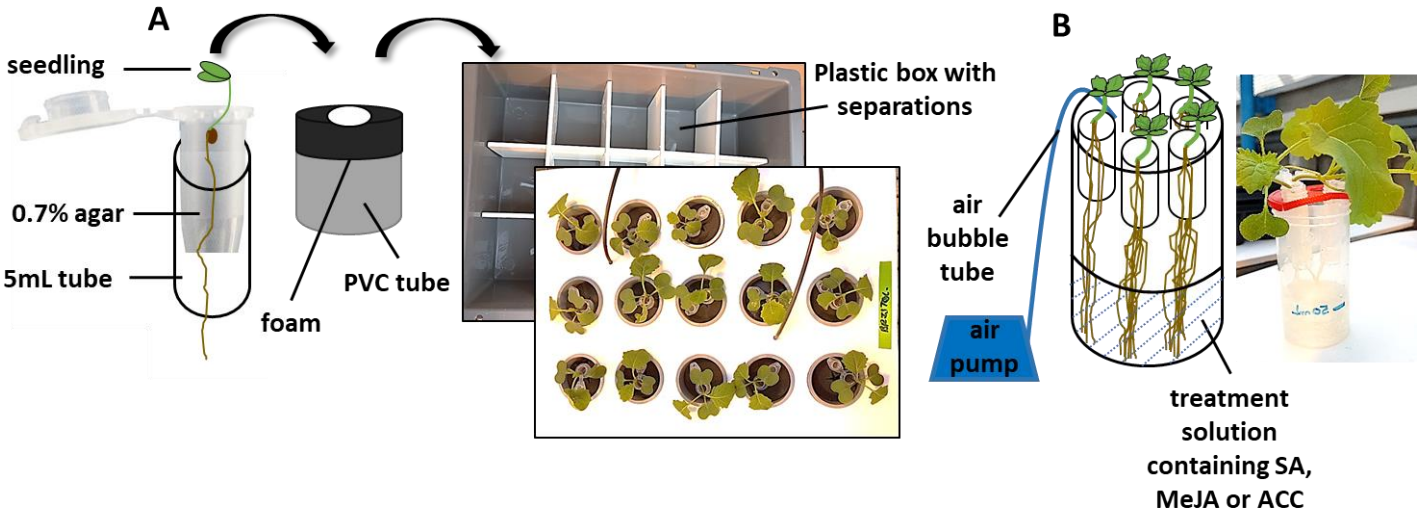

Figure S III-9. Experimental design for seedling production and plant screening.

(A) After being soaked for 48 hours at 4°C in 0.1% (w:v) agar solution, the seedlings were grown for 2.5 weeks in a hydroponic system at 21°C with 16h of light and 8h of dark period. (B) Treatment of plant after 18 days of growth in 150mL pots (five plants per pot) with 50 mL of nutrient solution containing the phytohormone (0,5 mM salicylic acid (SA), 50 µM methyl jasmonate (MeJA) or 20 µM 1-Aminocyclopropane-1-carboxylic acid (ACC) for 3, 6, 12, and 24 h. The shoots and the roots were harvested separately, stored at -80°C before ARN or protein extraction.

Table S III-2. P-values from Wilcoxon test for comparisons of the treated versus control samples for each gene and each sampling time.

Values in red correspond to gene expression above the control with p-values < 0.05. Values in green correspond to gene expression below the control with p-values < 0.05.

			Sampling time			
	Gene	Treatment	3h	6h	12h	24h
Defense marker genes	*BnPR1*	SA	0.06	**<0.05**	**<0.01**	**<0.01**
		MeJa	1.00	0.55	0.07	0.09
		ACC	0.69	0.55	0.06	0.21
	BnWRKY70	SA	**<0.01**	**<0.01**	**<0.01**	**<0.01**
		MeJa	**<0.01**	**<0.01**	**<0.01**	**<0.01**
		ACC	0.84	**<0.05**	0.42	0.09
	BnHEL	SA	**<0.01**	**<0.01**	**<0.01**	**<0.01**
		MeJa	**<0.01**	**<0.01**	**<0.01**	**<0.05**
		ACC	**<0.05**	**<0.01**	**<0.01**	**<0.01**
	BnPDF1.2	SA	0.67	0.30	**<0.05**	0.84
		MeJa	0.40	0.54	0.06	0.15
		ACC	0.40	0.22	0.15	0.83
	BnERF2	SA	**<0.01**	**<0.01**	**<0.01**	**<0.01**
		MeJa	0.30	0.09	**<0.01**	1.00
		ACC	**<0.01**	**<0.01**	**<0.01**	**<0.01**
	BnAOS	SA	**<0.01**	**<0.01**	**<0.01**	**<0.01**
		MeJa	**<0.01**	**<0.01**	**<0.01**	**<0.01**
		ACC	**<0.01**	**<0.01**	0.42	**<0.01**
FEH genes	*Bn6-FEH_A06*	SA	0.54	**<0.01**	**<0.01**	**<0.01**
		MeJa	**<0.01**	**<0.01**	**<0.01**	**<0.05**
		ACC	0.15	0.69	0.15	0.22
	Bn6-FEH_C06	SA	0.15	0.84	0.22	0.09
		MeJa	**<0.05**	0.30	0.06	0.22
		ACC	0.09	0.15	0.06	**<0.01**
	Bn6&1FEH_A10	SA	**<0.01**	**<0.01**	**<0.01**	**<0.01**
		MeJa	**<0.05**	**<0.05**	**<0.05**	**<0.05**
		ACC	0.22	0.54	0.84	0.15
	Bn6&1FEH_C03	SA	**<0.01**	**<0.01**	**<0.01**	**<0.01**
		MeJa	0.42	0.84	0.54	0.84
		ACC	0.60	1.00	0.42	0.42
	Bn6&1FEH_C09	SA	**<0.05**	**<0.01**	**<0.01**	**<0.01**
		MeJa	0.84	1.00	0.54	0.42
		ACC	0.67	**<0.05**	0.15	0.09
	Bn6&1FEH_A03	SA	**<0.01**	**<0.01**	**<0.01**	**<0.01**
		MeJa	0.42	0.09	0.29	**<0.05**
		ACC	0.34	0.15	0.42	0.15

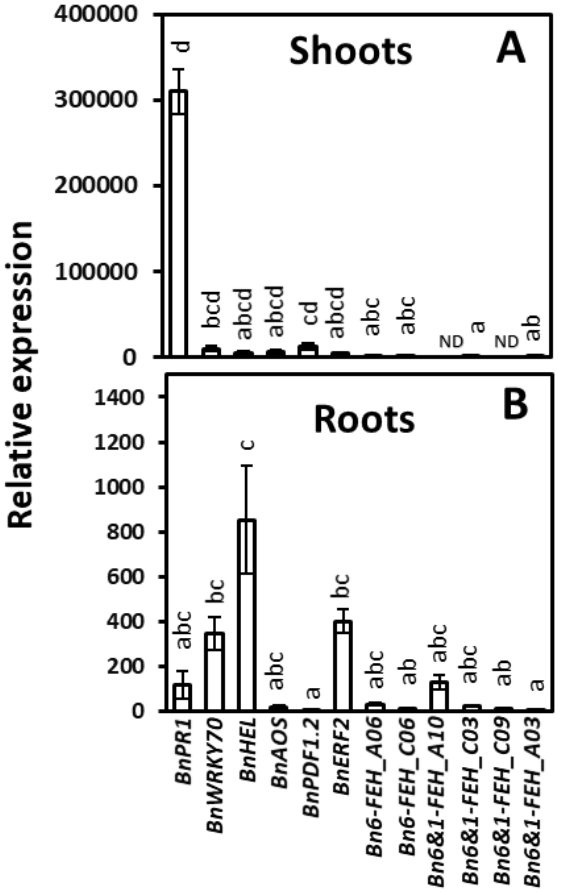

Figure S III-11. Relative expression of genes in B. napus cv. 'Tenor' shoots (A) and roots (B) after 12 hours of treatment with SA.

Data are the same as in Fig.2 but were normalized against the relative expression level of Bn6&1-FEH_C03 in shoots. Defense marker genes: BnPR1, BnWRKY70, BnHEL, BnDPF1.2, BnERF2, BnAOS. FEHs genes: Bn6-FEH_A06; Bn6-FEH_C06; Bn6&1-FEH_A10; Bn6&1-FEH_C09; Bn6&1-FEH_C03 and Bn6&1-FEH_A03. Shoots and roots were sampled after 12 hours of treatment with 0.5 mM salicylic acid (SA). Each data point is the average of five independent biological replicates and the bars indicate the standard errors. ND, not detected. Different letters indicate statistically significant differences between genes (Kruskal-Wallis test followed by a multi-comparison post-hoc rank test; p<0.05).

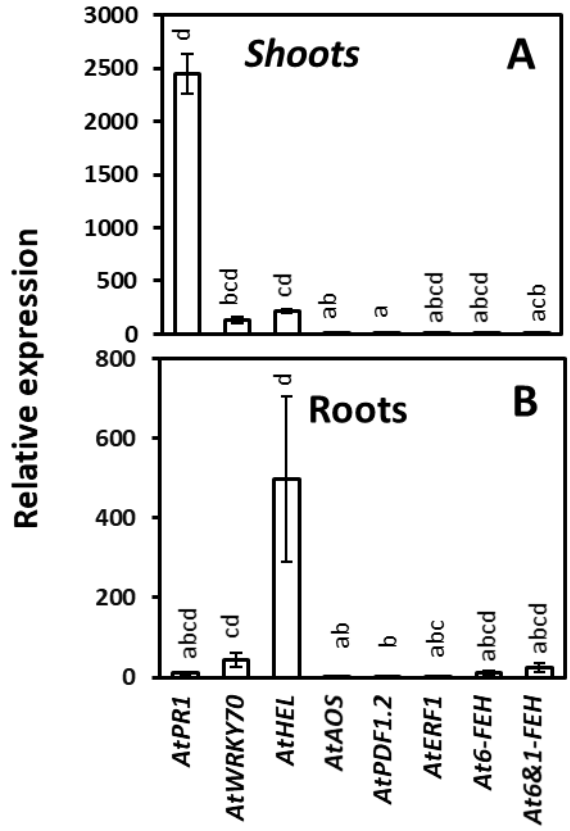

Figure S III-10. Relative expression of genes in A. thaliana shoots (A) and roots (B) after 12 hours of treatment with SA. Data are the same as in Fig.3 but were normalized against the relative expression level of At6&1-FEH in shoots. Defense marker genes: AtPR1, AtWRKY70, AtHEL, AtDPF1.2, AtERF1, AtAOS. FEHs genes: At6-FEH and At6&1-FEH. Shoots and roots were sampled after 12 h of treatment with 0.5 mM salicylic acid (SA). Each data point is the average of five independent biological replicates and the bars indicate the standard errors. Different letters indicate statistically significant differences between genes (Kruskal-Wallis test followed by a multi-comparison post-hoc rank test; p<0.05).

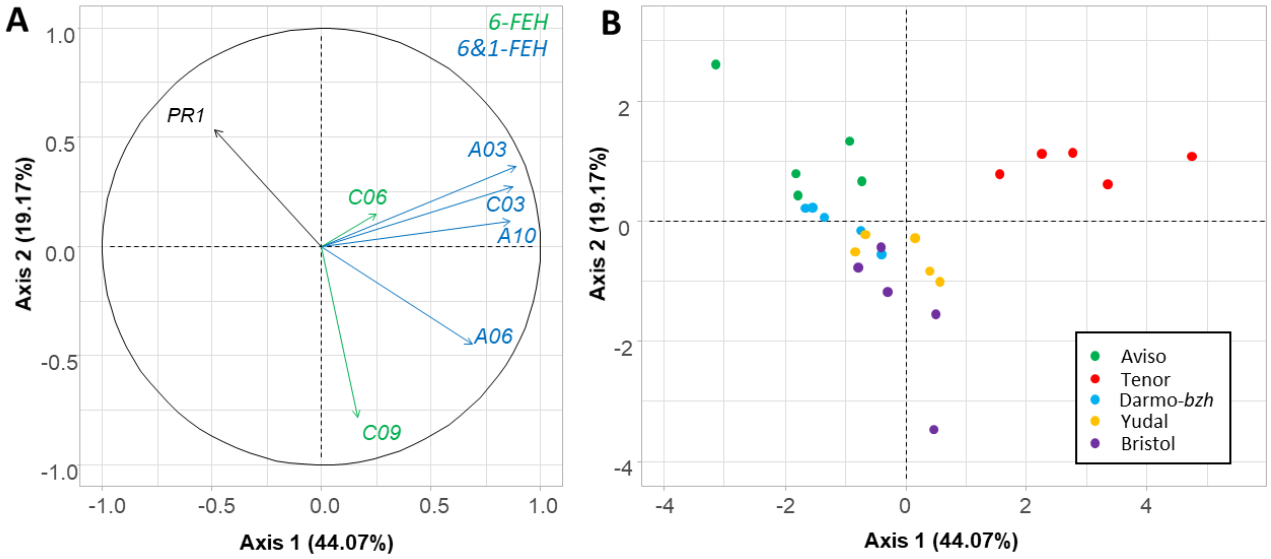

Figure S III-12. Principal component analysis performed with the relative expression of the defense marker BnPR1 and of the six FEHs genes

(Bn6-FEH_A06; Bn6-FEH_C06; Bn6&1-FEH_A10; Bn6&1-FEH_C09; Bn6&1-FEH_C03 and Bn6&1-FEH_A03) in B. napus roots after 12 hours of treatment with 0.5 mM SA for five genotypes ('Aviso', 'Tenor', 'Darmor-bzh', 'Yudal', 'Bristol') with five biological replicates for each genotype (n=25). A: graph of variables. B: graph of individuals.

Table S III-3. Primers used for qRT-PCR in this study.

F: forward; R: reverse. Bn: B. napus genes and At: A. thaliana genes.

Function		Gene name	Protein name	Accession	Primer sequence (5' to 3')	Reference for primers
Reference genes for RT-qPCR		*BnGAPDH*	Glyceraldehyde 3-phosphate dehydrogenase	FJ529182	Forward : CGCTTCCTTCAACATCATTCCCA Reverse : TCAGATTCCTCCTTGATAGCCTT	*Alkooranee et al.*, 2017
		BnEF1	Elongation factor 1	DQ312264	Forward: GCCTGGTATGGTTGTGACCT Reverse: GAAGTTAGCAGCACCCTTGG	*Nicot et al.*, 2005
		AtEF1α	Elongation factor 1- α	AT5G60390	Forward: CTGGAGGTTTTGAGGCTGGTAT Reverse: CCAAGGGTGAAAGCAAGAAGA	*Baud et al., 2003*
		AtActin	Actin constitutively expressed in vegetative tissues	AT3G18780	Forward: GCCATCCAAGCTGTTCTCTC Reverse: CCCTCGTAGATTGGCACAGT	*Pontier et al., 2005*
Defense marker genes	Antimicrobial protein SA responsive	*BnPR1*	Pathogenesis-related 1	AY623008	Forward: ATGCCAACGCTCACAACCA Reverse: CACGGGACCTACGCCTACT	*Wang et al.*, 2012
		AtPR1		AT2G14610	Forward: TTCTTCCCTCGAAAGCTCAA Reverse: AAGGCCCACCAGAGTGTATG	*Zhang et al.*, 2020
	Transcription factor SA responsive	*BnWRKY70*	Proteins with the highly conserve WRKY domain	EV113862	Forward: ACATACATAGGAAACCACACG Reverse : ACTTGGACTATCTTCAGAATGC	*Wang et al.*, 2012
		AtWRKY70		AT3G56400	Forward: CATGGATTCCGAAGATCACA Reverse: CTGGCCACACCAATGACAA	*Li et al.*,2013
	Antimicrobial peptides JA and ET responsive	*BnPDF1.2*	Plant Defensin 1.2	AY884023	Forward : CATCACCCTTCTCTTCGCTGC Reverse : ATGTCCCACTTGACCTCTCGC	*Wang et al.*, 2012
		AtPDF1.2		AT2G26020	Forward: ACCAACAATGGTGGAAGCAC Reverse : CACTTGTGAGCTGGGAAGAC	*Attard et al.*, 2010
	JA biosynthesis gene	*BnAOS*	Allene Oxide Synthase	EV124323	Forward: CGCCACCAAAACAACAAAG Reverse: GGGAGGAAGGAGAGAGGTTG	*Wang et al.*, 2012
		AtAOS		AT5G42650	Forward: ACTACGGTTTACCAATCGTAGGAC Reverse: TCTGTACACCGTGGAGTTGTATTT	*Matsuoka et al.*,2018
	Antimicrobial protein JA and ET responsive	*BnHEL*	Hevein-Like protein	FG577475	Forward : GGAACACAAGGACTAATGC Reverse : TTTCGATAGCCATCACCA	*Wang et al.*, 2012
		AtHEL		AT3G04720	Forward: TAGTGGACCAATGCAGCAAC Reverse : GATCAATGGCCGAAACAAG	*Attard et al.*, 2010
	Ethylene signaling transcription factor	*BnERF2*	Ethylene response transcription factor	FJ788940	Forward: GGAAATTCGCGGCGGAGAT Reverse : GGAACCACGCATCCTAAAAG	*This study*
		AtERF1		AT3G23240	Forward: ATTCTTTCTCATCCTCTTCTTCT Reverse : CGAATCTCTTATCTCCGCCG	*Mao et al.*, 2016
Fructan exohydrolase (FEH) genes	Hydrolysis of both β(2,6) and β(2,1) linkages of fructans	*Bn6&1-FEH_A03*	6&1-FEH	BnaA03G03670D	Forward: CCCTTTAGCTCCAGAGTTCA Reverse: TTCCGGTGTACAAGATCACA	*This study*
		Bn6&1-FEH_A10		BnaA10G20680D	Forward: TAACTTGGCTCCCCGATTCA Reverse: GTCCAGTGTATAGAATTACC	
		Bn6&1-FEH_C03		BnaC03G05170D	Forward: GTACACCGGAAGCGACACCA Reverse : TACTAGGTGGAACCATAACA	
		Bn6&1-FEH_C09		BnaC09G44700D	Forward: CAGTAATTCTCTACACTGGAC Reverse: TGGTAATAGAAACCGGGAAA	
		At 6&1-FEH		AT5G11920	Forward : TTACGGGCCTTTTGGATTGC Reverse : TCGCTGCTGCACATTACAAC	
	Hydrolysis of β(2,6) linkages of fructans	*Bn6-FEH_A06*	6-FEH	BnaA06G00510D	Forward: AAGACTTAACCGGAATGTGG Reverse: AACGTCTCGATCAAACTAAC	
		Bn6-FEH_C06		BnaC06G07120D	Forward: AGGAGTTAACCGGAATGTGG Reverse: AACGTCTCGATCAAACTCAT	
		At 6-FEH		AT1G55120	Forward : ATTGAGAAGGGTTGGTCTGGTC Reverse : TTGCCAGTTGACTTGTTGCC	

4. Involvement of bacterial levans and plant fructan exohydrolases (FEHs) in *Arabidopsis thaliana* root colonization by *Pseudomonas brassicacearum*

Abstract

Fructans are fructose polymers present in some plants and microorganisms including beneficial or pathogenic bacteria. In bacteria, fructans are mainly levans which are synthesized by levansucrases and are the exopolysaccharides. Fructan exohydrolases (FEHs) have been found in several non-fructan-accumulating plant species including *Arabidopsis thaliana.* Their discovery has led to the hypothesis that they could act as defense-related proteins in plant-bacteria interactions by hydrolyzing bacterial extracellular levans which form a protective layer and thereby produce fructo-oligosaccharide elicitors. To test this hypothesis, the interaction between the non-fructan-accumulating plant *A. thaliana* and the beneficial levan-producing bacteria *Pseudomonas brassicacearum* was investigated by using *A. thaliana* Col-0 and FEH knock-out mutants inoculated with *P. brassicacearum,* wild-type (NFM421), and the corresponding levansucrase deletion mutant (*Δlev*). Strong inhibition of primary root growth and stimulation of lateral root production was observed in *A. thaliana* Col-0 inoculated with NFM421. When Col-0 was inoculated with *Δlev*, root colonization was increased 3-fold and the root morphological changes tended to be stronger, indicating that the presence of levans did not facilitate the root colonization. Root morphological changes induced NFM421were stronger in all five FEH knockout mutants Col-0, indicating that the deletion of one of the two FEHs (*At6-FEH* or *At6&1-FEH*) reduce plant defense response. These preliminary results confirm the role of bacterial levans in plant-bacteria interaction and support the hypothesis of the involvement of plant FEHs in this interaction by acting directly on bacterial levans and/or by modulating sugar signaling. To confirm these results, *6-feh/6&1feh* double- mutants will be produced and challenged by fructan-producing rhizospheric microorganisms.

Introduction

Fructans are fructose polymers present in more than 15% of Angiosperms (Hendry, 1993) and in microorganisms, such as beneficial (*Gluconacetobacter diazotrophicus*; Hernández et al., 2000) or pathogenic bacteria (*Erwinia amylovora*; Öner et al., 2016) and fungi (*Aspergillus* and *Rhodotorula*; Trollope et al., 2015). In bacteria, fructans are mainly levans which are synthesized by extracellular levansucrases (EC 2.4.1.10) belonging to the GH68 family (Cantarel et al. 2009; Lammens et al., 2009). Levansucrases catalyze different reactions including the hydrolysis of sucrose, the synthesis of 6-kestotriose from sucrose, and the polymerization of levans using sucrose as a fructosyl donor (Martínez-Fleites et al., 2005).

Bacterial fructans are thus part of the exopolysaccharides (EPS) that contribute to biofilm formation, an assembly of microorganisms adhering to each other and/or to a surface and embedded in an EPS matrix (Morris and Monier, 2003; Velázquez-Hernández et al., 2009; Lembre et al., 2012; Dogsa et al., 2013). Interestingly, enzymes that hydrolyze fructans have been found in several non-fructan-accumulating plant species, *i.e. Beta vulgaris* (Van den Ende et al., 2003), *Arabidopsis thaliana* (De Coninck et al., 2005), and *Zea mays* (Zhao et al., 2019, Huang et al., 2020; Wu et al., 2021). They are fructan exohydrolases (FEHs) belonging to the GH32 family that hydrolyze the *O*-glycosidic linkage of the fructosyl unit at the end of fructan to release fructose (Lammens et al., 2009). In *A. thaliana*, the two FEHs were originally identified as invertases, AtcwINV3 and AtcwINV6 (cell wall invertase 3 and 6) based on the analysis of their amino acid sequences. Their functional characterization using heterologous expression in the yeast *Pichia pastoris* shows that these FEHs hydrolyze β-(2,6) (AtcwINV3) or both β-(2,1) and β-(2,6) linkages (AtcwINV6) (De Coninck et al., 2005). They were thus re-named At6-FEH and At6&1FEH, respectively.

The discovery of FEHs in non-fructan accumulating plants has led to the hypothesis that they could act as defense-related proteins in plant-microorganism interactions (Van den Ende et al., 2004) by hydrolyzing levan-containing slimes surrounding endophytic or phytopathogenic bacteria such as *Pseudomonas* or *Erwinia* (Hettwer et al., 1995; Bereswill et al., 1997). Indeed, levans form a separating layer between bacteria and plant cell wall polymers which prevents the plant to recognize the pathogen during the early stages of plant-pathogen interaction, (Hettwer et al., 1995). The disruption of the levansucrase gene in *Erwinia amylovora* (the fire blight agent of the *Pomoideae*) delayed the onset of symptoms in pear, indicating that the synthesis of levans increases the virulence of the bacteria by the formation of a protective layer which prevents the plant from perceiving the presence of bacteria (Geier and Geider, 1993; Koczan et al., 2009). Thus, plant FEHs could have a crucial role by preventing levan formation and consequently reducing pathogen infection (Van den Ende et al., 2004). Moreover, Van den Ende et al. (2004) suggested that plant FEHs could be involved in stabilizing symbiosis occurring between plants and fructan-producing beneficial bacteria such as in sugar beet (Tallgren et al., 1999) or sugar cane (Hernández et al., 2000). In addition, FEHs could play a role in plant-microorganism interactions by contributing to the production of the fructo-oligosaccharides from microbial fructans which act as elicitors triggering plant defense response (Versluys et al., 2017). Indeed, the pre-application of fructo-oligosaccharides reduced the impact of *Colletotrichum orbiculare* infection in cucumber (Zhang et al., 2009) and the infection caused by *Botrytis cinerea* in *Lactuca sativa* leaves (Tarkowski et al., 2019).

To further investigate the role of bacterial levans and plant FEHs in the interaction of plants with bacteria, we studied the interaction between the non-fructan-accumulating plant *A. thaliana* and the levan-producing bacteria *Pseudomonas brassicacearum. P. brassicacearum* is a Gram-negative bacterium isolated from the rhizosphere of two Brassicaceae, *A. thaliana* and *Brassica napus* (Achouak et al., 2000). *P. brassicacearum* is considered as a non-pathogenic commensal bacterium which is studied for its plant-growth promotion (PGP) and biocontrol properties (Gislason and Kievit, 2020).

We hypothesized that the colonization of *A. thaliana* roots by *P. brassicacearum* is facilitated by *i)* the production of levan by the bacteria and *ii)* the suppression of FEH synthesis by the plant. To test these hypotheses, we used *A. thaliana* FEH knock-out mutants and their corresponding wild-type Col-0 to study their responses to inoculation with two strains of *P. brassicacearum,* the wild-type strains NFM421 and a mutant strain which do not produce levans. We used two strains used in this study. The red fluorescent protein-tagged bacteria correspondto the reference strain for genome-based analysis (Ortet et al., 2011) and possess the levansucrase gene encoding the levan synthesizing enzyme (NFM421-I; Achouak et al., 2004). We also took advantage of corresponding levansucrase knock-out mutant strain (NFM421-I::Δlev, later named *⊿lev*) produced by LEMiRE team (Laboratoire d'Écologie Microbienne de la Rhizosphère et de l'Environnement Extrême, CEA, Cadarache).

The colonization of *A. thaliana* by *P. brassicacearum* NFM421 leads to a more branched and shorter root system as compared to control plant presumably due to a production of bacterial auxin (Persello-Cartieaux et al., 2001). The production of auxins by rhizobacteria is indeed a PGP trait of many plant-associated bacteria (Gislason and Kievit, 2020). However, besides its PGP effect, auxins can suppress the signaling cascade required for plant immunity and allow colonization of the plant by avoiding plant defense response (Gislason and Kievit, 2020). Thus, we used changes in root morphology as an indicator of plant defense response to bacterial colonization, with increased changes indicative of decreased plant defense. Specifically, we will assess whether i) *P. brassicacearum* levan suppression will increase bacterial recognition by *A. thaliana*, leading to an increase of plant defense response as revealed by a decrease of root colonization and root morphological changes ii) FEH suppression in *A. thaliana* will avoid *P. brassicacearum* levan degradation and reduce elicitor production, leading to a reduction of plant defense response as revealed by an increase in root morphology changes.

Materials and Methods

Bacterial strains

The strains are red or green fluorescent protein-tagged bacteria corresponding to the reference strain for genome-based analysis (Ortet et al., 2011) which contains the levansucrase gene encoding the levan synthesizing enzyme (NFM421-I::rfp or NFM421-I::gfp; later named NFM421) and the corresponding levansucrase knock-out mutant strain (NFM421-I::Δlev, later named *Δlev*) (Achouak et al., 2004). The levansucrase knock-out mutant strain *Δlev* was obtained by Sylvain Fochesato (Laboratoire d'Écologie Microbienne de la Rhizosphère et de l'Environnement Extrême - LEMiRE, Institut de Biosciences et biotechnologies d'Aix-Marseille – BIAM, CEA, Cadarache).

Arabidopsis T-DNA mutant

At6-FEH (At1g55120) and *At6&1-FEH* (At5g11920) *Arabidopsis thaliana* knock-out mutants were selected from the Colombia (Col-0) SALK T-DNA collection of the Nottingham Arabidopsis Stock Centre (NASC, Nottingham UK) (Table II-5 of Materiels and Methods). The three *6-feh* mutant lines are N675754-SALK 073323C (further named *6-feh-S073*), N671758-SALK 097556C (further named *6-feh-S097*) and N672154-SALK 134791C (further named *6-feh-S134*). The two *6&1-feh* mutant lines are N655172-SALK 127864C (further named *6&1-feh-S127*) and N655201-SALK 152299C (further named *6&1-feh-S152*).

For mutant genotyping, *A. thaliana* seeds (wild-type Col-0 and FEH knock-out mutants) were stratified for 48 h in 0.1% agar at 4°C in the dark and then sown in pots (9x9x10cm) filled with vermiculite with a 1cm layer of soil on top (Fig. 39A). The pots were placed in a plastic tank containing Hoagland ¼ nutrient solution which was renewed every 3-4 days. Plants were grown for approximately 8 weeks in a plant growth chamber with a PAR (Photosynthetically Active Radiations) of 110 µmol photons·m^{-2}·s^{-1} under a photoperiod of 16 h and a thermoperiod of 20/18°C day/night.

FEH knock-out mutants were tested by PCR-based genotyping to confirm the T-DNA insertion localization and homozygosity. The PCR primers used for genotyping are listed in table II-5 of Materiels and Methods. DNA is extracted from 100 mg of fresh young leaves using NucleoSpin™ Plant II kits (Macherey-Nagel, 740770.50). PCR was performed according to a protocol modified from O'Malley et al. (2015) using 3µL of DNA extract. Initial denaturation step at 94°C for 2 min was followed by 40 cycles including a denaturing step at 94°C for 30s, a primer hybridization step at various temperatures according to each pair of primers for 1 min

and an amplification step at 72°C for 1 min. Each PCR reaction was finished with a final step at 72°C for 10 min. Then, PCR products were separated by electrophoresis on 1.2% agarose gel in TAE 1X containing 50µL de BET (0.5 mg. mL^{-1}) and revealed by illumination with UV-light using a Gel-Doc TM EZ Scanner (Bio-Rad, Marnes-la-Coquette, France). In addition, FEH transcript level was also verified by using quantitative RT-PCR on the RNA extracted from leaves. The protocol is detailed in sections D.2 and D.3 of the M&M chapter. Seeds of homozygous plants were collected in 1.5 ml tubes and stored at 12°C.

The two *6&1-feh* mutant lines (*6&1-feh-S127* and *6&1-feh-S152*) are homozygote for the T-DNA insertion but *At6&1-FEH* transcript is detected in *6&1-feh-S152* (table II-6 of Materiels and Methods). Two *6-feh* mutant lines are homozygote for the T-DNA insertion (*6-feh-S097* and *6-feh-S134*) while the other is heterozygote (*6-feh-S073*). For the three *6-feh* mutant lines, the *At6-FEH* transcript is not detected (table II-6 of Materiels and Methods).

Bacterial inoculation

For the *in vitro* root colonization experiments with *P. brassicacearum*, *A. thaliana* seeds (wild-type Col-0 and FEH knock-out mutants) were placed in a 2 mL sterile Eppendorf tube. 2 mL of a sterilization solution containing 1 mL 2.5 % chlorine bleach, 9mL ethanol absolute, and 3 drops of Tween 80 (Sigma-Aldrich-V000749) were added to the seeds for 6 min. Then seeds were washed 4 times with absolute ethanol and dried naturally in a Petri dish under sterile conditions in horizontal laminar flow hoods before sowing. Two *P. brassicacearum* strains (NFM421 and *Δlev*) were grown in 10-fold-diluted tryptic soy broth (TSB/10; Difco Laboratories, Detroit) at 30°C for 24h. The optical density (OD) at 600 nm of overnight bacterial cultures was measured before the experiment to obtain approximately 200-1000 bacteria per plate culture. Bacterial suspensions were added to 150mL of half-strength Hoagland (Hoagland ½) medium containing 3.5g agar per liter (Arnon and Hoagland, 1940) and poured as a band where the seeds were sown. 7 sterile seeds were sown in a squared dish (15 x 15 cm) filled with Hoagland ½ medium and 0.4% phytagel (Sigma, St. Louis) (see Materials and Methods A.1). The dishes were sealed with micropore tape (3M, St. Paul, MN, U.S.A.) and incubated vertically at 21°C for 21 days with 16 h of light and 18°C at night (approximately 100 photons m^{-2} s^{-1}). Control experiments were performed by omission of bacteria. For this experiment, 9 technical replicates and 3 biological replicates were performed.

Monitoring root colonization by P. brassicacearum using bacterial colonies counting

The roots of five 21-d-old plants inoculated with one of the two strains (NFM421 or *Δlev*) were collected and ground in mortar in 1mL of 0.85% potassium chloride (KCl). Then, three dilutions of the ground root were plated on a 10-fold-diluted tryptic soy agar (TSA/10) medium. After 3 days at 25°C in the bacterial incubator, the bacterial colonies of the 3 most diluted points were counted. For this experiment, 5 biological replicates were performed.

Monitoring root colonization by P. brassicacearum using fluorescent microscopy

The roots of 14-d-old plants inoculated with one of the two strains (NFM421 or *Δlev*) were observed using a confocal scanning light microscopy (CSLM, Olympus) equipped with a krypton-argon laser, detectors, and filter sets for RFP monitoring. Shadow projections and optical sections were generated using the Fluoview software package. The observation was realized in three compartments of root including the basal part (1.5- to 2-cm), apical part (1-cm), and median part (variable lengths) (Achouak et al., 2004). For this experiment, 4 technical replicates and 3 biological replicates were done.

Observations of P. brassicacearum exopolysaccharide (EPS) production

Bacterial exopolysaccharide (EPS) production was observed using a fluorescent Concanavalin A probe (ConA, Texas Red™ Conjugate, Molecular Probes- C825, 1 mg/ml). A colony of *P. brassicacearum* NFM421 expressing a plasmid-borne GFP (NFM421-I::gfp) was scraped from the agar surface and deposited on a slide. 100µL of 1 mg/ml ConA was added and the slide was stored 15 min in the dark. The ConA solution was then discarded and the slide is rinsed 2 times with 40 mL of PBS for 15 min. Finally, a droplet of citifluor was delicately deposited on the sample and a coverslip is mounted to the slide before observing by CSLM. In addition, the roots of 14-d-old plants inoculated with the *P. brassicacearum* NFM421-I::gfp strain were removed from the plate and incubated into 100µL of ConA solution for 1h in the dark in the microscope slide. After discarding the ConA solution, roots were washed 2 times with 40 mL of PBS for 15 min. The roots were then observed in a droplet of citifluor after being covered with a coverslip by CSLM equipped with a krypton-argon laser, detectors and filter sets for simultaneous monitoring of GFP and RFP. For this experiment, 3 technical replicates and 2 biological replicates were performed.

Analysis of root system morphology

The morphology of root system of at least five plants of each genotype (Col-0 and FEHs knock-out mutant) was studied by analyzing scanned images. WinRHIZO Pro version 2007d (Regent Instruments, Canada) was used to measure two root traits which are indicators for a potential uptake of water and nutrients (Himmelbauer et al., 2004; Gruber et al., 2013), the total root length (cm) and surface area (cm^2). They were measured in the total root system of each plate and then divided by the number of plants to obtain the root length per plant ($cm.\ plant^{-1}$) as well as surface area per plant ($cm^2.plant^{-1}$). Moreover, the Fiji (Fiji is Just ImageJ), an image processing package of ImageJ2 (Schindelin et al., 2012; https://imagej.net/software/fiji/) was used to measure the total primary root length per plate (cm) and the lateral root number. Lateral root density (number/cm primary root) was calculated by dividing the total number of visible lateral roots in one plate by the total length of primary root (Lima et al., 2010; Gruber et al., 2013).

Statistical analysis

Data were analyzed with R software version 4.0.3 using the "Rcmdr" package (R Core Team, 2021). For each inoculation, the data correspond to five biological replicates (five individual plants). The comparison of control *versus* inoculated plants was undertaken using a one-way ANOVA with pairwise comparisons made using a Tukey test. Before ANOVA, a Shapiro–Wilk test and a Bartlett test were performed on each set of data to assess data normality and homogeneity of variances, respectively. For each test, the statistical effect is considered significant with $P<0.05$.

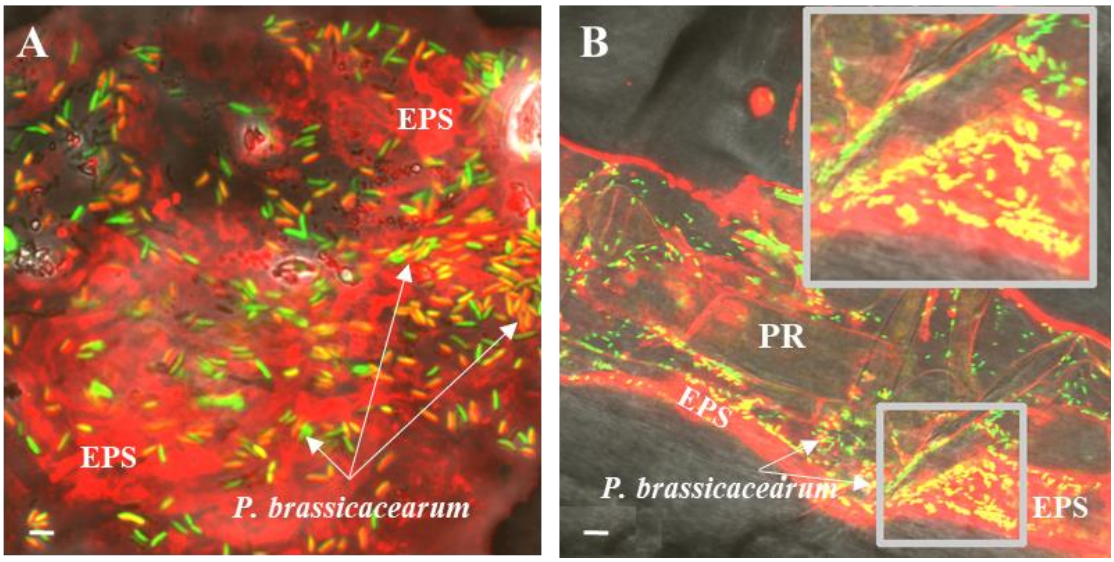

Figure III-24. Exopolysaccharide (EPS) of P. brassicacearum NFM421-I::gfp strain visualization using red fluorescent ConA probe.

(A) in vitro (B) in planta in 14-d-old Col-0 roots. PR: primary root. Scale bars: 5

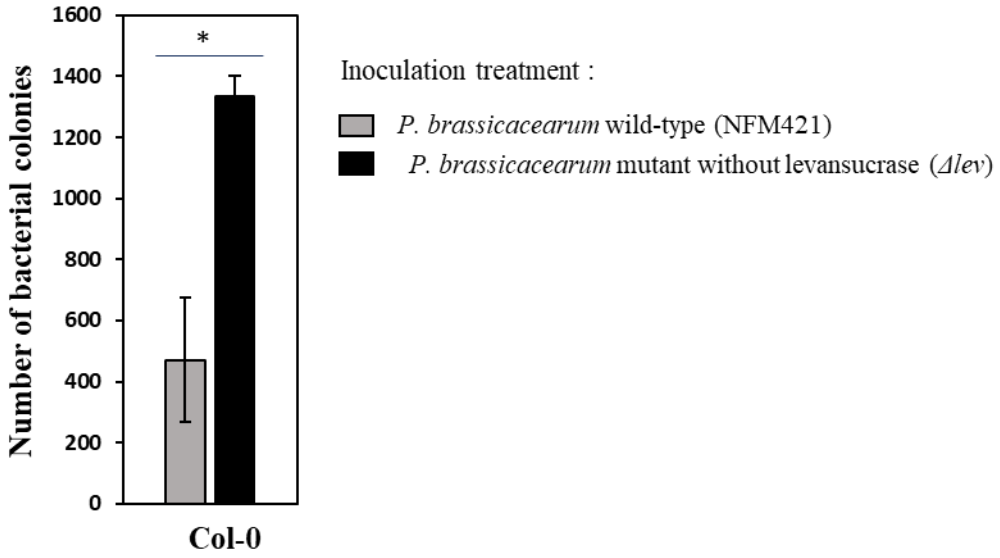

Figure III-23. Level of Arabidopsis Col-0 root colonization by P. brassicacearum.

*The roots of five 21-d-old plants inoculated with NFM421 or Δlev strains were collected and grown for 3 days at 25°C. Bacterial colonies of the three most diluted points were counted using ImageJ. * indicates an significant difference between inoculation treatments (P < 0.05; Student's test).*

Results

EPS production and colonization of Col-0 roots by P. brassicacearum.

By using a red fluorescent ConA probe, EPS production by *P. brassicacearum* NFM421 was confirmed *in vitro* (Fig. III-23A) and *in planta* (Fig. III-23B). Under both conditions, the bacteria were visualized by green fluorescence due to the expression of a plasmid-borne GFP and appeared embedded in a dense matrix of EPS visualized by red fluorescence.

The level of root colonization by *P. brassicacearum* was measured by growing *in vitro* the bacteria collected from the roots of 21-d-old plants inoculated by the levan producing strain (NFM421) or the levansucrase deletion mutant (*Δlev)*. Colony counting showed that root colonization was approximately 3-fold greater with *Δlev* than with NFM421 (Fig. III-24). Root colonization was confirmed by the observation of red fluorescent bacteria *in planta* (Fig. III-25).

The basal part of the root system was colonized by both strains but *Δlev* bacteria labeling was more visible on the surface of primary root than that of NFM421 (Fig. III-25A, B). Both strains were also observed at the median part of primary root**,** especially at the insertion of LRs (Fig. III-25C, D). Furthermore, both strains colonized the root tips (Fig. III-25E, F). In this zone, NFM421 labeling was much higher than *Δlev* labeling, especially in meristematic zone (Fig. III-25E).

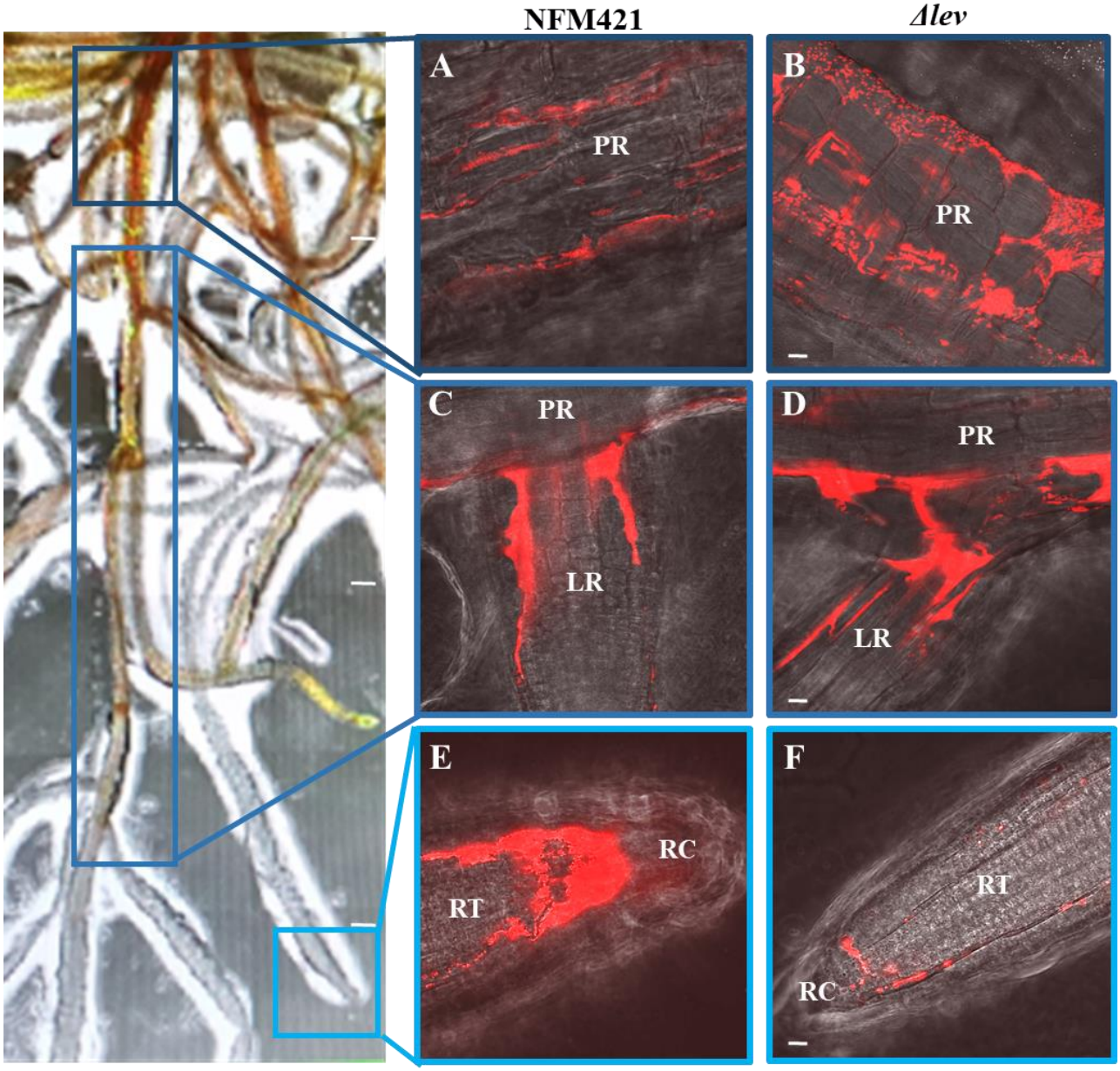

Figure III-25. Visualization of Arabidopsis Col-0 root colonization of by red fluorescent protein-tagged P. brassicacearum NFM421 (wild-type) and Δlev (levansucrase deletion mutant)

By using a confocal scanning light microscopy. Three root compartments were observed: (A, B) the basal part (1.5 to 2 cm); (C, D) median part (variable lengths), and (E, F) apical part (1cm from root apice). PR: primary root; LR: lateral root; RT: root tip; RC: root cap. Scale bars: 5 µm.

Effects of P. brassicacearum inoculation on root growth, morphology and mucilage production in Col-0

Figure III-26A shows the development of the root system in control conditions, *i.e.* for wild-type *A. thaliana* (Col-0) without inoculation. When Col-0 seeds were inoculated with *P. brassicacearum* strain producing levan (NFM421), root morphology was strongly modified (Fig. III-26B). Root system size decreased (Fig. III-26B) and total root length measured by image analysis tended to be lower (approximately 5.6 cm shorter than non-inoculated Col-0) (Fig. III-27A). The inoculation produced a very shallow and highly branched root system (Fig.III-26B, C), the inhibition of primary root growth in inoculated plants was indeed accompanied by an increase in the density of lateral roots (Fig. III-27G).

When Col-0 was inoculated with the mutant bacteria that do not produce levans (*Δlev*), the total root length was significantly reduced compared to the non-inoculated Col-0 and tended to be lower than with NFM421 inoculation (approximately 8 cm shorter than non-inoculated Col-0) (Fig. III-27A). The total root surface tended to be lower than non-inoculated plant (Fig. III-27D). The density of lateral roots was significantly enhanced compared to the non-inoculated Col-0 and tended to be higher than with NFM421 inoculation (Fig. III-27G).

The presence of mucilage at the root tip was investigated using negative staining with India ink. In non-inoculated Col-0, the dye-free zone around the root tip revealed the presence of mucilage surrounding border-like cells (BLCs) at the root cap periphery (Fig. III-28A). Interestingly, the presence of mucilage was strongly reduced in Col-0 inoculated with both NFM421 (Fig. III-28B) or *Δlev* (Fig. III-28C) *P. brassicacearum* strains. Moreover, in the presence of *P. brassicacearum*, the BLCs were firmly attached to the root cap and more difficult to observe (Fig. III-28B, C).

Effects of FEH deletion in Arabidopsis responses to P. brassicacearum inoculation.

The root system size (Fig. III-26A, D, G), as well as total root length and surface and lateral root density, were similar in Col-0, *6-feh* and *6&1feh* mutants (control plants without inoculation) (Fig. III-27A-I). This indicates that the T-DNA insertion in one of the two *FEH* genes (*At6-FEH* or *At6&1-FEH*) did not alter root growth and morphology.

Inoculation with NFM421 caused a greater root growth inhibition in FEH knockout mutants than in Col-0 with a reduction in root length and even more in total root surface (Fig. III-26D, E, G, H; Fig. III-27B, C, E, F). Similar root growth reductions were observed in FEH knockout

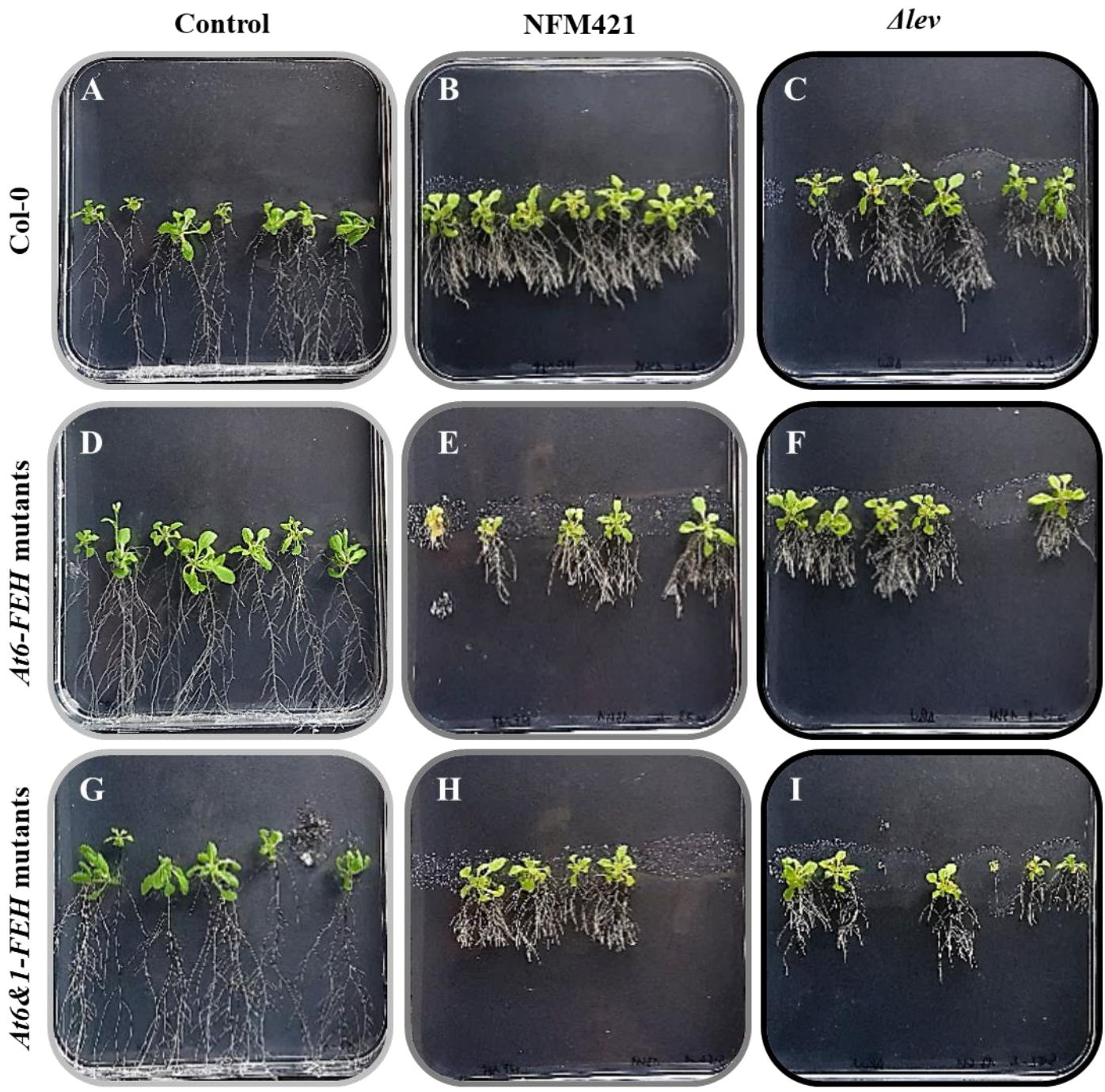

Figure III-26. Arabidopsis Col-0 and FEH knock-out mutants inoculated with P. brassicacearum

(A, B, C) Col-0; (D, E, F) 6-feh (a petri dish representative of Arabidopsis 6-FEH knockout mutants); (G, H, I) 6&1-feh (a dish representative of Arabidopsis 6&1-FEH knockout mutants). Plants were not inoculated (A, D, G) or inoculated with P. brassicacearum NFM421 (B, E, H) or Δlev (C, F, I). These images were used to analyse root system morphology by ImageJ and WinRHIZO.

mutants inoculated with *Δlev* (Fig. III-26F, I; Fig. III-27B, C, E, F). By comparison with Col-0, the total root length and surface were significantly reduced by inoculation with NF421 for two *6-feh* mutants (S097 and S134) and one 6&1-feh mutant (S127).

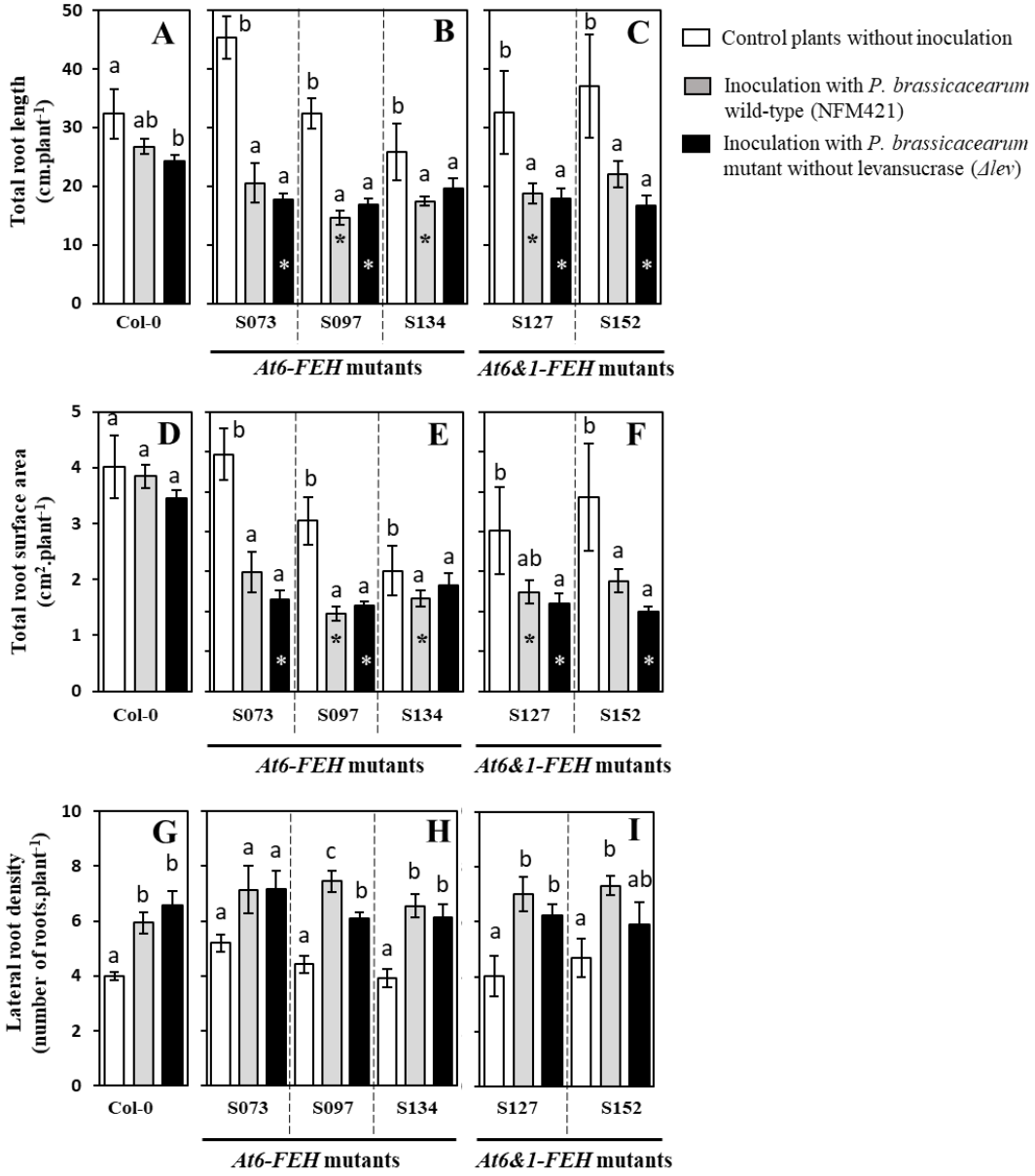

Figure III-27. The effect of P. brassicacearum inoculation on root morphology of Arabidopsis

Col-0 (A, D, G), Arabidopsis 6-FEH knock-out mutants (B, E, H) and Arabidopsis 6&1-FEH knock-out mutants (C, F, I . (A, B, C) total root length, (D, E, F) total rot surface area, (G, H, I) lateral root density. Plants were not inoculated or inoculated with P. brassicacearum NFM421 or Δlev. Each data point is the average of five independent biological replicates and the bars indicate the standard errors. The asterisk indicates a statistically significant differences at P < 0.05 (Student's test) between the mutant genotype and Col0 for the same inoculation treatment. Different letters indicate statistically significant differences between inoculation treatments for the same plant genotype (Tukey's test).

Total root length and surface were significantly reduced by inoculation with *Δlev* for two *6-feh* mutants (*S073* and *S097*) and the two *6&1-feh* mutants (*S127* and *S152*). As in Col-0, the inoculation of FEH knockout mutants with NFM421 or *Δlev* produced a very shallow and highly branched root system (Fig III-26E, F, H, I), and the increased lateral root density was more pronounced in FEH knockout mutants than in Col-0 and with NFM421 than *Δlev* inoculation (Fig. III-27G, H, I). Thus, the effects of inoculation on root growth and morphology were generally more pronounced in FEH knockout mutant lines which appeared to be more sensitive to the presence of bacteria than Col-0.

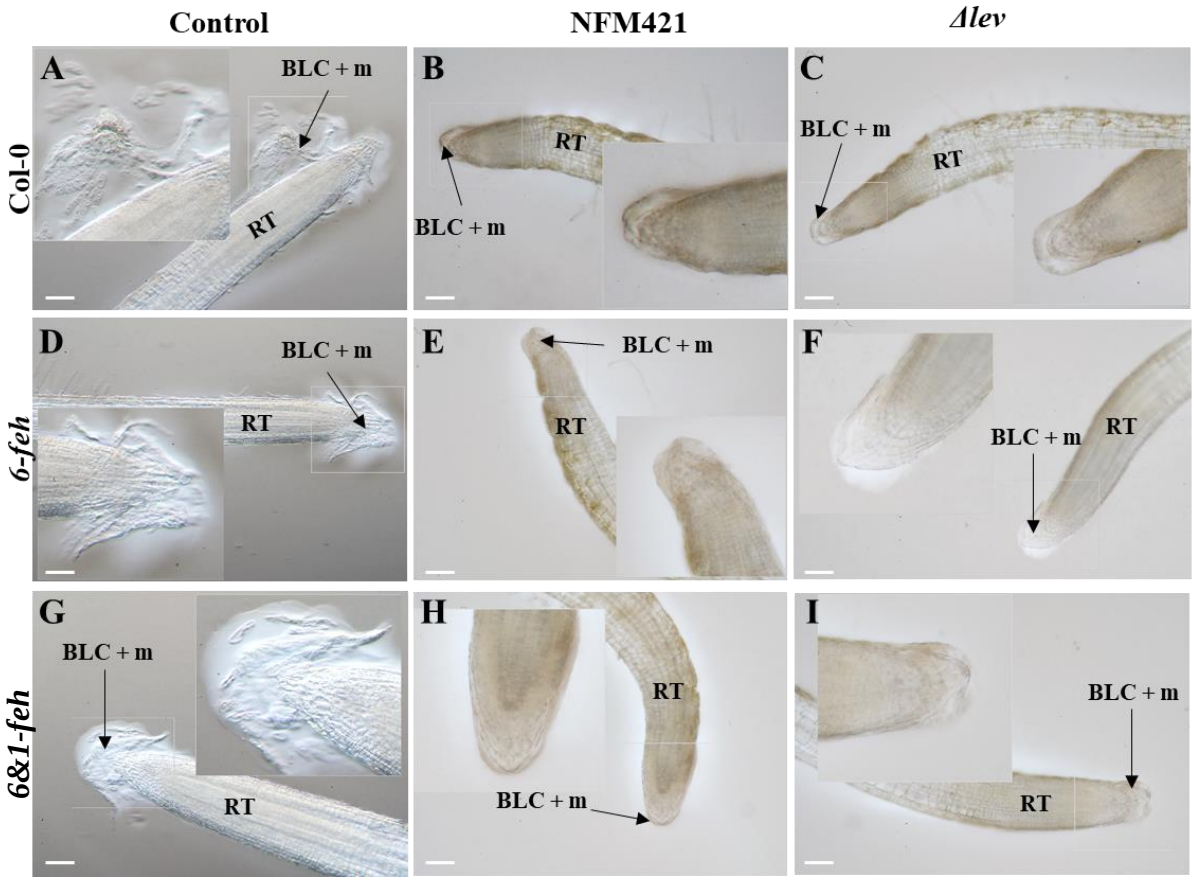

Figure III-28. Visualization by light microscopy of the mucilage forming a halo at the root tip (m) using India ink staining.

(A, B, C) Col-0; (D, E, F) 6-feh (a root representative of A. thaliana 6-FEH knockout mutants); (G, H, I) 6&1-feh (a root representative of A. thaliana 6&1-FEH knockout mutants). Plants were not inoculated (A, D, G) or inoculated with P. brassicacearum NFM421 (B, E, H) or Δlev (C, F, I). BLC: root-border cell; RT: root tip. Scale bars: 200 µm.

As in Col-0, the dye-free zone around the root tip revealed the presence of abundant mucilage secretions with numerous border-like cells (BLCs) surrounding the root cap periphery in FEH knock-out mutants (Fig. III-28D, G). Similar to Col-0, the presence of mucilage was strongly reduced in BLCs were firmly attached to the root cap in FEH knockout mutants inoculated with both NFM421 (Fig. III-28B, E, H) or *Δlev* (Fig. III-28C, F, I) strains.

Discussion

Many plant colonizing bacteria are capable of producing indole-3-acetic acid (IAA) or effectors that promote IAA accumulation (Spaepen et al., 2007; Navarro et al., 2006; Cui et al., 2005; Pel and Pieterse, 2013). IAA is the main auxin found in plants and it plays an important role in growth and development as well as response to abiotic stress (Benjamins and Scheres, 2008). Auxin strongly decelerates root elongation in a wide range of concentrations (Scott, 1972; Pilet, 2002; Tanimoto, 2005). This inhibition of growth was accompanied by elevated auxin accumulation at the root tip and enhanced lateral root elongation as well as initiation of lateral roots particularly in the upper zone of the primary root (Muday et al., 2012).

So, as expected and as previously reported by Persello-Cartieaux et al. (2001), we observed a strong inhibition of primary root growth and a stimulation of lateral root production in *A. thaliana* Col-0 inoculated with the wild-type levan-producing *P. brassicacearum* NFM421. The typical mucilage secretions along the root tip and border-like cells (BLCs) surrounding the root cap periphery (Vicré et al.,2005) which were observed in absence of bacteria were strongly reduced by inoculation with NFM421.

When Col-0 was inoculated with the levansucrase deletion mutant of *P. brassicacearum* (*Δlev*), root colonization was increased 3-fold and the root morphological changes tended to be stronger. Thus, conversely to that observed in plants inoculated by levansucrase deletion mutant of *E. amylovora* (Geier and Geider, 1993; Koczan et al., 2009) and to our first hypothesis, the presence of levans did not facilitate the root colonization. Indeed, suppression of levan synthesis in *P. brassicacearum* not only did not reduce root colonization but even increase it. This indicates that in *A. thaliana – P. brassicacearum* interaction, the absence of levans did not increase but decreased plant defense response suggesting that the production of auxins by bacteria might have suppressed the regulatory cascade required for plant immunity (Gislason and de Kievit, 2020). Moreover, the suppression of levan synthesis modified the pattern of root colonization, the levan-producing bacteria was mainly present in root tip meristematic zone as previously observed by Persello-Cartieaux et al. (2001) while *Δlev* preferentially colonized the upper part of primary root and the zones of insertion of lateral roots. This suggests that specific

root tip defense response was enhanced when *A. thaliana* is colonized by levan-free *P. brassicacearum*.

Since the presence or absence of levans in *P. brassicacearum* led to different patterns of plant response and root colonization, we investigated the involvement of plant FEHs in the plant-bacteria interaction. Indeed, FEHs are fructan degrading enzymes that might reduce bacterial levan layer and produce elicitors of plant defense response. In the T-DNA insertion in one of the two *A. thaliana* FEH genes (*At6-FEH* or *At6&1-FEH*) did not modify the morphology of the roots as long as they are not in contact with *P. brassicacearum*. We hypothesized that FEH suppression might prevent levan degradation and reduce elicitor production, leading to a reduction of plant defense response. As expected, root morphological changes induced by levan-producing *P. brassicacearum* were stronger in all five FEH knockout mutants than in Col-0, indicating that the deletion of one of the two FEHs reduces plant defense response.

This suggests that, in Col-0, the presence of the two FEHs allowed efficient hydrolysis of bacterial levans producing fructo-oligosaccharides (FOS) which triggered plant defense response (Versluys et al., 2017) reducing the effect of auxins. In presence of the levan-free *P. brassicacearum*, the absence of levans did not allow the production of elicitors of defense response by FEHs, so the regulation by auxin had continued and the modification of root morphology was greater.

In FEH knock-out mutants inoculated with NFM421 or *Δlev*, changes in root morphology could be explained by auxin regulation which was not antagonized by FOS production or degradation of the levan layer. Thus, the regulation by auxin continued resulting in more significant morphological changes compared to Col-0 and to non-inoculated plants. Moreover, the fact the inoculation with *Δlev* strain led to a greater total root length reduction in FEH knockout mutants than in Col-0 suggests that FEH are involved in other regulatory mechanisms. In the non-fructan plant *Zea mays*, 6&1FEH protein binds to cell-wall invertase (Cw-INV) inhibitor protein which may enhance Cw-INV activity (Zhao et al., 2019). The authors have proposed that the expression of this FEH at the site of plant-bacteria interaction could not only lead to levan degradation but also increase Cw-INV activity and thereby increase apoplastic sucrose hydrolysis (Zhao et al., 2019). Such modification of apoplastic sucrose metabolism by FEH might modulate plant defense response independently to levan degradation through sugar signaling (Ruan, 2014)

These preliminary results confirm the role of bacterial levans in plant-bacteria interaction and support the hypothesis of the involvement of plant FEHs in this interaction by acting directly on bacterial levans and/or by modulating sugar signaling. Before going further in result

interpretation, it is necessary to complete these preliminary experiments by measuring FEH activity in Col-0 and in the different *feh* lines. This is particularly needed for the *6&1-feh-S152* line in which *6&1-FEH* transcripts were detected by RT-qPCR but which showed a similar response than the other *feh* lines in response to *P. brassicacearum* inoculation. Moreover, in order to study the effect of the total suppression of FEH activity in response to root colonization by microorganisms, *6-feh/6&1feh* double- mutants will be produced and challenged by fructan-producing rhizospheric microorganisms.

IV. General discussion and Perspectives

Characterization of two monoclonal antibodies that recognized β-(2,1) and β-(2,6)-fructan epitopes

Cell imaging and immunolocalisation of epitopes carried by defense molecules are powerful tools to unravel the cellular and molecular mechanisms involved in plant response to biotic and abiotic stresses. Fructans are promising candidate for the concept of "sweet immunity" (Bolouri Moghaddam and Van den Ende, 2013; Trouvelot et al., 2014; Tarkowski et al., 2019; Svara et al., 2020) and the localization of their epitopes at tissue and cellular level becomes crucial to clarify their mechanisms of action in general and more particularly in root defense. However, despite a wide range of existing techniques for the analysis of fructans (Matros et al., 2020), no specific antibodies against fructans are currently commercially available. In this thesis, a collaboration of the society BIOTEM was initiated to produce antibodies against plant fructans. By immunizing mice with a mixture prepared from chicory inulins and timothy levans, two new monoclonal antibodies (mAbs) (BTM15A6 and BTM9H2) with high specificity against plant fructans with β-(2,1) and β-(2,6) linkages have been characterized. Their specificity was studied using immuno-dot blot assay. The two mAbs showed a high specificity for levans (β-(2,6)-linked fructans) and inulins (β-(2,1)-linked fructans) from various plant species including timothy (*Phleum pratense*), chicory (*Cichorium intybus*) as well as for WSC extracts obtained from fructan-accumulating grasses, *i.e.* perennial ryegrass (*Lolium perenne*) and cocksfoot (*Dactylis glomerata*), and from the Asteraceae dandelion (*Taraxacum officinalis*). Interestingly, their specificity towards β-(2,6)-linked fructans from plants was confirmed by the strong reaction with levans from timothy which have an average DP of about 75 (P-LEVAN, Megazyme) whereas no reaction was detected with bacterial levans from *Erwinia herbicola* (L8647, Sigma-Aldrich) which contains polymers with a DP greater than 100 and up to 10000 (Velázquez-Hernández et al., 2009). With other mono-, di-, oligo- and polysaccharides (starch, pectins, proteoglycans and hemicellulosic polysaccharides) found in plants, a weak insignificant reaction at the highest concentration tested or even no reaction was detected. Anti-glycan antibodies directed against cell-wall polysaccharides are commonly used to study cell wall organization in plant tissues (Knox, 2008) and to analyze the composition of the mucilage produced by root tip (Durand et al., 2009) or seeds (Voiniciuc et al., 2015) and more recently to localize starch granules in pea root cap (Rydahl et al., 2017). We took advantage of these previously described protocols to test in this study the fluorescence binding of BTM15A6 and BTM9H2 on tissues of fructan- and non-fructan-accumulating plants. The fact that fluorescence

labelling of BTM15A6 and BTM9H2 was detected at the root tip surface of the fructan-accumulating plants tested including perennial ryegrass, timothy and wheat and on sections of perennial ryegrass root tip and leaf bases while their epitopes were neither detected at the surface of root tips nor on root section of Arabidopsis, a non-fructan plant, confirms once again their specificity towards plant fructans. Interestingly, the difference of intensity of labeling obtained with the two anti-fructan mAbs when used for immunolocalization in different fructan-accumulating plants suggests that they have a slight difference in specificity.

The detection of BTM15A6 and BTM9H2 epitopes at the surface of the root elongation and meristematic zones can be explained by secretion from their subcellular localization (*i.e*. vacuole; Wagner et al., 1983) to the cell wall. This observation is consistent with previous reports of apoplastic localization of fructans in crown tissues of oat after cold hardening (Livingston and Henson, 1998) and in the phloem of *Agave deserti* (Wang and Nobel, 1998). The intracellular detection of the epitopes within root and mature leaf sheath cells on sections is consistent with their expected vacuolar localization (Vijn and Smeekens, 1999; Ritsema and Smeekens, 2003). The mAbs BTM15A6 and BTM9H2 enrich the family of antibodies against structural and non-structural polysaccharides already available for plant research (Rydahl et al., 2017; 2018) and allow to investigate the mechanisms of fructans involvement in plant metabolism and in their interaction with microorganisms.

The immunofluorescence labeling with BTM9H2 and BTM15A6 performed on roots and leaves sections from timothy (*Phleum pratense*) and chicory (*Cichorium intybus*) will further confirm their specificity since highly purified levans from timothy and inulins from chicory have been used to prepare antigenic compounds for producing these mAbs. In addition, to investigate in more details the localization of fructans epitopes using BTM9H2 and BTM15A6 at the subcellular level, immunogold analyses on longitudinal ultrathin sections from perennial ryegrass and timothy root tips by transmission electron microscopy should be tested. Besides, immunocytochemistry on soluble epitopes is a particularly delicate task as it cannot be excluded a re-localization of these epitopes during samples preparation. Cryofixation using high pressure freezing followed by freeze-substitution remained the optimal protocol to preserve both ultrastructure and antigenicity of plant cells. However, some adaptations of this method might be necessary in order to minimize fructan leakage during tissue fixation.

Microscopical characterization of the root extracellular trap (RET) of perennial ryegrass (*L. perenne*)

As mentioned previously, root system and the role of cell wall glycomolecules in the defense response constitute the main research focus of the thesis. In plants, the formation and release of RETs from the root cap to the rhizosphere are essential for protecting the root against biotic and abiotic stresses (Haichar et al., 2014; Driouich et al., 2019). To date, the RET was described in many plant species including plants belonging to the Poaceae family such as barley (Tamas et al., 2005) or maize (Canellas and Olivares, 2017). Although perennial ryegrass is a Poaceae of agronomic interest because of its role as an important grassland forage plant that accumulate fructans, research activities focus mainly on the aerial part more than on the roots. In this thesis, we provide the first characterization of the RET from perennial ryegrass. In this species, the RET comprises two different morphotypes of border cells with small spherical cells (sBC) and elongated cells (eBC). This result is consistent with the presence of difference types of border cells in barley (Tamas et al., 2005) and maize (Canellas and Olivares, 2017), which also belong to Poaceae family. The abundant mucilage surrounding border cells is found to cover the whole root cap as well as the meristematic zone of perennial ryegrass. One of the major findings is that the RET of *L. perenne* is particularly enriched in AGP epitopes compared to other plant species such as *A. thaliana* and pea. Although AGPs were present in the RET of these species, other glycomolecules such as homogalacturonan (Durand et al., 2009; Plancot et al., 2013) or xyloglucan epitopes (Ropitaux et al., 2019) were also detected in their RET. AGPs are known to be involved in response to various biotic and abiotic stresses (Cannesan et al. 2012; Nguema-Ona et al., 2013; Pereira et al., 2015; Koroney et al. 2016) and play a prominent role at the root surface during root colonization by pathogenic and symbiotic microbes (Vicré et al., 2005; Gaspar et al., 2004; Xie et al., 2012). Our study highlighted that both flg22 elicitation and water stress induce by PEG increased the quantity of mucilage in perennial ryegrass which forms a larger halo at the root tip. It is likely that AGPs from the RET of perennial ryegrass contribute to interactions between the root and soil-borne microbes as well as provide the protection for the root tip in water deficit condition. This agrees with previous reports which demonstrate that the alteration of AGPs in *A. thaliana* inhibited rhizobium bacteria attachment (Vicré et al., 2005) and increased the susceptibility of root to pathogenic cyst nematode (Baum et al., 2000; Bozbuka et al., 2018). Previously, their role in the salt adaptation processes (Olmos et al. 2017) and low-temperature tolerance (Yan et al. 2015) was also reported.

Further investigation about the alteration of AGPs from perennial ryegrass roots in response to other elicitors and/or phytohormones will allow to confirm their involvement in root defense. Moreover, the detection of fructan epitopes by immunolocalization with the two recently characterized mAbs BTM15A6 and BTM9H2 in perennial ryegrass root elicited by flg22, and other elicitors, or treated with PEG will be performed to assess the effect of these treatments on the potential secretion of fructans located in the cap cells in the RET of perennial ryegrass.

Evaluation of fructan exohydrolases (FEHs) as root defense genes in non-fructan plants.

The unknown role of FEHs present in various plant species which do not accumulate fructans challenges our curiosity. To date, six FEHs have been characterized in non-fructan plants, *At6-FEH* and *At6&1FEH* in Arabidopsis (De Coninck et al., 2005), *Bv6-FEH* in *Beta vulgaris* (Van den Ende et al., 2003b), *Zm-6&1-FEH1* (Zhao et al., 2019), *Zm-6-FEH* (Huang et al., 2020) and *Zm-6&1-FEH2* (Wu et al., 2021) in maize. This led us to study their role in plant defense in the model plant *A. thaliana* and the genetically related allopolyploid species *Brassica napus,* both well-known as non-fructan plants. By sequence homology with the two *A. thaliana* FEH genes *At6-FEH* and *At6&1-FEH* previously identified by De Coninck *et al.* (2005), we identified two genes with complete sequence coding for a putative 6-FEH (named *Bn6-FEH*) and four genes with complete sequence coding for a putative 6&1-FEH (named *Bn6&1-FEH*). Plant defense responses against pathogens involve different complex and interconnected hormonal pathways including those of SA, JA and ET (Wang et al., 2012; Lemarié et al., 2015; Zhang et al., 2020; Caarls *et al.*, 2016; Papadopoulou *et al.*, 2018). As a consequence, exogeneous phytohormones application is useful to clarify the hypothesis that FEHs are defense-related proteins in *A. thaliana* and *B. napus*.

The ability of phytohormones to trigger defense responses was confirmed by the strong induction of the well-known SA-responsive genes *PR1* and *WRKY70* (Li et al., 2004; van Loon et al., 2006) by SA treatment, *AOS* by MeJA treatment and *PDF1.2* and *ERF1/2* by treatment with the ET precursor ACC. *HEL*, a recognized marker of root defense response, was up-regulated by the three phytohormones. Interestingly SA treatment for 12 hours at root level strongly up-regulated all *6&1-FEH* genes in the five varieties of *B. napus* and in the model species *A. thaliana*. It should be noted that *PR1* and *HEL*, two well-known pathogen-induced antimicrobial proteins, and *WKRY70*, a marker of SA-mediated signaling were also up-regulated. Our findings clearly support the role of FEHs as defense proteins in non-fructan plants. We can then speculate that FEHs are involved in plant-microorganism interactions and may constitute, together with some cell-wall invertases, a new family of pathogenesis-related

(PR) proteins (Roitsch *et al.*, 2003; van Loon *et al.*, 2006). FEHs may play a specific role in these interactions through the production of MAMPs from microbial fructans and/or through the weakening of bacterial biofilm (Van den Ende *et al.*, 2003). A genotypic variability of SA-mediated FEH regulation was observed among five *B. napus* varieties, that may have consequences on the susceptibility to fructan synthesizing pathogens.

To further assess the role of FEHs in plant defense, At*6-FEH* and *At6&1-FEH* double knockout mutants are being produced and will be challenged by fructan-producing rhizospheric microorganisms. Besides, to determine whether up-regulation of FEH genes was associated with modification of β-fructosidase activities, the invertase (INV) and FEHs activities of the vacuolar and cell-wall fractions were measured on protein extracts from roots treated with the phytohormonones (i.e. SA, JA and ET) for 24 hours. Our preliminary results showed that vacuolar and cell-wall 1-FEH activities measured against plant β-(2,1)-linked fructans tended to increase in response to SA treatment and that cell-wall 6-FEH activity measured against plant β-(2,6)-linked fructans tended to increase in response to MeJA and ACC treatments. A slight increase trend was also observed for vacuolar 6-FEH activity measured against bacteria β-(2,6)-linked fructans in response to ACC treatment. For further investigation, FEH activities have to be monitored in kinetics from 6 to 48 h after the start of phytohormone treatment to optimize the detection of treatment effect on FEH activities.

Involvement of plant fructan exohydrolases (FEHs) and bacterial levans in *A. thaliana* root colonization by *P. brassicacearum*

Our results support that FEHs could act as defense-related proteins. We performed preliminary investigations on the interaction between the non-fructan-accumulating plant *A. thaliana* and the beneficial levan-producing bacteria *Pseudomonas brassicacearum*. To this end, we initiated a collaboration with W. Achouak. We used *A. thaliana* Col-0 and FEH knock-out single mutants inoculated with *P. brassicacearum* wild-type (NFM421) and the corresponding levansucrase deletion mutant (*Δlev*). As previously reported by Persello-Cartieaux et al. (2001), we observed a strong inhibition of primary root growth and a stimulation of lateral root production in *A. thaliana* Col-0 inoculated with the wild-type levan-producing *P. brassicacearum* NFM421. Border-like cells (BLCs) and the layer of mucilage surrounding the root cap periphery were observed in absence of bacteria as described in Vicré et al., (2005). However, the RET of *A. thaliana* was strongly reduced upon inoculation with NFM421. The suppression of levan synthesis in *P. brassicacearum* increased root colonization. It can be hypothesized that the absence of levans in bacterial EPS prevented the production of MAMPs

and the effect of auxins produced by bacteria was thus not counteracted by the regulatory cascade triggered by MAMPs and required for plant immunity (Gislason and de Kievit, 2020). The deletion of one of the two FEHs reduced plant defense response in the interaction with levan-producing *P. brassicacearum*. We observed an increased root morphological changes in all five FEH knockout mutants as compared to Col-0. We suggest that the presence of the two FEHs allowed efficient hydrolysis of bacterial levans producing fructo-oligosaccharides (FOS) which triggered plant defense response (Versluys et al., 2017). This will allow to reduce the effect of auxins. In presence of the levan-free *P. brassicacearum* (*Δlev*), the absence of levans did not allow the production of elicitors of defense response by FEHs. As a consequence, the regulation by auxin carried on and the modification of root morphology was increased.

Moreover, we propose that the expression of FEH at the site of plant-bacteria interaction could not only lead to levan degradation but also increase Cw-INV activity by interacting with proteinaceous invertase inhibitor (Zhao et al., 2019) and thereby increase apoplastic sucrose hydrolysis. Such modification of apoplastic sucrose metabolism by FEH might modulate plant defense response independently to levan degradation through sugar signaling (Ruan, 2014).

Our preliminary results support the hypothesis of the involvement of plant FEHs in Arabidopsis-*P. brassicacearum* interaction by acting directly on bacterial levans and/or by modulating sugar signaling. To confirm this hypothesis, the measurement of FEH and INV activities in Col-0 and the different FEH knockout mutants inoculated with *P. brassicacearum* is needed. Besides, the *6-feh/6&1feh* double-mutants which are being produced will be challenged with rhizospheric fructan-producing microorganisms to study the effect of the total suppression of FEH activity on the response of plants to root colonization by microorganisms.

Beyond their fundamental character, these results could lead to the definition of new strategies for bio-control and/or bio-stimulation of crop species.

V. Appendix

Appendix 1. List of the potential antigens and test oligo/polysaccharides used for this study.

	Subtracts	Description and source	Preparation method
Antigens	Levan (MEGAZYME, P-LEV)	Fructans with β-2,6 linkages from timothy (*Phleum pratense*)	Solubilization in distilled water at room temperature
	Inulin (MEGAZYME, P-INUL)	Fructans with β-2,6 linkages from chicory (*Cichorium intybus*)	Solubilization in distilled water (120°C, 10 min) and reheat before each test to 80°C (5 min)
Fructans	Levan (SIGMA, L8647)	Fructans with β-2,6 linkages from bacteria (*Erwinia herbicola*)	Solubilization in distilled water (120°C, 10 min) and reheat before each test to 80°C (5 min)
	Fructo-oligosaccharides (FOS-Megazyme, P-FOS28)	DP 3–10 fructans with β-2,1 linkages from chicory (*Cichorium intybus*)	Solubilization in distilled water at room temperature
	1,1-Kestotetraose (MEGAZYME, O-KTE)	DP4 fructanswith β-2,1 linkages	Solubilization in distilled water at room temperature
	1-Kestotriose (MEGAZYME, O-KTR)	DP3 fructanswith β-2,1 linkages	Solubilization in distilled water at room temperature
WSC extracts	Perennial ryegrass (*Lolium perenne*)	Mixture of soluble carbohydrates (inulin, neo-inulin and neo-levan type, sucrose, glucose, fructose)	Hot water extraction followed by removal of charged compounds by ion exchange.
	Cocksfoot (*Dactylis glomerata*)	Mixture of soluble carbohydrates (levan, sucrose, glucose, fructose)	Hot water extraction followed by removal of charged compounds by ion exchange.
	Dandelion (*Taraxacum officinalis*)	Mixture of soluble carbohydrates (inulin, sucrose, glucose, fructose)	Hot water extraction followed by removal of charged compounds by ion exchange.
	Purified fructans from *L. perenne*	β-2,1 linkages and β-2,6 linkages from *Lolium perenne*	Hot water extraction followed by removal of charged compounds by ion exchange and gel filtration on Sephadex G-25
Tri-saccharides	Raffinose (Sigma, R0514)	α-D-galactosylsucrose	Solubilization in distilled water at room temp.
Di-saccharides	Sucrose (Fluka, 84097)	α-D-glucopyranosyl-(1,2)-β-D-fructofuranoside	Solubilization in distilled water at room temp.
	Maltose (Sigma, M5895)	α-D-glucopyranosyl-(1,4)-α-D-glucopyranoside	
Mono-saccharides	Glucose (ACROS, 410955000)	D-(+)-glucose	Solubilization in distilled water at room temperature
	Fructose (Sigma, F0127)	D-(−)-Fructose	
	Arabinose (Sigma, A3131 and A3256)	D-(-)-Arabinose	
		L-(+)-Arabinose	
	Rhamnose (Sigma, R3875)	L-Rhamnose	
	Galactose (Sigma, G0750)	D-(+)-galactose	
	Xylose (Sigma, X2126)	DL-Xylose	
	Glucuronic acid (Sigma, G8645)	D-Glucuronic acid	
Poly-saccharides	Starch (Sigma, S5127)	α-1,4 and α-1,6 linkages from wheat (Triticum aestivum)	Solublization in Dimethyl sulfoxide (DMSO) (100°C, 5 min) supplemented with distilled water (Perez-Rea et al., 2015)
	Pectin (Fluka, 76280)	α-(1,4)-linked D-galacturonic acid and β (1,2) and (1,4) linkages from citrus peel	Solublizationin distilled water at room temp.
	Galactan (MEGAZYME, P-GALLU)	β-1,4 linkages from lupin seed	Solublizationin distilled water at room temp.
	Arabinan (MEGAZYME, P-ARAB)	α-1,5 linkages from sugar-beet pulp	Solublizationin distilled water at room temp.
	Arabinogalactan (Serva, 13717)	α-1,5 linkages from larch wood	Solublizationin distilled water at room temp.
	Gum arabic (Biosupplies Australia Pty Ltd)	1,3-linked β-D- galactopyranose from acacia trees	Solublizationin distilled water at room temp.
	Arabinoxylan (MEGAZYME, P-WAXYL, P-RAXY)	β-1,4 linkages from wheat flour	Solublizationin distilled water at room temp.
		β-1,4 linkages from rye flour	Solublizationin distilled water at room temp.
	Xyloglucan (MEGAZYME, P-XYGLN)	β-1,4, α-1,6 and β-1,6 linkages from tamarind seed	Solublizationin distilled water at room temp.
	Xylan (Megazyme, P-XYLNBE)	β-1,4 and α-1,2 from beechwood	Solublizationin distilled water at room temp.

*Appendix 2. Values of Kruskal-Wallis non-parametric test for immuno-dot blot data obtained with BTM9H2 mAb (Fig.1&3 data). *P < 0.05; **P < 0.01; ND, not detected.*

	Carbohydrates	Secondary antibody	χ2	p-value	
Antigens	Levans (*P. pratense*)	Goat anti-mouse	20.77	<0.01	**
	Inulins (*C. intybus*)		21.34	<0.01	**
	Levans (*P. pratense*)	Chicken anti-mouse	13.64	<0.05	*
	Inulins (*C. intybus*)		3.32	>0.05	
Fructans	Levans *(E. herbicola)*	Goat anti-mouse		ND	
	Fructo-oligosaccharides (FOS)		4.74	>0.05	
	1,1-Kestotetraose		3.71	>0.05	
	1-Kestotriose		2.12	>0.05	
WSC extracts	Perennial ryegrass *(L. perenne)*	Goat anti-mouse	2.71	>0.05	
	Cocksfoot (*D. glomerata*)		14.65	<0.05	*
	Dandelion (*T. officinalis*)		11.64	<0.05	*
	Purified fructan (*L.perenne*)	Chicken anti-mouse	11.38	<0.05	*
	WSC extract (*L. perenne*)		12.22	<0.05	*
Tri-saccharides	Raffinose	Goat anti-mouse		ND	
Di-saccharides	Sucrose	Goat anti-mouse		ND	
	Maltose		7.48	>0.05	
Mono-saccharides	Glucose	Goat anti-mouse	7.99	>0.05	
	Fructose			ND	
	D-(-)-Arabinose		1.46	>0.05	
	L-(+)-Arabinose		4.32	>0.05	
	Rhamnose			ND	
	Galactose			ND	
	Xylose	Chicken anti-mouse	1.79	>0.05	
	Glucuronic acid	Goat anti-mouse		ND	
Polysaccharides	Starch (wheat)	Goat anti-mouse	2.17	>0.05	
	Pectin (citrus peel)			ND	
	Galactan			ND	
	Arabinan			ND	
	Arabinogalactan		3.26	>0.05	
	Gum arabic		10.30	>0.05	
	Arabinoxylan (wheat)		8.84	>0.05	
	Arabinoxylan (rye)			ND	
	Xyloglucan			ND	
	Xylan (beechwood)	Chicken anti-mouse		ND	

*Appendix 3. Values of Kruskal-Wallis non-parametric test for immuno-dot blot data obtained with BTM15A6 mAb (Fig.2&4 data). *P < 0.05; **P < 0.01; ND, not detected.*

	Carbohydrates	Secondary antibody	χ2	p-value	
Antigens	Levans (*P. pratense*)	Goat anti-mouse	21.71	<0.01	**
	Inulins (*C. intybus*)		18.42	<0.01	**
	Levans (*P. pratense*)	Chicken anti-mouse	13.58	<0.05	*
	Inulins (*C. intybus*)		12.67	<0.05	*
Fructans	Levan *(E. herbicola)*	Goat anti-mouse		ND	
	Fructo-oligosaccharides (FOS)		9.16	>0.05	
	1,1-Kestotetraose		6.56	>0.05	
	1-Kestotriose		2.51	>0.05	
WSC extracts	Perennial ryegrass *(L. perenne)*	Goat anti-mouse	17.77	<0.01	**
	Cocksfoot (*D. glomerata*)		3.43	>0.05	
	Dandelion (*T. officinalis*)		3.82	>0.05	
	Purified fructan (*L.perenne*)	Chicken anti-mouse	12.46	<0.05	*
	WSC extract (*L. perenne*)		2.77	>0.05	
Tri-saccharides	Raffinose	Goat anti-mouse		ND	
Di-saccharides	Sucrose	Goat anti-mouse		ND	
	Maltose		7.67	>0.05	
Mono-saccharides	Glucose	Goat anti-mouse		ND	
	Fructose			ND	
	D-(-)-Arabinose		1.85	>0.05	
	L-(+)-Arabinose		3.43	>0.05	
	Rhamnose			ND	
	Galactose		7.65	>0.05	
	Xylose	Chicken anti-mouse	3.90	>0.05	
	Glucuronic acid	Goat anti-mouse		ND	
Polysaccharides	Starch (wheat)	Goat anti-mouse	9.12	>0.05	
	Pectin (citrus peel)			ND	
	Galactan		5.10	>0.05	
	Arabinan		5.22	>0.05	
	Arabinogalactan			ND	
	Gum arabic		0.56	>0.05	
	Arabinoxylan (wheat)		9.94	>0.05	
	Arabinoxylan (rye)			ND	
	Xyloglucan			ND	
	Xylan (beechwood)	Chicken anti-mouse	4.72	>0.05	

Appendix 4. Primary antibodies and associated epitopes of different cell wall polysaccharides used.

	Cell wall polymers	mAbs	Epitopes	References
Hemicelluloses	Xylan	LM10	(1,4)-β-xylosyl residues	McCartney et al., 2005
	Arabinoxylan and low-substituted xylan	LM11	(1,4)-β-xylosyl residues	McCartney et al., 2005
	Grass Heteroxylan	LM27	Unknown	Cornuault et al.,2015
	Glucuronoxylan	LM28	Glucuronosyl residues of xylan	Cornuault et al.,2015
	Feruloylated polymers	LM12	Feruloylated xylan	Pedersen et al., 2012; Bozbuga et al., 2018
	Mixed linkage glucan (MLG)	MLG	(1,3; 1,4)-β-D-glucan	Meıkle et al., 1994; Vega-Sánchez et al., 2013
Pectins	Homogalacturonans (HGs)	LM19	HG with low degree of esterification	Verhertbruggen et al., 2009; Ordaz-Ortiz et al., 2009
		LM20	HG with high degree of esterification	Verhertbruggen et al., 2009; Ordaz-Ortiz et al., 2009
	Galactan chains	LM5	(1,4)-β-D-galactan, Rhamnogalacturonan-I (RG-I)	Jones et al. ,1997; Willats et al., 1998; Ermel et al., 2000
	Arabinan chains	LM6	(1,5)-α-L-highly branched arabinan, RG-I	Willats et al., 1998; Lee et al., 2005; Moller et al., 2007
Extensins	Extensin from rice	LM1	Unknown	Smallwood et al.,1995
	Extensin from carrot	JIM11	Unknown	Smallwood et al.,1994; Yates et Knox, 1994
	Extensin from carrot	JIM12	Unknown	Smallwood et al.,1994
	Extensin from pea	JIM19	Unknown	Knox et al., 1995; Wang et al., 1995
	Extensin from pea	JIM20	Unknown	Smallwood et al.,1994; Pattathil et al., 2010
Arabinogalactan proteins (AGPs)	AGP from rice	LM2	β-D-GlcpA	Smallwood et al.,1996; Yates et al., 1996
	AGP from carrot	JIM13	β-D-GlcA-(1,3)-α-D-GalA-(1,2)-α-L-Rha	Yates and Knox, 1994; Yates et al.,1996
	AGP from carrot	JIM15	Unknown	Yates and Knox, 1994; Yates et al.,1996
	AGP from carrot	JIM16	Unknown	Yates and Knox, 1994; Yates et al.,1996
	AGP from sugar beet	JIM8	Unknown	Pennell et al.,1991

VI. References

Achouak W, Conrod S, Cohen V, Heulin T. 2004. Phenotypic variation of *Pseudomonas brassicacearum* as a plant root-colonization strategy. Molecular Plant-Microbe Interactions **17**, 872–879.

Achouak W, Sutra L, Heulin T, Meyer JM, Fromin N, Degraeve S, Christen R, Gardan L. 2000. *Pseudomonas brassicacearum* sp. nov. and *Pseudomonas thivervalensis* sp. nov., two root-associated bacteria isolated from *Brassica napus* and *Arabidopsis thaliana*. International Journal of Systematic and Evolutionary Microbiology **50**, 9–18.

Alberts B, Johnson A, Lewis J, Raff M, Roberts K, Walter P. 2002. Molecular biology of the cell, 4th edition (New York: Garland Science).

Alkooranee JT, Aledan TR, Ali AK, Lu G, Zhang X, Wu J, Fu C, Li M. 2017. Detecting the hormonal pathways in oilseed rape behind induced systemic resistance by *Trichoderma harzianum* TH12 to *Sclerotinia sclerotiorum*. PLoS One **12**, e0168850.

Allard G, Nelson CJ. 1991. Photosynthate partitioning in basal zones of tall fescue leaf blades. Plant Physiology **95**, 663–668.

An C, Mou Z. 2011. Salicylic acid and its function in plant immunity. Journal of Integrative Plant Biology **53**, 412–428.

Andème-Onzighi C, Girault R, His I, Morvan C, Driouich A. 2000. Immunocytochemical characterization of early-developing flax fiber cell walls. Protoplasma **213**, 235–245.

Apel K, Hirt H. 2004. Reactive oxygen species: metabolism, oxidative stress, and signal transduction. Annual Review of Plant Biology **55**, 373–399.

Arnaud C, Bonnot C, Desnos T, Nussaume L. 2010. The root cap at the forefront. Comptes Rendus Biologies **333**, 335–343.

Arnon DI, Hoagland DR. 1940. Crop production in artificial culture solutions and in soils with special reference to factors influencing yields and absorption of inorganic nutrients. Soil Science **50**, 463–485.

Arraño-Salinas P, Domínguez-Figueroa J, Herrera-Vásquez A, Zavala D, Medina J, Vicente-Carbajosa J, Meneses C, Canessa P, Moreno AA, Blanco-Herrera F. 2018. WRKY7, -11 and -17 transcription factors are modulators of the bZIP28 branch of the unfolded protein response during PAMP-triggered immunity in *Arabidopsis thaliana*. Plant Science **277**, 242–250.

Atsumi G, Kagaya U, Kitazawa H, Nakahara KS, Uyeda I. 2009. Activation of the salicylic acid signaling pathway enhances clover yellow vein virus virulence in susceptible pea cultivars. Molecular Plant-Microbe Interactions **22**, 166–175.

Attard A, Gourgues M, Callemeyn-Torre N, Keller H. 2010. The immediate activation of defense responses in Arabidopsis roots is not sufficient to prevent *Phytophthora parasitica* infection. New Phytologist **187**, 449–460.

Ausubel FM. 2005. Are innate immune signaling pathways in plants and animals conserved? Nature Immunology **6**, 973–979.

Bacete L, Mélida H, Miedes E, Molina A. 2018. Plant cell wall-mediated immunity: cell wall changes trigger disease resistance responses. The Plant Journal **93**, 614–636.

Bacic A, Harris PJ, Stone BA. 1988. Structure and function of plant cell walls. In: The Biochemistry of Plants, Vol 14. Ed. J Priess (Academic Press, New York), 297–371.

Bacic A, Moody SF, Clarke AE. 1986. Structural analysis of secreted root slime from maize (*Zea mays* L.). Plant Physiology **80**, 771–777.

Badri DV, Loyola-Vargas VM, Du J, Stermitz FR, Broeckling CD, Iglesias-Andreu L, Vivanco JM. 2008. Transcriptome analysis of Arabidopsis roots treated with signaling compounds: a focus on signal transduction, metabolic regulation and secretion. New Phytologist **179**, 209–223.

Badri DV, Vivanco JM. 2009. Regulation and function of root exudates. Plant, Cell & Environment **32**, 666–681.

Baetz U, Martinoia E. 2014. Root exudates: the hidden part of plant defense. Trends in Plant Science **19**, 90–98.

Bais HP, Weir TL, Perry LG, Gilroy S, Vivanco JM. 2006. The role of root exudates in rhizosphere interactions with plants and other organisms. Annual Review of Plant Biology **57**, 233–266.

Ball S, Colleoni C, Cenci U, Raj JN, Tirtiaux C. 2011. The evolution of glycogen and starch metabolism in eukaryotes gives molecular clues to understand the establishment of plastid endosymbiosis. Journal of Experimental Botany **62**, 1775–1801.

Balmer D, de Papajewski DV, Planchamp C, Glauser G, MauchMani B. 2013. Induced resistance in maize is based on organ-specific defence responses. The Plant Journal **74**, 213–225.

Balmer D, Mauch-Mani B. 2013. More beneath the surface? Root versus shoot antifungal plant defenses. Frontiers in Plant Science **4**, 256.

Bancal P, Henson CA, Gaudillère JP, Carpita NC. 1991. Fructan chemical structure and sensitivity to an exohydrolase. Carbohydrate Research **217**, 137–151.

Banguela A, Hernández L. 2006. Fructans: from natural sources to transgenic plants. Biotecnologia Aplicada **160**, 811–820.

Basu D, Liang Y, Liu X, Himmeldirk K, Faik A, Kieliszewski M, Held M, Showalter AM. 2013. Functional identification of a hydroxyproline-O-galactosyltransferase specific for arabinogalactan protein biosynthesis in *Arabidopsis*. Journal of Biological Chemistry **288**, 10132–10143.

Basu D, Tian L, Wang W, Bobbs S, Herock H, Travers A, Showalter AM. 2015a. A small multigene hydroxyproline-O-galactosyltransferase family functions in arabinogalactan-protein glycosylation, growth and development in Arabidopsis. BMC Plant Biology **15**, 295.

Basu D, Wang W, Ma S, DeBrosse T, Poirier E, Emch K, Soukup E, Tian L, Showalter AM. 2015b. Two hydroxyproline galactosyltransferases, GALT5 and GALT2, function in arabinogalactan-protein glycosylation, growth and development in Arabidopsis. PLoS One **10**, e0125624.

Basu U, Francis JL, Whittal RM, Stephens JL, Wang Y, Zaiane OR, Goebel R, Muench DG, Good AG, Taylor GJ. 2006. Extracellular proteomes of *Arabidopsis thaliana* and *Brassica napus* roots: analysis and comparison by MudPIT and LC-MS/MS. Plant and Soil **286**, 357–376.

Battey NH, Blackbourn HD. 1993. The control of exocitosis in plant cells. New Phytologist **125**, 307–308.

Baum T, Wubben MK, Hardyy KA, Su H, Rodermel SR. 2000. A screen for *Arabidopsis thaliana* mutants with altered susceptibility to *Heterodera schachtii*. Journal of Nematology **32**, 166–173.

Bellincampi D, Cervone F, Lionetti V. 2014. Plant cell wall dynamics and wall-related susceptibility in plant-pathogen interactions. Frontiers in Plant Science **5**, 228.

Benjamins R, Scheres B. 2008. Auxin: the looping StAR in plant development. Annual Review of Plant Biology **59**, 443–465.

Benkeblia N, Onodera S, Shiomi N. 2005. Variation in 1-fructo-exohydrolase (1-FEH) and 1-kestose-hydrolysing (1-KH) activities and fructo-oligosaccharide (FOS) status in onion bulbs. Influence of temperature and storage time. Journal of the Science of Food and Agriculture **85**, 227–234.

Bennett T, Scheres B. 2010. Root development-two meristems for the price of one? Current Topics in Development Biology **91**, 67–102.

Bennett T, van den Toorn A, Willemsen V, Scheres B. 2014. Precise control of plant stem cell activity through parallel regulatory inputs. Development **141**, 4055–4064.

Benot ML, Morvan-Bertrand A, Mony C, Huet J, Sulmon C, Decau ML, Prud'homme MP, Bonis A. 2019. Grazing intensity modulates carbohydrate storage pattern in five grass species from temperate grasslands. Acta Oecologica **95**, 108–115.

Berckmans B, Kirschner G, Gerlitz N, Stadler R, Simon R. 2020. CLE40 signaling regulates root stem cell fate. Plant Physiology **182**, 1776–1792.

Berendsen RL, Pieterse CM Bakker PA. 2012. The rhizosphere microbiome and plant health. Trends in Plant Science **17**, 478–486.

Bereswill S, Jock S, Aldridge P, Janse JD, Geider K. 1997. Molecular characterization of natural *Erwinia amylovora* strains deficient in levan synthesis. Physiological and Molecular Plant Pathology **51**, 215–225.

Berrocal-Lobo M, Molina A, Solano R. 2002. Constitutive expression of ETHYLENE-RESPONSE-FACTOR1 in Arabidopsis confers resistance to several necrotrophic fungi. The Plant Journal **29**, 23–32.

Berrocal-Lobo M, Molina A. 2008. Arabidopsis defense response against *Fusarium oxysporum*. Trends in Plant Science **13**, 145–150.

Bertin C, Yang X, Weston LA. 2003. The role of root exudates and allelochemicals in the rhizosphere. Plant and Soil **256**, 67–83.

Bertini L, Proietti S, Aleandri MP, Mondello F, Sandini S, Caporale C, Caruso C. 2012. Modular structure of HEL protein from Arabidopsis reveals new potential functions for PR-4 proteins. Biological Chemistry **393**, 1533–1546.

Bie X, Wang K, She M, Du L, Zhang S, Li J, Gao X, Lin Z, Ye X. 2012. Combinational transformation of three wheat genes encoding fructan biosynthesis enzymes confers increased fructan content and tolerance to abiotic stresses in tobacco. Plant Cell Reports **31**, 2229–2238.

Bogino P, Oliva M, Sorroche F, Giordano W. 2013. The role of bacterial biofilms and surface components in plant-bacterial associations. International Journal of Molecular Science **14**, 15838–15859.

Böhm H, Albert I, Oome S, Raaymakers TM, Van den Ackerveken G, Nürnberger T. 2014. A conserved peptide pattern from a widespread microbial virulence factor triggers pattern-induced immunity in *Arabidopsis*. PLoS pathogens **10**, e1004491.

Boller T, Felix G. 2009. A renaissance of elicitors: perception of microbe-associated molecular patterns and danger signals by pattern-recognition receptors. Annual Review of Plant Biology **60**, 379–406.

Bolouri Moghaddam MR, Van den Ende W. 2012. Sugars and plant innate immunity. Journal of Experimental Botany **63**, 3989–3998.

Bolouri Moghaddam MR, Van den Ende W. 2013. Sweet immunity in the plant circadian regulatory network. Journal of Experimental Botany **64**, 1439–1449.

Bonnett GD, Incoll LD. 1993. Effects on the stem of winter barley of manipulating the source and sink during grain-filling: II. Changes in the composition of water-soluble carbohydrates of internodes. Journal of Experimental Botany **44**, 83–91.

Bonnett GD, Simpson RJ. 1995 Fructan exohydrolase activities from *Lolium rigidum* that hydrolyze beta-2,1- and beta-2,6-glycosidic linkages at different rates. New Phytologist **131**, 199–209.

Borderies G, le Béchec M, Rossignol M, Lafitte C, Le Deunff E, Beckert M, Dumas C, Matthys-Rochon E. 2004. Characterization of proteins secreted during maize microspore culture: arabinogalactan proteins (AGPs) stimulate embryo development, European Journal of Cell Biology **83**, 205–212.

Bouton S, Leboeuf E, Mouille G, Leydecker MT, Talbotec J, Granier F, Lahaye M, Höfte H, Truong HN. 2002. QUASIMODO1 encodes a putative membrane-bound glycosyltransferase required for normal pectin synthesis and cell adhesion in Arabidopsis. Plant Cell **14**, 2577–2590.

Bowdish DME, Davidson DJ, Lau YE, Lee K, Scott MG, Hancock REW. 2005. Impact of LL-37 on anti-infective immunity. Journal of Leukocyte Biology **77**, 451–459.

Bradley DJ, Kjellbom P, Lamb CJ. 1992. Elicitor- and wound-induced oxidative cross-linking of a proline-rich plant cell wall protein: a novel, rapid defense response. Cell **70**, 21–30.

Brigham LA, Woo HH, Nicoll SM, Hawes MC. 1995. Differential expression of proteins and mRNAs from border cells and root tips of pea. Plant Physiology **109**, 457–463.

Brigham LA, Woo HH, Wen F, Hawes MC. 1998. Meristem-specific suppression of mitosis and a global switch in gene expression in the root cap of pea by endogenous signals. Plant Physiology **118**, 1223–1231.

Brinkmann V, Reichard U, Goosmann C, Fauler B, Uhlemann Y, Weiss DS, Weinrauch Y, Zychlinsky A. 2004. Neutrophil extracellular traps kill bacteria. Science **303**, 1532–1535.

Brocklebank KJ, Hendry GAF. 1989. Characteristics of plant species which store different types of reserve carbohydrates. New Phytologist **112**, 255–260.

Burton RA, Wilson SM, Hrmova M, Harvey AJ, Shirley NJ, Medhurst A, Stone BA, Newbigin EJ, Bacic A, Fincher GB. 2006. Cellulose synthase-like CslF genes mediate the synthesis of cell wall (1,3;1,4)-β-D-glucans. Science **311**, 1940-1942.

Caarls L, der Does D, van Hickman R, Jansen W, van Verk M C, Proietti S, Lorenzo O, Solano R, Pieterse CMJ, Van Wees SCM. 2016. Assessing the role of ETHYLENE RESPONSE FACTOR transcriptional repressors in salicylic acid-mediated suppression of jasmonic acid-responsive genes. Plant & Cell Physiology **58**, 266–278.

Caarls L, Pieterse CMJ, Van Wees SCM. 2015. How salicylic acid takes transcriptional control over jasmonic acid signaling. Frontiers in Plant Science **6**, 170.

Caffall KH, Mohnen D. 2009. The structure, function, and biosynthesis of plant cell wall pectic polysaccharides. Carbohydrate Research **344**, 1879–1900.

Cai M, Wang N, Xing C, Wang F, Wu K, Du X. 2013. Immobilization of aluminum with mucilage secreted by root cap and root border cells is related to aluminum resistance in *Glycine max* L. Environmental Science and Pollution Research **20**, 8924–8933.

Cairns AJ, Ashton JE. 1993. Species-dependent patterns of fructan synthesis by enzymes from excised leaves of oat, wheat, barley and timothy. New Phytologist **124**, 381–388.

Cairns AJ, Nash R, Machado De Carvalho MA, Sims IM. 1999. Characterization of the enzymatic polymerization of 2,6-linked fructan by leaf extracts from timothy grass (*Phleum pratense*). New Phytologist **142**, 79–91.

Calderan-Rodrigues MJ, Guimarães Fonseca J, de Moraes FE, Vaz Setem L, Carmanhanis Begossi A, Labate CA. 2019. Plant cell wall proteomics: a focus on monocot species, *Brachypodium distachyon*, *Saccharum* spp. and *Oryza sativa*. International Journal of Molecular Sciences **20**, 1975.

Canellas LP, Olivares FL. 2017. Production of border cells and colonization of maize root tips by *Herbaspirillum seropedicae* are modulated by humic acid. Plant and Soil **417**, 403–413.

Cannesan MA, Durand C, Burel C, Gangneux C, Lerouge P, Ishii T, Laval K, Follet-Gueye ML, Driouich A, Vicre-Gibouin M. 2012. Effect of arabinogalactan proteins from the root caps of pea and *Brassica napus* on *Aphanomyces euteiches* zoospore chemotaxis and germination. Plant Physiology **159**, 1658–1670.

Cannesan MA, Gangneux C, Lanoue A, Giron D, Laval K, Hawes M, Driouich A, Vicré-Gibouin M. 2011. Association between border cell responses and localized root infection by pathogenic *Aphanomyces euteiches*. Annals of Botany **108**, 459–469.

Cannon MC, Terneus K, Hall Q, Tan L, Wang Y, Wegenhart BL, Chen L, Lamport DTA, Chen Y, Kieliszewski MJ. 2008. Self-assembly of the plant cell wall requires an extensin scaffold. Proceedings of the National Academy of Sciences USA **105**, 2226–2231.

Cantarel BL, Coutinho PM, Rancurel C, Bernard T, Lombard V, Henrissat B. 2009. The Carbohydrate-Active EnZymes database (CAZy): an expert resource for glycogenomics. Nucleic Acids Research **37**, D233–8.

Carpita N, McCann M. 2000. The cell wall. In: Biochemistry and Molecular Biology of Plants. Eds. BB Buchanan, G Wilhelm, RL Jones (Rockville, IL: American Society of Plant Physiologists), 52–108.

Carpita NC, Gibeaut DM. 1993. Structural models of primary cell walls in flowering plants: consistency of molecular structure with the physical properties of the walls during growth. The Plant Journal **3**, 1–30.

Carpita NC, McCann MC. 2008. Maize and sorghum: genetic resources for bioenergy grasses. Trends in Plant Science **13**, 415–420.

Carpita NC. 1996. Structure and biogenesis of the cell walls of grasses. Annual Review of Plant Physiology and Plant Molecular Biology **47**, 445–476.

Carreras A, Bernard S, Durambur G, Gügi B, Loutelier C, Pawlak B, Boulogne I, Vicré M, Driouich A, Goffner D, Follet-Gueye ML. 2020. In vitro characterization of root extracellular trap and exudates of three Sahelian woody plant species. Planta **251**, 19.

Castilleux R, Plancot B, Ropitaux M, Carreras **A,** Leprince **J,** Boulogne **I,** Follet-Gueye **ML, Popper ZA,** Driouich **A,** Vicré **M**. 2018. Cell wall extensins in root–microbe interactions and root secretions. Journal of Experimental Botany **69**, 4235–4247.

Castilleux R, Plancot B, Gügi B, Attard A, Loutelier-Bourhis C, Lefranc B, Nguema-Ona E, Arkoun M, Yvin JC, Driouich A, Vicré M. 2020. Extensin arabinosylation is involved in root response to elicitors and limits oomycete colonization. Ann Bot **125**, 751-763.

Chaboud A, Rougier M. 1984. Identification and localization of sugar components of rice (*Oryza sativa* L.) root cap mucilage. Journal of Plant Physiology **116**, 323–330.

Chaboud A. 1983. Isolation, purification and chemical composition of maize root cap slime. Plant and Soil **73**, 395–402.

Chalhoub B, Denoeud F, Liu S, Parkin IAP, Tang H, Wang X, Chiquet J, Belcram H, Tong C, Samans B, Corréa M, Da Silva C, Just J, Falentin C, Koh CS, Le Clainche I, Bernard M, Bento P, Noel B, Labadie K, Alberti A, Charles M, Arnaud D, Guo H, Daviaud C, Alamery S, Jabbari K, Zhao M, Edger PP, Chelaifa H, Tack D, Lassalle G, Mestiri I, Schnel N, Le Paslier M-C, Fan G, Renault V, Bayer PE, Golicz AA, Manoli S, Lee T-H, Thi VHD, Chalabi S, Hu Q, Fan C, Tollenaere R, Lu Y, Battail C, Shen J, Sidebottom CHD, Wang X, Canaguier A, Chauveau A, Bérard A, Deniot G, Guan M, Liu Z, Sun F, Lim YP, Lyons E, Town CD, Bancroft I, Wang X, Meng J, Ma J, Pires JC, King GJ, Brunel D, Delourme R, Renard M, Aury JM, Adams KL, Batley J, Snowdon RJ, Tost J, Edwards D, Zhou Y, Hua W, Sharpe AG, Paterson AH, Guan C, Wincker P. 2014. Early allopolyploid evolution in the post-neolithic *Brassica napus* oilseed genome. Science **345**, 950–953.

Chambert R, Treboul G, Dedonder R. 1974. Kinetic studies of levansucrase of *Bacillus subtilis*. European Journal of Biochemistry **41**, 285–300.

Chatterton NJ, Harrison PA, Thornley WR, Bennett JH. 1993. Structures of fructan oligomers in Orchardgrass (*Dactylis glomarata* L.). Journal of Plant Physiology **142**, 552–556.

Chen F, Ro DK, Petri J, Gershenzon J, Bohlmann J, Pichersky E, Tholl D. 2004. Characterization of a root-specific Arabidopsis terpene synthase responsible for the formation of the volatile monoterpene 1,8-cineole. Plant Physiology **135**, 1956–1966.

Cheng LT, Zeng YJ, Chu CY, Wang HY. 2019. Development of a quick dot blot assay for the titering of bovine ephemeral fever virus. BMC Veterinary Research **15**, 313.

Cheong JJ, Choi YD. 2003. Methyl jasmonate as a vital substance in plants. Trends in Genetics **19**, 409–413.

Chevalier L, Bernard S, Ramdani Y, Lamour R, Bardor M, Lerouge P, Follet-Gueye ML, Driouich A. 2010. Subcompartment localization of the side chain xyloglucan-synthesizing enzymes within Golgi stacks of tobacco suspension-cultured cells. The Plant Journal **64**, 977–989.

Chuberre C, Plancot B, Driouich A, Moore JP, Bardor M, Gügi B, Vicré M. 2018. Plant immunity is compartmentalized and specialized in roots. Frontiers in Plant Science **9**, 1692.

Cimini S, Locato V, Vergauwen R, Paradiso A, Cecchini C, Vandenpoel L, Verspreet J, Courtin CM, D'Egidio MG, Van den Ende W, de Gara L. 2015. Fructan biosynthesis and degradation as part of plant metabolism controlling sugar fluxes during durum wheat kernel maturation. Frontiers in Plant Science **6**, 89.

Cochrane MP. 2000. Seed carbohydrates. In: Seed Technology and Its Biological Basis. Eds. M Black, JD Bewley (Boca Raton, FL: CRC Press), 85–120.

Coenen GJ, Bakx EJ, Verhoef RP, Schols HA, Voragen AGJ. 2007. Identification of the connecting linkage between homo- or xylogalacturonan and rhamnogalacturonan type I. Carbohydrate Polymers **70**, 224–235.

Collinge DB. 2009. Cell wall appositions: the first line of defense. Journal of Experimental Botany **60**, 351–352.

Cornuault V, Buffetto F, Rydahl MG, Marcus SE, Torode TA, Xue J, Crépeau MJ, Faria-Blanc N, Willats WG, Dupree P, Ralet MC, Knox JP. 2015. Monoclonal antibodies indicate low-abundance links between heteroxylan and other glycans of plant cell walls. Planta **242**, 1321–1334.

Cosgrove DJ, Jarvis MC. 2012. Comparative structure and biomechanics of plant primary and secondary cell walls. Frontiers in Plant Science **3**, 204.

Cosgrove DJ. 1997. Assembly and enlargement of the primary cell wall in plants. Annual Review of Cell and Developmental Biology **13**, 171–201.

Cosgrove DJ. 2005. Growth of the plant cell wall. Nature Reviews Molecular Cell Biology **6**, 850–861.

Cosgrove DJ. 2014. Re-constructing our models of cellulose and primary cell wall assembly. Current Opinion in Plant Biology **22**, 122–131.

Cosgrove DJ. 2018. Diffuse growth of plant cell walls. Plant Physiology **176**, 16–27.

Coventry HS, Dubery IA. 2001. Lipopolysaccharides from *Burkholderia cepacia* contribute to an enhanced defensive capacity and the induction of pathogenesis-related proteins in *Nicotianae tabacum*. Physiological and Molecular Plant Pathology **58**, 149–158.

Cui J, Bahrami AK, Pringle EG, Hernandez-Guzman G, Bender CL, Pierce NE, Ausubel FM. 2005. *Pseudomonas syringae* manipulates systemic plant defenses against pathogens and herbivores. Proceedings of the National Academy of Sciences USA **102**, 1791–1796.

Curlango-Rivera G, Huskey DA, Mostafa A, Kessler JO, Xiong Z, Hawes, MC. 2013. Intraspecies variation in cotton border cell production: rhizosphere microbiome implications. American Journal of Botany ***100***, 1706–1712.

Dangl JL, Jones JDG. 2001. Plant pathogens and integrated defence responses to infection. Nature **411**, 826–833.

Darvill AG, Albersheim P. 1984. Phytoalexins and their elicitors-a defense against microbial infection in plants. Annual Review of Plant Physiology **35**, 243–275.

Darvill JE, McNeil M, Darvill AG, Albersheim P. 1980. Structure of plant cell walls. XI. Glucuronoarabinoxylan, a second hemicellulose in the primary cell walls of suspension-cultured sycamore cells. Plant Physiology **66**, 1135–1139.

Daval S, Gazengel K, Belcour A, Linglin J, Guillerm-Erckelboudt AY, Sarniguet A, Manzanares-Dauleux MJ, Lebreton L, Mougel C. 2020. Soil microbiota diversity influences clubroot disease by modulating *Plasmodiophora brassicae* and *Brassica napus* transcriptomes. Microbial Biotechnology **13**, 1648–1672.

Davidsson PR, Kariola T, Niemi O, Palva ET. 2013. Pathogenicity of and plant immunity to soft rot pectobacteria. Frontiers in Plant Science **4**, 191.

De Coninck B, Le Roy K, Francis I, Clerens S, Vergauwen R, Halliday AM, Smith SM, Van Laere, A, Van den Ende W. 2005. Arabidopsis AtcwINV3 and 6 are not invertases but are fructan exohydrolases (FEHs) with different substrate specificities. Plant Cell & Environment **28**, 432–443.

De Coninck B, Van den Ende W, Le Roy K. 2007. Fructan exohydrolases (FEHs) in plants: properties, occurrence and 3-D structure. In: Recent advances in fructooligosaccharides research. Eds. N Shiomi, N Benkeblia, S Onodera (Research Signpost, India), 157–179.

De Roover J, Van Laere A, De Winter M, Timmermans JW, Van den Ende W. 1999. Purification and properties of a second fructan exohydrolase from the roots of *Cichorium intybus*. Physiologia Plantarum **106**, 28–34.

Dehors J, Mareck A, Kiefer-Meyer MC, Menu-Bouaouiche L, Lehner A, Mollet JC. 2019. Evolution of cell wall polymers in tip-growing land plant gametophytes: composition, distribution, functional aspects and their remodeling. Frontiers in Plant Science **10**, 441.

Deiana S, Gessa C, Palma A, Premoli A, Senette C. 2003. Influence of organic acids exuded by plants on the interaction of copper with the polysaccharidic components of the root mucilages. Organic Geochemistry **34**, 651–660.

Del Viso F, Puebla AF, Hopp HE, Heinz RA. 2009. Cloning and functional characterization of a fructan 1-exohydrolase (1-FEH) in the cold tolerant Patagonian species *Bromus pictus*. Planta **231**, 13–25.

De-la-Peña C, Lei Z, Watson BS, Sumner LW, Vivanco JM. 2008. Root microbe communication through protein secretion. Journal of Biological Chemistry **283**, 25247–25255.

Dennis PG, Miller AJ, Hirsch PR. 2010. Are root exudates more important than other sources of rhizodeposits in structuring rhizosphere bacterial communities? FEMS Microbiology Ecology **72**, 313–327.

Dewick PM. 2009. Medicinal natural products: a biosynthetic approach, 3rd edition. (Chichester, UK: AJ Wiley and Sons), 539.

Dhugga KS, Barreiro R, Whitten B, Stecca K, Hazebroek J, Randhawa GS, Dolan M, Kinney AG, Tomes D, Nichols S, Anderson P. 2004. Guar seed –mannan synthase is a member of the cellulose synthase super gene family. Science **303**, 363–366.

Doblin MS, Pettolino FA, Wilson SM, Campbell R, Burton RA, Fincher GB, Newbigin E, Bacic A. 2009. A barley cellulose synthase-like CSLH gene mediates (1,3;1,4)-β-D-glucan synthesis in transgenic Arabidopsis. Proceedings of the National Academy of Sciences USA **106**, 5996–6001.

Dodds PN, Rathjen JP. 2010. Plant immunity: towards an integrated view of plant-pathogen interactions. Nature Reviews Genetics **11**, 539–548.

Dogsa I, Brloznik M, Stopar D, Mandic-Mulec I. 2013. Exopolymer diversity and the role of levan in *Bacillus subtilis* biofilms. PLoS One **8**, e62044.

Driouich A, Cannesan MA, Dardelle F, Durand C, Plancot B, Bernard S, Follet-Gueye ML, Vicré-Gibouin M. 2012. Unity is strength: the power of border cells and border-like cells in relation with plant defense. In: Secretions and Exudates in Biological Systems. Eds. JM Vivanco, F Baluška (Berlin, Heidelberg: Springer Berlin Heidelberg), 91–107.

Driouich A, Durand C, Cannesan MA, Percoco G, Vicré-Gibouin M. 2010. Border cells versus border-like cells: are they alike? Journal of Experimental Botany **61**, 3827–3831.

Driouich A, Durand C, Vicré-Gibouin M. 2007. Formation and separation of root border cells. Trends in Plant Science **12**, 14–19.

Driouich A, Follet-Gueye ML, Vicré-Gibouin M, Hawes M. 2013. Root border cells and secretions as critical elements in plant host defense. Current Opinion in Plant Biology **16**, 489–495.

Driouich A, Gaudry A, Pawlak B, Moore JP. 2021. Root cap–derived cells and mucilage: a protective network at the root tip. Protoplasma **258**, 1179–1185.

Driouich A, Smith C, Ropitaux M, Chambard **M,** Boulogne **I,** Bernard **S,** Follet-Gueye **ML,** Vicré **M,** Moore **J**. 2019. Root extracellular traps versus neutrophil extracellular traps in host defence, a case of functional convergence? Biological Reviews **94**, 1685–1700.

Duchateau N, Karlheinz B, Simmen U, Wiemken A, Bancal P. 1995. Sucrose:fructan 6-fructosyltransferase, a key enzyme for diverting carbon from sucrose to fructan in barley leaves. Plant physiology **107**, 1249–1255.

Duchow S, Dahlke RI, Geske T, Blaschek W, Classen B. 2016. Arabinogalactan-proteins stimulate somatic embryogenesis and plant propagation of *Pelargonium sidoides*. Carbohydrate Polymers **152**, 149–155.

Dupuy L, Mackenzie J, Haseloff J. 2010. Coordination of plant cell division and expansion in a simple morphogenetic system. Proceedings of the National Academy of Sciences USA **107**, 2711–2716.

Durand C, Vicre-Gibouin M, Follet-Gueye ML, Duponchel L, Moreau M, Lerouge P, Driouich A. 2009. The organization pattern of root border-like cells of Arabidopsis is dependent on cell wall homogalacturonan. Plant Physiology **150**, 1411–1421.

Duran-Flores D, Heil M. 2017. Extracellular self-DNA as a damage-associated molecular pattern (DAMP) that triggers self-specific immunity induction in plants. Brain, Behavior, and Immunity **72**, 78–88.

Durrant WE, Dong X. 2004. Systemic acquired resistance. Annual Review of Phytopathology **42**, 185–209.

Ebringerová A, Hromádková Z, Heinze T. 2005. Hemicellulose. In: Polysaccharides I. Advances in Polymer Science, Vol 186. Ed. T Heinze (Springer, Berlin, Heidelberg).

Ellis M, Egelund J, Schultz CJ, Bacic A. 2010. Arabinogalactan-proteins: key regulators at the cell surface? Plant Physiology **153**, 403–419.

Endo I, Tange T, Osawa H. 2011. A cell-type-specific defect in border cell formation in the *Acacia mangium* root cap developing an extraordinary sheath of sloughed-off cells. Annals of Botany **108**, 279–290.

Erb M, Lenk C, Degenhardt J, Turlings TC. 2009. The underestimated role of roots in defense against leaf attackers. Trends in plant science **14**, 653–659.

Evidente A, Cimmino A, Fernández-Aparicio M, Andolfi A, Rubiales D, Motta A. 2010. Polyphenols, including the new Peapolyphenols A−C, from pea root exudates stimulate *Orobanche foetida* seed germination. Journal of Agricultural and Food Chemistry **58**, 2902–2907.

Faik A. 2010. Xylan biosynthesis: news from the grass. Plant Physiology **153**, 396–402.

Fangel JU, Ulvskov P, Knox JP, Mikkelsen MD, Harholt J, Popper ZA, Willats WGT. 2012. Cell wall evolution and diversity. Frontiers in Plant Science **3**, 152.

Felix G, Regenass M, Boller T. 1993. Specific perception of subnanomolar concentrations of chitin fragments by tomato cells: induction of extracellular alkalinization, changes in protein phosphorylation, and establishment of a refractory state. The Plant Journal **4**, 307–316.

Felix G, Duran JD, Volko S, Boller T.1999. Plants have a sensitive perception system for the most conserved domain of bacterial flagellin. Plant J **18**, 265–276

Ferrari S, Savatin DV, Gramegna G, Cervone F, De Lorenzo G. 2013. Oligogalacturonides: plant damage-associated molecular patterns and regulators of growth and development. Frontiers in Plant Science **4**, 49.

Fincher G. 2009. Exploring the evolution of (1,3;1,4)-beta-D-glucans in plant cell walls: comparative genomics can help! Current Opinion in Plant Biology **12**, 140–147.

Fincher GB, Stone BA, Clarke AE. 1983. Arabinogalactan-proteins: structure, biosynthesis, and function. Annual Review of Plant Biology **34**, 47–70.

Fopa Fomeju B, Falentin C, Lasalle G, Manzanares-Dauleux MJ, Delourme R. 2015. Comparative genomic analysis of duplicated homoeologous regions involved in the resistance of *Brassica napus* to stem canker. Frontiers in Plant Science **6**, 772.

Fragkostefanakis S, Sedeek KEM, Raad M, Zaki MS, Kalaitzis P. 2014. Virus induced gene silencing of three putative prolyl 4-hydroxylases enhances plant growth in tomato (*Solanum lycopersicum*). Plant Molecular Biology **85**, 459–471.

Frehner M, Keller F, Wiemken A. 1984. Localisation of fructan metabolism in the vacuoles isolated from protoplasts of jerusalem artichoke tubers (*Helianthus tuberosus* L.). Journal of Plant Physiology **16**, 197–208.

Fry SC, Nesselrode BH, Miller JG, Mewburn BR. 2008. Mixed-linkage (1-3,1-4)-beta-D-glucan is a major hemicellulose of *Equisetum* (horsetail) cell walls. New Phytologist **179**, 104–115.

Fry SC. 2004. Primary cell wall metabolism: tracking the careers of wall polymers in living plant cells. New Phytologist **161**, 641–675.

Fuchs A, Bruijn JMDE, Niedeveld CJ. 1985. Bacteria and yeasts as possible candidates for the production of inulinases and levanases. Antonie Van Leeuwenhoek **51**, 333–343.

Galindo-González L, Manolii V, Hwang SF, Strelkov SE. 2020. Response of *Brassica napus* to *Plasmodiophora brassicae* involves salicylic acid-mediated immunity: an RNA-seq-based study. Frontiers in Plant Science **11**, 1025.

Galloway TS, Cole M, Lewis C. 2017. Interactions of microplastic debris throughout the marine ecosystem. Nature Ecology & Evolution **1**, 116.

Gao Y, Lipton AS, Wittmer Y, Murray DT, Mortimer JC. 2020. A grass-specific cellulose–xylan interaction dominates in sorghum secondary cell walls. Nature Communications **11**, 6081.

Gaspar YM, Nam J, Schultz CJ, Lee LY, Gilson PR, Gelvin SB, Bacic A. 2004. Characterization of the Arabidopsis lysine-rich arabinogalactan-protein AtAGP17 mutant (rat1) that results in a decreased efficiency of *Agrobacterium* transformation. Plant Physiology **135**, 2162–2171.

Geier G, Geider K. 1993. Characterization and influence on virulence of the levansucrase gene from the fireblight pathogen *Erwinia amylovora*. Physiology and Molecular Plant Pathology **42**, 387–404.

Gibson LJ. 2012. The hierarchical structure and mechanics of plant materials. Journal of the Royal Society Interface **9**, 2749–2766.

Gislason AS, de Kievit TR. 2020. Friend or foe? Exploring the fine line between *Pseudomonas brassicacearum* and phytopathogens. Journal of Medical Microbiology **69**, 347–360.

Glazebrook J. 2005. Contrasting mechanisms of defense against biotrophic and necrotrophic pathogens. Annual Review of Phytopathology **43**, 205–227.

Goellner EM, Gramann JC, Classen B. 2013. Antibodies against Yariv's reagent for immunolocalization of arabinogalactan-proteins in aerial parts of *Echinacea purpurea*. Planta Medica **79**, 175–180.

Gohel V, Vyas P, Chhatpar HS. 2005. Activity staining method of chitinase on chitin agar plate through polyacrylamide gel electrophoresis. African Journal of Biotechnology **4**, 87–90.

Gómez-Gómez L, Boller T. 2002. Flagellin perception: a paradigm for innate immunity. Trends in Plant Science **7**, 251–256.

Gorshkova T, Morvan C. 2006. Secondary cell-wall assembly in flax phloem fibres: role of galactans. Planta **223**, 149–158.

Gouveia BC, Calil IP, Machado JP, Santos AA, Fontes EP. 2017. Immune receptors and co-receptors in antiviral innate immunity in plants. Frontiers in Microbiology **7**, 2139.

Griffin GJ, Hale MG, Shay FJ. 1976. Nature and quantity of sloughed organic matter produced by roots of axenic peanut plants. Soil Biology and Biochemistry **8**, 29–32.

Groot EP, Doyle JA, Nichol SA, Rost TL. 2004. Phylogenetic distribution and evolution of root apical meristem organization in dicotyledonous angiosperms. International Journal of Plant Science **165**, 97–105.

Gruber BD, Giehl RF, Friedel S, von Wirén N. 2013. Plasticity of the Arabidopsis root system under nutrient deficiencies. Plant Physiology **163**, 161–179.

Grudkowska M, Zagdańska B. 2004. Multifunctional role of plant cysteine proteinases. Acta Biochimica Polinica **51**, 609–624.

Guckert A, Breisch H, Reisinger O. 1975. Etude au microscope électronique des relations mucigel–argile–microorganismes. Soil Biology and Biochemistry **7**, 241–250.

Gunawardena U, Hawes MC. 2002. Tissue specific localization of root infection by fungal pathogens: role of root border cells. Molecular Plant-Microbe Interactions **15**, 1128–1136.

Gunawardena U, Rodriguez M, Straney D, Romeo JT, VanEtten HD, Hawes MC. 2005. Tissue-specific localization of pea root infection by *Nectria haematococca*. Mechanisms and consequences. Plant Physiology **137**, 1363–1374.

Gust AA, Pruitt R, Nürnberger T. 2017. Sensing danger: key to activating plant immunity. Trends in Plant Science **22**, 779–791.

Haberlandt G. 1914. Physiological plant antomy. London, Macmillan and Co.

Haichar FZ, Santaella C, Heulin T, Achouak W. 2014. Root exudates mediated interactions belowground. Soil Biology and Biochemistry **77**, 69–80.

Hall B, Bona C, Victor-Kobrin C. 1990. Binding specificities of inulin-binding immunoglobulins for sinistrin and oligosaccharides isolated from asparagus roots. Molecular Immunology **27**, 351–361.

Halverson TWR, Wilton M, Poon KKH, Petri B, Lewenza S. 2015. DNA is an antimicrobial component of Neutrophil Extracellular Traps. PLoS Pathogens **11**, 4593.

Hamamoto L, Hawes MC, Rost TL. 2006. The production and release of living root cap border cells is a function of root apical meristem type in dicotyledonous angiosperm plants. Annals of Botany **97**, 917–923.

Han Z, Liu Y, Deng X, Liu D, Liu Y, Hu Y, Yan Y. 2019. Genome-wide identification and expression analysis of expansin gene family in common wheat (*Triticum aestivum* L.). BMC Genomics **20**, 101.

Hano C, Addi M, Bensaddek L, Crônier D, Baltora-Rosset S, Doussot J, Maury S, Mesnard F, Chabbert B, Hawkins S, Lainé E, Lamblin F. 2006. Differential accumulation of monolignol-derived compounds in elicited *fl*ax (Linum usitatissimum) cell suspension cultures. Planta **223,** 975–989.

Harris PJ. 2006. Primary and secondary plant cell walls: a comparative overview. New Zealand Journal of Forestry Science **36**, 36–53.

Hatfield RD, Wilson JR, Mertens DR. 1999. Composition of cell walls isolated from cell types of grain sorghum stems. Journal of the Science of Food and Agriculture **79**, 891–899.

Hawes M, Allen C, Turgeon BG, Curlango-Rivera G, Minh Tran T, Huskey DA, Xiong Z. 2016. Root border cells and their role in plant defense. Annual Review of Phytopathology **54**, 143–161.

Hawes MC, Bengough G, Cassab G, Ponce G. 2003. Root caps and rhizosphere. Journal of Plant Growth Regulation **21**, 352–367.

Hawes MC, Brigham LA, Wen F, Woo HH, Zhu Y. 1998. Function of root border cells in plant health: pioneersin the rhizosphere. Annual Review of Phytopathology **36**, 311–327.

Hawes MC, Brigham LA. 1992. Impact of root border cells on microbial populations in the rhizosphere. Advances in Plant Pathology **8**, 119–148.

Hawes MC, Curlango-Rivera G, Wen F, White GJ, Van Etten HD, Xiong Z. 2011. Extracelluar DNA: the tip of root defenses. Plant Science **180**, 741–745.

Hawes MC, Curlango-Rivera G, Xiong Z Kessler JO. 2012. Roles of root border cells in plant defense and regulation of rhizosphere microbial populations by extracellular DNA 'trapping.' Plant and Soil **355**, 1–16.

Hawes MC, Gunawardena U, Miyasaka S, Zhao X. 2000. The role of root border cells in plant defense. Trends in Plant Science **5**, 128–133.

Hawes MC, Lin HJ. 1990. Correlation of pectolytic enzyme activity with the programmed release of cells from root caps of pea (*Pisum sativum*). Plant Physiology **94**, 1855–1859.

Hawes MC, Pueppke SG. 1986. Sloughed peripheral root cap cells: yield from different species and callus formation from single cells. American Journal of Botany **73**, 1466-1473.

Hellemans J, Mortier G, de Paepe A, Speleman F, Vandesompele J. 2007. qBase relative quantification framework and software for management and automated analysis of real-time quantitative PCR data. Genome Biology **8**, R19.

Hendry GAF. 1993. Evolutionary origins and natural functions of fructans - a climatological, biogeographic and mechanistic appraisal. New Phytologist **123**, 3–14.

Henry G, Thonart P, Ongena M. 2012. PAMPs, MAMPs, DAMPs and others: an update on the diversity of plant immunity elicitors. Biotechnology, Agronomy and Society and Environment **16**, 257–268.

Henson CA, Livingston DPIII. 1996. Purification and characterization of an oat fructan exohydrolase that preferentially hydrolyzes beta-2,6-fructans. Plant Physiology **110**, 639–644

Henson CA, Livingston DPIII. 1998. Characterization of a fructan exohydrolase purified from barley stems that hydrolyzes multiple fructofuranosidic linkages. Plant Physiology and Biochemistry **36**, 715–720.

Hermanns M, Slusarenko AJ, Schlaich NL. 2003. Organ-specificity in a plant disease is determined independently of R gene signaling. Molecular Plant-Microbe Interactions **16**, 752–759.

Hernández L, Sotolongo M, Rosabal Y, Menéndez C, Ramírez R, Caballero-Mellado J, Arrieta J. 2000. Structural levansucrase gene (lsdA) constitutes a functional locus conserved in the species *Gluconacetobacter diazotrophicus*. Archives of Microbiology **174**, 120–124.

Hettwer U, Gross M, Rudolph K. 1995. Purification and characterization of an extracellular levansucrase from *Pseudomonas syringae* pv. *phaseolicola*. Journal of Bacteriology **177**, 2834–2839.

Heyer AG, Schroeer B, Radosta S, Wolff D, Czapla S, Springer J. 1998) Structure of the enzymatically synthesized fructan inulin. Carbohydrate Research **313**, 165–174.

Hijazi M, Velasquez SM, Jamet E, Estevez JM, Albenne C. 2014. An update on post-translational modifications of hydroxyproline-rich glycoproteins: toward a model highlighting their contribution to plant cell wall architecture. Frontiers in Plant Science **5**, 395.

Himmelbauer M, Loiskandl W, Kastanek F. 2004. Estimating length, average diameter and surface area of roots using two different image analyses systems. Plant and Soil **260**, 111–120.

Hincha DK, Livingston DP, Premakumar R, Zuther E, Obel N, Cacela C, Heyer AG. 2007. Fructans from oat and rye: composition and effects on membrane stability during drying. Biochimica et Biophysica Acta **1768**, 1611–1619.

Hirao T, Fukatsu E, Watanabe A. 2012. Characterization of resistance to pine wood nematode infection in *Pinus thunbergii* using suppression subtractive hybridization. BMC Plant Biology **12**, 13.

His I, Andème-Onzighi C, Morvan C, Driouich A. 2001. Microscopic studies on mature flax fibers embedded in LR white: immunogold localization of cell wall matrix polysaccharides. Journal of Histochemistry and Cytochemistry **49**, 1525–1536.

Homann A, Biedendieck R, Götze S, Jahn D, Seibel J. 2007. Insights into polymer versus oligosaccharide synthesis: mutagenesis and mechanistic studies of a novel levansucrase from *Bacillus megaterium*. The Biochemical Journal **407**, 189–198.

Huang P-Y, Catinot J, Zimmerli L. 2016. Ethylene response factors in Arabidopsis immunity. Journal of Experimental Botany **67**, 1231–1241.

Huang X, Luo W, Wu S, Long Y, Li R, Zheng F, Greiner S, Rausch T, Zhao H. 2020. Apoplastic maize fructan exohydrolase Zm-6-FEH displays substrate specificity for levan and is induced by exposure to levan-producing bacteria. International Journal of Biological Macromolecules, **163,** 630–639.

Iijima M, Barlow PW, Bengough AG. 2003. Root cap structure and cell production rates of maize (*Zea mays*) roots in compacted sand. New Phytologist **160**, 127–134.

Iijima M, Griffiths B, Bengough AG. 2000. Sloughing of cap cells and carbon exudation from maize seedling roots in compacted sand. New Phytologist **145**, 477–482.

Iijima M, Higuchi T, Watanabe A, Bengough AG. 2004. Method to quantify root border cells in sandy soil. Soil Biology and Biochemistry **36**, 1517–1519.

Iiyama K, Lam TBT, Stone BA. 1990. Phenolic acid bridges between polysaccharides and lignin in wheat internodes. Phytochemistry **29**, 733–737.

Ingle RA, Carstens M, Denby KJ. 2006. PAMP recognition and the plant–pathogen arms race. BioEssays **28**, 880–889.

Ishii T. 1997. Structure and functions of feruloylated polysaccharides. Plant Science **127**, 111–127.

Jarvis MC. 1984. Structure and properties of pectin gels in plant-cell walls. Plant, Cell & Environment **7**, 153–164.

Jensen JK, Sorensen SO, Harholt J, Geshi N, Sakuragi Y, Moller I, Zandleven J, Bernal AJ, Jensen NB, Sorensen C, Pauly M, Beldman G, Willats WGT, Scheller HV. 2008. Identification of a xylogalacturonan xylosyltransferase involved in pectin biosynthesis in Arabidopsis. The Plant Cell **20**, 1289–1302.

Ji X, Van den Ende W, Schroeven L, Clerens S, Geuten K, Cheng S, Bennett J. 2007. The rice genome encodes two vacuolar invertases with fructan exohydrolase activity but lacks the related fructan biosynthesis genes of the Pooideae. New Phytologist **173**, 50–62.

Johnson KL, Cassin AM, Lonsdale A, Wong GKS, Soltis DE, Miles NW, Melkonian **M,** Melkonian **B,** Deyholos **MK,** Leebens-Mack **J,** Rothfels **CJ,** Stevenson **DW,** Graham **SW,** Wang **X,** Wu **S,** Pires **JC,** Edger **PP,** Carpenter **EJ,** Bacic **A,** Doblin **MS,** Schultz **CJ**. 2017. Insights into the evolution of hydroxyproline-rich glycoproteins from 1000 plant transcriptomes. Plant Physiology **174**, 904–921.

Johnson X, Lidgett A, Chalmers J, Guthridge K, Jones E, Cummings N, Spangenberg G. 2003. Isolation and characterisation of an invertase cDNA from perennial ryegrass (*Lolium perenne*). Journal of Plant Physiology **160**, 903–911.

Jones JDG, Dangl JL. 2006. The plant immune system. Nature **444**, 323–329.

Joseleau JP, Pérez S. 2016. The plant cell walls: complex polysaccharide nano-composites. Glycopedia.

Jost R, Altschmied L, Bloem E, Bogs J, Gershenzon J, Hähnel U, Hänsch R, Hartmann T, Kopriva S, Kruse C, Mendel RR, Papenbrock J, Reichelt M, Rennenberg H, Schnug E, Schmidt A, Textor S, Tokuhisa J, Wachter A, Wirtz M, Rausch T, Hell R. 2005. Expression profiling of metabolic genes in response to methyl jasmonate reveals regulation of genes of primary and secondary sulfur-related pathways in *Arabidopsis thaliana*. Photosynthesis Research **86**, 491–508.

Jourdan E, Ongena M, Thonart P. 2008. Caractéristiques moléculaires de l'immunité des plantes induite par les rhizobactéries non pathogènes. Biotechnologie, Agronomie, Société, Environnement **12**, 437–449.

Jung HJ. 2003. Maize stem tissues: ferulate deposition in developing internode cell walls. Phytochemistry **63**, 543–549.

Kamiya M, Higashio SY, Isomoto A, Kim JM, Seki M, Miyashima S, Nakajima K. 2016. Control of root cap maturation and cell detachment by BEARSKIN transcription factors in Arabidopsis. Development **143**, 4063–4072.

Kang X, Kirui A, Dickwella Widanage MC, Mentink-Vigier F, Cosgrove DJ, Wang T. 2019. Lignin-polysaccharide interactions in plant secondary cell walls revealed by solid-state NMR. Nature Communications **10**, 347.

Karve R, Suárez-Román F, Iyer-Pascuzzi AS. 2016. The transcription factor NIN-LIKE PROTEIN7 controls border-like cell release. Plant Physiology **171**, 2101–2111.

Katagiri F, Tsuda K. 2010. Understanding the plant immune system. Molecular Plant-Microbe Interactions **23**, 1531–1536.

Kawakami A, Yoshida M, Van den Ende W. 2005. Molecular cloning and functional analysis of a novel 6&1-FEH from wheat (*Triticum aestivum* L.) preferentially degrading small graminans like bifurcose. Gene **358**, 93–101.

Kawano T, Bouteau F. 2013. Salicylic acid-induced local and long-distance signaling models in plants. In: Long-distance systemic signalling and communication in plants. Ed. F Baluska (Springer-Verlag, Berlin), 23–52.

Keinath NF, Waadt R, Brugman R, Schroeder JI, Grossmann G, Schumacher K, Krebs M. 2015. Live cell imaging with R-GECO1 sheds light on flg22- and chitin-induced transient [Ca(2+)]cyt patterns in *Arabidopsis*. Molecular Plant **8**, 1188–1200.

Kieliszewski MJ, Lamport DTA. 1994. Extensin: repetitive motifs, functional sites, post-translational codes, and phylogeny. The Plant Journal **5**, 157–172.

Kirtel O, Lescrinier E, Van den Ende W, Öner ET. 2019. Discovery of fructans in Archaea. Carbohydrate Polymers **220**, 149–156.

Kitazawa K, Tryfona T, Yoshimi Y, Hayashi Y, Kawauchi S, Antonov L, Tanaka H, Takahashi T, Kaneko S, Dupree P, Tsumuraya Y, Kotake T. 2013. β-Galactosyl Yariv reagent binds to the β-1,3-galactan of arabinogalactan proteins. Plant Physiology **161**, 1117–1126.

Knee EM, Gong FC, Gao M, Teplitski M, Jones AR, Foxworthy A, Mort AJ, Bauer WD. 2001. Root mucilage from pea and its utilization by rhizosphere bacteria as a sole carbon source. Molecular Plant-Microbe Interactions **14**, 775–784.

Knoch E, Dilokpimol A, Geshi N. 2014. Arabinogalactan proteins : focus on carbohydrate active enzymes. Frontiers in Plant Science **5**, 198.

Knox JP, Linstead PJ, Peart J, Cooper C, Roberts K. 1991. Developmentally-regulated epitopes of cell surface arabinogalactan-proteins and their relation to root tissue pattern formation. The Plant Journal **1**, 317–326.

Knox JP, Peart J, Neill SJ. 1995. Identifcation of novel cell surface epitopes using a leaf epidermal strip assay system. *Planta* **196**, 266–270.

Knox JP. 2008. Revealing the structural and functional diversity of plant cell walls. Current Opinion in Plant Biology **11**, 308–313.

Koczan JM, McGrath MJ, Zhao Y, Sundin GW. 2009. Contribution of *Erwinia amylovora* exopolysaccharides amylovoran and levan to biofilm formation: implications in pathogenicity. Phytopathology **99**, 1237–1244.

Koo YM, Heo AY, Choi HW. 2020. Salicylic acid as a safe plant protector and growth regulator. Plant Pathology Journal **36**, 1–10.

Koornneef A, Leon-Reyes A, Ritsema T, Verhage A, Den Otter FC, Van Loon LC, Pieterse CMJ. 2008. Kinetics of salicylate-mediated suppression of jasmonate signaling reveal a role for redox modulation. Plant Physiology **147**, 1358–1368.

Koroney AS, Plasson C, Pawlak B, Sidikou R, Driouich A, Menu-Bouaouiche L, Vicré-Gibouin M. 2016. Root exudate of *Solanum tuberosum* is enriched in galactose-containing molecules and impacts the growth of *Pectobacterium atrosepticum*. Annals of Botany **118**, 797–808.

Kozlova LV, Nazipova AR, Gorshkov OV, Petrova AA, Gorshkova TA. 2020. Elongating maize root: zone-specific combinations of polysaccharides from type I and type II primary cell walls. Science Reports **10**, 10956.

Kumar M, Campbell L, Turner S. 2016. Secondary cell walls: biosynthesis and manipulation. Journal of Experimental Botany **67**, 515–531.

Kumar N, Iyer-Pascuzzi AS. 2020. Shedding the last layer: mechanisms of root cap cell release. Plants **9**, 308.

Kumpf RP, Nowack MK. 2015. The root cap: a short story of life and death. Journal of Experimental Botany **66**, 5651–5662.

Kunze G, Zipfel C, Robatzek S, Niehaus K, Boller T, Felix G. 2004. The N terminus of bacterial elongation factor Tu elicits innate immunity in Arabidopsis plants. The Plant Cell **16**, 3496–3507.

Lamb CJ, Lawton MA, Dron M, Dixon RA. 1989. Signals and transduction mechanisms for activation of plant defenses against microbial attack. Cell **56**, 215–224.

Lammens W, Le Roy K, Schroeven L, Van Laere A, Rabijns A, Van den Ende W. 2009. Structural insights into glycoside hydrolase family 32 and 68 enzymes: functional implications. Journal of Experimental Botany **60**, 727–740.

Lamport DTA, Kieliszewski MJ, Chen Y, Cannon MC. 2011. Role of the extensin superfamily in primary cell wall architecture. Plant Physiology **156**, 11–19.

Lampugnani ER, Khan GA, Somssich M, Persson S. 2018. Building a plant cell wall at a glance. Journal of Cell Science **131**, 207373.

Lasseur B, Lothier J, Wiemken A, Van Laere A, Morvan-Bertrand A, Van den Ende W, Prud'homme MP. 2011. Towards a better understanding of the generation of fructan structure diversity in plants: molecular and functional characterization of a sucrose:fructan 6-fructosyltransferase (6-SFT) cDNA from perennial ryegrass (*Lolium perenne*). Journal of Experimental Botany **62**, 1871–1885.

Le Berre JY, Gourgues M, Samans B, Keller H, Panabières F, Attard A. 2017. Transcriptome dynamic of Arabidopsis roots infected with *Phytophthora parasitica* identifies VQ29, a gene induced during the penetration and involved in the restriction of infection. PLoS One **12**, e019034.

Le Roy K, Lammens W, Verhaest M, De Coninck B, Rabijns A, Van Laere A, Van den Ende W. 2007a. Unraveling the difference between invertases and fructan exohydrolases: a single amino acid (Asp-239) substitution transforms Arabidopsis cell wall invertase1 into a fructan 1-exohydrolase. Plant physiology **145**, 616–625.

Lemarié S, Robert-Seilaniantz A, Lariagon C, Lemoine J, Manzanares-Dauleux MJ, Gravot A. 2015. Both the jasmonic acid and the salicylic acid pathways contribute to resistance to the biotrophic clubroot agent *Plasmodiophora brassicae* in Arabidopsis. Plant & Cell Physiology **56**, 2158–2168.

Lembre P, Cécile Lorentz C, Di Martino P. 2012. Exopolysaccharides of the biofilm matrix: a complex biophysical world. In: The Complex World of Polysaccharides. Ed. DN Karunaratne (London: Intech Open Science), 371–392.

Lerouxel O, Cavalier DM, Liepman AH, Keegstra K. 2006. Biosynthesis of plant cell wall polysaccharides - a complex process. Current Opinion in Plant Biology **9**, 621–630.

Li J, Brader G, Palva ET. 2004. The WRKY70 transcription factor: a node of convergence for jasmonate-mediated and salicylate-mediated signals in plant defense. The Plant Cell **16**, 319–331.

Li N, Han X, Feng D, Yuan D, Huang LJ. 2019. Signaling crosstalk between salicylic acid and ethylene/jasmonate in plant defense: do we understand what they are whispering? International Journal of Molecular Sciences, **20**, 671.

Liepman AH, Nairn CJ, Willats WGT, Sørensen I, Roberts AW, Keegstra K. 2007. Functional genomic analysis supports conservation of function among cellulose synthase-like a gene family members and suggests diverse roles of mannans in plants. Plant Physiology **143**, 1881–1893.

Lima JE, Kojima S, Takahashi H, von Wirén N. 2010. Ammonium triggers lateral root branching in Arabidopsis in an AMMONIUM TRANSPORTER1;3-dependent manner. The Plant cell **22**, 3621–3633.

Liu Z, Wu Y, Yang F, Zhang Y, Chen S, Xie Q, Tian X, Zhou JM. 2013. BIK1 interacts with PEPRs to mediate ethylene-induced immunity. Proceedings of the National Academy of Sciences USA **110**, 6205–6210.

Livingston DP, Henson CA. 1998. Apoplastic sugars, fructans, fructan exohydrolase and invertase in winter oat: responses to second-phase cold hardening. Plant Physiology **116**, 403–408.

Livingston DP, Hincha DK, Heyer AG. 2009. Fructan and its relationship to abiotic stress tolerance in plants. Cellular and Molecular Life Sciences **66**, 2007–2023.

Loix C, Huybrechts M, Vangronsveld J, Gielen M, Keunen E, Cuypers A. 2017. Reciprocal interactions between cadmium-induced cell wall responses and oxidative stress in plants. Fronters in Plant Science **8**, 1867.

Lombard V, Golaconda Ramulu H, Drula E, Coutinho PM, Henrissat B. 2014. The carbohydrate-active enzymes database (CAZy) in 2013. Nucleic Acids Research **42**, D490–5.

Lorenzo O, Piqueras R, Sánchez-Serrano JJ, Solano R. 2003. ETHYLENE RESPONSE FACTOR1 integrates signals from ethylene and jasmonate pathways in plant defense. The Plant Cell **15**, 165–178.

Lothier J, Lasseur B, Le Roy K, Van Laere A, Prud'homme MP, Barre P, Van den Ende W, Morvan-Bertrand A. 2007. Cloning, gene mapping and functional analysis of a fructan 1-exohydrolase (1-FEH) from *Lolium perenne* implicated in fructan synthesis rather than in fructan mobilization. Journal of Experimental Botany **58**, 1969–1983.

Lothier J, van Laere A, Prud'homme M-P, van den Ende W, Morvan-Bertrand A. 2014. Cloning and characterization of a novel fructan 6-exohydrolase strongly inhibited by sucrose in *Lolium perenne*. Planta **240**, 629–643.

Lynch JM, Whipps JM. 1990. Substrate flow in the rhizosphere. Plant and Soil **129**, 1–10.

Ma W, Muthreich N, Liao C, Franz-Wachtel M, Schütz W, Zhang F, Hochholdinger F, Li C. 2010. The mucilage proteome of maize (*Zea mays* L.) primary roots. Journal of Proteome Research **9**, 2968-2976.

Ma Y, Zeng W, Bacic A, Johnson KL. 2018. AGPs through time and space. In book: Annual Plant Reviews online, 1–38.

Maeda K, Kunieda T, Tamura K, Hatano K, Hara-Nishimura I, Shimada T. 2019. Identification of periplasmic root-cap mucilage in developing columella cells of *Arabidopsis thaliana*. Plant & Cell Physiology **60**, 1296–1303.

Makandar R, Nalam V, Chaturvedi R, Jeannotte R, Sparks AA, Shah J. 2010. Involvement of salicylate and jasmonate signaling pathways in Arabidopsis interaction with *Fusarium graminearum*. Molecular Plant-Microbe Interactions **23**, 861–870.

Malinovsky FG, Fangel JU, Willats WGT. 2014. The role of the cell wall in plant immunity. Frontiers in Plant Science **5**, 178.

Manceur AP, Zou W, Marcil A, Paquet E, Gadoury C, Jaentschke B, Li X, Petiot E, Durocher Y, Baardsnes J, Rosa-Calatrava M, Ansorge S, Kamen AA. 2017. Generation of monoclonal pan-hemagglutinin antibodies for the quantification of multiple strains of influenza. PLoS One **12**, e0180314.

Mancilla-Margalli N, Lopez MG. 2006. Water-Soluble Carbohydrates and fructan structure patterns from *Agave* and *Dasylirion* species. Journal of Agricultural and Food Chemistry **54**, 7832–7839.

Manzanares-Dauleux MJ, Delourme R, Baron F, Thomas G. 2000. Mapping of one major gene and of QTLs involved in resistance to clubroot in *Brassica napus*. Theoretical and Applied Genetics **101**, 885–891.

Mao JL, Miao ZQ, Wang Z, Yu LH, Cai XT, Xiang CB. 2016. Arabidopsis ERF1 mediates cross-talk between ethylene and auxin biosynthesis during primary root elongation by regulating ASA1 expression. PLoS Genetics **12**, e1005760.

Marcel S, Sawers R, Oakeley E, Angliker H, Paszkowski U. 2010. Tissue-adapted invasion strategies of the rice blast fungus *Magnaporthe oryzae*. The Plant Cell **22**, 3177–3187.

Martínez-Fleites C, Ortíz-Lombardía M, Pons T, Tarbouriech N, Taylor EJ, Arrieta JG, Hernández L, Davies GJ. 2005. Crystal structure of levansucrase from the Gram-negative bacterium *Gluconacetobacter diazotrophicus*. The Biochemical Journal **390**, 19–27.

Marx SP, Nösberger J, Frehner M. 1997a. Hydrolysis of fructan in grasses: a beta-(2-6)-linkage specific fructan-beta-fructosidase from stubble of *Lolium perenne*. Nature Biotechnology **135**, 279–290.

Marx SP, Nösberger J, Frehner M. 1997b. Seasonal variation of fructan-β- fructosidase (FEH) activity and characterization of a β-(2,1)-linkage specific FEH from tubers of Jerusalem Artichoke (*Helianthus tuberosus*). New Phytologist **135**, 267–277.

Marzec M, Szarejko I, Melzer M. 2015. Arabinogalactan proteins are involved in root hair development in barley. Journal of Experimental Botany **66**, 1245–1257.

Matros A, Peshev D, Peukert M, Mock HP, Van den Ende W. 2015. Sugars as hydroxyl radical scavengers: proof-of-concept by studying the fate of sucralose in Arabidopsis. The Plant Journal **82**, 822–839.

Matros A, Peukert M, Lahnstein J, Seiffert U, Burton R. 2019. Determination of fructans in plants: current analytical means for extraction, detection, and quantification. Annual Plant Reviews **2**, 1–39.

Mauch-Mani B, Baccelli I, Luna E, Flors V. 2017. Defense priming: an adaptive part of induced resistance. Annual Review of Plant Biology **68**, 485–512.

Mayers CN, Lee KC, Moore CA, Wong SM, Carr JP. 2005. Salicylic Acid-induced resistance to cucumber mosaic virus in squash and *Arabidopsis thaliana*: contrasting mechanisms of induction and antiviral action. Molecular Plant-Microbe Interactions **18**, 428–434.

McCartney L, Marcus SE, Knox JP. 2005. Monoclonal antibodies to plant cell wall xylans and arabinoxylans. Journal of Histochemistry and Cytochemistry **53**, 543–546.

McCully M. 1995. How do real roots work? (Some new views of root structure). Plant Physiology **109**, 1–6.

McCully ME. 1999. Roots in soil: unearthing the complexities of roots and their rhizospheres. Annual Review of Plant Physiology and Plant Molecular Biology **50**, 695–718.

Mellado-Mojica E, González de la Vara LE, López MG. 2017. Fructan active enzymes (FAZY) activities and biosynthesis of fructooligosaccharides in the vacuoles of *Agave tequilana* Weber Blue variety plants of different age. Planta **245**, 265–281.

Miedes E, Vanholme R, Boerjan W, Molina A. 2014. The role of the secondary cell wall in plant resistance to pathogens. Frontiers in Plant Science **5**, 358.

Millet YA, Danna CH, Clay NK, Songnuan W, Simon MD, Werck-Reichhart D, Ausubel FM. 2010. Innate immune responses activated in *Arabidopsis* roots by microbe-associated molecular patterns. The Plant Cell **22**, 973–990.

Mitchell RAC, Dupree P, Shewry PR. 2007. A novel bioinformatics approach identifies candidate genes for the synthesis and feruloylation of arabinoxylan. Plant Physiology **144**, 43–53.

Mohnen D. 2008. Pectin structure and biosynthesis. Current Opinion in Plant Biology **11**, 266–277.

Moody SF, Clarke AE, Bacic A. 1988. Structural analysis of secreted slime from wheat and cowpea roots. Phytochemistry **27**, 2857–2861.

Moore R, Evans ML, Fondern WM. 1990. Inducing gravitropic curvature of primary roots of *Zea mays* cv. Ageotropic. Plant Physiology **92**, 310–315.

Morel JL, Habib L, Plantureux S, Guckert A. 1991. Influence of maize root mucilage on soil aggregate stability. Plant and Soil **136**, 111–119.

Morris CE, Monier JM. 2003. The ecological significance of biofilm formation by plant-associated bacteria. Annual Review of Phytopathology **41**, 429–453.

Morvan A, Challe G, Prud'homme MP, Le Saos J, Boucaud J. 1997. Rise of fructan exohydrolase activity in stubble of *Lolium perenne* after defoliation is decreased by uniconazole, an inhibitor of the biosynthesis of gibberellins. New Phytologist **136**, 81–88.

Morvan-Bertrand A, Boucaud J, Le Saos J, Prudhomme MP. 2001. Roles of the fructans from leaf sheaths and from the elongating leaf bases in the regrowth following defoliation of *Lolium perenne* L. Planta **213**, 109–120.

Mravec J, Guo X, Hansen AR, Schückel J, Kračun SK, Mikkelsen MD, Mouille G, Johansen IE, Ulvskov P, Domozych DS, Willats WGT. 2017. Pea border cell maturation and release involve complex cell wall structural dynamics. Plant Physiology **174**, 1051–1066.

Mravec J, Kracun SK, Rydahl MG, Westereng B, Miart F, Clausen MH, Fangel JU, Daugaard M, Van Cutsem P, De Fine Licht HH, Höfte H, Malinovsky FG, Domozych DS, Willats WGT. 2014. Tracking developmentally regulated post-synthetic processing of homogalacturonan and chitin using reciprocal oligosaccharide probes. Development **141**, 4841–4850.

Muday GK, Rahman A, Binder BM. 2012. Auxin and ethylene: collaborators or competitors? Trends in Plant Science **17**, 181–95.

Navarro L, Dunoyer P, Jay F, Arnold B, Dharmasiri N, Mark E, Voinnet O, Jones JDG. 2006. A plant miRNA contributes to antibacterial resistance by repressing auxin signaling. Science **312**, 436–439.

Neik TX, Amas J, Barbetti M, Edwards D, Batley J. 2020. Understanding host–pathogen interactions in *Brassica napus* in the omics Era. Plants **9**, 1336.

Newman M-A, Sundelin T, Nielsen JT, Erbs G. 2013. MAMP (microbe-associated molecular pattern) triggered immunity in plants. Frontiers in Plant Science **4**, 1–14.

Ngou BPM, Ahn HK, Ding P, Jones JDG. 2021. Mutual potentiation of plant immunity by cell-surface and intracellular receptors. Nature **592**, 110–115.

Nguema-Ona E, Coimbra S, Vicré-Gibouin M, Mollet JC, Driouich A. 2012. Arabinogalactan proteins in root and pollen-tube cells: distribution and functional aspects. Annals of Botany **110**, 383–404.

Nguema-Ona E, Moore JP, Fagerström AD, Fangel JU, Willats WG, Hugo A, Vivier MA. 2013a. Overexpression of the grapevine PGIP1 in tobacco results in compositional changes in the leaf arabinoxyloglucan network in the absence of fungal infection. BMC Plant Biology **13**, 46.

Nguema-Ona E, Vicré-Gibouin M, Cannesan MA, Driouich A. 2013b. Arabinogalactan proteins in root–microbe interactions. Trends in Plant Science **18**, 440–449.

Nguema-Ona E, Vicré-Gibouin M, Gotté M, Plancot B, Lerouge P, Bardor M, Driouich A. 2014. Cell wall O-glycoproteins and N-glycoproteins: aspects of biosynthesis and function. Frontiers in Plant Science **5**, 499.

Nguyen NNT, Ranwez V, Vile D, Soulié MC, Dellagi A, Expert D, Gosti F. 2014. Evolutionary tinkering of the expression of PDF1s suggests their joint effect on zinc tolerance and the response to pathogen attack. Frontiers in Plant Science **5**, 70.

Nguyen QM, Iswanto A, Son GH, Kim SH. 2021. Recent advances in Effector-Triggered Immunity in plants: new pieces in the puzzle create a different paradigm. International Journal of Molecular Sciences, **22**, 4709.

Nicaise V, Roux M, Zipfel C. 2009. Recent advances in PAMP-Triggered Immunity against bacteria: Pattern Recognition Receptors watch over and raise the alarm. Plant Physiology **150**, 1638–1647.

Nishitani K, Nevins DJ. 1991. Glucuronoxylan xylanohydrolase. A unique xylanase with the requirement for appendant glucuronosyl units. Journal of Biological Chemistry **266**, 6539–6543.

Nishiyama Y. 2009. Structure and properties of the cellulose microfibril. Journal of Wood Science **55**, 241–249.

Norman-Setterblad C, Vidal S, Palva ET. 2000. Interacting signal pathways control defense gene expression in *Arabidopsis* in response to cell wall-degrading enzymes from *Erwinia carotovora*. Molecular Plant-Microbe Interactions **13**, 430–438.

Nothnagel E. 1997. Proteoglycans and related components in plant cells. International Review of Cytology **174**, 195–191.

O'Neill MA, Albersheim P, Darvill AG. 1990. The pectic polysaccharides of primary cell walls. In: Methods in Plant Biochemistry, 2. Ed. PM Dey (London: Academic Press), 415–441.

Ogawa-Ohnishi M, Matsubayashi Y. 2015. Identification of three potent hydroxyproline O-galactosyltransferases in Arabidopsis. The Plant Journal **81**, 736–746.

Oka T, Saito F, Shimma YI, Yoko-o T, Nomura Y, Matsuoka K, Jigami Y. 2010. Characterization of endoplasmic reticulum-localized UDP-D-Galactose: hydroxyproline O-galactosyltransferase using synthetic peptide substrates in Arabidopsis. Plant Physiology **152**, 332–340.

Olmos E, Garcia De La Garma J, Gomez-Jimenez MC, Fernandez-Garcia N. 2017. Arabinogalactan proteins are involved in salt-adaptation and vesicle trafficking in tobacco by-2 cell cultures. Frontiers in Plant Science **8, 1092.**

O'Malley RC, Barragan CC, Ecker JR. 2015. A user's guide to the Arabidopsis T-DNA insertion mutant collections. In: Plant Functional Genomics. Eds. J Alonso, A Stepanova (Humana Press, New York). Methods in Molecular Biology **1284**, 323–342.

Öner ET, Hernández L, Combie J. 2016. Review of levan polysaccharide: from a century of past experiences to future prospects. Biotechnology Advances **34**, 827–844.

Ortet P, Barakat M, Lalaouna D, Fochesato S, Barbe V, Vacherie B, Santaella C, Heulin T, Achouak W. 2011. Complete genome sequence of a beneficial plant root-associated bacterium, *Pseudomonas brassicacearum*. Journal of Bacteriology **193**, 3146.

Ould-Ahmed M. 2013. Métabolisme des fructanes au cours du développement et après récolte chez la fléole des prés (*Phleum pratense* L) : identification et analyse fonctionnelle de deux gènes codant des fructane exohydrolases (FEHs) à activité invertase. Thèse. Université du Québec en Abitibi Témiscamingue (Canada) et Université de Caen (France). 242p.

Ovide C, Kiefer-Meyer MC, Bérard C, Vergne N, Lecroq T, Plasson C, Burel C, Bernard S, Driouich A, Lerouge P, Tournier I, Dauchel H, Bardor M. 2018. Comparative in depth RNA sequencing of *P. tricornutum*'s morphotypes reveals specific features of the oval morphotype. Scientific Reports **8**, 14340.

Palin R, Geitmann A. 2012. The role of pectin in plant morphogenesis. Biosystems **109**, 397–402.

Panstruga R, Parker JE, Schulze-Lefert P. 2009. SnapShot: plant immune response pathways. Cell **136**, 978.

Papadopoulou GV, Maedicke A, Grosser K, van Dam NM, Martínez-Medina A. 2018. Defence signalling marker gene responses to hormonal elicitation differ between roots and shoots. AoB Plants **10**, ply031.

Park YB, Cosgrove DJ. 2015. Xyloglucan and its interactions with other components of the growing cell wall. Plant & Cell Physiology **56**, 180–194.

Parvanova D, Ivanov S, Konstantinova T, Karanov E, Atanassov A, Tsvetkov T, Alexieva V, Djilianov D. 2004. Transgenic tobacco plants accumulating osmolytes show reduced oxidative damage under freezing stress. Plant Physiology and Biochemistry **42**, 57–63.

Pattathil S, Avci U, Baldwin D, Swennes AG, McGill JA, Popper Z, Bootten T, Albert A, Davis RH, Chennareddy C, Dong R, O'Shea B, Rossi R, Leoff C, Freshour G, Narra R, O'Neil M, York WS, Hanh MG. 2010. *A comprehensive toolkit of plant cell wall glycan-directed monoclonal antibodies. Plant Physiology* **153***, 514–525.*

Pattathil S, Hahn MG, Dale BE, Chundawat SP. 2015. Insights into plant cell wall structure, architecture, and integrity using glycome profiling of native and AFEXTM-pre-treated biomass. Journal of Experimental Botany **66**, 4279–4294.

Pauly M, Gille S, Liu LF, Mansoori N, De Souza A, Schultink A, Xiong G. 2013. Hemicellulose biosynthesis. Planta **238**, 627–642.

Pauly M, Qin Q, Greene H, Albersheim P, Darvill A, York WS. 2001. Changes in the structure of xyloglucan during cell elongation. Planta **212**, 842–850.

Pavis N, Chatterton NJ, Harrison PA, Baumgartner S, Praznik W, Boucaud J, Prud'homme MP. 2001. Structure of fructans in roots and leaf tissues of *Lolium perenne*. The New Phytologist **150**, 83–95.

Pel MJC, Pieterse CMJ. 2013. Microbial recognition and evasion of host immunity. Journal of Experimental Botany **64**, 1237–1248.

Pennell RI, Janniche L, Kjellbom P, Scofield GN, Peart JM, Roberts K. 1991. Developmental regulation of a plasma membrane arabinogalactan protein epitope in oilseed rape flowers. The Plant Cell **3**, 1317–1326.

Penninckx IAMA, Thomma BPHJ, Buchala A, Métraux JP, Broekaerta WF. 1998. Concomitant activation of jasmonate and ethylene response pathways is required for induction of a plant defensin gene in Arabidopsis. The Plant Cell **10**, 2103–2113.

Penning BW, McCann MC, Carpita NC. 2019. Evolution of the cell wall gene families of grasses. Frontiers in Plant Science **10**, 1205.

Pereira AM, Pereira LG, Coimbra S. 2015. Arabinogalactan proteins: rising attention from plant biologists. Plant Reproduction **28**, 1–15.

Pérez S, Mazeau K, Hervé du Penhoat C. 2000. The three-dimensional structures of the pectic polysaccharides. Plant Physiology and Biochemistry **38**, 37–55.

Pérez-López AV, Simpson J, Clench MR, Gomez-Vargas AD, Ordaz-Ortiz JJ. 2021. Localization and composition of fructans in stem and rhizome of *Agave tequilana* Weber var. azul. Frontiers in Plant Science **11**, 608850.

Perilli S, Di Mambro R, Sabatini S. 2012. Growth and development of the root apical meristem. Current Opinion in Plant Biology **15**, 17–23.

Persello-Cartieaux F, David P, Sarrobert C, Thibaud MC, Achouak W, Robaglia C, Nussaume, L. 2001. Utilization of mutants to analyze the interaction between *Arabidopsis thaliana* and its naturally root-associated *Pseudomonas*. Planta **212**, 190–198.

Persello-Cartieaux F, Nussaume L, Robaglia C. 2003. Tales from the underground: molecular plant–rhizobacteria interactions. Plant, Cell & Environment **26**, 189–199.

Petricka JJ, Schauer MA, Megraw M, Breakfield NW, Thompson JW, Georgiev S, Soderblom EJ, Ohler U, Moseley MA, Grossniklaus U, **Benfey PN**. 2012. The protein expression landscape of the Arabidopsis root. Proceedings of the National Academy of Sciences USA **109**, 6811–6818.

Peukert M, Thiel J, Mock HP, Marko D, Weschke W, Matros A. 2016. Spatiotemporal dynamics of oligofructan metabolism and suggested functions in developing cereal grains. Frontiers in Plant Science **6**, 1245.

Pi L, Aichinger E, van der Graaff E, Llavata-Peris CI, Weijers D, Hennig L, Groot E, Laux T. 2015. Organizer-derived WOX5 signal maintains root columella stem cells through chromatin-mediated repression of CDF4 expression. Developmental Cell **33**, 576–588.

Pierret A, Doussan C, Capowiez Y, Bastardie F, Pagès L. 2007. Root functional architecture: a framework for modelling the interplay between roots and soil. Vadose Zone Journal **6**, 269–281.

Pieterse CMJ, Leon-Reyes A, Van der Ent S, Van Wees SCM. 2009. Networking by small-molecule hormones in plant immunity. Nature Chemical Biology **5**, 308–316.

Pilet PE. 2002. Root growth and gravireaction: a critical study of hormone and regulator implications. In: Plant Roots The Hidden Half (3rd Edition). Eds. Y Waisel, A Eshel, U Kafkafi (Marcel Dekker Inc., New York), 489–504.

Pilon-Smits EAH, Ebskamp MJM, Jeuken MJW, van der Meer IM, Visser RGF, Weisbeek P J, Smeekens SCM. 1996. Microbial fructan production in transgenic potato plants and tubers. Industrial Crops and Products **5**, 35–46.

Plancot B, Santaella C, Jaber R, Kiefer-Meyer **MC,** Follet-Gueye **ML,** Leprince **J,** Gattin **I,** Souc **C,** Driouich **A,** Vicré-Gibouin **M**. 2013. Deciphering the responses of root border-like cells of Arabidopsis and flax to pathogen-derived elicitors. Plant Physiology **163**, 1584–1597.

Pollock C, Cairns A. 1991. Fructan metabolism in grasses and cereals. Annual Review of Plant Biology **42**, 77–101.

Pollock CJ, Chatterton NJ. 1988. Fructans. In: The biochemistry of plants. A comprehensive treatise, Vol. 14, Carbohydrates. Ed. J Preiss (Academic Press, San Diego/London), 109–140.

Poncini L, Wyrsch I, Dénervaud Tendon V, Vorley T, Boller T, Geldner N, Métraux JP, Lehmann S. 2017. In roots of *Arabidopsis thaliana*, the damage-associated molecular pattern AtPep1 is a stronger elicitor of immune signalling than flg22 or the chitin heptamer. PLoS One **12**, e0185808.

Proseus TE, Boyer JS. 2007. Tension required for pectate chemistry to control growth in *Chara corallina*. Journal of Experimental Botany **58**, 4283–4292.

R Core Team. 2021. R: A language and environment for statistical computing. R Foundation for Statistical Computing, Vienna, Austria.

Raaijmakers JM, Paulitz TC, Steinberg C, Alabouvette C, Moënne-Loccoz Y. 2008. The rhizosphere: a playground and battlefield for soil borne pathogens and beneficial microorganisms. Plant and Soil **321**, 341–361.

Rabbi SMF, Tighe MK, Flavel RJ, Kaiser BN, Guppy CN, Zhang X, Young IM. 2018. Plant roots redesign the rhizosphere to alter the three-dimensional physical architecture and water dynamics. New Phytologist **219**, 542–550.

Rahni R, Efroni I, Birnbaum KD. 2016. A case for distributed control of local stem cell behavior in plants. Developmental Cell **38**, 635–642.

Ramirez-Prado JS, Abulfaraj AA, Rayapuram N, Benhamed M, Hirt H. 2018. Plant immunity: from signaling to epigenetic control of defense. Trends in Plant Science **23**, 833–844.

Reguera M, Abreu I, Brewin NJ, Bonilla I, Bolaños L. 2010. Borate promotes the formation of a complex between legume AGP-extensin and Rhamnogalacturonan II and enhances production of *Rhizobium* capsular polysaccharide during infection thread development in *Pisum sativum* symbiotic root nodules. Plant, Cell & Environment **33**, 2112–2120.

Rejeb IB, Pastor V, Mauch-Mani B. 2014. Plant responses to simultaneous biotic and abiotic stress: molecular mechanisms. Plants **3**, 458–475.

Rich-Griffin C, Eichmann R, Reitz MU, Hermann S, Woolley-Allen K, Brown PE, Wiwatdirekkul K, Esteban E, Pasha A, Kogel KH, Provart NJ, Ott S, Schäfer P. 2020. Regulation of cell type-specific immunity networks in Arabidopsis roots. The Plant Cell **32**, 2742–2762.

Richmond T, Somerville C. 2000. The cellulose synthase superfamily. Plant Physiology **124**, 495–498.

Ringli C. 2010. The hydroxyproline-rich glycoprotein domain of the Arabidopsis LRX1 requires Tyr for function but not for insolubilization in the cell wall. The Plant Journal **63**, 662–669.

Ritsema T, Smeekens S. 2003. Fructans: beneficial for plants and humans. Current Opinion in Plant Biology **6**, 223–230.

Röber M, Geider K, Müller-Röber B, Willmitzer L. 1996. Synthesis of fructans in tubers of transgenic starch-deficient potato plants does not result in an increased allocation of carbohydrates. Planta **199**, 528–536.

Rocha RO, Morais JKS, Oliveira JTA, Oliveira HD, Sousa DO, Souza BCA, Moreno FB, Monteiro-Moreira ACO, de Souza Junior JDA, Grossi de Sá MF, Vasconcelos IM. 2015. Proteome of soybean seed exudates contains plant defense-related proteins active against the root-knot nematode *Meloidogyne incognita*. Journal of Agricultural and Food Chemistry **63**, 5335–5343.

Roitsch T, Balibrea ME, Hofmann M, Proels R, Sinha AK. 2003. Extracellular invertase: key metabolic enzyme and PR protein. Journal of Experimental Botany **54**, 513–524.

Ropitaux M, Bernard S, Follet-Gueye ML, Vicré M, Boulogne I, Driouich A. 2019. Xyloglucan and cellulose form molecular cross-bridges connecting root border cells in pea (*Pisum sativum*). Plant Physiology and Biochemistry **139**, 191–196.

Ropitaux M, Bernard S, Schapman D, Follet-Gueye ML, Vicré M, Boulogne I, Driouich A. 2020. Root border cells and mucilage secretions of soybean, *Glycine max* (Merr) L.: characterization and role in interactions with the oomycete *Phytophthora parasitica*. Cells **9**, 2215.

Rose V. 1804. Über Eine Eigentümliche Vegetabilische Substanz. Gehlen's Journal der Chemie **3**, 217–219.

Rost TL. 2011. The organization of roots of dicotyledonous plants and the positions of control points. Annals of Botany **107**, 1213–1222.

Rougier M. 1981. Secretory activity of the root cap. In: Encyclopedia of plant physiology, New Series, Vol 13B Plant carbohydrates II. Eds. W Tanner, FA Loewus (Berlin: Springer-Verlag), 542–574.

Ruan YL. 2014. Sucrose metabolism: gateway to diverse carbon use and sugar signaling. Annual Review of Plant Biology **65**, 33–67.

Ruta V, Longo C, Lepri A, De Angelis V, Occhigrossi S, Costantino P, Vittorioso P. 2020. The DOF transcription factors in seed and seedling development. Plants **9**, 218.

Rydahl MG, Hansen AR, Kračun SK, Mravec J. 2018. Report on the current inventory of the toolbox for plant cell wall analysis: proteinaceous and small molecular probes. Frontiers in Plant Science **9**, 581.

Rydahl MG, Kračun SK, Fangel JU, Michel G, Guillouzo A, Génicot S, Mravec J, Harholt J, Wilkens C, Motawia MS, Svensson B, Tranquet O, Ralet M-C, Jørgensen B, Domozych DS, Willats WGT. 2017. Development of novel monoclonal antibodies against starch and ulvan - implications for antibody production against polysaccharides with limited immunogenicity. Scientific Reports **7**, 9326.

Saito F, Suyama A, Oka T, Yoko-o T, Matsuoka K, Jigami Y, Shimma Y. 2014. Identification of novel peptidyl serine α-galactosyltransferase gene family in plants. Journal of Biological Chemistry **289**, 20405–20420.

Sakamoto S, Somssich M, Nakata MT, Unda **F,** Atsuzawa **K,** Kaneko **Y,** Wang **T,** Bågman **AM,** Gaudinier **A,** Yoshida **K,** Brady **SM,** Mansfield **SD,** Persson **S,** Mitsuda **N**. 2018. Complete substitution of a secondary cell wall with a primary cell wall in Arabidopsis. Nature Plants **4**, 777–783.

Sarilmiser HK, Ates O, Ozdemir G, Arga KY, Öner ET. 2015. Effective stimulating factors for microbial levan production by *Halomonas smyrnensis* AAD6T. Journal of Bioscience and Bioengineering **119**, 455–463.

Sarkar AK, Luijten M, Miyashima S, Lenhard M, Hashimoto T, Nakajima K, Scheres B, Heidstra R, Laux T. 2007. Conserved factors regulate signalling in *Arabidopsis thaliana* shoot and root stem cell organizers. Nature **446**, 811–814.

Saulnier L, Vigouroux J, Thibault JF. 1995. Isolation and partial characterization of feruloylated oligosaccharides from maize bran. Carbohydrate Research **272**, 241–253.

Scheller HV, Ulvskov P. 2010. Hemicelluloses. Annual Review of Plant Biology **61**, 263–289.

Schindelin J, Arganda-Carreras I, Frise E, Kaynig V, Longair M, Pietzsch T, Cardona A. 2012. Fiji: an open-source platform for biological-image analysis. Nature Methods **9**, 676–682.

Schlink K. 2009. Down-regulation of defense genes and resource allocation into infected roots as factors for compatibility between *Fagus sylvatica* and *Phytophthora citricola*. Functional & Integrative Genomics **10**, 253–264.

Schnyder H. 1993. The role of carbohydrate storage and redistribution in the sourcesink relations of wheat and barley during grain filling - a review. New Phytologist **123**, 233–245.

Schröder R, Atkinson RG, Redgwell RJ. 2009. Re-interpreting the role of endo- β-mannanases as mannan endotransglycosylase/hydrolases in the plant cell wall. Annals of Botany **104**, 197–204.

Schultink A, Liu L, Zhu L, Pauly M. 2014. Structural diversity and function of xyloglucan sidechain substituents. Plants **3**, 526–542.

Schwessinger B, Ronald PC. 2012. Plant innate immunity: perception of conserved microbial signatures. Annual Review of Plant Biology **63**, 451–482.

Scott TK. 1972. Auxins and roots. Annual Review of Plant Physiology **23**, 235–258.

Seifert GJ, Roberts K. 2007. The biology of arabinogalactan proteins. Annual Review of Plant Biology **58**, 137–161.

Shah J, Klessig DF. 1999. Salicylic acid: signal perception and transduction. New Comprehensive Biochemistry **33**, 513–541.

Shi CL, von Wangenheim D, Herrmann U, Wildhagen M, Kulik I, Kopf A, Ishida T, Olsson V, Anker MK, Albert M, Butenko **MA,** Felix **G,** Sawa **S,** Claassen **M,** Friml **J,** Aalen **RB**. 2018. The dynamics of root cap sloughing in Arabidopsis is regulated by peptide signalling. Nature Plants **4**, 596–604.

Shiomi N. 1989. Properties of fructosyltransferases involved in the synthesis of fructan in Liliaceous plants. Journal of Plant Physiology **134**, 151–155.

Showalter AM, Basu D. 2016. Extensin and arabinogalactan-protein biosynthesis: glycosyltransferases, research challenges, and biosensors. Frontiers in Plant Science **7**, 814.

Showalter AM, Varner JE. 1989. Plant hydroxyproline-rich glycoproteins. In: The Biochemistry of Plants, Vol. 15. Eds. PK Stumpf, EE Conn (New York: Academic Press), 485–520.

Showalter AM. 2001. Arabinogalactan-proteins: structure, expression and function. Cellular and Molecular Life Sciences **58**, 1399–1417.

Showalter MA. 1993. Structure and function of plant cell wall proteins. The Plant Cell **5**, 9–23.

Simmons TJ, Mortimer JC, Bernardinelli OD, Pöppler AC, Brown SP, deAzevedo ER, Dupree R, Dupree P. 2016. Folding of xylan onto cellulose fibrils in plant cell walls revealed by solid-state NMR. Nature Communications **7**, 13902.

Simpson RJ, Bonnett GD. 1993. Fructan exohydrolase from grasses. New Phytologist **123**, 453–469.

Smallwood M, Beven A, Donovan N, Neill SJ, Peart J, Roberts K, Knox JP. 1994. Localization of cell wall proteins in relation to the developmental anatomy of the carrot root apex. The Plant Journal ***5***, 237–246.

Smallwood M, Martin H, Knox JP. 1995. An epitope of rice threonine- and hydroxyproline-rich glycoprotein is common to cell wall and hydrophobic plasma-membrane glycoproteins. Planta ***196***, 510-522.

Smallwood M, Yates EA, Willats WGT, Martin H, Knox JP. 1996. Immunochemical comparison of membrane-associated and secreted arabinogalactan-proteins in rice and carrot. Planta ***198***, 452–459.

Smith BG, Harris PJ. 1999. The polysaccharide composition of Poales cell walls: Poaceae cell walls are not unique. Biochemical Systematics and Ecology **27**, 33–53.

Song DD, Jacques NA. 1999. Purification and enzymic properties of the fructosyltransferase of *Streptococcus salivarius* ATCC 25975. Biochemical Journal **341**, 285–291.

Spaepen S, Vanderleyden J, Remans R. 2007. Indole-3-Acetic acid in microbial and microorganism-plant signaling. FEMS Microbiology Review **31**, 425–448.

Sprenger N, Bortlik K, Brandt A, Boller T, Wiemken A. 1995. Purification, cloning, and functional expression of sucrose:fructan 6-fructosyltransferase, a key enzyme of fructan synthesis in barley. Proceedings of the National Academy of Sciences USA **92**, 11652–11656.

Srikanth R, Reddy CHSSS, Siddartha G, Ramaiah MJ, Uppuluri KB. 2015. Review on production, characterization and applications of microbial levan. Carbohydrate Polymers **120**, 102–114.

Stahl Y, Grabowski S, Bleckmann A, Kühnemuth R, Weidtkamp-Peters S, Pinto KG, Kirschner GK, Schmid JB, Wink RH, Hülsewede A, Felekyan S, Seidel CA, Simon R. 2013. Moderation of Arabidopsis root stemness by CLAVATA1 and ARABIDOPSIS CRINKLY4 receptor kinase complexes. Current Biology **23**, 362–371.

Stahl Y, Simon R. 2009. Is the Arabidopsis root niche protected by sequestration of the CLE40 signal by its putative receptor ACR4? Plant Signaling & Behavior **4**, 634–635.

Stahl Y, Wink RH, Ingram GC, Simon R. 2009. A signaling module controlling the stem cell niche in Arabidopsis root meristems. Current Biology **19**, 909–914.

Stanley CE, Shrivastava J, Brugman R, Heinzelmann E, van Swaay D, Grossmann G. 2018. Dual-flow-RootChip reveals local adaptations of roots towards environmental asymmetry at the physiological and genetic levels. New Phytologist **217**, 1357–1369.

Steeghs M, Bais HP, de Gouw J, Goldan P, Kuster W, Northway M, Fall R, Vivanco JM. 2004. Proton-transfer-reaction mass spectrometry as a new tool for real time analysis of root-secreted volatile organic compounds in Arabidopsis. Plant Physiology **135**, 47–58.

Stone BA, Clarke AE. 1992. Chemistry and Biology of (1→3)-β-Glucans. (Bundoora, Australia: La Trobe University Press).

Stoyanova S, Geuns J, Hideg E, Van den Ende W. 2011. The food additives inulin and stevioside counteract oxidative stress. International Journal of Food Sciences and Nutrition **62**, 207–214.

Sturm A. 1999. Invertases. Primary structures, functions and roles in plant development and sucrose partitioning. Plant Physiology **121**, 1–7.

Suárez-González EM, Suárez PAP, Cruz-Rubio JM, Martínez-Gallardo NA, Hernández IC, Délano-Frier JP, Gómez-Leyva JF. 2016. Differential fructan accumulation and expression of fructan biosynthesis, invertase and defense genes is induced in *Agave tequilana* plantlets by sucrose or stress-related elicitors. Agri Gene **2**, 17–28.

Sujkowska-Rybkowska M, Borucki W. 2014. Accumulation and localization of extensin protein in apoplast of pea root nodule under aluminum stress. Micron **67**, 10–19.

Svara A, Tarkowski ŁP, Janse van Rensburg HC, Deleye E, Vaerten J, De Storme N, Keulemans W, Van den Ende W. 2020. Sweet Immunity: the effect of exogenous fructans on the susceptibility of apple (*Malus* × *domestica Borkh*.) to *Venturia inaequalis*. International Journal of Molecular Sciences **21**, 5885.

Tallgren AH, Airaksinen U, von Weissenberg R, Ojamo H, Kuusisto J, Leisola M. 1999. Exopolysaccharide-producing bacteria from sugar beets. Applied Environmental Microbiology **65**, 862–864.

Tamura KI, Sanada Y, Tase K, Komatsu T and Yoshida M. 2011. *Pp6-FEH1* encodes an enzyme for degradation of highly polymerized levan and is transcriptionally induced by defoliation in timothy (*Phleum pratense* L.). Journal of Experimental Botany **62**, 3421–3431.

Tan L, Eberhard S, Pattathil S, Warder C, Glushka J, Yuan C, Hao Z, Zhu X, Avci U, Miller JS, Baldwin **D,** Pham **C,** Orlando **R,** Darvill **A,** Hahn **MG,** Kieliszewski **MJ,** Mohnen **D**. 2013. An arabidopsis cell wall proteoglycan consists of pectin and arabinoxylan covalently linked to an arabinogalactan protein. The Plant Cell **25**, 270–287.

Murashige T and Skoog F. 1962. A revised medium for rapid growth and bio-assays with tobacco tissue cultures. Physiologia Plantarum **15**, 473-497.

Tan L, Showalter AM, Egelund J, Hernandez-Sanchez A, Doblin MS, Bacic A. 2012. Arabinogalactan-proteins and the research challenges for these enigmatic plant cell surface proteoglycans. Frontiers in Plant Science **3**, 140.

Tan L, Varnai P, Lamport DTA, Yuan C, Xu J, Qiu F, Kieliszewski MJ. 2010. Plant O-hydroxyproline arabinogalactans are composed of repeating trigalactosyl subunits with short bifurcated side chains. Journal of Biological Chemistry **285**, 24575–24583.

Tanaka K, Choi J, Cao Y, Stacey G. 2014. Extracellular ATP acts as a damage-associated molecular pattern (DAMP) signal in plants. Frontiers in Plant Science **5**, 446.

Tanimoto E. 2005. Regulation of root growth by plant hormones—roles for auxin and gibberellin. Critical Reviews in Plant Sciences **24**, 249–265.

Tarkowski Ł, Van de Poel B, Höfte M, Van den Ende W. 2019. Sweet immunity: inulin boosts resistance of lettuce (*Lactuca sativa*) against grey mold (*Botrytis cinerea*) in an ethylene-dependent manner. International Journal of Molecular Science **20**, 1052.

Thakur M, Sohal BS. 2013. Role of elicitors in inducing resistance in plants against pathogen infection: a review. International Scholarly Research Notices Biochemistry **2013**, 762412.

Thomas LH, Forsyth VT, Sturcova A, Kennedy CJ, May RP, Altaner CM, Apperley **DC,** Wess **TJ,** Jarvis **MC**. 2013. Structure of cellulose microfibrils in primary cell walls from collenchyma. Plant Physiology **161**, 465–476.

Tian T, Sun B, Shi H, Gao T, He Y, Li Y, Liu Y, Li X, Zhang L, Li S, Wang Q, Chai Y. 2021. Sucrose triggers a novel signaling cascade promoting *Bacillus subtilis* rhizosphere colonization. The ISME Journal **15**, 2723–2737.

Timotiwu PB, Sakurai N. 2002. Identification of mono-, oligo-, and polysaccharides secreted from soybean roots. Journal of Plant Research **115**, 77–85.

Tran TM, MacIntyre A, Hawes M, Allen C. 2016. Escaping underground nets: extracellular DNases degrade plant extracellular traps and contribute to virulence of the plant pathogenic bacterium *Ralstonia solanacearum*. PLoS Pathogens **12**, e1005686.

Traoré O, Groleau-Renaud V, Plantureux S, Tubeileh A, Boeuf-Tremblay V. 2000. Effect of root mucilage and modelled root exudates on soil structure. European Journal of Soil Science **51**, 575–581.

Trollope KM, van Wyk N, Kotjomela MA, Volschenk H. 2015. Sequence and structure-based prediction of fructosyltransferase activity for functional subclassification of fungal GH32 enzymes. The FEBS Journal **282**, 4782–4796.

Trollope KM. 2015. Engineering a fungal β-fructofuranosidase. Thèse. Stellenbosch University (Afrique du Sud). 215p.

Trouvelot S, Héloir MC, Poinssot B, Gauthier A, Paris F, Guillier C, Combier M, Trda L, Daire X, Adrian M. 2014. Carbohydrates in plant immunity and plant protection: roles and potential application as foliar sprays. Frontiers in Plant Science **5**, 1–14.

Tytgat TOG, Verhoeven KJF, Jansen JJ, Raaijmakers CE, BakxSchotman T, McIntyre LM, van der Putten WH, Biere A, van Dam NM. (2013). Plants know where it hurts: root and shoot jasmonic acid induction elicit differential responses in *Brassica oleracea*. PLoS One **8**, e65502.

Ueno K, Ishiguro Y, Yoshida M, Onodera S, Shiomi N. 2011. Cloning and functional characterization of a fructan 1-exohydrolase (1-FEH) in edible burdock (*Arctium Zappa* L.). Chemistry Central Journal **5**, 16.

Underwood W. 2012. The plant cell wall: a dynamic barrier against pathogen invasion. Front Plant Sci **3,** 85.

Urban CF, Ermert D, Schmid M, Abu-Abed U, Goosmann C, Nacken W, Brinkmann V, Jungblut PR, Zychlinsky A. (2009). Neutrophil Extracellular Traps contain calprotectin, a cytosolic protein complex involved in host defense against *Candida albicans.* PLoS Pathogens **5**, e1000639.

Valluru R, Lammens W, Claupein W, Van den Ende W. 2008. Freezing tolerance by vesicle-mediated fructan transport. Trends in Plant Science **13**, 409–414.

Van Arkel J, Sévenier R, Hakkert JC, Bouwmeester HJ, Koops AJ, van der Meer IM. 2013. Tailor-made fructan synthesis in plants: a review. Carbohydrate Polymers **93**, 48–56.

Van Balken JAM, van Dooren TJGM, van den Tweel WJJ, Kamphuis J, Meijer EM. 1991. Production of 1-kestose with intact mycelium of *Aspergillus phoenicis* containing sucrose-1F fructosyltransferase. Applied Microbiology and Biotechnology **35**, 216–221.

Van den Ende W, Clerens S, Van Riet L, Van Laere A, Yoshida M, Kawakami A. 2003a. Fructan 1-exohydrolases. β-(2,1)-trimmers during graminane biosynthesis in stems of wheat? Purification, characterization, mass mapping and cloning of two fructan 1-exohydrolase isoforms. Plant Physiology **131**, 621–631.

Van den Ende W, Clerens S, Vergauwen R, Boogaerts D, Le Roy K, Arckens L, Van Laere A. 2006. Cloning and functional analysis of a high DP fructan:fructan 1-fructosyl transferase from *Echinops ritro* (Asteraceae): comparison of the native and recombinant enzymes. Journal of Experimental Botany **57**, 775–789.

Van den Ende W, De Coninck B, Clerens S, Vergauwen R, Van Laere A. 2003b. Unexpected presence of fructan 6-exohydrolases (6-FEHs) in non-fructan plants: characterization, cloning, mass mapping and functional analysis of a novel 'cell-wall invertase-like' specific 6-FEH from sugar beet (*Beta vulgaris* L.). The Plant Journal **36**, 697–710.

Van den Ende W, De Coninck B, Van Laere A. 2004. Plant fructan exohydrolases: a role in signaling and defense? Trends in Plant Science **9**, 523–528.

Van den Ende W, Michiels A, De Roover J, Van Laere A. 2002. Fructan biosynthetic and breakdown enzymes in dicots evolved from different invertases. Expression of fructan genes throughout chicory development. The Scientific World Journal **2**, 1281–1295.

Van den Ende W, Michiels A, De Roover J, Verhaert P, Van Laere A. 2000a. Cloning and functional analysis of chicory root fructan 1-exohydrolase I (1-FEH I): a vacuolar enzyme derived from a cell wall invertase ancestor? Mass fingerprint of the 1-FEH I enzyme. The Plant Journal **24**, 447–456.

Van den Ende W, Michiels A, Van Wonterghem D, Clerens SP, De Roover J, Van Laere AJ. 2001. Defoliation induces fructan 1-exohydrolase II in witloof chicory roots. Cloning and purification of two isoforms, fructan 1- exohydrolase lia and fructan 1-exohydrolase lib. Mass fingerprint of the fructan 1-exohydrolase II enzymes. Plant Physiology **126**, 1186–1195.

Van den Ende W, Yoshida M, Clerens S, Vergauwen R, Kawakami A. 2005. Cloning, characterization and functional analysis of novel 6-kestose exohydrolases (6-KEHs) from wheat (*Triticum aestivum*). The New Phytologist **166**, 917–932.

Van den Ende W. 2013. Multifunctional fructans and raffinose family oligosaccharides. Frontiers in plant science **4**, 247.

Van der Weele CM, Spollen WG, Sharp RE, Baskin TI. 2000. Growth of *Arabidopsis thaliana* seedlings under water deficit studied by control of water potential in nutrient-agar media. Journal of Experimental Botany **51**, 1555–1562.

Van Laere A, Van Den Ende W. 2002. Inulin metabolism in dicots: chicory as a model system. Plant, Cell & Environment **25**, 803–813.

Van Loon LC, Rep M, Pieterse CMJ. 2006. Significance of inducible defense-related proteins in infected plants. Annual Review of Phytopathologist **44**, 135–162.

Van Riet L, Altenbach D, Vergauwen R, Clerens S, Kawakami A, Yoshida M, Van den Ende W, Wiemken A, Van Laere A. 2008. Purification, cloning and functional differences of a third fructan 1-exohydrolase (1-FEHw3) from wheat (*Triticum aestivum* L.). Physiologia plantarum **133**, 242–253.

Van Riet L, Nagaraj V, Van den Ende W, Clerens S, Wiemken A, Van Laere A. 2006. Purification, cloning and functional characterization of a fructan 6- exohydrolase from wheat (*Triticum aestivum* L.). Journal of Experimental Botany **57**, 213-223.

Vandenbosch KA, Bradley DJ, Knox JP, Perotto S, Butcher GW, Brewin NJ. 1989. Common components of the infection thread matrix and the intercellular space identifed by immunocytochemical analysis of pea nodules and uninfected roots. The EMBO Journal **8**, 335–341.

Velasquez M, Salter JS, Dorosz JG, Petersen BL, Estevez JM. 2012. Recent advances on the posttranslational modifications of EXTs and their roles in plant cell walls. Frontiers in Plant Science **3**, 93.

Velasquez SM, Ricardi MM, Poulsen CP, Oikawa A, Dilokpimol A, Halim A, Mangano S, Denita Juarez SP, Marzol E, Salgado Salter JD, Dorosz **JG,** Borassi **C,** Möller **SR,** Buono **R,** Ohsawa **Y,** Matsuoka **K,** Otegui **MS,** Scheller **HV,** Geshi **N,** Petersen **BL,** Iusem **ND,** Estevez **JM**. 2015. Complex regulation of prolyl-4-hydroxylases impacts root hair expansion. Molecular Plant **8**, 734–746.

Velasquez SM, Ricardi MM. Dorosz JG, Fernandez PV, Nadra AD, Pol-Fachin L, Egelund J, Gille S, Harholt J, Ciancia M, Verli **H,** Pauly **M,** Bacic **A,** Olsen **CE,** Ulvskov **P,** Petersen **BL,** Somerville **C,** Iusem **ND,** Estevez **JM**. 2011. O-Glycosylated cell wall proteins are essential in root hair growth. Science **332**, 1401–1403.

Velázquez-Hernández ML, Baizabal-Aguirre VM, Bravo-Patiño A, Cajero-Juárez M, Chávez-Moctezuma MP, Valdez-Alarcón JJ. 2009. Microbial fructosyltransferases and the role of fructans. Journal of Applied Microbiology **106**, 1763–1778.

Verslues PE, Agarwal M, Katiyar-Agarwal S, Zhu J, Zhu JK. 2006. Methods and concepts in quantifying resistance to drought, salt and freezing, abiotic stresses that affect plant water status. The Plant Journal **45**, 523-539. Erratum in: The Plant Journal **46**, 1092.

Versluys M, Porras-Domínguez JR, de Coninck T, van Damme EJM, van den Ende W. 2021. A novel chicory fructanase can degrade common microbial fructan product profiles and displays positive cooperativity. Journal of Experimental Botany **73**, 1602–1622.

Versluys M, Tarkowski ŁP, Van den Ende W. 2017b. Fructans as DAMPs or MAMPs: evolutionary prospects, cross-tolerance, and multistress resistance potential. Frontiers in Plant Science **7**, 2061.

Vicré M, Santaella S, Blanchet S, Gateau A, Driouich A. 2005. Root Border Like Cells of Arabidopsis. Microscopical characterization and role in the interaction with Rhizobacteria. Plant Physiology **138**, 998–1008.

Vijn I, Smeekens S. 1999. Fructan: more than a reserve carbohydrate? Plant Physiology **120**, 351–359.

Vijn I, van Dijken A, Sprenger N, van Dun K, Weisbeek P, Wiemken A, Smeekens S. 1997. Fructan of the inulin neoseries is synthesized in transgenic chicory plants (*Cichorium intybus*

L.) harbouring onion (*Allium cepa* L.) fructan:fructan 6G-fructosyltransferase. The Plant Journal **11**, 387–398.

Vogel J. 2008. Unique aspects of the grass cell wall. Current Opinion in Plant Biology **11**, 301–307.

Voiniciuc C, Günl M, Schmidt MHW, Usadel B. 2015. Highly branched xylan made by IRREGULAR XYLEM14 and MUCILAGE-RELATED21 links mucilage to Arabidopsis seeds. Plant Physiology **169**, 2481–2495.

Volaire F, Morvan-Bertrand A, Prud'homme MP, Benot ML, Augusti A, Zwicke M, Roy J, Landais D, Picon-Cochard C. 2020. The resilience of perennial grasses under two climate scenarios is correlated with carbohydrate metabolism in meristems. Journal of Experimental Botany **71**, 370–385.

Von Köckritz-Blickwede M, Nizet V. 2009. Innate immunity turned inside-out: antimicrobial defense by phagocyte extracellular traps. Journal of Molecular Medicine **87**, 775–783.

Wagner W, Keller F, Wiemken A. 1983. Fructan metabolism in cereals: induction in leaves and compartmentation in protoplasts and vacuoles. Zeitschrift Für Pflanzenphysiologie **112**, 359–372.

Wan J, He M, Hou Q, Zou L, Yang Y, Wei Y, Chen X. (2021). Cell wall associated immunity in plants. Stress Biology **1**, 3.

Wang N, Nobel PS. 1998. Phloem transport of fructans in the crassulacean acid metabolism species *Agave deserti*. Plant Physiology **116**, 709–714.

Wang P, Chen X, Goldbeck C, Chung E, Kang BH. 2017. A distinct class of vesicles derived from the trans-Golgi mediates secretion of xylogalacturonan in the root border cell. The Plant Journal **92**, 596–610.

Wang Y, Chantreau M, Sibout R, Hawkins S. 2013. Plant cell wall lignification and monolignol metabolism. Frontiers in Plant Science **4**, 220.

Wang Z, Tan X, Zhang Z, Gu S, Li G, Shi H. 2012. Defense to *Sclerotinia sclerotiorum* in oilseed rape is associated with the sequential activations of salicylic acid signaling and jasmonic acid signaling. Plant Science **184**, 75–82.

Watt M, McCully ME, Jeffree CE. 1993. Plant and bacterial mucilages of the maize rhizosphere: comparison of their soil binding properties and histochemistry in a model system. Plant and Soil **151**, 151–165.

Weiller F, Moore JP, Young P, Driouich A, Vivier MA. 2016. The Brassicaceae species *Heliophila coronopifolia* produces root border-like cells that protect the root tip and secrete defensin peptides. Annals of Botany **119**, 803–813.

Wen F, Curlango-Rivera G, Hawes MC. 2007a. Proteins among the polysaccharides: a new perspective on root cap "slime." Plant Signaling & Behavior **2**, 410–412.

Wen F, Curlango-Rivera G, Huskey DA, Xiong Z, Hawes MC. 2017. Visualization of extracellular DNA released during border cell separation from the root cap. American Journal of Botany **104**, 970–978.

Wen F, VanEtten HD, Tsaprailis G, Hawes MC. 2007b. Extracellular proteins in pea root tip and border cell exudates. Plant Physiology **143**, 773–783.

Wen F, White GJ, VanEtten HD, Xiong Z, Hawes MC. 2009. Extracellular DNA is required for root tip resistance to fungal infection. Plant Physiology **151**, 820–829.

Wen F, Zhu Y, Hawes MC. 1999. Effect of pectin methylesterase gene expression on pea root development. The Plant Cell **11**, 1129–1140.

Willats WG, McCartney L, Mackie W, Knox JP. 2001. Pectin: cell biology and prospects for functional analysis. Plant Molecular Biology **47**, 9–27.

Wilson SM, Ho YY, Lampugnani ER, Van de Meene AM, Bain MP, Bacic A, Doblin MS. 2015. Determining the subcellular location of synthesis and assembly of the cell wall polysaccharide (1,3; 1,4)-β-D-glucan in grasses. The Plant Cell **27**, 754–771.

Woo HH, Hawes MC. 1997. Cloning of genes whose expression is correlated with mitosis and localized in dividing cells in root caps of *Pisum sativum* L. Plant Molecular Biology **35**, 1045–1051.

Wu S, Greiner S, & Ma C, Zhong J, Huang X, Rausch T, Zhao H. 2021. A fructan exohydrolase from maize degrades both inulin and levan and co-exists with 1-kestotriose in maize. International Journal of Molecular Sciences **22**, 5149.

Wu Y, Williams M, Bernard S, Driouich A, Showalter AM, Faik A. 2010. Functional identification of two non-redundant Arabidopsis α-(1,2)-fucosyltransferases specific to arabinogalactan proteins. Journal of Biological Chemistry **285**, 13638–13645.

Xia Y, Petti C, Williams MA, DeBolt S. 2014. Experimental approaches to study plant cell walls during plant-microbe interactions. Frontiers in Plant Science **5**, 540.

Xie D, Ma L, Šamaj J, Xu C. 2011. Immunohistochemical analysis of cell wall hydroxyproline-rich glycoproteins in the roots of resistant and susceptible wax gourd cultivars in response to *Fusarium oxysporum* f. sp. *Benincasae* infection and fusaric acid treatment. Plant Cell Reports **30**, 1555–1569.

Xie F, Williams A, Edwards A, Downie JA. 2012. A plant arabinogalactan-like glycoprotein promotes a novel type of polar surface attachment by *Rhizobium leguminosarum*. Molecular Plant-Microbe Interactions **25**, 250–258.

Yamamoto S, Mino Y. 1985. Partial purification and properties of phleinase induced in stem base of orchardgrass after defoliation. Plant Physiology **78**, 591–595.

Yan Y, Takáč T, Li X, Chen H, Wang Y, Xu E, Xie L, Su Z, Šamaj J and Xu C. 2015. Variable content and distribution of arabinogalactan proteins in banana (*Musa* spp.) under low temperature stress. Frontiers in Plant Science **6**, 353.

Yariv J, Lis H, Katchalski E. 1967. Precipitation of arabic acid and some seed polysaccharides by glycosylphenylazo dyes. Biochemical Journal **105**, 1–2.

Yates EA, Knox JP. 1994. Investigations into the occurrence of plant cell surface epitopes in exudate gums. Carbohydrate Polymers **24**, 281-286.

Yates EA, Valdor JF, Haslam SM, Morris HR, Dell A, Mackie W, Knox JP. 1996. Characterization of carbohydrate structural features recognized by anti-arabinogalactan-protein monoclonal antibodies. Glycobiology **6**, 131–139.

Yazawa T, Kawahigashi H, Matsumoto T, Mizuno H. 2013. Simultaneous transcriptome analysis of sorghum and *Bipolaris sorghicola* by using RNA-seq in combination with *de novo* transcriptome assembly. PLoS One **8**, e62460.

Yokoyama R Nishitani K. 2004. Genomic basis for cell-wall diversity in plants. A comparative approach to gene families in rice and Arabidopsis. Plant & Cell Physiology **45**, 1111–1121.

York LM, Carminati A, Mooney SJ, Ritz K, Bennett MJ. 2016. The holistic rhizosphere: integrating zones, processes, and semantics in the soil influenced by roots. Journal of Experimental Botany **67**, 3629–3643.

Yoshida M. 2021. Fructan Structure and Metabolism in Overwintering Plants. Plants **10**, 933.

Yu K Pieters CMJ, Bakker PAHM, Berendsen RL. 2019. Beneficial microbes going underground of root immunity. Plant, Cell & Environment **42**, 2860–2870.

Yuan M, Jiang Z, Bi G, Nomura K, Liu M, Wang Y, Cai B, Zhou JM, He SY, Xin XF. 2021. Pattern-recognition receptors are required for NLR-mediated plant immunity. Nature **592**, 105–109.

Yuan S, Le Roy K, Venken T, Lammens W, Van den Ende W, De Maeyer M. 2012. pKa modulation of the acid/base catalyst within GH32 and GH68: a role in substrate/inhibitor specificity? PLoS One **7**, e37453.

Yulia D, Yusriana B. 2006. Current thought of plant cell wall: structure, biosynthesis, and future application. Biota **XI**, 190–195.

Yun JW, Kim DH, Kim BW, Song SK. 1997. Production of inulo-oligosaccharides from inulin by immobilized endoinulinase from *Pseudomonas* sp., Journal of Fermentation and Bioengineering **84**, 369–371.

Zablackis E, Jing H, Muller B, Darvill AG, Albersheim P. 1995. Characterization of the cell-wall polysaccharides of *Arabidopsis thaliana* leaves. Plant Physiology **107**, 1129–1138.

Zandleven J, Sørensen SO, Harholt J, Beldman G, Schols HA, Scheller HV, Voragen AJ. 2007. Xylogalacturonan exists in cell walls from various tissues of *Arabidopsis thaliana*. Phytochemistry **68**, 1219–1226.

Zhang J, Zhou JM. 2010. Plant immunity triggered by microbial molecular signatures. Molecular Plant **3**, 783–793.

Zhang PY, Wang JC, Liu SH, Chen KS. 2009. A novel burdock fructooligosaccharide induces changes in the production of salicylates, activates defence enzymes and induces systemic acquired resistance to *Colletotrichum orbiculare* in cucumber seedlings. Journal of Phytopathology **157**, 201–207.

Zhang X, Ménard R, Li Y, Coruzzi GM, Heitz T, Shen WH, Berr A. 2020. Arabidopsis SDG8 potentiates the sustainable transcriptional induction of the Pathogenesis-Related genes PR1 and PR2 during plant defense response. Frontiers in Plant Science **11**, 277.

Zhang Y, Xin Li X. 2019. Salicylic acid: biosynthesis, perception, and contributions to plant immunity. Current Opinion in Plant Biology **50**, 29–36.

Zhao H, Greiner S, Scheffzek K, Rausch T, Wang G. 2019. A 6&1-FEH encodes an enzyme for fructan degradation and interact with invertase inhibitor protein in maize (*Zea mays* L.). International Journal of Molecular Science **20**, 3807.

Zhao X, Misaghi IJ, Hawes MC. (2000a) Stimulation of border cell production in response to increased carbon dioxyde levels. Plant Physiology **122**, 181–188.

Zhao X, Schmitt M, Hawes MC. 2000b. Species-dependent effects of border cell and root tip exudates on nematode behavior. Phytopathology **90**, 1239–1245.

Zhou F, Emonet A, Tendon VD, Marhavy P, Wu D, Lahaye T, Geldner N. 2020. Co-incidence of damage and microbial patterns controls localized immune responses in roots. Cell **180**, 440–453.

Zhou JM, Zhang Y. 2020. Plant immunity: danger perception and signaling. Cell **181**, 978–989.

Zhu Y, Wu N, Song W, Yin G, Qin Y, Yan Y, Hu Y. 2014. Soybean (*Glycine max*) expansin gene superfamily origins: segmental and tandem duplication events followed by divergent selection among subfamilies. BMC Plant Biology **14**, 1–19.

Zipfel C. 2008. Pattern-recognition receptors in plant innate immunity. Current Opinion in Immunology **20**, 10–16.

Zuther E, Kwart M, Willmitzer L, Heyer AG. 2004. Expression of a yeast-derived invertase in companion cells results in long distance transport of a trisaccharide in an apoplastic loader and influences sucrose transport. Planta **218**, 759–766.

Thi Ngoc Hanh NGUYEN
Doctorante en Sciences agronomiques, Biotechnologies agro-alimentaires

Situation actuelle

Depuis septembre 2018 : Doctorante dans le cadre d'une collaboration initiée entre les deux laboratoires d'accueil de la thèse :

-Laboratoire EVA (Écophysiologie Végétale, Agronomie & nutritions N.C.S.) - UMR INRAE-UNICAEN 950 - Université de Caen, sous la direction de Mme. Annette BERTRAND et Mme. Marie-Pascale PRUD'HOMME.

-Laboratoire GlycoMEV (Glycobiologie et Matrice Extracellulaire Végétale) - UPRES EA 4358 - Université de Rouen, sous la direction de Mme. Maïté VICRE et Mme. Marie-Laure FOLLET-GUEYE.

Sujet : Rhizo-sweet : Glycomolécules de la rhizosphère et défense des plantes.

Cursus universitaire

Septembre 2018 - présent : Doctorat en Sciences agronomiques, biotechnologies agro-alimentaires à l'Université de Caen et l'Université de Rouen, France (en cours).

2018 : Master biologie végétale : parcours Phytoressources et phytosciences à l'Université Claude Bernard Lyon 1, France.

2013 : Diplôme universitaire en Biotechnologie (Bac+4) à l'Université de technologie de Ho Chi Minh ville (HUTECH), Vietnam.

Expériences professionnelles

Cadarache, 2019 : Séjour scientifique (7 semaines) - LEMIRE - Laboratoire d'Ecologie Microbienne de la rhizosphère et d'environnements extrêmes.
Sujet : Etude du rôle des fructane-exohydrolases (FEHs) d'*Arabidopsis thaliana* dans les interactions entre les racines et la bactérie *Pseudomonas brassicacearum*.

Portes-lès-Valence, 2018 : Stage M2 (6 mois) - Laboratoire de recherche en Pathologie des Semences (PRS) - HM-Clause
Sujet : Amélioration de la méthode d'isolement et de détection de l'*Acidovorax valerianellae* sur semences de mâche.

Lyon, 2017 : Stage M1 (3 mois) - Laboratoire Reproduction et Développement des Plantes - ENS Lyon
Sujet : Rôle des microtubules de la papille stigmatique dans la germination et la croissance du tube pollinique chez *Arabidopsis thaliana*.

Contact

☎ 06 95 32 04 64
✉ hanh.nguyen@unicaen.fr
nguyenngochanh05@yahoo.com
8-10 Boulevard Gambetta
76000 Rouen
10/02/1990 (31 ans)

Compétences

Cultures de plantes (sur milieu gélosé et en hydroponie) : *A. thaliana, Lolium perenne, Brassica napus, Phleum pratense.*

Techniques d'imagerie
Microscopie Optique et Confocale :
Colorations histochimiques et immunocytochimiques des composés pariétaux / Utilisation de sondes fluorescentes.

Techniques de biologie moléculaire
Extraction et analyse d'acides nucléiques (ADN, ARN) :
Dosage au BioPhotometer, séparation électrophorétique sur gel d'agarose, analyses bio-informatiques, conception d'amorces, RT-PCR, PCR en temps réel (qPCR).

Techniques de biochimie
Caractérisation d'anticorps monoclonaux dirigés contre des glycomolécules par Dot-Blot.
Extraction des protéines solubles et pariétales.
Dosage d'activité enzymatique (invertase, β-fructosidases).

Vietnam, 2013 : Stage de fin d'études (2 mois) - Agri -Business Incubator compagnie
Sujet : Etude de la reproduction et processus de culture in vitro d'*Anthurium Andraeanum* (langue de feu) et les orchidées ; suivi de la croissance de ces plantes in vitro en pépinière.

Vietnam, 2012-2013 : Recherche de fin d'études (9 mois) - Université HUTECH (Ho Chi Minh City University of Technology)
Sujet : Recherche de la gamme d'hôtes des nématodes entomopathogènes (EPN) et de la virulence des entérobactéries vivant en association symbiotique avec des nématodes sur les insectes ravageurs de cultures.

Communications et publications

2021 - **Nguyen TNH**, Leclerc L, Prud'homme M-P, Follet-Gueye M-L, Morvan-Bertrand A, Vicré M, Manzanares M. *Fructan exohydrolases are upregulated by the salicylic acid-dependent defense response in the roots of two Brassicaceae*. (Article en cours de rédaction).

17-18 Mai 2021 - **Nguyen TNH**, Vicré M, Follet-Gueye M-L, Driouich A, Morvan-Bertrand A, Prud'homme M-P. *Molecular characterization of the Root Extracellular Trap (RET) in ryegrass (Lolium perenne), a fructan-producing plant.* (Poster des Journées de l'ED Normande de Biologie Intégrative, Santé, Environnement – XXIIIe Edition).

19-20 Septembre 2019 - **Nguyen TNH**, Leclerc L, Vicré M, Follet-Gueye M-L, Driouich A, Morvan-Bertrand A, Prud'homme M-P. *Les fructane exohydrolases (FEHs) et immunité végétale : un cas d'étude, les racines de colza (Brassica napus).* (Présentation orale pour des Secondes Journées Scientifiques « Root Days » - Nguyen TNH.).

28-29 Mai 2019 - **Nguyen TNH**, Leclerc L, Prud'homme M-P, Follet-Gueye M-L, Driouich A, Morvan-Bertrand A, Vicré M. *Glycomolecules in root defense.* (Poster des 3èmes journées de la SFR NORVEGE).

28-29 Mai 2019 - Leclerc L, **Nguyen TNH**, Prud'homme M-P, Vicré M, Morvan-Bertrand A. *Les fructane exohydrolases (FEHs) et immunité végétale : un cas d'étude, les racines de colza (Brassica napus).* (Présentation orale pour des 3èmes journées de la SFR NORVEGE - Leclerc L.).

18 Octobre 2018 - Leclerc L, **Nguyen TNH**, Prud'homme M-P, Vicré M, Morvan-Bertrand A. *Les fructane exohydrolases (FEHs) et l'immunité végétale : étude de l'expression des gènes Bn6-FEH et Bn6&1-FEH dans les racines de colza (Brassica napus).* (Présentation orale pour des Premières Journées Scientifiques « Root Days » - Morvan-Bertrand A.).

Informatique
Microsoft Office, analyse d'image (LAS AF Lite, ImageJ, Imaris), traitement statistique (R), GIMP, ZOTERO.

Langues
Français :
Compréhension et expression écrite et orale.
Anglais scientifique :
Compréhension et expression écrite et orale.
Vietnamien : langue maternelle.

Encadrement de stagiaires
Encadrement ponctuel technique des stagiaires (niveau L3, M1, M2) pour les formations de Dot blot, RT-qPCR, extraction enzymatique.

Collaboration scientifique
avec CEA Cadarache, IGEPP Rennes, ISA Nice.

Référents

Mme. Annette BERTRAND (MCU-HDR) – Université de Caen
annette.bertrand@unicaen.fr

Mme. Maïté VICRE (MCU-HDR) – Université de Rouen
maite.vicre@univ-rouen.fr

Mme. Marie-Pascale PRUD'HOMME (Professeur) - Université de Caen
marie-pascale.prudhomme@unicaen.fr

Mme. Marie-Laure FOLLET-GUEYE (MCU-HDR) – Université de Rouen
marie-laure.follet-gueye@univ-rouen.fr

Rhizo-sweet: glycomolecules of the rhizosphere and plant defense

Abstract. To date, root immunity remains poorly investigated as compared to the aerial part. In this thesis, we aimed to evaluate the role of glycomolecules in root defense with a particular interest on fructans and fructan metabolizing enzymes. *Lolium perenne* (perennial ryegrass), a Poaceae of regional interest due to its role as a grassland forage plant was chosen as fructan accumulating plant. Two non-fructan Brassicaceae were also selected: the plant model *Arabidopsis thaliana* and oilseed rape (*Brassica napus*) for its agronomical interest. Fructans are water-soluble fructose polymers containing β-(2,1) and/or β-(2,6) linked fructose residues found in some plant species and in exopolysaccharides produced by some beneficial or pathogenic bacteria. In plants, fructans constitute a carbohydrate reserve and act in the protection against abiotic and biotic stresses according to the theory of the « sweet immunity ». To unravel the mechanisms of action of fructans, their precise localization at tissue and cellular level in various environmental conditions need to be clarified. One of the major task of our study is the production of two novel monoclonal antibodies (mAbs) named BTM15A6 and BTM9H2 towards plant fructans with β-(2,1) and/or β-(2,6) linkages. In depth characterization of their specificity was performed by immune-dot blot assays using a wide range of carbohydrates including polysaccharides. Immunolocalization of fructans by cell imaging confirmed that the recognized epitopes were detected in three fructan plant species but not in the non-fructan plant Arabidopsis. Interestingly the presence of fructan epitopes was also detected in the root system of perennial ryegrass. The root extracellular trap (RET) is known to be an important actor of root protection. By investigating the RET composition of *L. perenne*, we found that both mucilage and cell wall surface of border cells were particularly enriched in arabinogalactan-proteins (AGPs) epitopes. The amount of the AGP-containing mucilage was increased in response to treatment with the bacterial elicitor flagellin 22 and the water-stress inducer PEG. This suggests that AGPs play an essential role in root protection in *L. perenne*. Although fructan epitopes were not detected within the mucilage, their presence in the root cap cells suggests that they might also be involved in biotic and/or abiotic stress protection. In addition, we evaluated the regulation of fructan exohydrolases (FEHs) found in non-fructan-accumulating plant species including *A. thaliana* and *B. napus* in response to root treatment with defense-related phytohormones. Salicylic acid increased the transcript level of the two FEHs (6-FEH and 6&1-FEH) in both species. These data support a role of these FEHs in root immunity. Furthermore, preliminary results obtained with Arabidopsis FEH knockout mutants suggest a role of these enzymes in root interaction with the beneficial bacteria *Pseudomonas brassicacearum*.

Keywords. Fructans, monoclonal antibodies, border cells, mucilage, Root Extracellular Trap, perennial ryegrass, arabinogalactan-proteins, fructan exohydrolases, salicylic acid, oilseed rape, Arabidopsis, FEH knock-out mutants, *Pseudomonas brassicacearum.*

Rhizo-sweet : glycomolécules de la rhizosphère et défense des plantes

Résumé. L'immunité et la protection racinaire restent encore peu étudiées par comparaison avec le système aérien des plantes. Ce travail de thèse porte sur l'évaluation du rôle des glycomolécules dans la défense racinaire avec un accent particulier sur les fructanes, et les enzymes les métabolisant. Le ray-grass anglais (*Lolium perenne*), une Poacée d'intérêt régional pour son rôle de plante fourragère prairiale, est choisie comme modèle d'étude de plantes accumulant des fructanes. De plus, deux espèces végétales appartenant à la famille des Brassicacées et ne produisant pas de fructanes ont été sélectionnées : la plante modèle *Arabidopsis thaliana* et une espèce d'intérêt agronomique majeur, le colza (*Brassica napus*). Les fructanes sont des polymères solubles de résidus fructosyles liés en β-(2,1) et/ou en β-(2,6) présents chez certaines espèces végétales et dans les exopolysaccharides de bactéries bénéfiques ou pathogènes. Chez les plantes, les fructanes constituent une réserve glucidique et agissent également dans la protection contre les stress abiotiques et biotiques selon le concept de la « Sweet-Immunity ». Pour approfondir la compréhension de leurs mécanismes d'action, leur localisation précise au niveau tissulaire et cellulaire dans diverses conditions environnementales doit être élucidée. Pour cette étude, deux nouveaux anticorps monoclonaux (mAbs) appelés BTM15A6 et BTM9H2 dirigés contre les fructanes portant des liaisons β-(2,1) et/ou β-(2,6) ont été produits. Leur caractérisation a été réalisée par des tests d'immuno-dot blot sur une large gamme de glucides incluant de nombreux polysaccharides. Des approches d'imagerie cellulaire ont révélé la présence de ces épitopes chez trois espèces de plantes à fructanes. La présence des épitopes associés aux fructanes a également été détectée dans le système racinaire de *L. perenne*. Le Root Extracellular Trap (RET) constitué de cellules frontières et de mucilage joue un rôle important dans la défense de la racine. Chez *L. perenne*, nous avons mis en évidence que le RET était particulièrement enrichi en épitopes associés aux arabinogalactane-protéines (AGPs). La quantité de mucilage contenant des AGPs est augmentée en réponse à un traitement avec la flagelline 22, un éliciteur bactérien, et au PEG, qui induit un stress hydrique. Nous émettons l'hypothèse que les AGPs jouent un rôle essentiel dans la protection racinaire chez *L. perenne*. Bien que les épitopes associés aux fructanes n'aient pas été détectés dans le mucilage, leur présence dans les cellules de coiffe suggère qu'ils pourraient être impliqués dans la protection contre les stress biotiques et/ou abiotiques. En outre, nous avons évalué la régulation de l'expression des fructanes exohydrolases (FEHs) présentes chez les deux espèces végétales *A. thaliana* et *B. napus* qui n'accumulent pas de fructanes. L'acide salicylique augmente le niveau des transcrits des deux FEHs (6-FEH et 6&1-FEH) chez les deux espèces suggérant leur implication dans la réponse immunitaire. De plus, des résultats préliminaires obtenus avec les mutants knock-out correspondant à ces gènes chez Arabidopsis indiquent un rôle des FEHs dans les interactions avec la bactérie bénéfique productrice de fructanes *Pseudomonas brassicacearum*.

Mots clés. Fructanes, anticorps monoclonaux, cellules bordantes, mucilage, Root Extracellular Trap, ray-grass anglais, arabinogalactanes, fructanes exohydrolases, acide salicylique, colza, mutants FEH knock-out, *Pseudomonas brassicacearum.*